THESIS SUBMITTED AS A PARTIAL FULFILMENT OF THE REQUIREMENTS FOR THE DEGREE OF D.PHIL.

NUFFIELD DEPARTMENT OF OBSTETRICS AND GYNAECOLOGY

UNIVERSITY OF OXFORD

STRUCTURE-FUNCTION STUDIES OF FIBRONECTIN DOMAINS IN THE HUMAN ENDOMETRIUM

MAY GEE YEE MOK

ST. CATHERINE'S COLLEGE

HILARY TERM 2008

Contents in Brief

Acknowledgements		x
Abbreviations		xi
Abstract		xv
Chapter 1	Introduction	1
Chapter 2	Materials and Methods	88
Chapter 3	Synthesis and Remodelling of ECM during *in vitro* decidualization of human endometrial stromal cells	116
Chapter 4	Modulation of FN levels in endometrial stromal cells by endometrial cytokines and growth factors	145
Chapter 5	Role of EDIIIA+FN in supporting blastocyst adhesion	159
Chapter 6	Structural and functional roles of EDIIIA and EDIIIB inclusion in FN	185
Chapter 7	General discussion and future directions	228
References		235

Full Contents

Acknowledgements ..... **x**

Abbreviations ..... **xi**

Abstract ..... **xv**

Chapter 1 Introduction **1**

1.1 The Endometrium 1

1.1.1. Menstrual cycle 2

1.1.2. Decidualization 5

1.1.2.1 Functions of the decidua 6

1.1.2.2 Models of *in vitro* decidualization in human endometrial stromal cells 8

1.2 Implantation 10

1.2.1. Pre-implantation embryo development 11

1.2.2. Uterine receptivity 12

1.2.3. Apposition 14

1.2.4. Attachment 15

1.2.5. Invasion 18

1.3 Endometrial growth factors and cytokines 21

1.3.1. EGF family 21

1.3.2. IL-6 family 24

1.3.3. TGF-β superfamily 26
1.3.4. IL-1 family 27
1.3.5. TNFα 29
1.3.6. bFGF 30
1.4 The Extracellular Matrix 33
1.4.1. Collagens 35
1.4.1.1 Collagen type I 37
1.4.1.2 Collagen type IV 39
1.4.2. Laminins 41
1.4.3. Tenascins 44
1.4.4. Vitronectin 46
1.4.5. Fibronectins 49
1.4.5.1 Structural organisation 49
1.4.5.2 Posttranslational modifications 54
1.4.5.3 Structure and Function of EDIIIA and EDIIIB variants 55
1.4.5.4 Modulation of FN splicing 59
1.4.5.5 Matrix assembly 61
1.4.5.6 Biological roles of FN and the ECM 62
1.4.6. Constitutive and cycle-dependent expression of ECM proteins in the endometrium 65
1.4.7. Expression of fibronectins in the endometrium 67
1.4.8. Roles of ECM glycoproteins in the endometrium 68
1.5 Integrins 72
1.5.1. Introduction 72
1.5.2. Integrins α5β1 and αvβ3 78

1.5.3. The α4 and α9 subset of integrins 78
1.5.4. Integrin-mediated signalling 79
1.5.5. Integrins in the endometrium 83
1.6 Hypothesis and Objectives 87

Chapter 2 Materials and Methods 88

2.1 Materials 88
2.1.1. Chemicals and buffers 88
2.1.2. Plasmids 88
2.1.3. Antibodies and conjugates 89
2.1.3.1 Primary antibodies 89
2.1.3.2 Secondary antibodies and conjugates 89
2.1.4. Bacterial media 89
2.1.5. Eukaryotic media 89
2.1.6. Bacterial strains 90
2.1.6.1 Preparation of bacterial competent cells 90
2.1.7. Eukaryotic cells: human endometrial stromal cells 90
2.1.7.1 Tissue collection and isolation of human endometrial stromal cells 90
2.1.7.2 Passaging and maintenance of human endometrial stromal cells 91
2.1.7.3 In vitro decidualization of endometrial stromal cells 91
2.1.7.4 Extraction of cell lysates 91

2.2 General DNA manipulation techniques 92
2.2.1. Transformation of *E.coli* with plasmid DNA 92
2.2.2. Glycerol stock of plasmid containing *E.coli* 92
2.2.3. Purification of plasmid DNA 92
2.2.4. Analytical agarose gel electrophoresis 93
2.2.5. DNA sequencing 93
2.3 Protein expression, purification and detection methods 93
2.3.1. Large-scale expression and affinity purification of recombinant fibronectin fragments 93
2.3.1.1 GST-fusion proteins 93
2.3.1.2 His-tag-fusion proteins 95
2.3.2. Affinity purification of integrins α5β1 and αvβ3 95
2.3.3. Determination of protein concentration 96
2.3.3.1 Coomassie assay 96
2.3.3.2 *DC* protein assay 97
2.3.4. Analysis of proteins by SDS-PAGE 97
2.3.5. Immunoblotting and antibody detection of proteins 97
2.4 Crystallization trials 98
2.5 Enzyme-linked immunosorbent assays (ELISAs) 99
2.5.1. Determining protein/integrin coating efficiency 99
2.5.2. Integrin-ligand binding assays 100
2.5.3. Modulation of FN expression in endometrial stromal cells by cytokines and growth factors 101
2.6 Cell adhesion assays 103

2.6.1. Maintenance and preparation of cells 103

2.6.2. Protocols for quantification of cell attachment and spreading 103

2.7 FAK phosphorylation assays 104

2.7.1. Extraction and detection of Focal Adhesion Kinase (FAK) 104

2.8 Immunofluorescence detection methods 105

2.8.1. Immunohistochemistry on tissue sections 105

2.8.2. Immunocytochemistry on cultured cell lines 105

2.8.2.1 Preparation of samples 105

2.8.2.2 Staining protocols 106

2.9 Cell proliferation assay 107

2.9.1. Maintenance and preparation of cells 107

2.9.2. Proliferation assays with immobilised fibronectin 107

2.9.3. Determining cell growth 107

2.10 *In vitro* blastocyst adhesion model 108

2.10.1. Human embryo culture 108

2.10.2. Embryo attachment assays 108

2.10.3. Immunofluorescent labelling of human blastocysts 109

2.11 Data analysis 109

2.11.1. General data processing, statistical analysis and molecular graphics 109

2.11.2. Densitometric quantification of immunoblotting 110

2.11.3. Image capturing and analysis 110

Chapter 3 Synthesis and Remodelling of ECM during *in vitro* decidualization of human endometrial stromal cells 116

3.1 Introduction....116

3.2 Results 118

3.2.1. Endometrial stromal cells undergo decidualization in response to cAMP after six days....118

3.2.2. Levels of ECM components collagen types I and IV, laminin, and vitronectin are not altered during *in vitro* decidualization of ESCs....120

3.2.3. Levels of TN, FN, EDIIIA+FN and EDIIIB+FN are modulated during *in vitro* decidualization of ESCs....128

3.2.4. Levels of focal adhesion proteins vinculin and paxillin appear to be reduced in response to *in vitro* decidualization of ESCs 135

3.3 Discussion....139

Chapter 4 Modulation of FN levels in endometrial stromal cells by endometrial cytokines and growth factors... 145

4.1 Introduction....145

4.2 Results 147

4.2.1. Effect of the EGF family of growth factors on FN levels....147

4.2.2. Effect of the IL-6 superfamily of cytokines on FN levels 149

4.2.3. Effect of IL-1β on FN levels....151

4.2.4. Levels of FN are decreased in response to TNFα in 0% serum....152

4.2.5. Effect of bFGF on FN levels....153

4.2.6. Effect of TGFβ on FN levels.....154

4.3 Discussion.....155

Chapter 5 The function of EDIIIA+FN in blastocyst adhesion.. 159

5.1 Introduction.....159

5.2 Results 164

5.2.1. Expression and purification of His-EDIIIA 164

5.2.2. EDIIIA had no effect on human blastocyst adhesion and trophoblast outgrowth 168

5.2.3. Integrin subunits α4 and α9 are expressed by post-implantation human blastocysts 172

5.3 Discussion.....182

Chapter 6 Structural and functional roles of EDIIIA and EDIIIB inclusion in FN..... 185

6.1 Introduction.....185

6.2 Results 187

6.2.1. Expression and purification of recombinant fibronectin fragments....187

6.2.2. EDIIIA and EDIIIB does not modulate cell adhesive activities of FIII7-12 199

6.2.3. Inclusion of EDIIIA decreases binding affinity to integrin α5β1.....204

6.2.4. Inclusion of EDIIIA and EDIIIB does not modulate FAK phosphorylation....210
6.2.5. ESCs adhered to FIII7-12A±B± display spread morphologies with formation of actin stress fibres and focal adhesions. 215
6.2.6. EDIIIA and EDIIIB does not modulate proliferative capacities of ESCs....217
6.2.7. Structural studies....220
6.3 Discussion....222

Chapter 7 General discussion and future directions.... 228

7.1 Overview of data presented in this thesis 228
7.2 Wider implications....230
7.3 Limitations....231
7.4 Future studies....233

Acknowledgements

First of all I would like to express my deep gratitude to my supervisor Professor Helen J. Mardon, her support, guidance and inspiration made this thesis possible. It has been a privilege to be part of her research group and to be able to work with all the fantastic people in the department.

I am grateful to fellow members of the Mardon research group, to Kristina Mills, Seema Grewal, Harri Altroff and Natasha Karpovich for their kind assistance and sound advice. My warmest thanks go to Janet Carver and Céline Jones, for their technical expertise and constant encouragement, helping me through the difficult times in and out of the lab and providing me with so many laughs and memories. I am extremely grateful to all the patients that donated tissue samples and embryos for research, and the clinical staff at the Women's Centre, John Radcliffe Hospital, especially Dorothea Borsi for her help in tissue collection.

I wish to thank my friends for being my surrogate family during my stay here in Oxford and for all the emotional support, entertainment, and caring they provided. In particular, Kris, Anna and Sajida for making sure I always made time for coffee, cake and the pub. Their words of encouragement especially in the last few months have helped me believe that I will get there in the end, I am extremely grateful to have found such wonderful friends. Life in Oxford would not have been the same without my housemates Petra, Pernilla and Güro, thanks for putting up with me and keeping me sane during my months of writing up.

Finally, I wish to thank my family for providing a loving environment for me, to my brother and cousins for being so supportive and such good listeners. Lastly, and most importantly, I wish to thank my parents for their endless patience, love and encouragement. To them I dedicate this thesis.

Abbreviations

Note: acronyms most commonly used in molecular biology are not listed below; the same applies for certain gene, protein and organism names.

AR	amphiregulin
bFGF	basic fibroblast growth factor
BMP-1	bone morphogenetic protein-1
BSA	bovine serum albumin
BTC	betacellulin
cAMP	cyclic adenosine monophosphate
CCBD	central cell-binding domain
CN	collagen
CSF	colony stimulating factor
CTB	cytotrophoblast
DAPI	4',6-diamidino-2-phenylindole
DD	death domain
DMEM	Dulbecco's Modified Eagle's Medium
DOC	deoxycholate
E2	estrogen, estradiol-17b
ECD	extracellular domain
ECL	enhanced chemiluminescence
ECM	extracellular matrix
EDIIIA/B	alternatively spliced domain A / B
EDTA	ethylene diamine tetracetic acid
EEC	endometrial epithelial cell
EGF	epidermal growth factor
EGFL	EGF-like repeats
ER	estrogen receptor
ErbBs	EGF receptors
ESCs	endometrial stromal cells
ESEs	exon splicing enhancers
FA	focal adhesion
FADD	fas-associated DD protein

FAK	focal adhesion kinase
FAT	FA-targeting
FCS	foetal calf serum
fFN	FN fragment
FG Globe	globular fibrinogen-homology domain
FGF	fibroblast growth factor
FI/FII/FIII	fibronectin type I / II / III
FITC	fluorescein isothiocyanate
FN	fibronectin
GAG	glycosaminoglycan
GE	glandular epithelium
GM-CSF	granulocyte/macrophage-colony stimulating factor
gp	glycoprotein
GPCR	G-protein coupled receptors
GST	glutathione-S-transferase
HAS	human serum albumin
HB-EGF	heparin binding EGF-like growth factor
hCG	human chorionic gonadotrophin
HGF/SF	hepatocyte growth factor/scatter factor
HRP	horseradish peroxidase
HS	heparan sulphate
HSPG	heparan sulphate proteoglycans
ICE	IL-1 converting enzyme, caspase-1
ICM	inner cell mass
IFN	interferon
IGF	insulin-like growth factor
IGFBP-1	insulin-like growth factor binding protein-1
IL	interleukin
IL-1R	IL-1 receptor antagonist
IL-1ra	IL-1 receptor antagonist
IGFBP-1	insulin-like growth factor binding protein-1
IL	interleukin
IL-1R	IL-1 receptor antagonist

IL-1ra	IL-1 receptor antagonist
IL-1RAcP	IL-1 receptor accessory protein
IPTG	isopropyl-b-D-thiogalactopyranoside
ISP	implantation serine proteases
JAK	janus kinase
KGF	keratinocyte growth factor
K_D	dissociation constant
LAP	latency-associated peptide
LE	luminal epithelium
LH	luteinizing hormone
LIF	leukaemia inhibitory factor
LLC	large latent complexes
LN	laminin
LNG	laminin N-terminal globular
LPS	lipopolysaccharides
LTBP	latent TGF-β binding protein
MAPK	mitogen-activated protein kinase
MIDAS	metal ion-dependent adhesion site
MIP	macrophage inflammatory protein
MLCK	myosin light chain kinase
MMPs	matrix metalloproteinases
MT-MMP	membrane-type MMP
NFκB	nuclear factor κB
NK	natural Killer
OPD	*o*-Phenylenediamine dihydrochloride
OPN	osteopontin
OSM	oncostatin-M
P_4	progesterone
PAI	Plasminogen activator inhibitor
PAs	plasminogen activators

PDGF	platelet-derived growth factor
PE	perlecan
PHSRN	Pro-His-Ser-Arg-Asn
PI3K	phosphatidylinositol 3-kinase
PKA	protein kinase A
PMSF	phenylmethylsulfonyl fluoride
PR	progesterone receptor
PRL	prolactin
RGD	Arg-Gly-Asp
SFK	src family kinase
SOCS	suppressors of cytokine signalling
SR	serine/arginine-rich
STATs	signal transducer and activator of transcription
TA	TN assembly
TE	trophectoderm
TF	transcription factors
TGF	transforming growth factor
TIMPs	tissue inhibitors of metalloproteinases
TLR	toll-like receptor
TN	tenascin
TNF	tumour necrosis factor
TNfn3	third FN type III repeat in TN
TNFR	TNF receptor
tPA	tissue-type PA
TRADD	TNFR-associated DD protein
TRAFs	TNF receptor-associated factors
TSP	thrombospondin
uPA	urokinase-type PA
VCAM	vascular cell adhesion molecule
VEGF	vascular endothelial growth factor
VN	vitronectin
VNTR	variable number tandem repeat

STRUCTURE-FUNCTION STUDIES OF FIBRONECTIN DOMAINS IN THE HUMAN ENDOMETRIUM

May G.Y. Mok
St. Catherine's College, University of Oxford
D.Phil. thesis
Hilary Term 2008

ABSTRACT

The function of the endometrium is to mediate implantation of the embryo. During the early stages of implantation, the endometrial stroma undergoes differentiation known as decidualization, a process critical for successful embryo implantation. The precise mechanisms involved are not clearly understood but extracellular matrix (ECM) remodelling is a key feature. Fibronectins (FNs) are large glycoproteins abundant in the ECM of the human endometrium. Up to twenty isoforms of FNs are generated from alternative splicing, including the EDIIIA+ and EDIIIB+ variants.

This thesis investigated changes in endometrial stromal ECM levels, in particular FN and its splice variants, during decidualization and in response to the endometrial cytokines and growth factors that drive the implantation process. Furthermore, the influence of these splice variants on the functional properties of FN was explored, including cell attachment, spreading and proliferation, integrin binding and focal adhesion kinase activation. Structural studies including crystallization trials were carried out to investigate how the insertion of EDIIIA modulates the conformation of FN and accessibility of its integrin binding sites. These combined studies allow us to test the hypothesis that the regulation of alternative splicing provides a biological mechanism for modulating function of FN in the endometrium. The main findings from this study can be summarized as follows:

- Immunocytochemistry and immunoblotting demonstrated reduced endometrial stromal levels of EDIIIA+FN, total FN and tenascin during *in vitro* decidualization.
- Substrate-associated FN production by endometrial stromal cells was reduced in response to the endometrial cytokine TNFα as detected by ELISA.
- Recombinant FIII7-12A±B± fragments were expressed, purified and mediated endometrial stromal cell adhesion.
- Inclusion of EDIIIA in the recombinant FIII7-12 fragment decreased binding affinities to integrin α5β1.

These findings suggest that production of FNs in the endometrial stroma is modified during *in vitro* decidualization and in response to endometrial TNFα. This modification in ECM composition is likely to result in modulation of cellular processes, perhaps to allow for cellular differentiation and migration that is required for invasion of the implanting embryo.

Chapter 1

Introduction

1.1 The Endometrium

The function of the uterus is to receive the embryo, support the foetus during pregnancy, and deliver the newborn at term. The uterus is a muscular organ with a triple-layered wall consisting of the perimetrium or loose surrounding tissue, the myometrium, a muscular outer layer composed mainly of smooth muscle and the endometrium, the inner lining of uterine cavity (Figure 1-1).

The endometrium consists of a single layer of surface or luminal epithelium (LE) and its basal lamina, uterine glands, and a cell-rich connective tissue, the stroma, which contains a rich supply of spiral arteries in the secretory stage at the time of implantation (Figure 1-1). The surface epithelium penetrates into the underlying stroma to form the tubular uterine glands, and therefore is the glandular epithelium (GE). Overall, there are two layers of endometrium, a functional layer adjacent to the uterine cavity which undergoes cyclic regeneration during the menstrual cycle, and the basal layer adjacent to the myometrium which is not shed during menstruation.

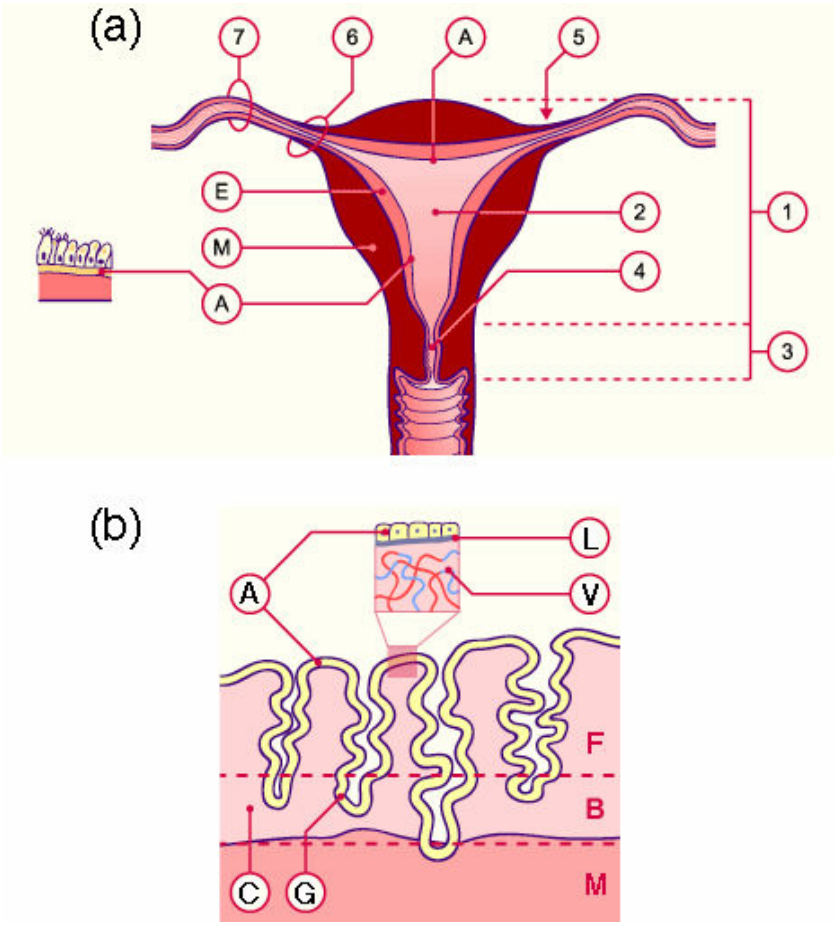

Figure 1-1 Schematic drawing of (a) the uterus and other female reproductive organs and (b) the endometrium (adapted from www.embryology.ch). 1- uterine body, 2- uterine cavity, 3- uterine cervix, 4- cervical canal, 5- isthmus of the tube, 6- interstitial segment, 7- fallopian tube, A- single-layered prismatic epithelium, B- basal layer, C- connective tissues or stroma, E- endometrium, F- superficial, functional layer, G- uterine glands, L- basal lamina, M- myometrium, V- blood vessels.

1.1.1. Menstrual cycle

The endometrium undergoes unique and extensive regulated cyclical regeneration and remodelling in preparation for implantation of the embryo in each menstrual cycle (Figure 1-2). It undergoes cycles of proliferation, differentiation and apoptosis in response to changes in expression in ovarian estradiol-17β (E_2) and progesterone (P_4) levels, which in turn are regulated by the hormones of the hypothalamic-pituitary axis.

If no implantation occurs, the outermost functional layer is shed in menstruation and remodelled in preparation for the next cycle (Wynn 1969). In the event of implantation, the endometrial lining is not shed and remains as the decidua, which becomes part of the placenta. The cyclic changes in endometrial structure are coincident with cyclic changes in the ovarian cycle that regulates ovulation.

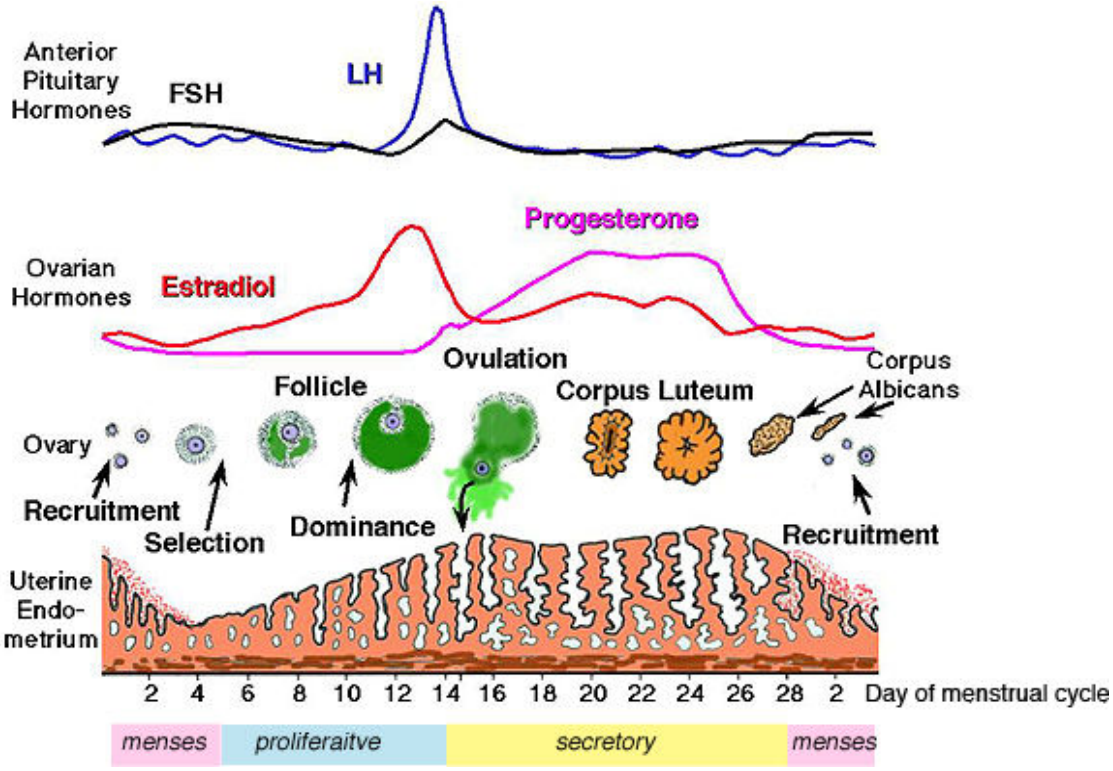

Figure 1-2 Human menstrual cycle showing the change in estradiol, progesterone, follicle-stimulating hormone (FSH) and luteinising hormone (LH) levels and how these affect the endometrium (adapted from http://www.wisc.edu).

The length of the human menstrual cycle is normally described as being twenty-eight days, but it varies from twenty-five to thirty-five days. It can be divided into three phases, the proliferative phase (days five to fourteen), the secretory phase (days fourteen to twenty-eight) and menses (days one to four) if no implantation occurs. The endometrium undergoes morphological changes during the menstrual cycle; it is

compact in the proliferative phase with elongated fibroblasts, and becomes more hydrated in the mid- and late- secretory phase.

At the end of menstruation, after the functional layer (functionalis) of the endometrium has been shed, the endometrial surface is covered by epithelial cells proliferating from basal glands. Under the influence of ovarian estrogen secreted from the growing ovarian follicle, the proliferative phase begins and intensive mitosis of epithelium and stroma occurs, to increase endometrial thickness from one to between three and four mm by the time of ovulation. Re-epithelialization, growth of stromal and glandular elements and production of the extracellular matrix (ECM) occurs and some surface epithelial cells become ciliated.

The estradiol peak at the end of the proliferative phase triggers a positive feedback mechanism at the level of the pituitary, and ovulation occurs about sixteen hours after the surge in LH. The oocyte matures within the follicle and is released from the ovary. LH stimulates remaining follicle cells to form the corpus luteum, which produces E_2 and P_4.

Under the influence of P_4 produced in the corpus luteum of the ovary, the endometrium differentiates to prepare the uterine inner lining for implantation. During this secretory phase, mitoses in epithelial cells cease, there is infiltration by lymphocytes and the glandular epithelium synthesizes and secretes glycogen into the glandular lumen. Secretory activity in epithelial cells peak at around day twenty-one. The endometrium becomes receptive to blastocyst implantation six to eight days after ovulation and remains receptive for approximately four days; this period of maximal

uterine receptivity between days twenty to twenty-four is described as the window of implantation (Psychoyos 1973; Bergh *et al.* 1992).

The uterine vessel network displays selective sensitivity to the cyclic hormonal alterations. The spiral arteries of the functional layer are hormone sensitive and constrict on progesterone withdrawal if no implantation occurs, leading to interruption of blood supply and dying out of the endometrial functional layer, resulting in menstruation. This intense vasoconstriction in the spiral arteries lasts for four to twenty-four hours before the onset of endometrial bleeding. The necrotic tissue is shed together with blood which does not coagulate due to a local fibrinolytic factor, and bleeding into the stroma is accompanied by breakdown, remodelling and repair of the functional layer (Fraser 1990).

1.1.2. Decidualization

During the late secretory phase of the menstrual cycle after ovulation, the endometrial stroma undergoes complex molecular and cellular changes in response to the postovulatory rise in progesterone, in preparation for potential embryo implantation. This differentiation process, known as decidualization, is crucial for embryo implantation, formation of the placenta and maintenance of pregnancy, though decidualization is initiated independently of conception in humans. The hormonally-induced process of decidualization is likely to be regulated by locally acting soluble and ECM-incorporated signalling molecules.

Decidualization involves remodelling of the stromal ECM, endometrial stromal cell proliferation and differentiation to a distinct morphological appearance, the elongated

fibroblast-like stromal cells become larger, rounder decidual cells (Wynn 1974; Telgmann *et al.* 1998). Decidualization is first apparent around day twenty-three of a normal menstrual cycle, in stromal cells surrounding spiral arteries of the endometrium. During pregnancy, under the continued influence of estradiol and progesterone as well as blastocyst-derived signals including human chorionic gonadotrophin (hCG), decidualization extends throughout the endometrial stroma, forming a dense cellular matrix that allows coordinated trophoblast invasion and protects the conceptus from maternal and environmental insults (Kliman 2000).

The decidualizing stromal cells have a unique biosynthetic and secretory phenotype, with coordinated expression of numerous cellular products, including ECM components, protease inhibitors, cytokines, growth factors, hormones such as prolactin (PRL) and binding proteins such as insulin-like growth factor binding protein-1 (IGFBP-1)(Telgmann *et al.* 1998). These factors critically regulate coordinated trophoblast invasion and differentiation and placenta formation. Microarray studies have shown that decidualization involves sequential reprogramming of genes within specific functional groups involved in ECM organisation, cell adhesion, cytoskeletal organisation, signal transduction, metabolism, differentiation and apoptosis (Brar *et al.* 2001; Giudice 2004).

1.1.2.1 Functions of the decidua

By forming a dense cellular matrix the decidua acts as a physical barrier to cell penetration. The decidua can regulate the coordinated trophoblast invasion and differentiation in a number of ways. During decidualization the stromal ECM undergoes remodelling, producing ECM components laminin (LN), collagen (CN) type IV, fibronectin (FN) and heparan sulphate proteoglycans (HSPG) (Aplin *et al.*

1988; Church *et al.* 1996; Salamonsen *et al.* 2002). These ECM components present in the basement membrane and decidual stroma can affect trophoblast cell adhesion, migration and differentiation, as well as their expression of matrix metalloproteinases (MMPs) and their tissue inhibitors (TIMPs), thereby regulating trophoblast invasiveness; this will be further discussed in Section 1.2.5

Trophoblast invasiveness can also be regulated by the secretion of growth factors and IGFBP-1 by the decidua. The production of transforming growth factor (TGF)-β and TIMP-1 by trophoblast and decidual cells was found to inhibit trophoblast invasiveness (Graham *et al.* 1992). TIMPs inhibit the action of MMPs, and TGF-β was found to induce TIMP-1 secretion and promote differentiation of invasive trophoblast cells into the presumably non-invasive multinucleated giant cells. Conversely, the secretory product of decidualized stromal cells IGFBP-1 increases trophoblast invasiveness by inducing the gelatinolytic activity of trophoblasts (Bischof *et al.* 1998).

The decidua also provides mechanical support of the conceptus, embryo nourishment (Finn 1971), protection of the foetal allograft from the maternal immune response (Lala *et al.* 1984), and secretion as an endocrine organ (Gibori *et al.* 1984).

A number of factors secreted by decidualizing endometrial stromal cells (ESCs) act as chemotactic stimuli to confer immunotolerance towards the invading trophoblast (Dimitriadis *et al.* 2006), including macrophage inflammatory protein (MIP)-1β, interleukin (IL)-15, and PRL. These are involved in the increase in uterine natural killer (uNK) cells in the endometrium in the secretory phase, by recruitment of

peripheral NK cells to the uterus or proliferation of existing uNK cells (Dosiou *et al.* 2005). The uNK cells provides local immunosuppression at the maternal-fetal interface, via the progesterone-regulated expression of the immunomodulatory proteins glycodelin A and galectin-1, which regulate T cell proliferation and activation (Koopman *et al.* 2003). A number of cytokines produced by uNK cells including granulocyte/macrophage-colony stimulating factor (GM-CSF), colony stimulating factor (CSF)-1, tumour necrosis factor (TNF)-α and interferon (IFN)-γ (Jokhi *et al.* 1994), influence the decidual and trophoblast microenvironment, to regulate trophoblast growth and differentiation.

1.1.2.2 Models of *in vitro* decidualization in human endometrial stromal cells

The decidualization of human ESCs can be induced *in vitro* in response to exogenous factors such as estrogen and progesterone and to analogues of cyclic adenosine monophosphate (cAMP), exhibiting similar morphological and biochemical changes to those observed *in vivo* (Daly *et al.* 1983; Huang *et al.* 1987; Tang *et al.* 1993; Mizuno *et al.* 1998).

Treatment with progesterone alone or together with estrogen induces expression of the decidual markers PRL or IGFBP-1 *in vitro*, but at low levels and can take eight or more days (Daly et al. 1983). The progesterone-dependent decidualization is suggested to be mediated by cAMP (Brar et al. 2001), elevated intracellular cAMP levels correlated with PRL secretion in the model of progesterone-dependent decidualization of human ESCs. A much more rapid response is observed for ligands that trigger an increase in intracellular cAMP levels, such as prostaglandin E_2 and

relaxin (Huang et al. 1987; Mizuno et al. 1998), inducing expression of decidual marker genes but are not maintained in long term cultures. These factors bind to G-protein coupled receptors (GPCR) on ESCs, activate adenylate cyclase, generate cAMP and finally activate the protein kinase A (PKA) pathway. The *in vitro* decidualization of ESCs can also be induced with the cAMP analogue 8-Bromo-cAMP (8-Br-cAMP) (Tang et al. 1993), a long-acting derivative of cAMP. This is an activator of the PKA pathway, but resistant to degradation by cAMP phosphodiesterase. Full decidualization and persistent expression of decidualization markers can be induced by both progesterone and elevated cAMP levels (Gellersen *et al.* 2003). This reflects *in vivo* conditions where endometrial stroma in the secretory phase is exposed to progesterone and factors that can bind to GPCRs to produce cAMP and activate the PKA signalling pathway.

1.2 Implantation

Implantation failure remains an unsolved problem in reproductive medicine and is considered to be the major cause of infertility in otherwise healthy women. Implantation rates are low despite advances in assisted reproductive technologies, the average implantation rate in IVF being approximately 25% (de los Santos *et al.* 2003). Inadequate uterine receptivity is thought to be responsible for approximately two-thirds of implantation failures, however there are no reliable diagnostic methods to predict adequate uterine receptivity (Simón *et al.* 1998; Ledee-Bataille *et al.* 2002; Achache *et al.* 2006). A better understanding of the mechanisms regulating embryo implantation may allow potential markers of receptive endometrium to be identified, which may improve treatment for infertility, prevent early pregnancy loss and allow the development of new contraceptive approaches.

Implantation involves the apposition and attachment of trophoblast cells of the blastocyst to the endometrial LE (Thie *et al.* 2002) and invasion of the blastocyst through the basement membrane and into the endometrial stromal ECM. It requires the synchronised development of the blastocyst to implantation competency and differentiation of the uterus to receptive stage, determining the window of implantation. This is achieved by coordinated effects of steroid hormones progesterone and estrogen, but also requires interaction between the blastocyst and endometrium, mediated by cytokines, growth factors and adhesion molecules.

1.2.1. Pre-implantation embryo development

Fertilization occurs on fusion of sperm with receptors on the surface of the oocyte, which then undergoes cleavage and morphogenesis as it migrates along the fallopian tube (Figure 1-3). At around day four, at the eight- to sixteen-cell stage, the cleaving conceptus undergoes compaction to produce a morula and establishes surface polarity. This polarity of cells within the embryo results in the formation of two cell lineages with subsequent cell divisions. Cells on the 'inside' of the embryo become the inner cell mass (ICM), which eventually forms the foetus, whilst those on the outside differentiate to form a polarized epithelium, the trophectoderm (TE) which gives rise to the placenta.

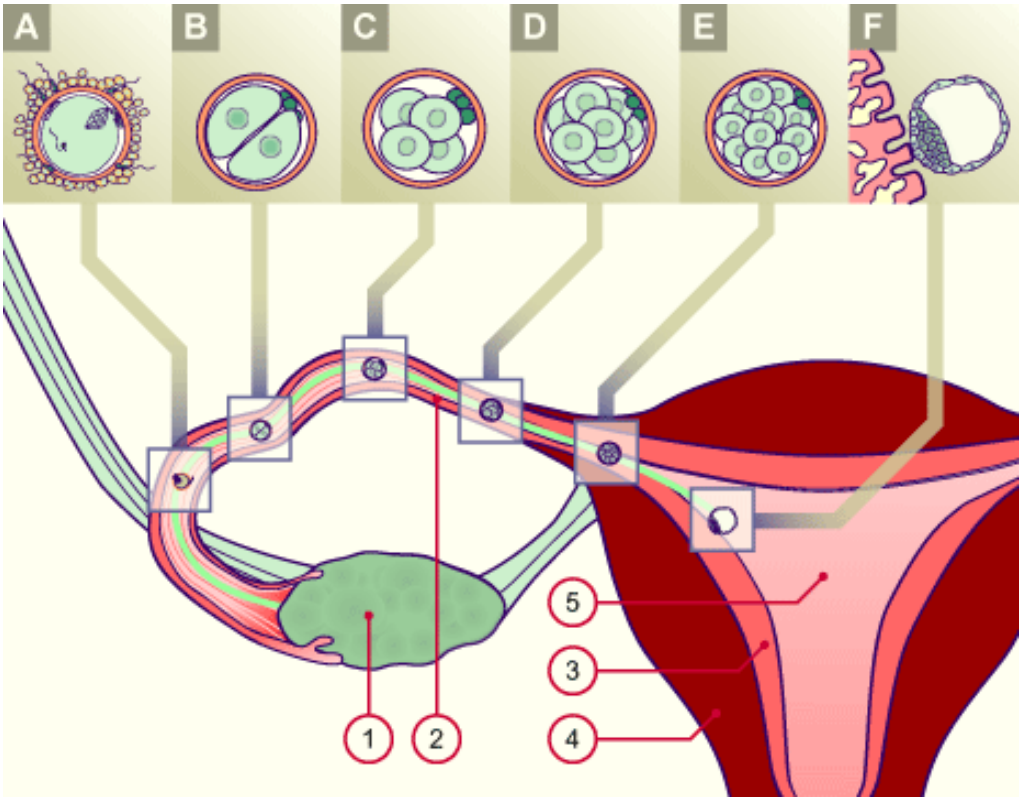

Figure 1-3 Human embryo development, migration of the embryo through the fallopian tube (from www.embryology.ch). 1- ovary, 2- fallopian tube, 3- endometrium, 4- myometrium, 5- uterine cavity, A- spermatozoon penetrates into the oocyte (conception), day 0; B- two-cell stage, day 1; C- four-cell stage, day 2; D- eight-cell stage, day 3; E- morula (16-32 cells), day 4; F- free blastocyst (following hatching), day 6.

The morula divides further to become a blastocyst and reaches the uterus around day five and implants into the uterine wall around day six. During development from fertilization to blastocyst, the conceptus is enclosed within the zona pellucida. For successful implantation of the blastocyst, the zona pellucida must be removed. The hatching process which occurs around day six, is mediated by the serine proteases ISP1 and ISP2 (implantation serine proteases), produced by the embryo and uterine glands respectively. The TE makes the initial physical and physiological connection with the uterine luminal epithelium. An intrinsic embryonic development program directs trophoblast cell differentiation to adhesion competency. Extrinsic signals, including growth factors and other soluble bioactive molecules secreted by the oviduct and uterus, can accelerate the rate of trophoblast differentiation and cause protein trafficking to the surface of trophoblast cells, allowing the embryo to acquire receptors to mediate interactions with the uterine LE (Armant 2005). This development of blastocyst adhesion competency needs to be co-ordinately regulated with endometrial differentiation to maximal receptivity by endometrial-embryonic crosstalk, as described in the following sections.

1.2.2. Uterine receptivity

The uterus differentiates into a state where it is receptive to blastocyst growth, attachment and the subsequent steps of implantation. In addition to ovarian hormones, the window of implantation is determined by a number of locally produced signalling molecules, cytokines, growth factors, homeobox transcription factors, lipid mediators and morphogens. A number of genes implicated in implantation in the mouse have been identified by knockout studies and microarray analysis (Carson *et al.* 2002; Kao *et al.* 2002; Borthwick *et al.* 2003; Riesewijk *et al.* 2003; Mirkin *et al.* 2005).

The ovarian steroid hormones P_4 and E_2 are the main effectors in directing uterine receptivity, binding to nuclear receptors estrogen receptor (ER)-α, ER-β and progesterone receptor (PR)-A and PR-B. These act as ligand-dependent transcription factors (Tsai *et al.* 1994) and their expression in the endometrium undergoes cycle-dependent changes (Mylonas *et al.* 2007). The ovarian P_4 and E_2 elicit their actions on cell proliferation and differentiation via locally produced cytokines, growth factors, adhesion molecules, transcription factors and vasoactive mediators, and their receptors as described in the following sections.

Many cytokines and their receptors are expressed in the uterus and blastocyst during the pre-implantation period suggesting potential roles in implantation (Section 1.3). However gene-targeting studies in mice demonstrated that the loss of TNFα, IL-1β, IL-1 receptor antagonist, IL-1 receptor type 1, IL-6 or GM-CSF did not result in reproductive defects (Stewart *et al.* 1997). Other cytokines are also important for fertility. Mice with null mutation of the *Lif* gene were shown to have implantation failure (Stewart *et al.* 1992). Leukaemia inhibitory factor (LIF) is a member of the IL-6 family of cytokines and was suggested to be crucial for uterine preparation for implantation. In the $Lif^{-/-}$ mice, blastocysts fail to implant and do not develop, but are viable and can implant and develop to term when transferred to wild-type pseudopregnant recipients. This suggests that maternal LIF is essential for mouse blastocyst implantation. In humans, LIF expression in the GE is upregulated at the secretory stage and its deficiency is linked with unexplained recurrent abortions and infertility in women (Hambartsoumian 1998).

Several homeobox transcription factors are also crucial for uterine receptivity and implantation in the mouse. The *Abdominal-B*-like *Hox* genes *Hoxa10* and *Hoxa11* are upregulated in the human uterus during the secretory phase and may have roles in uterine receptivity (Taylor *et al.* 1998). In mice, *Hoxa10*$^{-/-}$ females exhibit uterine factor infertility, mainly due to reduced stromal cell proliferation and failure to decidualize (Lim *et al.* 1999). The females can ovulate normally, but do not support the pre-implantation embryo or allow implantation, and mutant embryos are viable when placed in a surrogate (Satokata *et al.* 2002).

1.2.3. Apposition

During the process of apposition, the hatched blastocyst becomes closely apposed to the endometrial LE, with the ICM oriented proximally. The apical epithelial surfaces are normally non-adhesive; however during implantation changes occur in the epithelial cell organisation to allow for apical interaction between the TE and LE. These include modifications in gap junction distribution and complexity in the LE lateral membrane (Jahn *et al.* 1995), apico-lateral distribution of cell surface molecules such as integrin α6 (Albers *et al.* 1995) and adherens junctions as indicated by changes in E-cadherin expression (Fujimoto *et al.* 1996). Morphological, including both histological and ultrastructural, changes occur in the LE around the time of implantation. There is a decrease in the density of desmosomes, the intracellular junctions that confer strong cell-cell adhesion and which are important in the maintenance of tissue integrity (Sarani *et al.* 1999). Cells become flatter and microvilli are replaced with pinopodes, bleb-like protrusions found on the apical surface of the endometrial epithelium (Nikas 1999; Usadi *et al.* 2003). These may participate directly in blastocyst adhesion to the LE, as human blastocysts co-cultured

with endometrial epithelial cells attached to sites where pinopodes were present (Bentin-Ley *et al.* 1999).

1.2.4. Attachment

The attachment reaction between the trophoblast and uterine LE is mediated by the expression of complementary surface molecules, including mucins, HSPG, lectins, the trophinin-tastin-cystin complex, heparin-binding EGF-like growth factor (HB-EGF) and its receptors, and integrins (Aoki *et al.* 2000; Kimber *et al.* 2000).

The endometrial epithelium contains an apical glycocalyx which inhibits cell adhesion and provides protection from infectious agents. This natural barrier contains the cell surface mucin MUC1, which has both adhesive and anti-adhesive properties. Its large extracellular domain contains a variable number tandem repeat (VNTR) sequence that can undergo extensive glycosylation and extends outwards from the apical cell surface, perhaps masking receptors mediating cell adhesion and therefore inhibiting cell attachment by steric hindrance. The glycosylation and the negative charges associated with sialo- and sulphoglycans may have a role in the regulation of embryo attachment, possibly by interacting with lectin-like trophoblast molecules acting as recognition structures (Hey *et al.* 1994; Hey *et al.* 1995; Aplin *et al.* 1998). In an *in vitro* model of human implantation, the embryo could induce paracrine cleavage of endometrial epithelial expression MUC1 at the implantation site; its disappearance from the small area of cells surrounding the attached embryo suggests MUC1 may act as an endometrial anti-adhesive molecule and needs to be locally removed by the human blastocyst in the adhesion phase (Meseguer *et al.* 2001).

Once the embryo is tethered via carbohydrate ligands on the LE, the closer proximity allows firmer contacts to be established in preparation for penetration. Heparan sulphate proteoglycans and HB-EGF receptors expressed on the surface of blastocysts can bind to HB-EGF expressed on the LE to promote embryo attachment in mice (Raab *et al.* 1996). In humans, cells that express transmembrane HB-EGF have been shown to adhere to the HB-EGF receptor ErbB4 expressed on the surface of the trophectoderm in peri-implantation human blastocysts (Chobotova *et al.* 2002). The trophinin-tastin-cystin complex, shown to mediate cell adhesion between human trophoblast and endometrial adenocarcinoma cell lines, also potentially mediates the initial attachment of the blastocyst to the uterine epithelium (Fukuda *et al.* 1995; Suzuki *et al.* 1998).

Integrins are a family of transmembrane heterodimeric cell surface receptors that can bind to most ECM glycoproteins to mediate cell adhesion, migration, differentiation and survival (Aplin *et al.* 1998); they will be further discussed in Section 1.5. Integrins are expressed on embryonic cell surfaces continuously from fertilized egg through to peri- and post- implantation period, and on the maternal LE and GE in a temporally and spatially regulated manner throughout the menstrual cycle (Table 1-1).

The integrin αvβ3 is specifically expressed at the LE and GE during the window of implantation (Lessey 1994), and its aberrant epithelial expression is associated with infertility (Lessey *et al.* 1996), suggesting a possible role for αvβ3 in the initial embryo-endometrial interaction. This integrin can bind to a wide variety of ECM components, including FN, vitronectin (VN) and osteopontin (OPN). It recognizes the Arg-Gly-Asp (RGD) tripeptide motif which has been shown to be involved in

trophoblast adhesion and migration. The integrin αvβ3 is also present on the external surface of the expanded blastocyst (Campbell *et al.* 1995). A possible attachment mechanism involving αvβ3 integrins would require a bifunctional ligand to span between the receptors on the maternal and embryonic surfaces. One possible αvβ3 ligand for this role is OPN, which is expressed on the apical surface region of the endometrial epithelium and secreted into the lumen during the window of implantation (Brown *et al.* 1992; Coutifaris 1999; Apparao *et al.* 2001).

Integrins are expressed in the blastocyst throughout pre-implantation and in order to mediate blastocyst adhesion to the ECM they must become localized to the apical surface of trophoblast cells. Juxtacrine signalling between the trophoblast and LE cells induces trafficking of integrins including α5β1 in the blastocyst for it to gain adhesion competency, allowing it to become anchored to the endometrial basal lamina and stromal ECM (Schultz *et al.* 1997).

Following attachment of the blastocyst, luminal epithelial cells undergo apoptosis to expose the underlying basement membrane. Contact of the adhesion-competent blastocyst with the basement membrane and decidual ECM activates integrin signalling for strong trophoblast adhesion and differentiation of the blastocyst to an invasive phenotype. Newly expressed integrins such as α1, α2, α6 and α7 appear on the blastocyst surface after attachment to the uterine epithelium. These can bind to LN and CN, potentially supporting invasion of the epithelium and facilitate migration into the stroma. During differentiation to an invasive phenotype, the adhesion-competent blastocysts undergo specific cellular changes in cell polarity and

adhesiveness, resulting in trophoblast outgrowth and invasion of the decidua (Armant 2005).

1.2.5. Invasion

The process of trophoblast cell invasion involves the degradation and remodelling of the ECM, which is mainly mediated by the matrix degradation enzymes MMPs and plasminogen activators (PAs), to allow the trophoblast to penetrate into the decidua and invade the vasculature.

MMPs are a family of zinc-containing endopeptidases that collectively can cleave and degrade most ECM proteins. They are synthesized as secreted or transmembrane proenzymes which can be activated on removal of their amino-terminal propeptide. The expression of MMPs and their inhibitors, TIMPs, is regulated by cytokines and hormones in both uterine cells (Huang *et al.* 1998) and trophoblast (Meisser *et al.* 1999). On stimulation by IL-1β, ESCs showed decreased expression of TIMP-1 and TIMP-3, and increased expression of MMP-9 (Huang et al. 1998). The secretion of MMPs-1, 9 and 11 in endometrial fibroblasts is induced by a number of cytokines (Singer *et al.* 1999), including EGF, platelet-derived growth factor (PDGF)-BB, TNFα and IL-1α.

Plasminogen activators, both urokinase-type (uPA) and tissue-type (tPA) are serine proteases that cleave and activate plasminogen to the serine protease plasmin (Vassalli *et al.* 1991), which plays a role in tissue remodelling and cell migration. The proteolytic activity of the activators is controlled by specific inhibitors PAI-1 and PAI-2. Plasmin mediates tissue invasion by the degradation of ECM proteins and activation of MMPs (Murphy *et al.* 1992).

These matrix degrading enzymes digest various components of the endometrial basement membrane, causing the ECM to be more porous for the invasion of the embryo. The MMPs-2 and 9 have been shown to be important for trophoblast invasion *in vitro* (Librach *et al.* 1991); these mainly degrade a number of ECM proteins, such as CN types I, IV, V, VII, IX, and FN, LN, VN and elastin (Murphy *et al.* 1991; Woessner 1991).

The ECM components present in the basement membrane and decidual stroma can affect trophoblast expression of MMPs and TIMPs (Xu *et al.* 2001). Trophoblasts grown in the presence of VN, LN or FN secreted more MMP-9 than in the presence of CNI or CNIV, and TIMP-3 was inhibited by the presence of VN. The integrin αvβ3 binds to and activates MMPs and PAs in the ECM, acting both as a receptor for the embryo at the endometrial surface epithelium and as stimulator for trophoblast invasion (Brooks *et al.* 1996).

Cell invasion into the decidua is a complex and dynamic process involving cell adhesion to matrix proteins, degradation of ECM and cell migration. The differentiation of trophoblasts to invasive cytotrophoblast (CTB) cells is accompanied by temporally and spatially regulated switching of their integrin repertoire, upregulating expression of integrins α5β1 and α1β1 (Damsky *et al.* 1994). Interaction between CTBs and the ECM provides counterbalancing mechanisms that contribute to the regulation of trophoblast invasion; the inhibition of α1β1 interaction with LN and CNIV inhibited invasion, whilst inhibition of α5β1 interaction with FN accelerated invasion by CTB cells.

The extent and timing of trophoblast invasion must be carefully regulated. In addition to the influence of the basement membrane and stromal ECM, trophoblast invasion can be regulated by various cytokines and growth factors.

Epidermal growth factor (EGF) has been shown to be involved in implantation in several ways (Staun-Ram *et al.* 2005). It is expressed both in decidual and trophoblastic cells and induces trophoblast invasion, differentiation and proliferation (Li *et al.* 1997). EGF has also been shown to increase the activities of MMP-2 and 9, uPA and PAI-1 in trophoblastic cells, to induce cell invasion. LIF has been shown to directly block the proteolytic potential of trophoblast cells, recombinant human LIF blocks the activity of gelatinases secreted by cytotrophoblast cells *in vitro* (Bischof 1995).

The invasive and proliferative capacity of trophoblast cells can be inhibited by TGF-β, expressed by both endometrial and trophoblastic cells (Bischof *et al.* 2000), by stimulating TIMP secretion and decreasing MMP activation through downregulation of PAs (Graham *et al.* 1994; Lash *et al.* 2005). The migratory potential of first trimester invasive trophoblasts was also inhibited by TGF-β *in vitro* (Irving *et al.* 1995).

A main secretory product of the decidualized endometrium, IGFBP-1 can increase trophoblast invasiveness by inducing the gelatinolytic activity of trophoblasts (Bischof et al. 1998) and increasing cell migration (Hamilton *et al.* 1998), possibly by interaction of its RGD sequence with α5β1 integrin (Irving *et al.* 1995).

In summary, the implantation process depends on appropriate timing and expression of various factors of both maternal and embryonic origin for the synchronised development of the blastocyst to implantation competency and a receptive endometrium.

1.3 Endometrial growth factors and cytokines

Cytokines are small multifunctional glycoproteins that can exert multiple biological functions through binding to specific receptors, triggering activation of intracellular signalling cascades. These cytokine-mediated signals produce variable and sometimes opposing effects in different cell types. The binding of cytokines to receptors induces dimerization of receptors, triggering activation of intracellular signalling cascades including Janus kinase (JAK) and mitogen-activated protein kinase (MAPK) signaling pathways. Several cytokines and growth factors are known to be produced by or act on the endometrium, and these are discussed in the following sections.

1.3.1. EGF family

Members of the EGF superfamily of growth factors and their receptors (ErbBs) are expressed in the peri-implantation uterus and embryo in a spatiotemporal manner, suggesting a role as local mediators of embryo-uterine interactions during implantation (Das *et al.* 1997). This superfamily includes EGF, TGF-α, HB-EGF, amphiregulin (AR) and betacellulin (BTC), which are mitogens and stimulate cell proliferation and differentiation. Members are characterized by presence of one or

several EGF structural units defined by six conserved cysteines that can form three disulphide bonds. The EGF family polypeptides are synthesized as membrane-bound pro-peptides, with the EGF homology domain located in the membrane-proximal portion of the extracellular domain. Both the transmembrane and mature forms of the cytokines are biologically active, the soluble forms are released by tissue-specific proteolytic cleavage at the C-terminus of the EGF domain (Massague *et al.* 1993).

They exert biological effects via binding to the EGF family receptors EGFR/ErbB1, HER-2/ErbB2, HER-3/ErbB3 and HER-4/ErbB4, which are type I receptor kinases (Atalay *et al.* 2003). Ligand binding induces dimerization of receptors to form homodimers or heterodimers, the combination of dimerization partner determining the type and number of downstream effectors activated. Upon dimerization, intracellular tyrosine kinase domains are phosphorylated and provide docking sites for several adaptor proteins and signalling enzymes to activate downstream intracellular protein kinases and signalling cascades including PI3K and MAPK pathways, to regulate a wide variety of cellular processes including cell proliferation, apoptosis and angiogenesis.

EGF is immunolocalized in the human endometrium throughout the menstrual cycle (Hofmann *et al.* 1991), and is expressed in both the endometrial epithelium and stroma (Reis *et al.* 2005). It has been shown that EGF improved pre-implantation embryo development by increasing cell metabolism and proliferation (Adamson 1993).

TGF-α signals predominantly as a transmembrane ligand in the uterine luminal epithelium (Bush *et al.* 1998). This immunolocalization disappears in the early to mid-secretory phase, suggesting this period to be the most active period of membrane-bound TGF-α cleavage (Hansard *et al.* 1997). TGF-α/EGFR signalling between endometrial cells, and between the LE and pre-implantation embryo may occur, as EGFR is present in the endometrium (Troche *et al.* 1991) and in the trophectoderm of human blastocysts (Hofmann *et al.* 1992; Chia *et al.* 1995).

HB-EGF is expressed in the human endometrium throughout the menstrual cycle (Yoo *et al.* 1997; Leach *et al.* 1999), and is thought to regulate endometrial proliferation, secretion and decidualization (Simon *et al.* 2000). Expression is maximal in the receptive endometrium, with the transmembrane form of HB-EGF localized to the apical surface of the LE at the mid-secretory stage (Chobotova et al. 2002). Cells that express transmembrane HB-EGF could adhere to the HB-EGF receptor ErbB4 expressed on the surface of the trophectoderm in peri-implantation human blastocysts (Chobotova et al. 2002), suggesting that HB-EGF may be involved in the regulation of blastocyst implantation. HB-EGF has also been suggested to directly modulate blastocyst growth and function: its addition to mouse blastocysts in culture stimulated EGFR phosphorylation, increased the rate of zona hatching, blastocyst cell number and trophoblast outgrowth (Das *et al.* 1994). In humans, HB-EGF enhanced the development of *in vitro* fertilization-derived embryos to blastocysts (Martin *et al.* 1998).

1.3.2. IL-6 family

The IL-6 family of cytokines, including IL-6, LIF, IL-11, and OSM (Heinrich *et al.* 2003), can activate genes involved in differentiation, survival, apoptosis and proliferation, and are important in inflammation, immune response, embryonic development and fertility. They are pleiotropic cytokines and bind to plasma membrane receptor complexes containing the common signal transducing receptor gp (glycoprotein) 130. This shared usage of gp130 in receptor complexes explains the functional redundancy within the IL-6 family of cytokines (Taga 1996).

Signal transduction from receptors of the IL-6 family of cytokines activates the JAK-STAT and MAPK signalling cascades. The ligand-specific receptor chains and gp130 contain no intrinsic tyrosine kinase domains, but associate with and activate members of the JAK family of cytoplasmic tyrosine kinases after ligand-induced homo- or heterodimerization of gp130. This activation results in the tyrosine phosphorylation and activation of STAT3, a member of the signal transducer and activator of transcription (STAT) family and a latent cytoplasmic transcription factor. Signal transduction from cytokines acting through the JAK-STAT signalling pathway is attenuated via the suppressors of cytokine signalling (SOCS) family of cytoplasmic proteins in a negative feedback loop (Alexander 2002).

IL-11 and its receptor IL-11Rα are expressed in the human endometrium throughout the menstrual cycle (Karpovich *et al.* 2003) and the expression of IL-11 is hormonally regulated and upregulated by E_2. IL-11 expression is mainly in the GE (Rango 2004), whereas IL-11Rα expression is predominantly in stromal cells and colocalizes with

the ligand in the epithelium largely on the apical surface. The expression of gp130 is constant throughout the menstrual cycle (Dimitriadis *et al.* 2000).

Studies of the *IL-11Rα* mutant have shown IL-11 to be crucial for decidualization in mice since females with null mutation of IL-11Rα are infertile due to defective decidualization (Robb *et al.* 1998). In humans, IL-11 increased cell viability in *in vitro* cAMP-induced decidualized ESCs (Tanaka *et al.* 2001).

Another IL-6 family member, LIF has been suggested to be crucial for the preparation of the uterus for implantation in mice. As mentioned in Section 1.2.2, $Lif^{-/-}$ mice lacking a functional LIF gene are fertile but their blastocysts fail to implant; however they are viable and can implant when transferred to wild-type recipients (Stewart et al. 1992).

In humans, LIF mRNA and protein are localized in uterine GE and LE and in the stroma (Vogiagis *et al.* 1996). Their expression is menstrual cycle-dependent, being maximal in the mid-late secretory phase in the GE and also in first trimester decidual tissue. LIFR mRNA is restricted to LE and probably also GE in the mid-secretory phase (Cullinan *et al.* 1996), and is also detected in human blastocysts, which may be capable of responding to LIF, in advance of or during implantation (Charnock-Jones *et al.* 1994; Arici *et al.* 1995). In addition a number of cytokines and growth factors including IL-1, TNFα, PDGF, EGF, TGF-β could induce LIF expression by ESCs in culture and this induction is inhibited by IFN-γ (Arici et al. 1995).

1.3.3. TGF-β superfamily

The TGF-β superfamily of structurally related polypeptides regulates numerous physiological processes including embryonic development, inflammation, homeostasis and wound healing. There are nearly thirty members including activins, inhibins, bone morphogenic proteins, and the TGF-β isoforms TGF-β1, 2, and 3 (Moustakas *et al.* 2002; Shi *et al.* 2003). The three isoforms of TGF-β are homodimeric proteins that regulate numerous cellular processes including cell growth, differentiation, migration and survival. They inhibit proliferation in most cell types, induce apoptosis of epithelial cells and stimulate mesenchymal cells to proliferate and produce ECM.

TGF-βs are secreted as large latent complexes (LLCs), the latent or inactive state maintained by noncovalent association of the bioactive TGF-β peptide with its NH_2-terminal propeptide, the latency-associated peptide (LAP). The LLC also comprises the latent TGF-β-binding protein (LTBP) which is bound via a disulphide bond to the LAP, and targets the LLC to the ECM (Annes *et al.* 2003). They exert their biological effects by binding to cell surface receptors, TGF-βRI, II and III, serine-threonine kinases that signal through the Smad family of transcriptional activators, recruiting other transcription factors to activate the expression of target genes.

All three isoforms of TGF-β are expressed in the human endometrium throughout the menstrual cycle in a spatiotemporal manner, with maximal expression observed during the secretory phase (Chegini *et al.* 1994; Godkin *et al.* 1998). The three isoforms are expressed in both stromal and epithelial cells, and receptors TGF-βRI and TGF-βRII are both expressed on human endometrial epithelium (Osterlund *et al.*

2000), whereas only TGF-βRI is present in human blastocysts (Piestrzeniewicz-Ulanska *et al.* 2002).

The TGF-βs can regulate some cellular processes by stimulating the formation of ECM and its receptors, increasing synthesis of protease inhibitors and suppressing activity of ECM degrading proteases (Rizzino 1988). TGF-βs are expressed by both endometrial and trophoblastic cells (Bischof *et al.* 2000). They may play a role in human implantation via their influence on ECM production, for example via stimulation of FN expression (Feinberg *et al.* 1994), promotion of trophoblast cell adhesion to the ECM (Irving *et al.* 1995), or via influences on ECM degrading protease activity. TGF-β2 was identified to mediate the progesterone-induced, stromal-derived suppression of MMP-7 expression in the epithelium (Bruner *et al.* 1995), and inhibited MMP-9 and plasmin expression by trophoblast cells (Graham 1991, 1997). In addition, TGF-β1 has been shown to decrease MMP and uPA activity in human ESCs (Huang et al. 1998; Chung *et al.* 2001), the expression of TIMPs-1 and 3 was increased and components of the uPA system decreased on stimulation with TGF-β, which is produced by both the decidua and trophoblasts in the latent and active forms respectively (Graham *et al.* 1992).

1.3.4. IL-1 family

The pro-inflammatory cytokine IL-1β has multiple functions in a range of tissues (Bankers-Fulbright et al. 1996; Dinarello 1997). It belongs to the IL-1 family which includes ligands IL-1α and IL-1β, the receptor antagonist (IL-1ra), cell-surface receptors IL-1R1 and IL-1R2 and a non-binding receptor accessory protein (IL-1RAcP). IL-1β is synthesized as precursors which undergo proteolytic cleavage to

the biologically active form by the intracellular protease IL-1 converting enzyme (caspase-1), which removes the N-terminal portion of the precursor protein, to release the mature, latent and pro-piece forms of IL-1 from the cell. The latent form can undergo extracellular activation by enzymes including elastase, chymase, chymotrypsin and MMPs-2, 3 and 9. IL-1β signalling is mediated by binding to both IL-1R1 and IL-1RAcP, activating the MAPK and nuclear factor κB (NFκB) pathways and modulating target gene transcription (Dimitriadis *et al.* 2005).

The mRNA of IL-1β is expressed in the endometrium throughout the menstrual cycle with maximal expression during the late secretory phase, and the protein localised in endometrial stromal cells, macrophages and endothelial cells (Kauma *et al.* 1990; Sahakian *et al.* 1993; Simon *et al.* 1993). Only the IL-1R1 receptor is functionally active in the human endometrium, present predominantly in the GE throughout the menstrual cycle (Simon et al. 1993), and also in the stroma with maximal expression from the mid-late secretory phase (Bigonnesse *et al.* 2001). The receptor antagonist IL-1ra is also detected throughout the menstrual cycle (Tabibzadeh *et al.* 1992) and in decidua during early implantation (Simon *et al.* 1994).

All major components of the IL-1 system, IL-1β, IL-1ra and IL-1R1 were identified at the mRNA and protein level in single pre-implantation embryos (De los Santos *et al.* 1996; Krussel *et al.* 1998). The embryonic secretion of IL-1β was suggested to induce localised changes in the endometrium (Simon *et al.* 1997); binding of embryonic IL-1α and IL-1β to endometrial epithelial IL-1R1 upregulates endometrial epithelial integrin β3 subunit expression and facilitates adhesion of human blastocysts (Simon et al. 1997). IL-1 also stimulates production of a number of MMPs and

components of the uPA/PA-I cascade from endometrial stromal cells (Huang et al. 1998; Singer et al. 1999; Chung et al. 2001; Salamonsen *et al.* 2002), thereby influencing the ECM remodelling processes critical to implantation and decidualization. MMP-1 and 3 secretion by endometrial fibroblasts was stimulated by IL-1β (Braundmeier *et al.* 2006), which also downregulated ESC expression of TIMPs-1 and 3, and augmented collagenase expression (Huang et al. 1998).

IL-1β also induces the phosphorylation of p38 MAPK, a major signal transducer of proinflammatory stimuli, resulting in increased expression of IL-6, IL-8, MCP-1 and COX-2 in ESCs. This IL-1β-induced p38 MAPK phosphorylation response is suppressed during cAMP-induced decidualization (Yoshino *et al.* 2003). Interestingly, IL-1β and another proinflammatory cytokine TNFα inhibits *in vitro* decidualization of human ESCs, regardless of the stimulus being progesterone or cAMP (Kariya *et al.* 1991; Inoue *et al.* 1994; Frank *et al.* 1995).

1.3.5. TNFα

The proinflammatory cytokine TNFα elicits a diverse range of biological responses including apoptosis in many cell types. It is expressed as a membrane-bound precursor protein with a highly conserved presequence that anchors it to the membrane and undergoes proteolytic cleavage. The processed TNFα exists in solution as a homotrimer and exerts biological effects by binding as a trimer to three receptor molecules, resulting in the clustering of high-affinity receptors TNF-αRI and TNF-αRII present on cell membranes (Idriss *et al.* 2000). The receptors belong to the TNF receptor superfamily (TNFR), which also includes Fas, CD40, CD27 and RANK. The cytoplasmic domains of TNFRs function as docking sites for signalling

molecules, signalling occurs through two cytoplasmic adaptor proteins TRAFs (TNF receptor–associated factors) or 'death domain' (DD) molecules (Locksley et al. 2001). The TRAF family of adaptor proteins link the cell surface receptors with downstream kinase cascades, resulting in the activation of transcription factors NFκB and activator protein-1 (Inoue *et al.* 2000). TRAF-mediated signals are important in regulating cell survival, proliferation and stress responses. The association of TNFRs with DD signalling adaptors such as Fas-associated DD protein (FADD) and TNFR-associated DD protein (TRADD) causes caspase activation and cell death.

TNFα displays menstrual cycle-dependent expression in the human endometrium, which is minimal throughout the proliferative, early and mid-secretory phases, and is increased in the late secretory phase and during endometrial bleeding (Tabibzadeh *et al.* 1999). Endometrial epithelial cells (EECs) are the major source of *TNFα* mRNA and protein, and the receptors TNF-αRI and TNF-αRII have been localized to both the endometrial epithelium and stroma (Tabibzadeh *et al.* 1995), with increased expression by ESCs during decidualization (Popovici *et al.* 2000). EECs treated with TNFα undergo changes resembling those that occur during the menstrual phase, including induction of apoptosis, loss of expression of adhesion molecules, and dissociation of epithelial cells leading to glandular fragmentation and loss of filamentous actin. TNFα also stimulates the release of MMP-1 and -3 by endometrial fibroblasts (Braundmeier *et al.* 2006).

1.3.6. bFGF

The fibroblast growth factors (FGFs) are a family of mitogenic growth factors with pleiotrophic actions, having both mitogenic and angiogenic properties (Gospodarowicz *et al.* 1987). Acidic and basic FGF (aFGF and bFGF) are

intracellular peptides that lack secretory signal sequences, and their heparin-binding properties provide protection from heat, acid and protease digestion (Smith 1995). The FGF receptors, FGFR-1 and FGFR-2 have intrinsic tyrosine kinase activities (Friesel *et al.* 1989). The extracellular domain contains three immunoglobulin-like repeats, and alternative splicing in the third immunoglobulin-like domain confers specificity in binding between aFGF and bFGF.

Both bFGF and its receptor FGF-R1 are constitutively expressed in the human endometrium throughout the menstrual cycle (Sangha *et al.* 1997). The mRNA of bFGF is expressed in endometrial glandular epithelial and stromal cells and FGF-R1 is localized in endothelial cells. The ESC expression of both bFGF and FGF-R1 appears to increase in the secretory phase endometrium. As it has no secretory signal sequence, bFGF is likely to be released from cells during menstruation, and then stored by binding to heparin or HSPGs in the ECM or on the surface of epithelial cells (Ruoslahti *et al.* 1991), and released subsequently by proteases.

A number of growth factors including bFGF, EGF and vascular endothelial growth factor (VEGF) are considered to be angiogenic factors, with a role in initiating angiogenesis (Folkman *et al.* 1987). Angiogenesis is the process of neovascularization from pre-existing blood vessels. It can occur in response to angiogenic factors, which cause an increase in the permeability of blood vessels, proliferation of endothelial cells, and stimulation of proteolytic degradation of the vascular basement membrane and remodelling of the ECM, in order to allow endothelial cells to migrate and invade into the surrounding tissue (Zygmunt *et al.* 2003; Rundhaug 2005). The vascular network is required to provide nutrients and

oxygen for the implanting embryo and decidua, and angiogenesis is needed for the formation of new vasculature to support the implanting embryo. The angiogenic growth factors VEGF, bFGF and EGF are all co-expressed in the endometrium with their receptors (Moller *et al.* 2001).

It is well established that endometrial function is under control of ovarian steroids, the action of which is mediated by cytokines and growth factors. Cytokines are secreted by uterine glands, stromal fibroblasts, decidual cells and trophoblast. These can act separately or in concert on trophoblast, on endometrial epithelium, and contribute to the events of implantation in the initial blastocyst attachment to the endometrium, decidualization of the stroma and the invasion process.

Cytokines generally stimulate ECM remodelling by enhancing MMP expression; for example IL-1β and TNFα can stimulate MMP secretion whilst TGF-β provides ECM stability by inhibiting MMP expression. Both decidualization and the invasion process involve tissue remodelling of the ECM, mediated partly by the MMPs and their inhibitors, TIMPs. The ECM and its role in the endometrium will be further discussed in the following sections.

1.4 The Extracellular Matrix

The ECM is a complex network of proteins and polysaccharides secreted locally, creating a special environment in the extracellular space between cells. It provides structural support for cell adhesion, migration, and tissue organization, as well as external regulation of cellular functions. The ECM provides substrates for cell adhesion for the support and anchorage of cells, and ligands that activate intracellular signalling pathways within cells to regulate cell proliferation, survival and differentiation. It also acts as a reservoir for growth factors and cytokines by sequestering them in the ECM, and their release allows for local and rapid activation of cellular functions. The ECM also maintains space between cells to permit cell migration and controls macromolecular transport across basal lamina permeation barriers. Their interaction with the integrin family of cell surface receptors regulate cellular processes involved in tissue growth and homeostasis, and aberrant regulation of the ECM is often associated with diseases such as cancer.

The ECM constantly undergoes changes in response to a variety of cellular stimuli, ranging from dynamic homeostasis in resting-state adult organs, to tissue remodelling during development, inflammation, wound healing and cancer which involves major alterations in both ECM structure and composition. The remodelling of the ECM is an essential process for endometrial functions including decidualization, implantation and menstruation. Remodelling of the ECM needs to be tightly regulated, both in the synthesis and deposition of ECM components, its contraction and their proteolytic degradation by MMPs and PAs. The expression of several MMPs in the human endometrium is ultimately controlled by ovarian steroids and mediated by local

regulatory factors, such as cytokines and growth factors and varies throughout the menstrual cycle (Singer et al. 1999).

The major constituents of the ECM include the insoluble collagen fibre, which provides strength and structural support, hyaluronan, a large polysaccharide that forms a highly hydrated gel for resilience to compression, and two classes of soluble proteins, the proteoglycans which cushions cells, and glycoproteins such as FN which can bind to cell-surface adhesion receptors such as integrins.

Proteoglycans are a set of ubiquitous glycoproteins that are heavily glycosylated, and their functions are mediated by their protein cores and covalently attached glycosaminoglycan (GAG) side chains. These GAG chains may be chondroitin sulphate, dermatan sulphate, keratin sulphate, heparin and heparan sulphate (HS). The high content of charged polysaccharides results in the proteoglycans being highly hydrated, contributing to the volume of the ECM and permitting diffusion of small molecules between cells. The strongly polyanionic HS side chains of HSPGs contain specific binding sites for numerous growth factors, cytokines and morphogens with cationic binding domains, including FGF, HB-EGF, TGF-β, GM-CSF and PDGF, to sequester them to the ECM or cell surfaces, restricting their diffusion and range of action and modulating the cellular responses to growth factors (Kreis *et al.* 1999).

Many ECM glycoproteins are unusually large with extended conformations and can be divided into domains; these distinct structural modules such as immunoglobulin, fibronectin type III (FIII) and EGF repeats can form binding sites for cells, other ECM glycoproteins, proteoglycans, glycosaminoglycans, glycolipids, growth factors,

and proteases or protease inhibitors. For example, EGF repeats are homologous to EGF and they are found in many ECM glycoproteins and proteoglycans including LN, entactin, thrombospondin (TSP) and TN. They may mediate protein-protein interactions, or function in a similar manner to EGF by interacting with receptors to trigger intracellular signalling cascades (Swindle *et al.* 2001) and regulate cell proliferation.

1.4.1. Collagens

The CN superfamily of proteins is the major constituent of the ECM. They are the main structural proteins responsible for providing structural integrity in tissues, allowing connective tissues such as tendon, skin and bone to withstand tensile forces. To date at least twenty-seven members have been identified, displaying significant diversity in molecular and supramolecular organization, tissue distribution and function (Olsen *et al.* 1999; Canty *et al.* 2005). All CNs contain at least one triple-helical domain, formed by three polypeptide strands (α chains), each containing a $(Gly\text{-}X\text{-}Y)_n$ repetitive sequence motif, X being frequently proline and Y hydroxyproline. Each polypeptide strand is a left-handed helix, and the three α chains are twisted together into a right-handed triple helix and stabilized by numerous hydrogen bonds (Figure 1-4). To achieve this triple-helical conformation, the third amino acid in each α chain is a glycine, the only residue small enough to accommodate the close packing of every third residue along the triple-helical axis. The tropocollagen triple helices can form supramolecular aggregates such as fibrils, filaments or networks, either alone or with other ECM proteins.

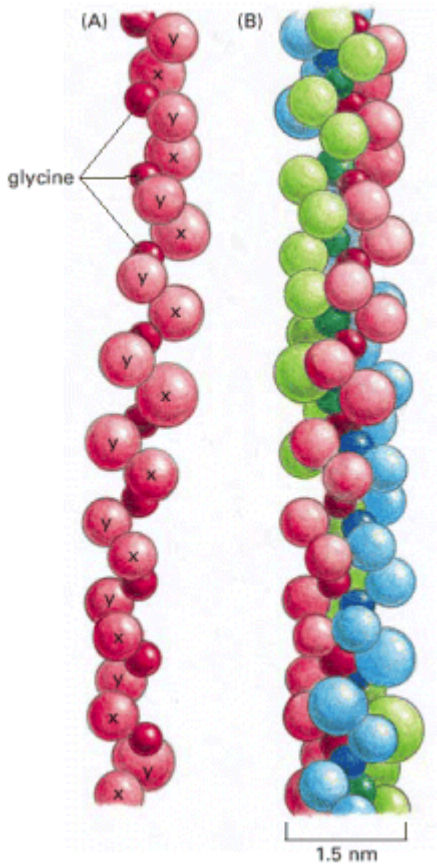

Figure 1-4 The structure of a typical CN molecule. (A) A model of part of a single collagen α chain, single amino acids are represented by a sphere. It is arranged as a left-handed helix, with three amino acids per turn and glycine every third amino acid. (B) A model of part of a collagen molecule, three α chains, each shown in a different colour are twisted around each other to form a triple helix (Alberts *et al.* 2002).

The collagens can be divided into several sub-families based on sequence homologies, similarities in structural organisation and supramolecular assembly. The fibrillar collagens comprising CN types I, II, III, V, XI form banded or cross-striated fibrils, which can further associate with the FACIT CNs including types IX, XII, XIV, XVI and XIX. The short chain CN types VIII and X are short dumb-bell shaped molecules forming part of the basement membranes for CNVIII or hypertrophic cartilage for CNX. The basement membrane CNs consists of different molecules collectively known as CN type IV (CNIV), and is the major collagenous component in basement

membranes. Also found in the basement membrane regions are the multiplexins CNV and CNXVIII, these are molecules with multiple short triple-helical domains. The MACITs, or CNs with transmembrane domains, include CN types XIII and XVII, which are cell surface molecules with multiple extracellular triple-helical domains connected to the cytoplasmic region by a transmembrane segment. In addition other CN molecules can form specialized structures, for example CNVI forms microfibrils and CNVII forms anchoring fibrils. This thesis will focus on CNI and CNIV as their expression in the endometrium has been suggested to be modulated during decidualization.

1.4.1.1 Collagen type I

The fibrillar CN type I can form fibrils with molecules packed in quarter-staggered arrays, providing supramolecular scaffolds for mechanical support and an environment for cellular migration, attachment and differentiation (Hulmes 2002; Ricard-Blum *et al.* 2005). They are heterotrimers with two or three different α chains. Each fibrillar α chain contains over three hundred repeats of the Gly-X-Y triplet sequence, flanked by short non-triplet sequences, the telopeptides. The fibrillar α chains are synthesised as precursors, pro-α chains which contains the central $(Gly\text{-}X\text{-}Y)_n$ -containing domain flanked by amino (N) and carboxyl (C) propeptides. During intracellular assembly of the trimeric procollagen molecules within the rough endoplasmic reticulum, the trimeric C-propeptide domain directs chain association. The C-propeptide domain itself folds first, followed by folding of the triple-helical domain from the C- to N-terminus of the trimeric molecule in a zipper-like manner, the rate being limited by *cis-trans* isomerization of peptidyl prolyl bonds.

Following or during secretion of procollagens into the ECM, propeptides undergo proteolytic cleavage by specific procollagen N- and C-proteinases. The C-propeptide prevents fibril formation by maintaining high solubility of the procollagen molecule, whereas the N-propeptide does not prevent fibril formation, but can influence fibril shape and diameter. After procollagen processing to remove the propeptides, the fibrillar collagens can undergo spontaneous self-assembly and aggregate into highly ordered collagen fibrils in the extracellular space. Within the fibrils, collagen molecules are arranged in quarter-staggered arrays, the long rod-like molecules overlap with their ends to produce a periodic structure with areas of loosely and densely packed molecules, producing a cross-striated pattern when the fibrils are positively stained.

Collagen fibrils are usually heterotypic in that they can contain more than one type of fibrillar collagen. For example, CN types I, III and V are found in most connective tissues and CN types II and XI in cartilage. The presence of small amounts of CN types V and XI within fibrils provides a mechanism for diameter control of heterotypic collagen fibrils. The steric hindrance caused by the incomplete removal of their N-propeptides during procollagen processing limits fibril diameters. Therefore, a greater ratio between CN types V and I, or XI and II will produce thinner fibrils. The relative composition and amounts of different collagen types co-assembled into heterotypic fibrils determines the structure and organization of the matrix network, to determine biomechanical properties of tissues. In addition to acting as stabilizing scaffolds in the ECM, fibrillar collagens can influence cell differentiation and migration during development, and interact with cells through the integrins.

1.4.1.2 Collagen type IV

The main collagenous component of basement membranes, CNIV, forms a network structure with other basement membrane components such as LN, HSPG and nidogen (Timpl 1996). The CNIV molecules are composed of three α chains, and have six distinct forms (α1-α6). Molecules composed of α1(IV) and α2(IV) chains are broadly expressed in basement membranes, while those containing combinations of α3(IV)-α6(IV) are components of specialized basement membranes. Each α chain contains at least three distinct domains, an N-terminal cysteine-rich (7S) domain, a central triple-helical domain and a C-terminal non-triple-helical domain (NC1). Unlike the fibrillar collagens, they are not cleaved after secretion, but interact via the uncleaved terminal domains to assemble into a flexible multilayered network.

Three α chains form the triple-helical monomer, the triple helix is interrupted by several non-helical segments that insert flexible kinks in the molecule. The CNIV monomer can associate into dimers between NC1 domains, or into tetramers between the N-termini 7S domain, both types of interactions are stabilized by disulphide bonds. The assembly of these dimers and tetramers, together with lateral associations between α-chains, forms the supramolecular network CNIV molecules (Figure 1-5).

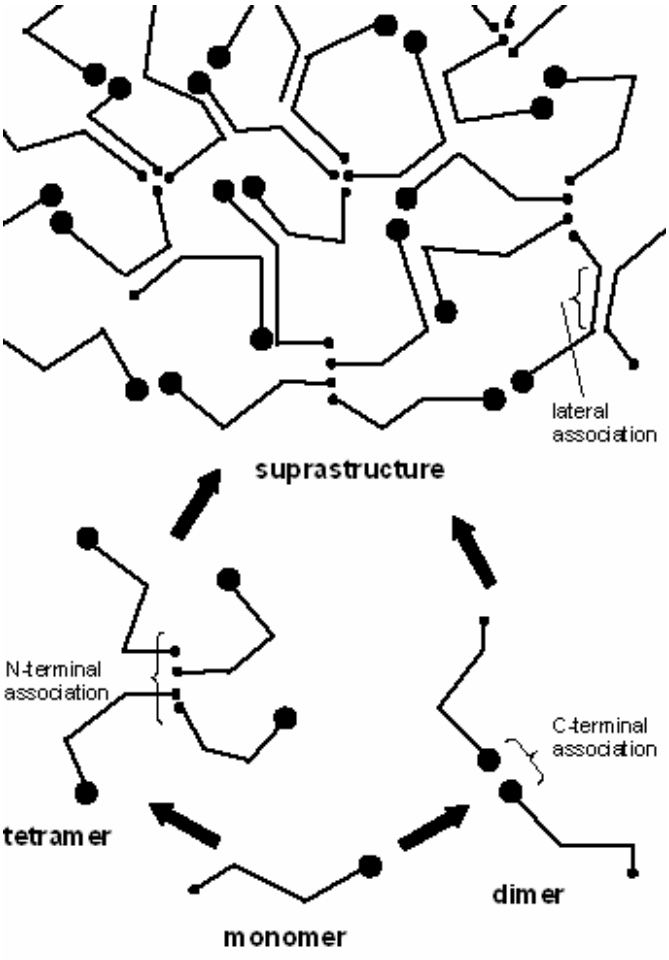

Figure 1-5 Schematic diagram of the supramolecular assembly of CNIV adapted from (Lodish *et al.* 2000).

Other basement membrane components such as laminin, nidogen and the HSPG perlecan are incorporated into the CNIV network. The CNIV network is highly cross-linked and thought to provide mechanical stability, while the LN networks are mainly non-covalent and may be more dynamic than the CNIV network. The two networks are thought to be bridged by the perlecan and nidogen, which can bind to both networks. The CNIV can also interact with cells via a major cell binding site localized about 100 nm from the N-terminus of α1(IV)/α2(IV) heterotrimers, which interacts with integrins α1β1 and α1β2.

1.4.2. Laminins

Laminins (LN) are a family of large, flexible heterotrimeric proteins, composed of three polypeptide chains (α, β, and γ) arranged in the shape of an asymmetric cross (Figure 1-6). At least fifteen laminin heterotrimers have been identified in mammals, formed from different combinations of several isoforms of each type of chain: five types of α chains, four types of β chains, and three types of γ chains are known to exist. All the chains have a globular, a rod-like and a coiled-coil domain of about eighty heptad sequence repeats close to the C-terminal end that is crucial for heterotrimer assembly. The assembly of the coiled-coil domain is determined by heptad motif interactions such that there is only one α, one β and one γ chain in each laminin, forming a three-stranded super α helix held by hydrophobic and polar interactions between the three chains. This assembly process occurs intracellularly and is required for secretion.

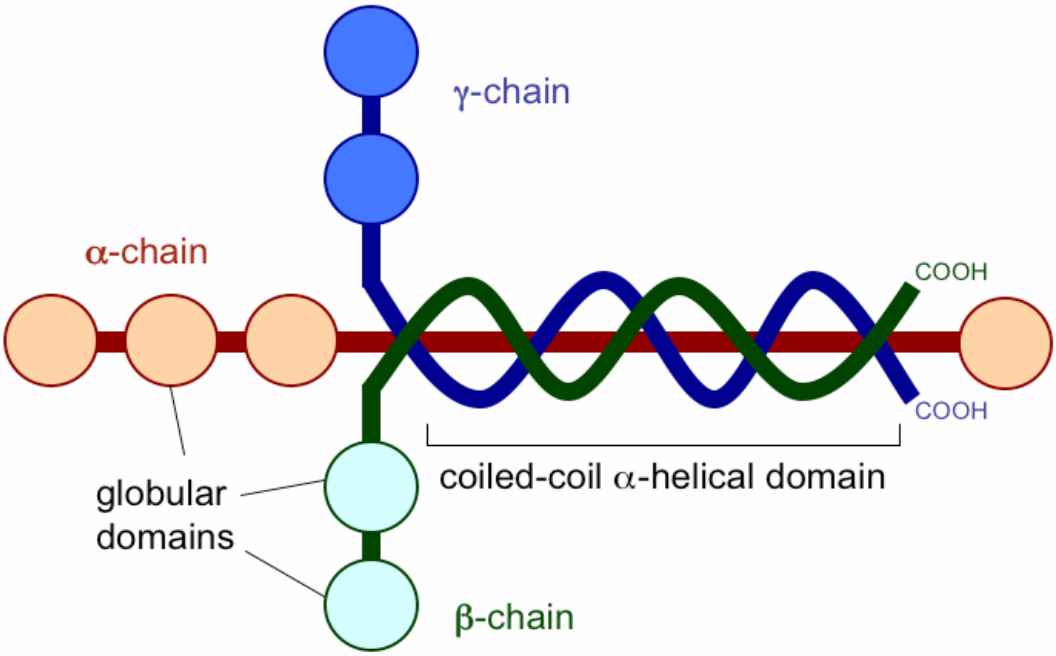

Figure 1-6 Structure of laminin; this multidomain glycoprotein contains globular domains and a coiled-coil region, where the three polypeptides (α, β, and γ) are covalently linked by disulphide bonds into an asymmetric cross-shaped structure (Alberts *et al.* 2002).

The various LN isoforms have a large variety of functional and biological activities, due to the different combinations of α, β and γ chains and the activities associated with the functional domains located on them. As a generalization, most noncellular ECM binding is confined to the short arms of all three subunits, whereas most receptor-mediated interactions to integrins or α-dystroglycan are mapped to the N- and C-terminal domains of the α subunit. The domain locations of activities for LNs-1 to 5 are shown in Figure 1-7.

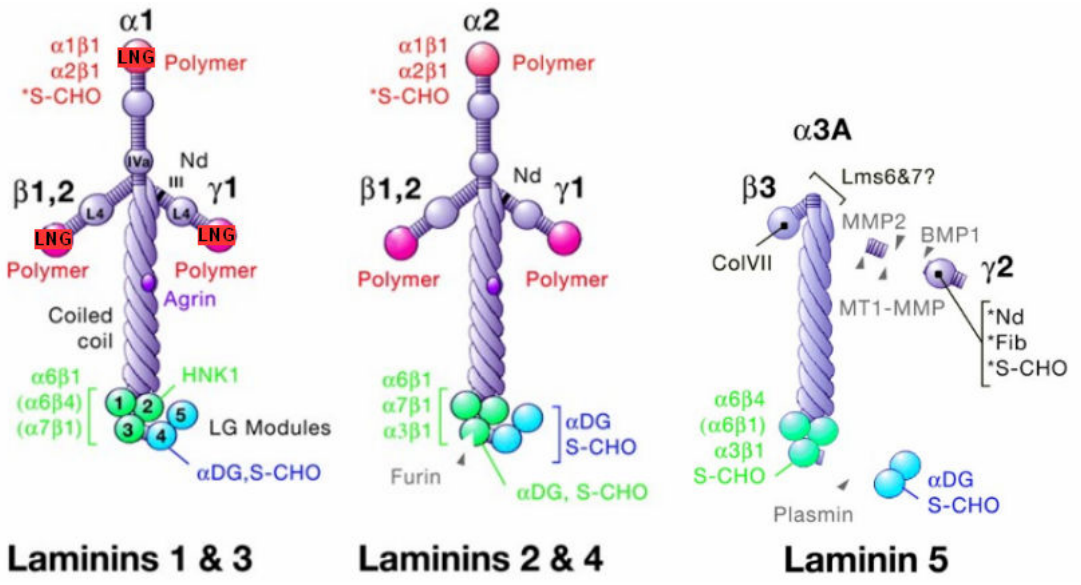

Figure 1-7 Domain locations of activities for LNs-1 to 5, from (Miner *et al.* 2004).

The isoforms LN-1 through 4 each possess three short arms with LN N-terminal globular (LNG) domains, rod-like domains consisting of laminin-type EGF-like repeats, and internal globular (L4, IV) domains, and a coiled-coil long arm terminating in the G-domain (Figure 1-7). The α2-LNs (LN-2 and 4) are cleaved by the protease furin in LG-3. LN-5 is the only known γ2 and β3 chain-containing laminin, it is a rod-like laminin with major truncations in the short arms. Several proteases, bone morphogenetic protein-1 (BMP1), MMP-2, membrane type (MT)1-MMP, and plasmin can cleave and release the N-terminal moiety of the γ2 short arm and the terminal two LG modules, to remove nidogen-, fibulin-, and heparin-binding sites, affecting LN incorporation into the ECM (Miner *et al.* 2004). Polymerization is thought to be mediated by the calcium-dependent bonding of three LNG domains of LNs 1 through 4, 10 and 11 to form layered sheets, which contributes to basement membrane assembly. The polymerization of LN has been suggested to be cooperative with LN-receptor interactions. Attachment to cell surfaces occurs via integrins, dystroglycan and other receptors for the LN long arm, and the increase in

concentration of receptor-engaged LN then drives LN self-assembly and polymerization through short arm interactions. The combination of polymerization-driven reorganization of receptors and receptor ligation drives the rearrangement and remodelling of actin filaments, to form laminin-cortical networks and assembly of basement membranes (Colognato *et al.* 2000).

1.4.3. Tenascins

The Tenascin (TN) family of large multimeric ECM proteins includes five members, TN-C, TN-R, TN-X, TN-Y and TN-W. Expression is often transient and restricted to embryonic development. TN expression is less abundant in adult tissues but re-occurs during tissue remodelling, wound healing, inflammation and tumourigenesis, and can be induced by mechanical stress (Jones *et al.* 2000). The best characterized member of the TN family, TN-C is a hexameric ECM protein with different subunit variants generated from alternative splicing of the primary transcript. Each subunit has a modular composition (Figure 1-8) that includes the heptad repeats in the TN assembly (TA) domain that enables subunits to trimerize through formation of triple coiled-coil α helices, EGF-like repeats (EGFL), FN type III domains some of which can be alternatively spliced, and a C-terminal globular fibrinogen-homology domain (FG globe). Other TNs contain the same types of domains arranged in similar order with varying numbers of domains.

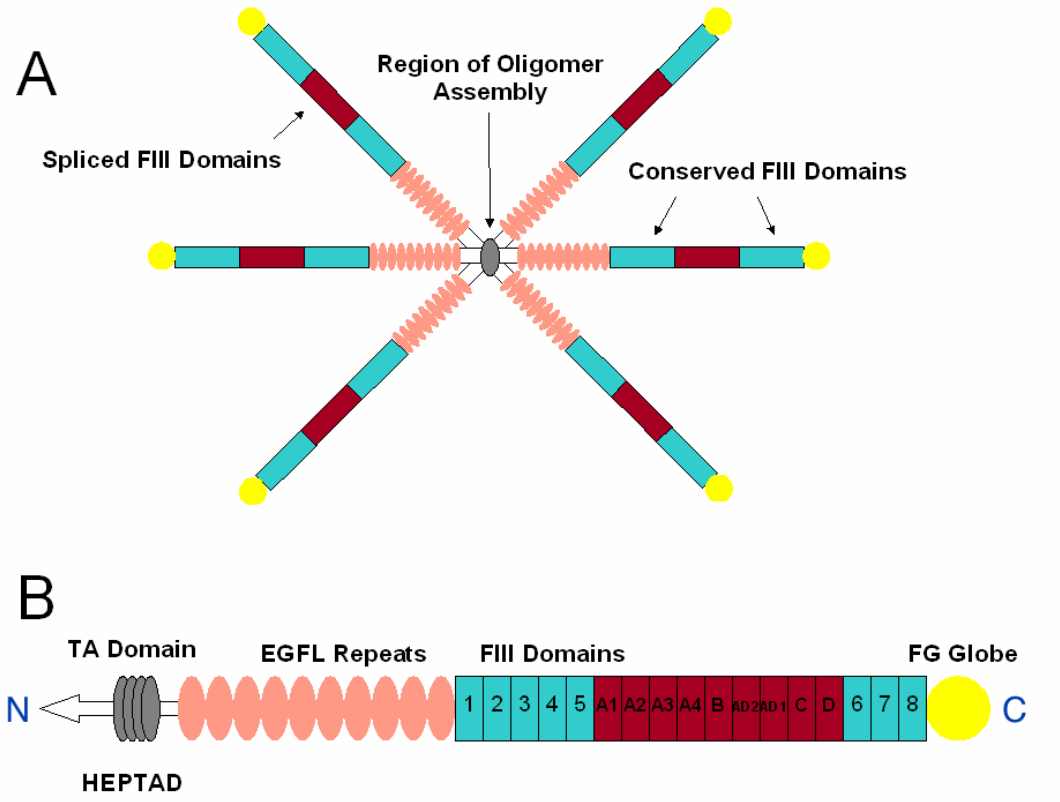

Figure 1-8 Structure of TN-C: (A) model of a TN-C hexamer; and (B) schematic representation of an individual TN-C polypeptide, N and C denotes the N- and C-terminal. The TA domain allows six polypeptides to associate via coiled-coil interactions that occur at the heptad repeat (Jones *et al.* 2000).

Three TN-C polypeptides associate in a triple-stranded coiled-coil by the α-helical heptad repeats, to form trimers that are stabilized through interchain disulfide bonds. Interaction of two trimers leads to the formation of hexamers, which is further stabilized by interchain disulphide linkages. The incorporation of TN-C into the ECM is thought to be mediated by its interactions with FN, integrins α5, αv and β1 and the HSPG perlecan. It can interact with cellular receptors including integrins α2β1, αvβ3, α8β1 and α9β1, and syndecan to regulate numerous cellular processes such as cell adhesion, proliferation and migration. Contrary to many ECM proteins, TN-C promotes only weak cell attachment and cell spreading is limited, and has been

suggested to be an adhesion-modulating or anti-adhesive protein as it inhibited cell adhesion to FN (Orend *et al.* 2000). A possible mechanism for the inhibition of cell spreading could be through the binding of TN-C to FIII-13 repeat of FN, which is required for interaction of FN with syndecan-4 to promote full cell spreading. This inhibition of syndecan-4 binding to FN also suppressed the proliferation of normal cells (Chiquet-Ehrismann 2004). In addition, TN-C has been shown to suppress focal adhesion kinase and RhoA activity (Midwood *et al.* 2002). These are key molecules in the regulation of cell shape via their influence on the actin cytoskeleton, and may result in the TN-C-mediated stimulation of cell migration as observed previously (Chung *et al.* 1996). The effect of TN-C on proliferation could be mediated by the direct binding and activation to the EGF-receptor by its EGF-repeats (Swindle *et al.* 2001).

1.4.4. Vitronectin

VN is a multifunctional glycoprotein found abundantly in the blood plasma where it regulates the complement, fibrinolytic and coagulation systems. It is also found in the ECM of many tissues, where it binds collagens and heparin-like GAGs, and to cell surface receptors including integrins such as αvβ3 and αIIbβ3, the urokinase receptor and proteoglycans to mediate cell adhesion, migration and invasion (Preissner *et al.* 1998; Schvartz *et al.* 1999).

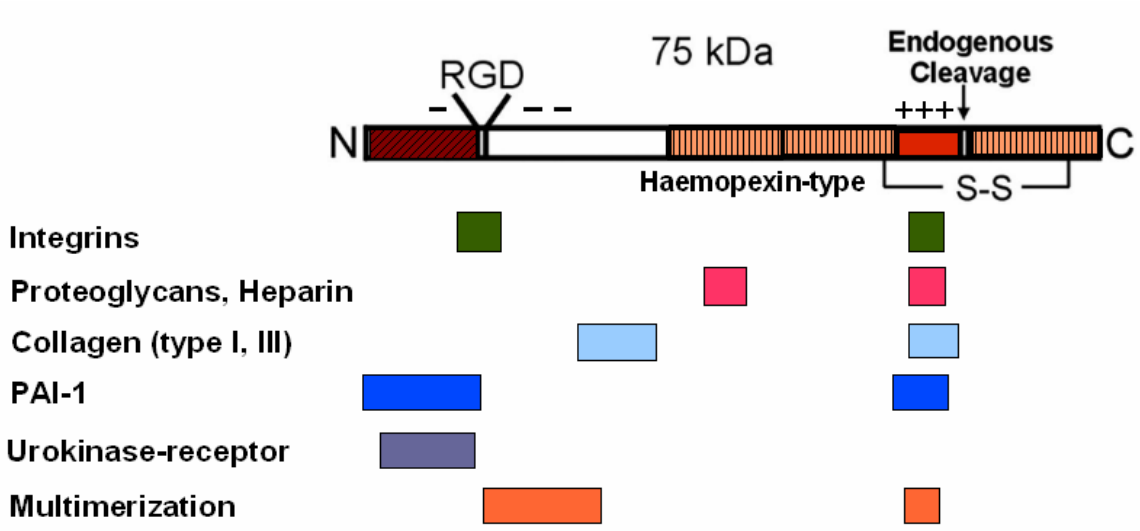

Figure 1-9 A schematic representation of the domain organization of human VN, indicating the somatomedin-B region at the N-terminus (dark brown diagonally-shaded box), the major RGD cell attachment site, haemopexin-type repeats (light brown vertically-striped boxes), the glycosaminoglycan-binding site (+++), the endogenous protease cleavage site. Binding sites for macromolecular ligands are listed at the left margin and highlighted by coloured bars according to their position along the primary structure. Many binding domains are concentrated around the acidic (--) N-terminus and the basic (+++) C-terminus, believed to be partially cryptic in the circulating plasma protein and exposed upon conformational activation. Adapted from (Preissner *et al.* 1998)

VN is synthesised as a single chain that is cleaved by signal peptidase, *N*-glycosylated, phosphorylated and sulphated prior to secretion. The somatomedin B domain at the N-terminus contains a binding site for PAI-1, following this domain is the RGD sequence that mediates cell attachment and spreading. Adjacent to the RGD sequence is a segment of amino acids including two sulphated tyrosine residues involved in binding of the thrombin–antithrombin III complex, and in neutralizing at least part of the polycationic domain present at the C-terminal end. The ionic interaction between these acidic and basic stretches is probably involved in stabilizing the three-

dimensional structure of VN, and in the formation of its multimers. Collagen binding is mediated by functional groups from two regions; one adjacent to the RGD sequence and another adjacent to the heparin binding domain. In the middle of the VN molecule is a region containing six haemopexin repeats, which anchor a disulphide bridge linking the endogenously cleaved ten kDa fragment to the rest of the molecule. In the C-terminal of VN is a cluster of basic amino acids containing two consensus heparin binding sequences, another PAI-1 binding site and GAG-binding sites (Figure 1-9).

There are two molecular forms of VN, a seventy-five kDa single chain and two chains of sixty-five and ten kDa held together by a disulphide bond. It is found in blood plasma as a folded monomer stabilised by ionic interactions between its polyanionic and polycationic segment. The conformation of VN is labile, and changes in ligand and cell binding properties are linked to conformational changes in the C-terminal heparin-binding domain and N-terminal acidic portion. The ligand-binding sites in these regions are cryptic in native plasma and are exposed upon denaturation or multimerization of VN. In the ECM, VN is present in the disulphide-linked multimeric form, exhibiting differential ligand properties to the monomeric form (Schvartz *et al.* 1999).

1.4.5. Fibronectins

FNs are a group of multifunctional adhesive ECM glycoproteins found abundantly in the plasma and ECM of most tissues including the endometrium. Integrin-mediated cell adhesion to FN regulates numerous cellular processes such as cell proliferation, migration, differentiation and apoptosis, and is therefore implicated in processes associated with endometrial regeneration and embryo implantation.

1.4.5.1 Structural organisation

FN is a large glycoprotein composed of two nearly identical subunits of approximately two hundred and fifty kDa linked by a pair of disulphide bonds near the COOH-terminus (Ruoslahti 1988). The complete amino acid sequence of the FN polypeptide determined from cloned cDNA (Kornblihtt *et al.* 1985) revealed it to be a modular protein composed of three types of homologous domains termed fibronectin types I, II and III (FI, FII and FIII, Figure 1-11). These independently folded modules are arranged as 'beads on a string' along the extended FN polypeptide. The FN gene transcript can undergo alternative splicing, resulting in the inclusion or exclusion of the domains EDIIIA, EDIIIB and IIICS in the FN molecule. These are found in cellular FN but not in the plasma form of FN. The biological significance of alternative splicing is not known, but it may affect the functions of FN. A schematic diagram of the structural organisation of FN is given in Figure 1-10.

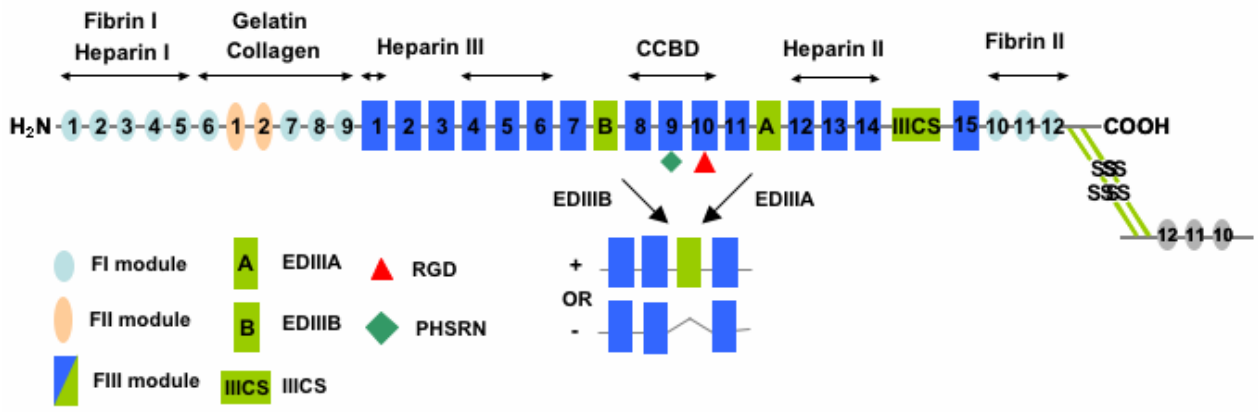

Figure 1-10 Structural organisation of FN showing three types of repeating homologous modules: FI, FII, FIII; alternatively spliced domains EDIIIA, EDIIIB, IIICS; cell binding motifs RGD in FIII10 and synergy site PHSRN in FIII9, the central cell-binding domain (CCBD) and binding sites for other ECM components are indicated above the diagram.

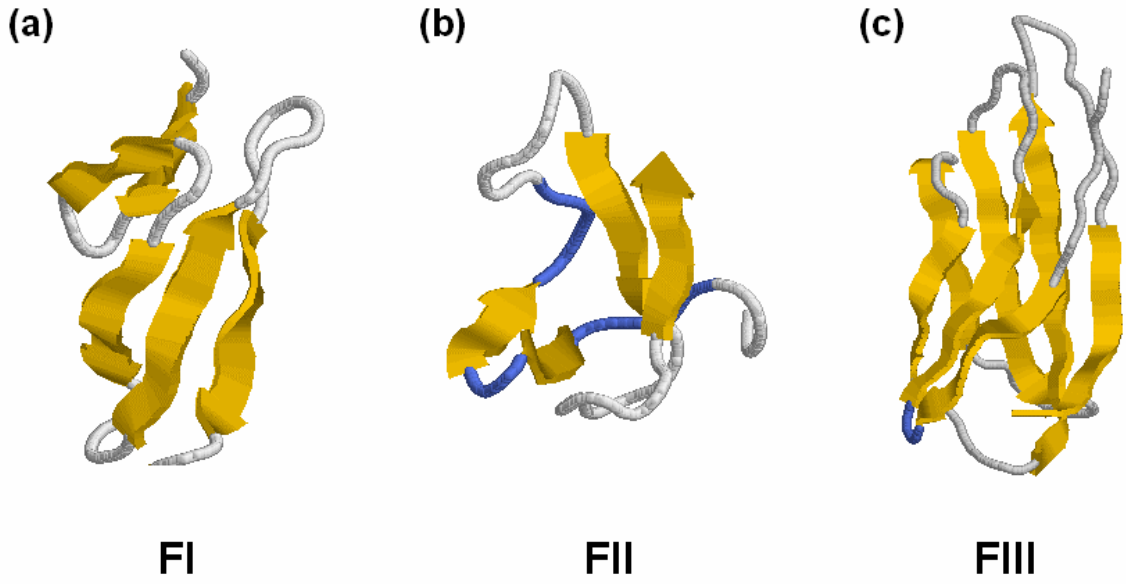

Figure 1-11 Diagrams of the (a) FI, (b) FII and (c) FIII domains, structures are of the FI4 (Williams *et al.* 1994), FII2 (Sticht *et al.* 1998) and FIII10 (Main *et al.* 1992). β-strands are coloured yellow and turns are coloured blue. The figure was made with the program RASMOL (Sayle *et al.* 1995).

In the middle of the FN polypeptide is a contiguous array of between fifteen to seventeen FIII repeats, depending on variations in RNA splicing. The FIII modules are the most common and largest of the FN sub-domains, and unlike the FI and FII repeats they do not contain disulphide bonds. They are composed of around ninety amino acids arranged in a conserved β sandwich fold, seven β-strands form two anti-parallel β-sheets of three and four strands packed against each other (Figure 1-11(c)). The sheets enclose a hydrophobic core, from which protrude more flexible loops joining the strands. Interactions with other proteins are mediated largely by the diverse surface loops, and the right spatial separation and position of FIII modules are important in determining specific binding properties and functional activity of FN (Main *et al.* 1992; Potts *et al.* 1994).

FN has a wide range of activities besides binding to cell surfaces through integrins. It can bind to a number of ECM molecules including collagens, heparin, and fibrin, and these interactions are mediated by a number of structural and functional domains in the FN polypeptide (Figure 1-10)(Ruoslahti 1988). The five major domains identified by controlled proteolysis include a NH_2-terminal domain, isolated as a twenty-nine kDa fragment this domain contains a fibrin-binding site (Fibrin I), a heparin-binding site (Heparin I), and one of the sites for transglutaminase-activated crosslinking and participates in FN matrix assembly. A CN-binding domain is mapped to the two FII repeats, binding far more effectively to gelatin which is primarily denatured CNI than to native CN. Next to the CN-binding domain towards the COOH-terminus is the DNA-binding domain. In addition, the principal heparin-binding domain is located in three FIII domains near the COOH-terminal (HepII/IIICS region), which also mediates cell binding and cell migration (Clark *et al.* 2003). Recently, the IIICS

region has been identified as a novel zinc-binding module, a FN fragment of FIII12-15 and IIICS can bind the divalent cations Ni^{2+}, Cu^{2+} and Zn^{2+}. Zinc coordination may be required for intra-molecular structural interactions and inter-molecular stability, and mediates interactions with other zinc-binding ECM molecules (Askari *et al.* 2007).

The major cell-adhesive domain, the central cell binding domain (CCBD) is located in the central portion of FN and promotes cell attachment. It contains the RGD sequence in FIII10 (Ruoslahti 1988) which provides a recognition site for at least eleven members of integrins. Recognition of the RGD sequence depends on flanking residues, its three-dimensional presentation and individual features of the integrin-binding pockets. The synergistic motif Pro-His-Ser-Arg-Asn (PHSRN) located on FIII9, enhances binding to and signalling through several RGD-dependent integrins including α5β1 and αIIbβ3; αvβ3 is believed to not require this synergistic effect (Bowditch *et al.* 1994; Akiyama *et al.* 1995). Synthetic peptides containing the sequence Arg-Gly-Asp-Ser (RGDS) can block attachment of cells to FN (Pierschbacher *et al.* 1984), and the deletion of RGD and PHSRN reduces cell attachment to FN (Obara *et al.* 1988).

From the 2.0 Å crystal structure of FIII7-10 (Figure 1-12), the FN fragment was shown to be an extended rod-like molecule, with a long axis of approximately 140 Å and highly variable tilt and rotation angles between adjacent FIII domains (Leahy et al. 1996). The interdomain surface between FIII9 and FIII10 is smaller than that between the other domains, with the RGD sequence located on a flexible loop of FII10, extending approximately 10 Å away from the FIII7-10 core. The unusually

small rotation between FIII9 and FIII10 results in the exposure of the RGD loop on FIII10 and the synergy site in FIII9 on the same side of the molecule, creating a binding site for integrins (Leahy et al. 1996). The FIII9-10 domain pair may represent a flexible hinge region; there is unusually high interdomain flexibility as shown by NMR (Altroff *et al.* 2004). The flexibility of the FIII9-10 pair may thus allow for conformational changes required to accommodate binding to integrin headpiece.

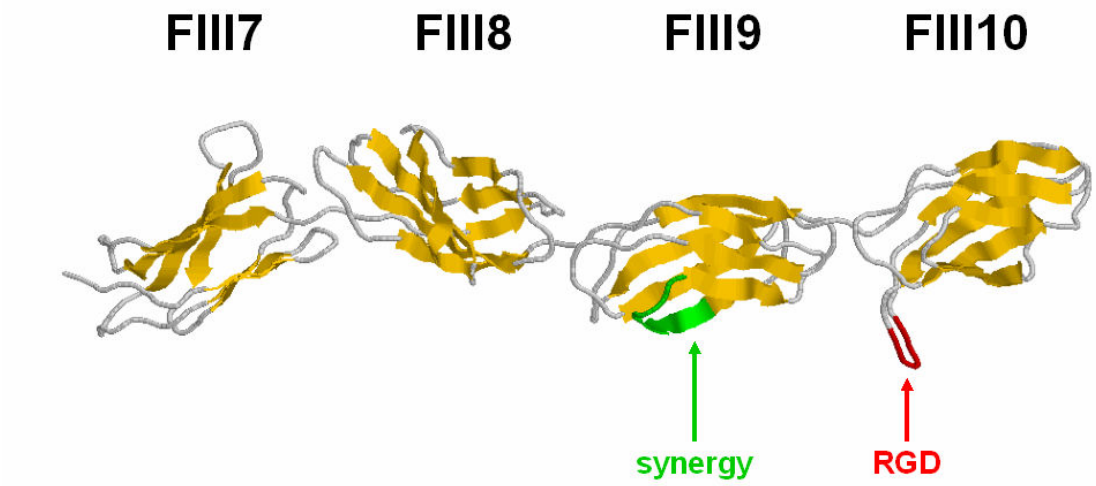

Figure 1-12 A ribbon diagram of the FIII7-10 structure (Leahy et al. 1996); β-strands are coloured yellow, the RGD loop is red and the synergy region is green. The figure was made with the program RASMOL (Sayle *et al.* 1995).

Integrin binding and specificity of the FIII9-10 pair is determined by the interdomain tilt between the two modules (Altroff *et al.* 2004). The introduction of a disulphide bond across the interdomain interface between the domains FIII9 and FIII10 increases

the stability of the FIII9-10 pair and attenuates the synergistic effect of FIII9 on α5β1 binding and recognition of αvβ3 by the FIII9-10 pair. Integrin binding activity was regained on reduction of the disulphide bond. The introduction of the interdomain disulphide bridge reduces the average interdomain tilt from approximately twenty eight to five degrees, to straighten the protein structure, which correlated with a reduction in biological activity and binding with α5β1 and αvβ3.

Transmission electron microscopy and single particle image analysis of a recent stable, soluble complex of FIII7-10B+ with the αvβ3 ectodomain (Adair *et al.* 2005) did not display the rod-like extensions seen in the crystal structure of FIII7-10 (Leahy et al. 1996), suggestive of bending between FIII domains as seen in electron micrographs of full-length FN (Erickson *et al.* 1983).

1.4.5.2 Posttranslational modifications

There are several FN types differing in both their primary structure and post-translational modifications. The FNs are glycoproteins that contain four to eight percent of carbohydrate depending on the source of protein. There is a low carbohydrate content in FN from adult plasma and normal adult skin fibroblasts, and more sugars in FNs from embryonic sources or tumour cells. There are at least six sites for both N- and O-linked glycosylations, with additional sites found for the IIICS and EDIIIB domains. The carbohydrates are thought to protect FN from proteolysis, and do not seem to have functional consequences on biological activities of FN (Olden *et al.* 1979; Ruoslahti 1988). Other posttranslational modifications include serine phosphorylations (Ali *et al.* 1981), sulphation of tyrosines (Paul *et al.* 1984)

and acylations (Lange-Mutschler 1986), however the significance of these modifications are unknown.

1.4.5.3 Structure and Function of EDIIIA and EDIIIB variants

The single FN primary transcript can undergo alternative splicing resulting in at least twenty different variants of FN (Borsi *et al.* 1987; Zardi *et al.* 1987). The alternatively spliced domains EDIIIA and EDIIIB are FIII repeats and encoded by a single exon each and can be spliced out completely by exon skipping (Figure 1-10) (Schwarzbauer *et al.* 1983; Fattorusso *et al.* 1999; Niimi *et al.* 2001).

Only insoluble cellular FN secreted by cells and organized into cellular matrices contain alternatively spliced sequences, plasma FN does not. Evidence suggests that alternative splicing of the FN transcript is regulated in a tissue-specific and developmental manner. Expression of the alternative splice variants EDIIIA and EDIIIB are minimal in normal adult tissues, but are expressed during embryonic development, wound healing and tumour progression (Ffrench-Constant *et al.* 1989; Hynes 1990; Jarnagin *et al.* 1994; Ffrench-Constant 1995; Peters *et al.* 1996; Scarpino *et al.* 1999). Because of their expression in cells of high proliferative and migratory potential, FNs containing EDIIIA and/or EDIIIB domains were suggested to play a role in promoting cell proliferation and migration (Manabe *et al.* 1999; Shimao *et al.* 1999). Mice devoid of EDIIIA exon-regulated splicing have shown that EDIIIA splicing regulation is required for proper skin wound healing and normal life span (Muro *et al.* 2003). However, the biological functions of these alternatively spliced isoforms are still poorly understood.

There has been inconsistent evidence as to how the inclusion of EDIIIA and EDIIIB in FN regulates cell adhesion and migration. Full length EDIIIA+FN enhanced cell adhesion and migration irrespective of the presence of EDIIIB, and binding affinity to integrin α5β1 was increased approximately two-fold on EDIIIA inclusion, the percentage of bound integrin α5β1 liposomes was increased from 3 % on recombinant full length FN to 7.5 % on recombinant full length EDIIIA+FN (Figure 1-13)(Manabe *et al.* 1997). The increase in α5β1 binding affinity was proposed to occur via the alteration of the global conformation of FN, and not by providing an additional cell interactive site. As function-blocking antibodies against the CCBD or integrin α5β1 inhibited EDIIIA+FN-mediated cell spreading almost completely, whilst those against the EDIIIA domain showed no inhibition. Full-length EDIIIA+FN isoforms were also more potent than EDIIIA-FN in promoting cell cycle progression through up-regulation of integrin-mediated mitogenic signal transduction (Manabe et al. 1999). In a separate study using recombinant FN fragments EDIIIB increased and EDIIIA decreased cell adhesion and spreading, whilst the presence of both EDIIIA and EDIIIB domains had no affect on cell adhesion and spreading (Hashimoto-Uoshima *et al.* 1997).

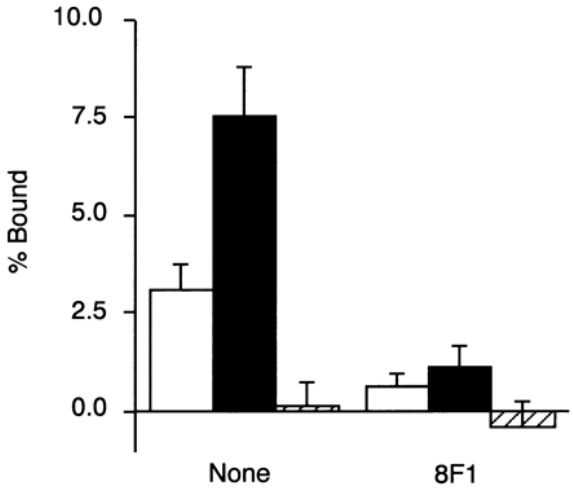

Figure 1-13 Binding of integrin α5β1 liposomes to plates coated with recombinant full length FN (open bars) and full length EDIIIA+FN (closed bars) or vitronectin (hatched bars) in the presence or absence of the anti-integrin α5 mAb 8F1. Quantities of bound integrin α5β1 liposomes are expressed as percentage of the total input radioactivity after subtraction of the radioactivity bound to plates coated only with BSA. Each bar represents the mean ± SD (n = 6). (Manabe *et al.* 1997).

From the crystal structure of the FIII7-10 fragment (Leahy *et al.* 1996), it was suggested that insertion of the EDIIIA segment would induce conformational changes in the FN molecule. Inclusion of spliced regions may alter the conformation of the RGD sequence by modification of neighbouring modules (Ffrench-Constant 1995). The insertion of EDIIIA could modify domains FIII11 and FIII12 by readjusting intermodular rotations and tilts, which could in turn alter the conformation of their neighbouring modules including FIII10 so as to optimize the conformation of the RGD-containing loop.

Another possibility is that the insertion of the EDIIIA segment may rotate the NH_2-terminal two-thirds up to 180° relative to the COOH-terminal one-third (Leahy et al. 1996). This could alter the global conformation of FN, increasing the accessibility of the RGD motif in CCBD to integrins and also induce partial unfolding of the FIII10

module by altering the tension and/or torsion applied to CCBD, thereby altering cell adhesive properties of FN and its interactions with other ECM molecules. In addition, the EDIIIA domain has been shown to be a ligand for integrins α9β1 and α4β1 (Liao et al. 2002), see Section 1.5.3.

Cellular FNs containing EDIIIA are produced in response to tissue injury (Jarnagin *et al.* 1994) and may play a role in the inflammatory response. EDIIIA+FN fragments produce cellular responses similar to those provoked by bacterial lipopolysaccharides (LPS), including the induction of genes involved in inflammatory responses such as those for pro-inflammatory cytokines and MMPs. For example, EDIIIA can activate MMP-1, 3, and 9 in synovial cells by an IL-1-dependent mechanism (Saito *et al.* 1999). One way by which cells can sense EDIIIA is via the activation of toll-like receptor (TLR) 4, a signalling receptor that is stimulated by LPS. Both TLR and IL-1R signal through a common pathway, resulting in downstream activation of the NFκB and MAPK signalling pathways, to induce cytokine production and apoptosis (Abrahams *et al.* 2004). The stimulation of TLR4 by EDIIIA was not observed with other recombinant FN domains, and was dependent on the co-expression of MD-2, a TLR4 accessory protein (Okamura *et al.* 2001). Therefore EDIIIA+FN may play a role in promoting expression of genes involved in inflammatory responses.

The alternatively spliced domain EDIIIB is considered to be a marker for angiogenesis. Expression of EDIIIB+FN is undetectable in mature vessels, but is highly up-regulated during angiogenesis, for example in the functional layer of the endometrium during the proliferative phase (Castellani *et al.* 1994).

The NMR structure of the EDIIIB domain indicated differences from other FIII domains, mainly in the loop regions buried at interdomain interfaces which could alter the global conformation of FN (Fattorusso *et al.* 1999). The crystal structure of FIII7-10 has demonstrated the four FIII domains to have highly conserved global folds differing only in their loop regions (Leahy *et al.* 1996). These loop regions found at interdomain interfaces are reported to influence interdomain interactions and orientations between adjacent domains, which determine particular biological functions (Spitzfaden *et al.* 1997). Comparison of EDIIIB with FIII8 revealed differences in the conformation of loop regions; the solvent-exposed BC loop of EDIIIB differs from the buried BC loop of FIII8 found at the FIII7-8 interface, and so may not be buried at the FIII7-EDIIIB interface. The resulting differences in interdomain distances will influence the relative orientations between adjacent domains, and so EDIIIB inclusion may modulate biological functions of FN. In addition a solvent-exposed hydrophobic cluster of residues found amongst the negatively charged protein surface of EDIIIB could be a potential specific recognition site (Fattorusso *et al.* 1999).

1.4.5.4 Modulation of FN splicing

The splicing pattern of many pre-mRNAs including FN are altered by extracellular cues such as growth factors, cytokines, hormones, and membrane depolarization (Stamm *et al.* 2005). Many of these extracellular cues may act through different signalling transduction cascades, to alter the relative abundance, subcellular localization or activation state of splicing factors such as the serine/arginine-rich (SR) proteins, which play a role in splice site selection. For example, TGF-β1, PDGF-BB and IL-1β altered splicing of the IIICS domain in a malignant renal cell line (McKay

et al. 1994) and EDIIIA and EDIIIB splicing in cultured normal skin fibroblasts are increased by TGF-β1 (Borsi *et al.* 1990). The splicing of domains EDIIIA, EDIIIB and IIICS by IMR-90 fibroblasts and MG63 osteocarcinoma cells are also increased by serum and TGF-β1 (Magnuson *et al.* 1991). The growth factors hepatocyte growth factor/scatter factor (HGF/SF), keratinocyte growth factor (KGF), aFGF, bFGF and EGF upregulate the inclusion of EDIIIA and IIICS in the mouse mammary epithelial cell line SCp2 (Blaustein *et al.* 2004). EDIIIA splicing was unresponsive to TGF-β1 in SCp2 cells, although it has previously been considered to be one of the main regulators of EDIIIA splicing; this correlates with the ability of TGF-β1 to exert a variety of effects under different conditions.

Extracellular stimuli such as growth factors can alter the nuclear and cytoplasmic activities of SR proteins, proposed to be via a Ras-PI 3-kinase-AKT pathway (Blaustein et al. 2005). Several consensus motifs for AKT phosphorylation have been identified in SR proteins, the phosphorylation of which may potentiate binding to mRNA to enhance the reimport of free cytoplasmic SR proteins into the nucleus and/or directly stimulate nuclear and cytoplasmic activities of SR proteins (Blaustein et al. 2005), thereby altering alternative splicing of EDIIIA. However, EDIIIA and EDIIIB splicing appear to be independent events (Paolella et al. 1988) and the mechanisms regulating the splicing of EDIIIB are less well understood.

In summary, the regulation of alternative splicing is hypothesized to provide a biological mechanism for modulating cell adhesion properties of FN. The insertion of the EDIIIA domain may alter the local and/or global conformation of the FN molecule, and affect the stability of other FIII domains. The EDIIIA domain may

also interact with other receptors such as integrins α4β1 and α9β1 to influence matrix assembly or interaction of FN with other proteins to induce cellular responses.

1.4.5.5 Matrix assembly

The matrix assembly of FN converts soluble FN into insoluble FN fibrillar matrices, a tightly regulated process involving integrins and the cytoskeleton. The stepwise assembly proceeds from initiation through elongation to stabilization; the critical step is considered to be the self-association of FN into aggregates and fibrils. Each step involves multiple FN domains for binding to cells, to other FN molecules and ECM components like CN or heparin. Some sites are exposed for binding whilst others are cryptic and are accessible on conformational changes induced on integrin binding (Sechler *et al.* 2001).

During the initiation stages, integrin binding immobilizes dimeric FN and promotes the formation of deoxycholate (DOC)-insoluble fibrils. There are two possible mechanisms as to how integrin binding can promote FN assembly. Interactions between the RGD and the synergy site with integrins such as α5β1 are necessary for the initiation of fibril formation, but not for fibril elongation (Sechler *et al.* 1997). An alternate RGD-independent assembly pathway initiated by α4β1 binding to the IIICS region of FN also promotes FN assembly (Sechler *et al.* 2000), but does not result in the reorganization of actin filaments into stress fibres or changes in growth rates, suggesting that there are multiple mechanisms of FN assembly. As a dimeric ligand, FN can induce receptor clustering by binding to two integrins. Integrin–FN clusters can create relatively high local concentrations of FN to help promote self association. Also, integrin binding may lead to the 'activation' of FN by releasing constraints on

binding domains and exposing additional FN binding sites for more accessible FN-FN interactions (Schwarzbauer *et al.* 1999).

Assembly then progresses into a growth phase where FN dimers are incorporated into fibrils, followed by fibril elongation and conversion of fibrils into the DOC-insoluble form. The matrix is further stabilized as high molecular mass multimers are formed. FN fibrillogenesis is also accompanied by the directed translocation of α5β1 out of focal adhesions into fibrillar adhesions. This movement along the actin cytoskeleton stretches and organizes the bound FN into fibrils (Pankov *et al.* 2000).

The major interaction site throughout the assembly process is the N-terminal assembly domain consisting of FI1-5, which can interact with other FN binding sites in FIII1-2, FIII10 and the C-terminal HepII domains to regulate interactions between FN molecules and matrix assembly (Sechler et al. 2001). Interactions with other ECM components are also important, for example HSPGs are likely to influence protein-protein and protein-heparin sulphate interactions in the ECM (Ruoslahti 1988). However, CN does not appear to be needed for FN deposition (Chen *et al.* 1978).

1.4.5.6 Biological roles of FN and the ECM

The ECM provides tissues with mechanical strength and elastic properties, and can influence cellular functions via interaction with specific cell-surface receptors, mainly integrins and also members of the collagen family, proteoglycans, or cell-surface-associated components. The activation of specific receptors transduces signals either directly to the intracellular cytoskeleton or via different signalling cascades. Therefore besides determining shape and orientation of cells, cell-matrix interactions

can also regulate cellular functions including cell adhesion, migration, proliferation, differentiation and gene expression.

The FN matrix is important for normal cell adhesion and growth, many transformed and tumour-derived cell lines have decreased levels of surface-associated FN, resulting from reduced biosynthesis and elevated degradation of FN (Hynes 1990). The FN matrix also plays a critical role in early development, since mice lacking FN have an embryonic lethal phenotype resulting from defects in mesodermal development and vasculogenesis (George *et al.* 1993).

The cell adhesion promoting properties of FN are well established; most cell types exhibit strong attachment and extensive spreading on surfaces coated with FN or FN-derived adhesive fragments (Hynes 1990). The same soluble fragments or specific peptides can detach cells from FN substrates (Hayman *et al.* 1983). Cells can adhere to FN via integrin and non-integrin receptors, the RGD and PHSRN synergy cell attachment sequences in FIII9 and FIII10 supports maximal fibroblast attachment, and specific sequences within heparin domain and IIICS region are also required for migration on FN.

Fibroblast migration on FN requires the cooperation of multiple integrin and non-integrin receptors, including integrins α5β1, αvβ3 and α4β1, CD44 proteoglycan and syndecan-4 (Clark et al. 2003). This stringency of cell migration places a constraint on normal mesenchymal cell mobility, and the loss of such restraint may be critical for migration through ECM; such a loss of migratory constraint on FN can occur in embryogenesis and in malignancy (Clark et al. 2003).

Most types of normal cells require attachment to the ECM for cell growth and proliferation, and the inhibition of FN matrix assembly results in the inhibition of cell proliferation (Bourdoulous *et al.* 1998). In addition, the EDIIIA+FN splice variant potentiated the ability of FN to promote cell cycle progression by inducing G_1-S phase transition (Manabe et al. 1999).

There is evidence that FN can affect differentiation in some cell types. For example, the process of chondrogenesis where mesenchymal stem cells differentiate towards chondrocytes, involves the coordinated effects of growth and differentiation factors and ECM components including FN (Djouad *et al.* 2007). The conversion of hepatic lipocytes to myofibroblast-like cells can be mediated by EDIIIA+FN (Jarnagin et al. 1994), which also has a role in the differentiation of fibroblasts to myofibroblasts, an effect that can be induced by TGF-β1 (Serini *et al.* 1998).

The ECM can influence growth factor signalling by its ability to associate with growth factors, including insulin-like growth factor (IGF), fibroblast growth factor (FGF), TGF-β and HGF (Taipale *et al.* 1997), facilitating their storage in a latent or unavailable form, which can be rapidly released and activated in a readily available form. FN can complex with VEGF via a binding domain in the HepII domain on FIII13-14 of FN to modulate VEGF activity. The cell-binding domain of FN together with the VEGF-binding domain is required to enhance VEGF-mediated cell migration, proliferation, or growth factor signalling (Wijelath *et al.* 2006). The release of growth factors from matrix storage and activation of latent forms can induce rapid and

localized changes in their activity, which controls cell proliferation, differentiation, synthesis and remodelling of the ECM.

1.4.6. Constitutive and cycle-dependent expression of ECM proteins in the endometrium

During the menstrual cycle, the endometrium undergoes morphological and functional changes in response to ovarian steroid hormones (Section 1.1.1). The components of the ECM are expected to have a role in the regulation of the cellular events involved in the cyclical regeneration and remodelling of the endometrium. The constitutive and cycle-dependent expression of ECM proteins is well established in the human endometrium (Kisalus *et al.* 1987; Aplin et al. 1988; Burrows *et al.* 1995; Iwahashi *et al.* 1996; Beliard *et al.* 1997; Harrington *et al.* 1999). The two major ECM glycoproteins, LNs and FNs, have key roles in epithelial cell attachment (Engel 1992) and stromal cell adhesion to the interstitial matrix (Yamada 1989).

The interstitial ECM components CN types I, III and V are present in the endometrial stroma but not in glands throughout the menstrual cycle and in first trimester decidua. They undergo changes in their distribution during decidualization, from the fibrillar arrangement throughout the endometrial stroma to occupying the matrix-filled space between decidual cells in first trimester decidua. This change is thought to accommodate the morphological changes during decidualization, when the elongated fibroblast-like stromal cells of the proliferative phase become enlarged epithelioid decidual cells. It also preserves the extracellular scaffolding to prevent collapse as tissue hydration increases during decidualization. VN is present in the basement membrane and apical surface of the glandular epithelium, and showed diffuse staining

in the ECM of stromal cells throughout the menstrual cycle, and in some blood vessels in first trimester decidua.

Basement membrane components CNIV, LN and HSPG are all present in glandular epithelial and endothelial basement membranes throughout the proliferative and secretory phase. The CNIV and LN also display staining in the ECM surrounding stromal cells throughout the menstrual cycle, and are organised into a pericellular aura surrounding stromal cells in first trimester decidua. The expression of LN is increased during progesterone-induced *in vitro* differentiation of human ESCs (Brar *et al.* 1995).

The expression of TN is positive in vascular and glandular basal membranes, epithelial cells and throughout the stromal ECM of the proliferative endometrium, but is confined to the stroma immediately adjacent to glandular epithelium in the secretory stage (Tan *et al.*; Harrington *et al.* 1999; Sedele *et al.* 2002). This temporal and spatial regulation of TN expression suggests a function in the regeneration of endometrial stroma, in regulating endometrial growth and proliferation. The intense deposition of TN fibrils in the stromal ECM immediately subjacent to the uterine epithelium showed the highest proportion of cells positive for the mitotic marker ki-67, and during the secretory phase, reduction in TN expression is correlated with a reduced proliferative index of the epithelium (Taguchi *et al.* 1999). The expression of TN has been suggested to be adhesion-modulatory or anti-adhesive (Orend *et al.* 2000), and its localization in the stroma adjacent to the glandular epithelium may facilitate embryo penetration by disrupting uterine cell adhesion to the underlying

basal lamina (Julian *et al.* 1994) and also by the 'loosening' of stromal contacts with ECM components (Chiquet-Ehrismann 1991).

1.4.7. Expression of fibronectins in the endometrium

The FNs are constitutively expressed in the endometrial stroma throughout the menstrual cycle and in first trimester decidua. They are present in the epithelial basement membrane and stromal cell ECM, where they are arranged as tightly packed fibrils. During decidualization their expression levels persist in the stroma but they become less tightly packed and distributed pericellularly around each stromal cell, perhaps to allow for the morphological changes that occur during decidualization and in preparation for potential implantation (Aplin *et al.* 1988; Burrows *et al.* 1995; Harrington *et al.* 1999).

During implantation the embryo must attach and adhere to the luminal epithelium, invade and migrate through the epithelium to infiltrate the stroma (Section 1.2). The expression of FNs in the epithelial basement membrane and endometrial stroma suggests that FNs have a role in supporting blastocyst attachment and activation of signals such as integrin trafficking required for subsequent invasion into the stroma. FNs effectively promote attachment of mouse blastocysts and outgrowth of trophoblast cells *in vitro* (Armant et al. 1986); they could act as bridging molecules binding the TE with the luminal surface of the endometrium, however fibronectin null mouse embryos do implant normally (George et al. 1993). Human pre-implantation blastocysts constitutively express integrin subunits α3, αv, β1, β3, β4 and β5 (Campbell *et al.* 1995), and these can form integrin receptors that can bind to FN. Staining for β5 in both the trophectoderm cytoplasm and at the outer surface of the

TE suggests that αvβ5 may be expressed in the human blastocyst and involved in the initial interaction with the luminal epithelium (Bloor *et al.* 2002).

1.4.8. Roles of ECM glycoproteins in the endometrium

Immunolocalisation of first trimester human decidual tissue showed that the relative amounts of CNV and CNI increases with decidualization, along with accumulation of basement membrane components CNIV and LN around decidual cells (Iwahashi et al. 1996). The increase in CNV to CNI ratio suggests that the CN fibrils formed are thinner (Section 1.4.1.1), which would affect the structure and organization of the matrix network in the decidua, altering its biomechanical properties. The pericellular distribution of basement membrane components observed in first trimester decidua is likely to restrict motility of decidual cells. Interstitial components, FN and CN types I, III and V become less tightly packed in the endometrial stroma, perhaps to allow for morphological changes during decidualization, and to 'loosen' the tissue for potential implantation and subsequent trophoblast invasion into the decidua.

A number of genes encoding ECM molecules were identified by RNA profiling to be dynamically regulated in the endometrium at the time of implantation or during decidualization. In one study comparing gene expression by ESCs in the window of implantation with the late proliferative stage, expression of LN and OPN were up-regulated and CN type XVI, TN and integrins α6 and β5 were down-regulated (Kao et al. 2002). In a separate study comparing changes in gene expression between early-secretory and mid-secretory or receptive phase endometrial tissue (Carson et al. 2002), the expression of genes encoding OPN and integrins α9 and β7 were up-regulated, whilst CN type VII, integrins αIIb, α5 and β2 were down-regulated. Gene profiling of

decidual fibroblasts from human term decidua, which closely resemble ESCs showed reduced expression of integrin α4, LN, FN, CN types I, IV, X, XI and XVI during differentiation (Brar et al. 2001).

Induction of expression of specific ECM components such as FN at the site of implantation has been shown in rodents (Rider *et al.* 1992). It is unclear what changes occur in the ECM at the implantation site in the human, and what factors regulate ECM synthesis during ECM remodelling and differentiation of decidualization.

Blastocyst implantation involves trophoblast attachment to the endometrium, invasion through the uterine epithelium and infiltration of the stroma (Section 1.2). The ECM has a role in supporting attachment and activation of signals such as integrin trafficking required for subsequent invasion into the stroma. A number of ECM components have been shown to support mouse trophoblast attachment and outgrowth *in vitro*, including FN and LN (Armant et al. 1986) (Yelian *et al.* 1995), VN (Armant *et al.* 1986), CN types I through IV (Carson et al. 1988; Sutherland *et al.* 1988) and TSP (O'Shea *et al.* 1990).

When proteolytic FN fragments containing the major functional domains of FN were assessed for blastocyst adhesion and trophoblast outgrowth, only those containing the RGD cell recognition motif supported adhesion and outgrowth (Yelian et al. 1995), an effect that was inhibited by the RGD-containing hexapeptide GRGDSP. This included a one hundred and twenty kDa FN fragment (fFN) containing the CCBD and RGD. The recombinant protein ProNectin F, containing thirteen copies of the RGD-

containing decapeptide VTGRGDSOAS could also support blastocyst adhesion and trophoblast outgrowth. A forty kDa C-terminal fFN containing the heparin-binding region and an alternate non-RGD cell-binding site was inactive in supporting trophoblast adhesion.

Mouse blastocyst attachment and trophoblast outgrowth is also supported by VN and CN types I through VI (Armant *et al.* 1986; Carson *et al.* 1988). Adhesion is RGD-dependent for VN, CNII and denatured CNIV, as RGD-containing hexapeptides effectively attenuated mouse trophoblast outgrowth on these ECM components. Attachment to CN types I, V, VI however were not inhibited by RGD peptides. Blastocyst adhesion on LN and TSP are also RGD-independent, the E8 proteolytic LN fragment appears to be the main adhesive domain and can promote outgrowth; it contains a heparan-binding domain and other sites recognised during cell adhesion and neurite outgrowth (Armant 1991; Sutherland *et al.* 1993). Outgrowth on TSP was inhibited by anti-TSP antibodies but not by the GRGDSP peptide (O'Shea et al. 1990). These observations suggest that multiple adhesion systems mediate attachment to the various endometrial ECM components present *in vivo*.

In the invasive phase of implantation, uterine epithelial cells detach from the underlying basement membrane during decidualization and trophoblasts become embedded in the underlying stroma, where the trophoblasts interact with a variety of ECM components including FN, LN, CN and proteoglycans secreted by the decidua. An *in vitro* model of trophoblast adhesion and outgrowth on ECM components is a likely representation of the interactions involved, where trophoblast cells attach to and

degrade FN and LN-containing basement membranes that underlies epithelium and invades the stroma (Armant et al. 1986).

Mouse blastocysts exhibit strong binding to FN only after exposure to FN (Schultz *et al.* 1997), and this upregulation of trophoblast adhesion is mediated by ligation of integrins α5β1 and αvβ3, elevating cytoplasmic free Ca^{2+} levels (Wang *et al.* 2002). Ca^{2+} signalling induces trafficking of proteins including integrin αIIbβ3 to the apical plasma membrane (Rout *et al.* 2004), to strengthen trophoblast adhesion to the ECM and subsequent invasion into the stroma. There is an ECM-dependent selectivity of integrin activation: only FN upregulates FN-binding activity and only LN upregulates LN binding activity (Armant 2005), suggesting that contact with different ECM components will activate the appropriate receptors, allowing for efficient adhesion to complex mixtures of ECM encountered *in vivo*.

1.5 Integrins

1.5.1. Introduction

Integrins are a family of cation-dependent transmembrane heterodimeric receptors, composed of non-covalently linked α and β subunits. At least twenty-four functional integrin dimers have been identified, formed from eighteen α and eight β subunits (Figure 1-14) (Hynes 2002).

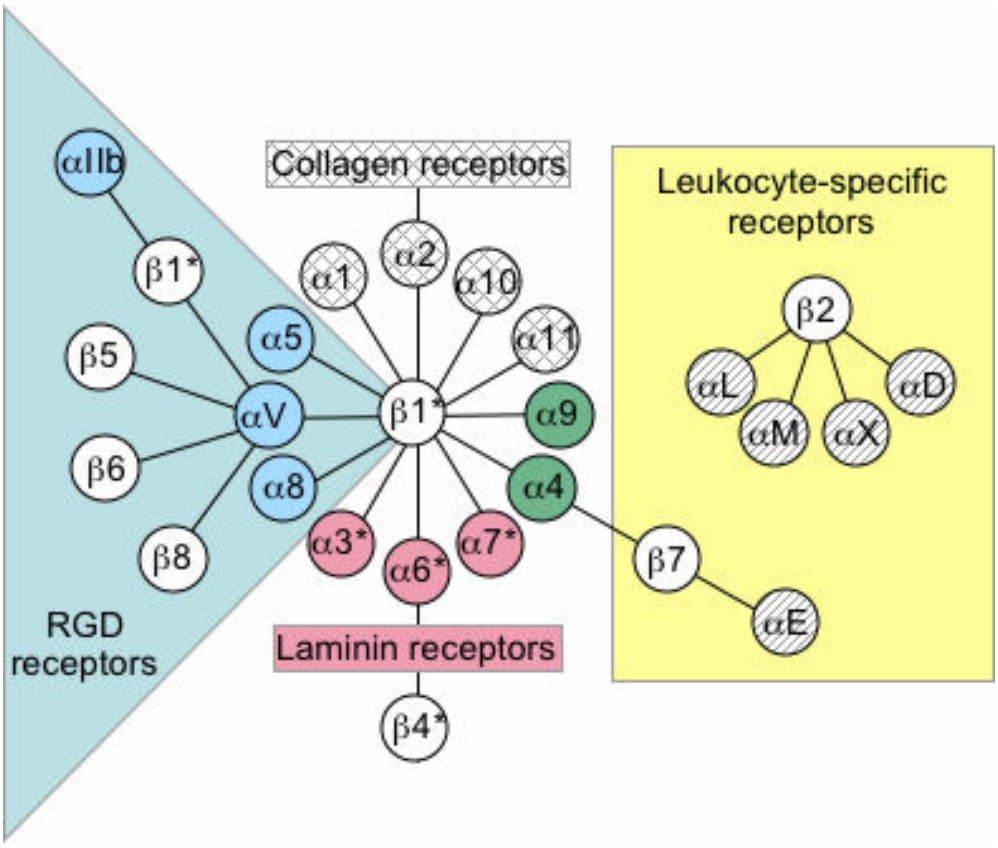

Figure 1-14 Mammalian integrin subunits and their αβ associations; 8 β subunits can assort with 18 α subunits to form 24 distinct integrins. Several subfamilies of α subunits are coloured based on ligand specificity; α subunits with grey hatching have an inserted I domain; α4 and α9 can recognise both ECM proteins and Ig-superfamily cell surface coreceptors (green). Asterisks denote alternatively spliced cytoplasmic domains (Hynes 2002).

A feature of integrins is the ability of individual members to recognise multiple ligands. They can bind to a diverse range of ligands including ECM proteins, cell surface proteins and plasma proteins, with ligand specificity being determined by the specific combination of α and β subunits.

Integrin α and β subunits are type I transmembrane proteins, both consists of a large N-terminal extracellular domain responsible for ligand binding, a single transmembrane (TM) segment and a relatively short C-terminal cytoplasmic tail. A schematic diagram of an integrin dimer is shown in Figure 1-15.

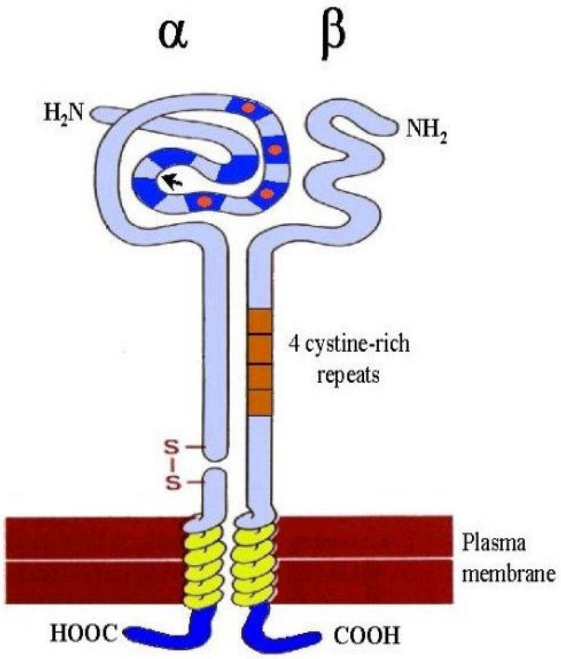

Figure 1-15 Schematic drawing of a typical integrin dimer. Arrow shows region where an I domain is inserted in some α subunits, not all α subunits are posttranslationally cleaved. Internal disulphide bonds within subunits not shown. Dark blue regions in the head segment of α subunit represent homologous repeats. Those with the EF-hand consensus sequence are marked with red circles to denote binding sites for divalent metal ion. From http://www.obs-gyn.ox.ac.uk/research/mardon/fibronectin.

The extracellular segment of the integrin is an asymmetric structure forming a 'head' carried on two 'legs'. The head is formed from a predicted seven-bladed β-propeller domain from the α-subunit and a predicted α-like domain (βA) from the β-subunit. The N-terminal region of all α-subunits contain seven repeats forming the β-propeller, the final three or four contain inserted sequences, EF-hand-like domains which can mediate bivalent-cation-binding. In a subset of integrins, an extra domain, αA or I domain is inserted between repeats two and three to mediate ligand binding. At the apex of αA is a metal ion-dependent adhesion site (MIDAS) motif.

The binding of ligands to integrins is bivalent-cation-dependent, stimulated by Mg^{2+} and Mn^{2+} and inhibited by Ca^{2+}. There are four potential sites for bivalent cation binding: the αA-domain, the βA-domain, the EF-hand-like sequences in the α subunit β-propeller, and in a site in the β-propeller (Humphries 2000). The divalent cation binding sites are of relatively low affinity, with the bound divalent ions affecting ligand binding strength and specificity.

Integrins are capable of transmitting bidirectional signals across the plasma membrane, altering its conformation and ligand-binding affinities to control integrin activation. Inside-out signalling occurs in response to intracellular signals which affect integrin cytoplasmic domains, to trigger changes in the conformation and ligand-binding affinity in the extracellular domain. The mechanisms by which integrins transmit these signals remain unclear. Intracellular signals include the binding of intracellular proteins such as talin to the β-subunit cytoplasmic tail. The phosphotyrosine-binding (PTB) domain in the F3 domain of talin has been shown to bind to membrane-proximal (MP) region of integrin β-subunit cytoplasmic domains, resulting in integrin

activation (Wegener *et al.* 2007). The talin/MP interaction is suggested to promote activation by disruption of TM helix interactions, where the TM domains are further out of the membrane, shifting the equilibrium towards the active conformation. The binding of extracellular ligands produces intracellular signals, by outside-in signalling, including changes in tyrosine phosphorylation and cytoskeletal organization to influence cell shape, migration, growth, and survival (Zhu *et al.* 2007)

In the resting state where integrins exhibit low affinity for the ligand, the extracellular domain of the integrin is in a compact bent conformation, stabilized by specific interfaces between the α and β subunits in the extracellular, TM and cytoplasmic domains. From X-ray crystal structures of the αvβ3 extracellular domain, the legs were shown to be severely bent in a V-shaped topology where the head domain is closely juxtaposed to the membrane-proximal portions of the legs (Luo *et al.* 2007).

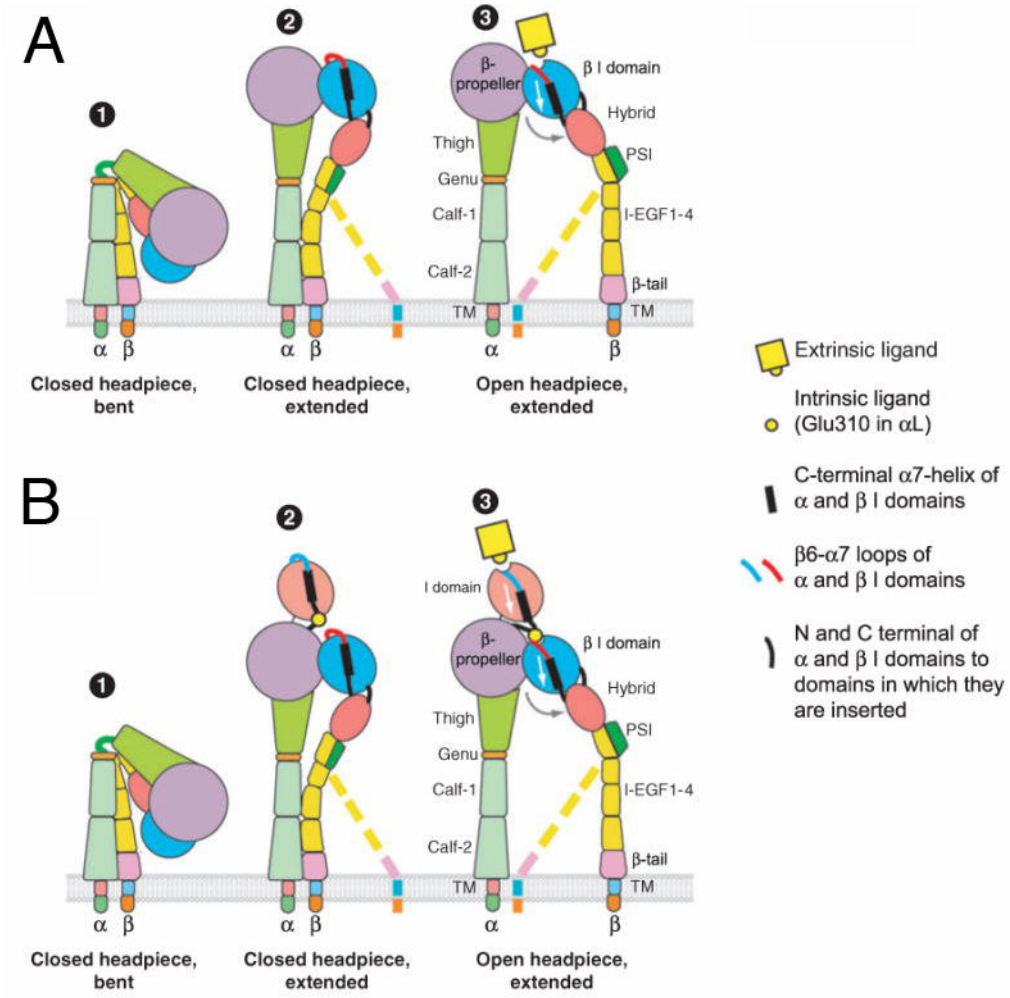

Figure 1-16 Schematic diagram of rearrangement of domains during activation of integrins that lack (A) or contain (B) an α I domain. The β subunit lower legs are flexible and are therefore shown in what may be the predominant (*solid representation*) and less predominant (*dashed lines*) orientations. From (Luo *et al.* 2007).

Integrin activation occurs as a result of priming by intracellular signals and ligand binding to induce extension and separation of the α and β legs at the TM and cytoplasmic domains. The integrin extends with a switchblade-like motion, these global rearrangements are linked to intradomain conformational changes associated with affinity modulation and ligand binding. Transformation to the high-affinity ligand-binding site is allosterically linked to the downward movement of the α7-helix of both α and β subunit I domains, causing rotation and remodelling of the interface

between the hybrid and β-I domains, swing-out of the hybrid domain from the α subunit (Xiao *et al.* 2004), movement of the PSI domain and separation of the integrin knees (Figure 1-16). Therefore there are two structurally-linked mechanisms for activating integrin adhesiveness. Integrin extension moves the ligand binding head further away from the cell surface, orientating it for adhesion to other cells or the ECM. Integrin extension also enables hybrid domain swing-out to induce increased ligand binding affinity.

However, there is controversy for the requirement of extension in the activation of some integrins, and an alternative deadbolt model was proposed (Arnaout *et al.* 2005; Luo *et al.* 2006). In one EM study, soluble αvβ3 bound to a FN fragment was still in the bent conformation. The 'deadbolt' interaction is at a small 60Å^2 interface between the β-tail domain CD loop (deadbolt) and the β-I domain β6 strand-α7 helix region in the unliganded αvβ3. However, mutation of the β-tail domain CD loop had no effect on ligand binding by αIIbβ3 or αvβ3, and integrins locked in the bent conformation are resistant to inside-out activation, indicating that integrin extension is required for ligand binding during integrin inside-out signalling and that the deadbolt may not regulate integrin activation (Zhu *et al.* 2007).

A number of integrin recognition sequences have been identified in ECM proteins (Ruoslahti 1996), the integrins recognise a core ligand motif centred on an acidic residue. The RGD sequence was originally identified in FN that engages integrin α5β1, and is a recognition motif found in multiple ligands for several different integrins. The interaction with RGD-containing ligands is determined by the context of the RGD sequence, including flanking residues, three-dimensional presentation and

individual features of the integrin binding pockets (Haas *et al.* 1994). The integrin α4β1 can interact with a number of sequences in FN, including the alternatively spliced sequences IIICS and EDIIIA (Mould *et al.* 1990; Liao *et al.* 2002).

1.5.2. Integrins α5β1 and αvβ3

The FN receptor α5β1 (Argraves *et al.* 1987) recognises the RGD motif in the central cell-binding domain of FN, enhanced by the adjacent synergistic PHSRN motif in the FN molecule. Integrin α5β1 has a role in the regulation of adhesion and migration on FN, and also regulates FN matrix assembly (Akiyama *et al.* 1989; Roman *et al.* 1989). Another FN receptor, αvβ3, primarily recognises RGD-containing ligands. It can bind to more than a dozen different ligands in addition to FN including VN, fibrinogen, OPN and TN, and mediates FN matrix assembly in cells lacking α5β1 (Wu *et al.* 1996). The α5 subunit sequence is forty-six percent homologous to the αv subunit, though αv can dimerize with a greater selection of β subunits. The recognition of the RGD motif by αvβ3 does not require the synergistic effect of the PHSRN motif (Chen *et al.* 1996). In this thesis, the main fibronectin receptor integrin α5β1, and αvβ3 which is expressed at the LE and GE at the time of implantation (Lessey et al. 1996) will be investigated in more detail.

1.5.3. The α4 and α9 subset of integrins

The α4 and α9 integrin subfamily are different from the other integrin subsets in that the α subunits do not contain the I domain inserted close to the N terminus, nor a disulphide-linked cleavage site (Palmer *et al.* 1993). A number of ligands have been identified for α9β1, including the third FN type III repeat in TN (TNfn3) and the FN alternative splice domain, EDIIIA (Liao *et al.* 2002). Other ligands such as OPN and VCAM-1 can also bind to α4β1.

The α4 and α9 integrins do not recognise the RGD motif: recognition sites in several α4β1-binding ligands contain a homologous tripeptide composed of leucine (L) or isoleucine (I) and an acidic residue, followed by a neutral amino acid with a small chain, such as *LDV* in IIICS, *IDAP* in HepII and *KLDAPT* in FIII5 of FN, and *IDSP* in VCAM-1. Similarly, the α9β1 recognition sequences *AEIDGIEL* in TNfn3 and *EDGIHEL* in EDIIIA also contain this homologous tripeptide sequence (Yokosaki *et al.* 1998; Liao et al. 2002).

Integrin α4β1 regulates cellular functions differently from other β1 integrins: α4β1 integrin-mediated cell adhesion results in increased cell migration, reduced cell spreading and focal adhesion formation. The α4-mediated cell migration depends on the specific interaction of the α4 cytoplasmic domain with the adaptor protein paxillin, which facilitates recruitment and activation of FAK (Liu *et al.* 2002). It has previously been shown that FAK can bind paxillin (Turner 2000), and stimulates migration and FA disassembly (llic *et al.* 1995). Integrin α9β1-mediated cell adhesion also accelerated cell migration, an effect which depends on the α9 cytoplasmic domain, but was paxillin-independent unlike α4β1 (Young *et al.* 2001).

1.5.4. Integrin-mediated signalling

The main functions of integrins are to mediate cell-cell binding and cell-matrix interactions. In addition to their involvement with cell adhesion, integrins make transmembrane connections to the cytoskeleton. For example, integrin binding promotes formation of focal contacts where integrins associate with F-actin to regulate cell shape and activates intracellular signalling pathways to regulate cell

migration, proliferation, differentiation and survival (Hynes 1992; Clark *et al.* 1995; Giancotti 1997). The integrins differ from cell-surface receptors for hormones and soluble signalling molecules in that they bind their ligands with relatively low affinity, and usually they are at high concentrations on the cell surface. By binding weakly to a large numbers of matrix molecules, it allows cell motility without losing all attachment to receptors.

Integrins function as two-way signalling molecules, in regulating affinity and conformation of the receptor from inside the cell (inside-out signalling) and triggering intracellular signalling by ligand binding to the receptor (outside-in signalling) (Figure 1-17). The activation of integrins to switch from low to high affinity for ligand binding is triggered by both inside-out signals, to release intracellular constraints exerted on the cytoplasmic tails of the integrin, or by outside-in signalling when ligand-occupied integrins undergo conformational changes.

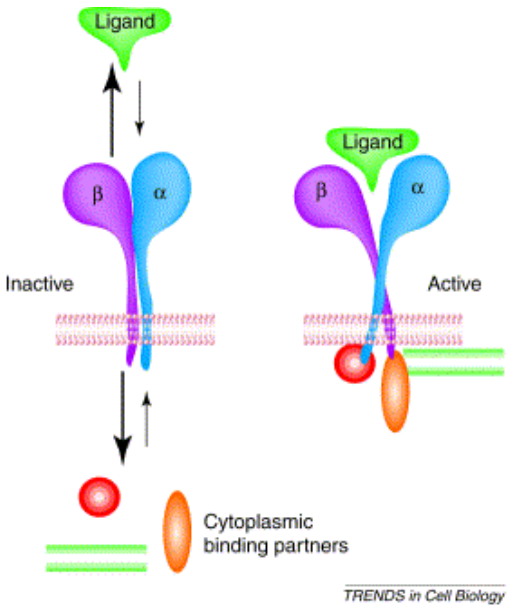

Figure 1-17 Bidirectional signalling of integrins. For inactive integrins, the extracellular domain has low affinity for ECM ligands, the α and β cytoplasmic domains are associated with each other to

induce low affinity for intracellular cytoskeletal and signalling binding partners. Activated or occupied integrins have high affinity for ECM ligands outside the cell, disruption of the intramolecular tail interactions increases affinity for tail interactions and affinity for intracellular components (Schwartz 2001).

The binding of ligands can trigger signal transduction in two ways: firstly by clustering of receptors to trigger post-translational modifications and/or effector molecule engagement, and secondly by inducing conformational changes in receptors, to create effector binding sites and/or expose sites to modifying enzymes. Clustering is considered to increase avidity, not affinity of molecular interactions, and this increases receptor occupancy by increasing the on-rate of binding. This occurs bidirectionally both inside the cell for signalling and cytoskeletal proteins and outside of the cell for ligands. For example, the adhesion of cells to multivalent ligands in the ECM or other cell surfaces causes accumulation of signalling complexes on the cytoplasmic face of the plasma membrane, to induce formation of cytoskeletal and signalling complexes, which further recruits integrins via linker proteins (Humphries 2000).

The engagement and clustering of integrins at focal adhesions (FA) recruits cytoskeletal proteins, and the cytoplasmic tails of the integrin β subunit can bind to several cytoskeletal proteins including talin, paxillin, vinculin, tensin and α-actinin. These actin-binding proteins recruit and bundle actin filaments to form actin-rich stress fibres, which have a role in maintaining cell shape and polarity (Calderwood *et al.* 2000). The FAs are sites of cell adhesion to the ECM, forming a structural link between the ECM and the actin cytoskeleton. They also mediate signal transduction as components of FAs propagate signals arising from integrin activation. Integrin-

mediated adhesion also activates the small GTP-binding protein Rho, which is required for the formation of stress fibres and FAs.

The clustering of integrins also triggers tyrosine phosphorylation and activation of focal adhesion kinase (FAK) and Src family kinases (SFKs). The non-receptor protein tyrosine kinase FAK has a central catalytic domain separating the N-and C-terminal domains. The former binds to β1 integrin cytoplasmic domain peptides. The C-terminal domain contains a FA-targeting (FAT) sequence and binding sites for at least two FA proteins, paxillin and talin (Burridge *et al.* 1996).

The activation of FAK on tyrosine phosphorylation at multiple sites occurs in response to a number of stimuli, including integrin-meditated adhesion, growth factors, neuropeptides, mechanical stimuli and reagents that stimulate G-protein coupled receptors. In quiescent and adherent cells, FAK is localized to vinculin-enriched focal contacts through association with paxillin and talin. Cell spreading on matrix proteins promotes integrin clustering and FAK activation through both intermolecular clustering and intramolecular release of conformational restraints. The phosphorylation at FAK Tyr-397 forms docking binding sites for the SH2-domain of SFKs, FAK-binding proteins Cas and paxillin, and other SH2-domain containing proteins including PI3-kinase and phospholipase Cγ. Subsequent SFK-mediated phosphorylation of FAK at Tyr-576/577 located in the kinase activation loop is important for the maximal activation of FAK and downstream signalling events (Parsons 2003). FAK can also be activated by growth factor-dependent pathways involving Rho family proteins that are implicated in the regulation of the actin cytoskeleton (Zachary *et al.* 1992; Seufferlein *et al.* 1995).

Evidence suggests a role for FAK in the regulation of cell migration: FAK-deficient cells spread more slowly on ECM proteins, exhibit an increased number of FAs and migrate poorly in response to chemotactic (PDGF and EGF) and haptotactic (FN) signals. Cell migration can be restored upon reconstitution with wild-type FAK, whereas FAK mutants lacking kinase activity or the ability to bind SFKs (Y397 mutation) could not restore cell migration. It was suggested that FAK regulates the assembly and dynamic turnover of FAs required for efficient cell movement (Sieg *et al.* 1999; Sieg *et al.* 2000).

1.5.5. Integrins in the endometrium

Integrins display spatial and temporal patterns of expression within the endometrium throughout the menstrual cycle. Some of the known αβ pairings identified in reproductive and early embryonic tissues are indicated in Figure 1-18. Their expression in the uterine epithelium and stroma, as well as on the pre-implantation embryo and their ECM ligands are summarized in Table 1-1.

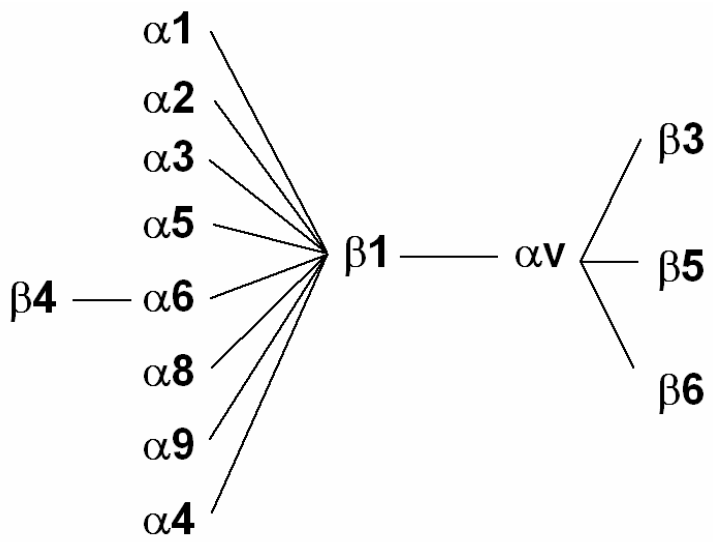

Figure 1-18 Known integrin subunits and αβ pairings identified in reproductive and early embryonic tissues (Bowen *et al.* 2000).

Integrin	Human blastocyst	LE	GE	Stromal	Ligands
α1β1		r+	r+	r+	LN, CN, PE
α2β1		+	+	r+	CN, TN
α3β1	+	+	+	+	FN, CN, LN
α4β1			r+		FN, VCAM-1, OPN
α5β1				+	FN
α6β1	?	?	?	r+	LN
α6β4	?	+	+	+	LN
α9β1		+	r+		TN, FN, OPN
αvβ1		?	?		FN, VN, OPN
αvβ3	+	r+	r+	r+	FN, VN, TN, OPN, PE, TSP
αvβ5	+	+			FN, VN, OPN
αvβ6		+			FN, TN

Table 1-1 Integrins present in blastocyst, LE, GE, endometrial stroma. r, regulated expression during the menstrual cycle; ?, constituent subunits are present but specific association not determined. Ligands: CNs, FNs, LNs, OPN, PE (perlecan), TN, TSP, VN, vascular cell adhesion molecule-1 (VCAM-1) (Aplin 1997; Bowen *et al.* 2000; Reddy *et al.* 2003).

Integrins recognising the basement membrane components collagens and/or laminin, primarily α2β1, α3β1 and α6β4, are expressed on the glandular epithelium

throughout the menstrual cycle. The α2β1 and α3β1 integrins show a pericellular distribution whereas α6β4 shows basolateral localization, adjacent to the basement membrane of endometrial glands where its ligands laminin and collagens are expressed. In the LE, α2β1 undergoes cycle-dependent changes, whereas α3β1 and α6β4 are constitutively expressed. The FN receptor α5β1 was not detected in either the glandular nor luminal epithelium, but was uniformly expressed in the stroma throughout the menstrual cycle (Lessey *et al.* 1992; Lessey et al. 1996).

The integrin αvβ3 has been implicated in human implantation. It is expressed at the LE and GE at the time of implantation and its aberrant epithelial expression has been associated with infertility (Section 1.2.4)(Lessey et al. 1996). Integrins α4β1 and α9β1 are also expressed in the GE at the time of implantation, with α9β1 localised in the LE throughout the menstrual cycle. Neither integrin has been demonstrated in ESCs (Lessey *et al.* 1996).

The expression of certain integrins can be regulated by growth factors and cytokines. The expression of α1β1 in cultured ESCs is induced by EGF, TGF-α and TGF-β1, and there is decreased expression of the α6 subunit in response to IL-1α, IL-1β and TNFα (Grosskinsky *et al.* 1996). In Ishikawa cells, a well differentiated endometrial adenocarcinoma cell line, EGF and TGF-α increase expression of the integrin αvβ3 (Somkuti *et al.* 1997). These alterations could be due to the action of both steroid hormones and the implanting embryo, via paracrine-autocrine cytokine systems such as the IL-1 system. The embryo can secrete components of the IL-1 system in the presence of EECs (De los Santos et al. 1996), and IL-1 upregulates integrin β3 expression by EECs in culture (Simon et al. 1997).

The integrin β1 and FAK are localised in FAs of human decidual cells (Hanashi *et al.* 2003), and have a role in mediating mouse embryo outgrowth but not attachment on the human decidual cells, suggesting that this integrin β1-cytoskeletal linkage at FAs on decidual cells may be important mediators of implantation.

A number of *in vitro* decidualization studies have suggested that FAs and the cytoskeleton are disrupted in the process. During *in vitro* decidualization of human ESCs induced by estradiol and progesterone, there is breakdown of the actin-based cytoskeleton and loss of FAs in the decidualized ESCs. The phosphorylation of FAK and paxillin remains constant but vinculin does not localize at distinct focal contacts, instead vinculin are diffusively localized in the cytosol (Maruyama *et al.* 1999). In addition, the cAMP-induced decidualization of human uterine fibroblasts is accompanied by the downregulation of α-smooth muscle actin, β-tubulin and redistribution of vinculin (Ihnatovych *et al.* 2007). It is known that in fibroblasts the activation of the cAMP/PKA signalling pathway, which is suggested to be activated during decidualization, disrupts focal adhesion plaques and the actin cytoskeleton through the downregulation of myosin light chain kinase (MLCK). The cytoskeleton has a role in numerous cellular processes including smooth muscle contraction, mitosis, cell growth and motility (Ayscough *et al.* 2004). Cytoskeletal organization and plasticity is determined by actin-myosin II interactions, which are regulated by the phosphorylation of myosin light chain and mediated mainly by MLCK. The destabilization of the cytoskeleton by inhibitors of MLCK could accelerate decidualization induced by cAMP, suggesting the regulation of cytoskeletal dynamics to be important for decidualization (Ihnatovych *et al.* 2007). The observed

breakdown of actin-based cytoskeleton and focal contacts may contribute to the decidualization process; cytochalasin D which disrupts the actin cytoskeleton has previously been shown to increase IGFBP-1 expression and accelerate decidualization (Kim *et al.* 1999). Perhaps disruption of the cytoskeleton and loss of FA is required for the morphological and biochemical changes in ESCs during decidualization.

1.6 Hypothesis and Objectives

The thesis aims to test the hypothesis that implantation of the human embryo depends upon tightly regulated modulation of ECM components in the endometrium. This was investigated using an *in vitro* decidualization model to determine alterations in the levels of various ECM components, including FN and its splice variants EDIIIA and EDIIIB, during decidualization of human endometrial stromal cells. The role of EDIIIA, which increases in endometrial stroma adjacent to the LE during the window of implantation, in mediating blastocyst attachment was studied using an *in vitro* blastocyst adhesion assay. The effect of locally secreted cytokines and growth factors on the production of FNs in endometrial stromal cells was investigated by ELISA.

The biological significance of EDIIIA+FN and EDIIIB+FN remains unclear. The functional consequences of their inclusion in the FN molecule was determined using FN fragments FIII7-12A±B± in a number of functional assays, including integrin binding, endometrial stromal cell adhesion and proliferation assays. Preliminary experiments aimed at determining the structural basis for modulations in functional properties was performed, using the recombinant FN fragments FIII7-12A+B- and FIII8-12A+B- in crystallization trials.

Chapter 2

Materials and Methods

2.1 Materials

2.1.1. Chemicals and buffers

All chemicals were of analytical grade and, unless otherwise stated, were purchased from Sigma-Aldrich Ltd. (Poole, U.K.). The composition of various buffer solutions used is given in Table 2-3.

2.1.2. Plasmids

Fusion protein expression vectors pGEX2T and pGEX4T3 were purchased from Pharmacia Biotech AB (Uppsala, Sweden), pET-22b from Novagen (Madison, WI, U.S.A.) and pRSETA from Invitrogen Life Technologies (Paisley, U.K.). Plasmid constructs pGEX-FIII7-12A+B+, pGEX-FIII7-12A+B-, pGEX-FIII7-12A-B+, pGEX-FIII7-12A-B-, pET-EDIIIA, pRSET-FIII7-12A+B- and pRSET-FIII8-12A+B- were provided by Dr. J. Asselin (Nuffield Dept. of Obstetrics and Gynaecology, University of Oxford, Oxford). Construction of pGEX-FIII8-9 (Mardon *et al.* 1994) and pGEX-FIII9-10L2P (van der Walle *et al.* 2002) has been reported previously. The schematic representations of all plasmids used in this study for protein expression are given in Figure 2-1 and Figure 2-2.

2.1.3. Antibodies and conjugates

2.1.3.1 Primary antibodies

Details of primary antibodies used in experiments are shown in Table 2-4.

2.1.3.2 Secondary antibodies and conjugates

Horseradish peroxidase (HRP) conjugated sheep anti-mouse IgG were obtained from Sigma, and HRP-conjugated rabbit anti-goat IgG from DAKO (Glostrup, Denmark). Biotin-conjugated rabbit anti-mouse IgG, fluorescein isothiocyanate (FITC)-conjugated donkey anti-mouse IgG, FITC-conjugated donkey anti-rabbit IgG, biotin-conjugated rabbit anti-mouse IgG and HRP-conjugated streptavidin were purchased from Jackson Immunoresearch Laboratories (Baltimore, PA, U.S.A.). Texas Red-conjugated phalloidin was obtained from Invitrogen Life Technologies.

2.1.4. Bacterial media

Liquid Luria-Bertani (LB) and LB-agar media, containing 15 g of bacto-agar per litre of LB were prepared as published previously (Sambrook *et al.* 1987). Ampicillin and chloramphenicol were added to the media to obtain final concentrations of 100 μg/ml and 170 μg/ml, respectively. All reagents were purchased from Sigma-Aldrich.

2.1.5. Eukaryotic media

Human endometrial stroma cells were maintained in Dulbecco's Modified Eagle's Medium (DMEM) (Invitrogen) supplemented with 10% fetal calf serum (FCS, PAA Laboratories, Pasching, Austria), 100 IU/ml penicillin, and 100 μg/ml streptomycin. Cells were passaged when confluent, using trypsin-ethylene diamine tetracetic acid (trypsin-EDTA) and the proteolytic effects of trypsin-EDTA neutralized using

DMEM during maintenance of cells, or soybean trypsin inhibitor for experiments. All tissue culture reagents were obtained from Sigma unless stated otherwise.

2.1.6. Bacterial strains

Escherichia coli strains BL21pLysS were purchased from Promega (Southampton, U.K.) and TOP10 from Invitrogen.

2.1.6.1 Preparation of bacterial competent cells

Bacteria strains TOP10 and BL21pLysS were inoculated into a small volume of LB, in the presence of 170 µg/ml chloramphenicol for BL21pLysS and grown overnight at 37^{o}C in a shaking incubator. They were then diluted into fresh LB and incubated for 2-6 hours until an optical density at 600 nm (OD_{600}) of 0.6 is reached. Cells were then pelleted by centrifugation at 4^{o}C, resuspended in cold 50 mM $CaCl_2$ and left on ice for 30 minutes. Finally the cells were centrifuged and resuspended in cold 15 % glycerol in 50 mM $CaCl_2$, and stored at -80^{o}C.

2.1.7. Eukaryotic cells: human endometrial stromal cells

2.1.7.1 Tissue collection and isolation of human endometrial stromal cells

Endometrial tissues were obtained with informed consent from patients undergoing sterilization or hysterectomy for benign conditions in accordance with the requirements of the Oxfordshire Clinical Research Ethics Committee (OxREC). Patients had normal endometrium with proven fertility, with regular menstrual cycles of 26–30 days and had not used hormonal medication for the three months before surgery. Samples were obtained from secretory stage endometrium (Table 2-1), the tissues were staged according to the last menstrual period (LMP) and standard

histological criteria (Noyes *et al.* 1975). Endometrial stromal cells (ESCs) were prepared by Ms Janet Carver according to a protocol described previously (Fernandez-Shaw *et al.* 1992).

2.1.7.2 Passaging and maintenance of human endometrial stromal cells

ESCs were used between passages 2 and 6 and were at least 84% and 92% positive for Thy-1 and vimentin, respectively. Cells were maintained and passaged when confluent as described in Section 2.1.5.

2.1.7.3 In vitro decidualization of endometrial stromal cells

ESCs were seeded onto cell culture grade plates (Nunc, Hereford, U.K.) at 1 x 10^5 cells/ml and grown until confluence. Decidualization was induced *in vitro* by the addition of 0.5 mM 8-Br-cAMP (Sigma-Aldrich) as described previously (Mizuno *et al.* 1998) for 6 days. Phase contrast microscopy was used to observe morphological changes associated with decidualization. The culture supernatants were collected, centrifuged, and stored at –20°C. Levels of secreted prolactin were measured in culture supernatants using the Immulite Prolactin Kit (Diagnostic Products Corp., Llanberis, U.K.), according to the manufacturer's instructions. The concentrations were normalized to the amount of total protein in each well.

2.1.7.4 Extraction of cell lysates

ESCs cultured on cell-culture grade 6-well plates were grown until confluence and induced to decidualize *in vitro* as described in Section 2.1.7.3. Cells were washed twice with ice-cold phosphate-buffered saline (PBS), treated with 115 µl/well of ice-cold Cell Lysis buffer (Table 2-3) for 30 minutes on ice. The cell lysates were collected with a cell scraper (Nunc) and transferred to an eppendorf tube and left at -

80°C for at least 10 minutes. Total protein concentrations were measured using the DC protein assay as described in Section 2.3.3.2

2.2 General DNA manipulation techniques

2.2.1. Transformation of *E.coli* with plasmid DNA

Competent *E.coli* strains (Section 2.1.6.1) were incubated with plasmid DNA on ice for 10 minutes, heat shocked for 2 minutes at 42°C, left on ice for a further 10 minutes before incubation with LB for 60 minutes at 37°C. Cells were pelleted by centrifugation, resuspended in LB and plasmid-containing cells were selected for resistance by plating them onto ampicillin-containing LB-agar dishes and growing overnight at 37°C.

2.2.2. Glycerol stock of plasmid containing *E.coli*

Bacteria containing the plasmid of interest were grown in LB broth in the presence of 100 µg/ml ampicillin overnight at 37°C. An additional 170 µg/ml chloramphenicol was included for BL21pLysS cells. Aliquots of the bacterial cultures in a final glycerol concentration of 40 % were stored at -80°C.

2.2.3. Purification of plasmid DNA

Bacteria containing the plasmid of interest were grown overnight at 37°C in LB containing 100 µg/ml ampicillin. The cells were collected by centrifugation and cell lysis and DNA extraction were preformed using the QIAprep Spin Miniprep Kit from Qiagen Ltd. (Crawley, U.K.) according to the manufacturer's instructions. Purity and concentration of plasmid DNA was determined spectrophotometrically as described previously (Sambrook *et al.* 1987).

2.2.4. Analytical agarose gel electrophoresis

Agarose gel electrophoresis was conducted as described previously (Sambrook *et al.* 1987), using gel preparations containing 1% agarose in TAE buffer (Table 2-3) and 1 µg/ml ethidium bromide. DNA samples were mixed with 1/6 volume of DNA loading buffer (Table 1-1) before loading. GeneRuler 1kb DNA Ladder from Fermentas (Ontario, Canada) was used as a molecular size reference. Separated DNA species were visualized under ultraviolet (UV) light.

2.2.5. DNA sequencing

Sequencing reactions were carried out by the DNA Sequencing Facility (Dept. of Biochemistry, University of Oxford, Oxford) and processed on an ABI Prism 3730xl DNA Analyser. Sequence data were analysed using the software program Chromas, version 1.45.

2.3 Protein expression, purification and detection methods

2.3.1. Large-scale expression and affinity purification of recombinant fibronectin fragments

Recombinant FIII domains that were produced as either glutathione-S-transferase (GST) or His-tag fusion proteins are described in Figure 2-1 and Figure 2-2.

2.3.1.1 GST-fusion proteins

Protein expression and purification was performed as previously published (Mardon *et al.* 1994) with some modifications. Transformed cultures of BL21pLysS *E.coli* were inoculated into 50 ml of LB in the presence of 100 µg/ml ampicillin and 170 µg/ml chloramphenicol and grown overnight at 37^{o}C in a shaking incubator. Cells

were diluted 1 in 10 into 500 ml of LB with 100 µg/ml of ampicillin and 170 µg/ml of chloramphenicol and incubated until OD_{600} reaches 0.6. Protein expression was then induced with 0.1 mM (isopropyl-β-D-thiogalactopyranoside) IPTG and the cultures further incubated for 3-6 hours. Bacteria were pelleted by centrifugation at 2744 x *g* for 10 minutes at 4°C, resuspended in 15 ml ice-cold PBS per litre of culture, and lysed by freeze-thawing using liquid N_2 and sonication at 3000 µm. Protease activity was inhibited by addition of 1 mM phenylmethylsulfonyl fluoride (PMSF). Cell debris were removed by centrifugation at 32815 x *g* at 4°C for 1 hour, the supernatant was passed through 1 µm and 0.22 µm filters and Triton X-100 was added to a final concentration of 1%. The solution was then incubated with 2ml of Glutathione-Sepharose 4B beads (Pharmacia Biotech) for 5 minutes at 4°C and the beads were washed once with PBS containing 1% Triton X-100, followed by 3 washes with PBS. The fusion proteins were eluted from the beads with 3 ml of 10 mM glutathione, 50 mM Tris-HCl, pH 8.0, and the beads rinsed with 3 x 2 ml of the same buffer. Positive fractions were identified by SDS-PAGE, pooled and dialyzed against 2 x 2 L of PBS for 24 hours at 4°C. The proteins were purified by FPLC gel filtration on a Sephadex 200 column (Amersham Pharmacia Biotech), and eluted peak fractions pooled and concentrated using Vivaspin centrifugal concentrators (Sartorius Ltd, Epsom, U.K.), and stored at -80°C. Purity of the proteins was assessed by SDS-PAGE as described in Section 2.3.4. Several FIII proteins that had been produced earlier in the laboratory following the above-described protocol had previously also been analysed by electrospray mass spectrometry (Mardon *et al.* 1994; Grant *et al.* 1997) and found to be sufficiently pure for use in functional assays.

2.3.1.2 His-tag-fusion proteins

His-tag fusion FIII proteins were produced as in Section 2.3.1.1 but with the following modifications. The bacteria pellet was resuspended in 15 ml of ice-cold Lysis buffer (Table 1-1) per litre of culture. The lysed culture was then incubated with 2 ml of Ni-NTA Superflow beads (Qiagen), washed 3 times with Wash buffer (Table 2-3), and the His-tag protein eluted with 5 x 4 ml Elution buffer (Table 2-3). The eluate was assessed by SDS-PAGE and mass spectrometry, and dialyzed as described in Section 2.3.1.1.

2.3.2. Affinity purification of integrins α5β1 and αvβ3

Integrins α5β1 and αvβ3 were purified from human placental tissues by affinity chromatography with Sepharose-conjugated rat anti-α5 antibody BIIG-2 and Sepharose-conjugated mouse anti-αvβ3 antibody HB11029 (both made in-house) by Mrs Céline Jones (Nuffield Dept. of Obstetrics and Gynaecology, University of Oxford, Oxford), using a method derived from (Mould *et al.* 1996; Sharma *et al.* 1997). All the buffers used below are described in Table 2-3.

Placental material was homogenized in 400 ml of ice-cold buffer A, centrifuged at 2744 x *g* for 15 minutes at 4°C and the pellet resuspended in 600 ml of ice-cold buffer A. The mixture was centrifuged again at 2744 x *g* for 15 minutes at 4°C, the pellet resuspended in 400 ml of buffer B and incubated for 1 hour at 4°C. This was finally centrifuged at 32816 x *g* first for 15 minutes and then at 48400 x *g* for 1 hour at 4°C, with the pellet discarded to remove tissue debris and any lysed material. In order to remove excess amounts of immunoglobulins present in placental preparations, the supernatant was loaded onto a protein G-Sepharose column (GE Healthcare, Chalfont,

U.K) that had been equilibrated with 10 bed volumes of Buffer C. The flow-through was then loaded onto the anti-α5 and anti-αvβ3 columns pre-equilibrated with 10 bed volumes of Buffer C, and the column washed with 2 volumes of Buffer D without Triton X-100. Finally, the integrins were eluted with 2 volumes of Buffer E in 1.5 ml fractions into neutralising 2M Tris pH8.0 and the pH adjusted to pH 7.4. The fractions were analysed by SDS-PAGE and stored at 4°C. The quality of integrin purity was determined by ELISA as described in Section 2.5.1.

2.3.3. Determination of protein concentration

The concentration of purified proteins was calculated from light absorbance data at 280nm (A_{280}), obtained with a Cecil CE 2021 spectrophotometer (Cecil Instruments Ltd., Cambridge, U.K.). The calculations were based on the known extinction coefficient (ε) values that were specific for each protein. The formula used was as follows:

$$\text{Protein concentration (mg/ml)} = \frac{A_{280} \times \text{protein molecular weight (g mol}^{-1})}{\varepsilon\ (\text{M}^{-1}\ \text{cm}^{-1}) \times \text{length of the light path (cm)}}$$

2.3.3.1 Coomassie assay

Total protein concentrations of cell lysates were determined by the Coomassie Plus Protein assay (Pierce Ltd., Tattenhall, U.K.). The method is based on the Bradford protein assay; Coomassie Plus Assay reagent was added to equal volumes of sample and standards, mixed and the absorbance at 595 nm was measured. Protein concentration was determined using a bovine serum albumin (BSA) standard curve.

2.3.3.2 *DC* protein assay

The *DC* (detergent compatible) protein assay (BioRad, Hemel Hempstead, U.K.) was used to measure protein concentration following detergent solubilization. Briefly, 5 µl of sample was mixed with 25 µl reagent A and 200 µl reagent B in wells of a 96-well plate (Nunc), and the absorbance at 750 nm was measured.

2.3.4. Analysis of proteins by SDS-PAGE

Electrophoresis on SDS-polyacrylamide gels with acrylamide content varying from 6% to 12% was conducted as described elsewhere (Laemmli 1970). Protein samples to be analysed were mixed with 1/6 volume of protein loading buffer (Table 2-3), boiled for 5 minutes and loaded onto gels prepared according to the recommendations by (Sambrook *et al.* 1989) using reagents provided by BioRad. Broad-range molecular weight markers were also purchased from BioRad. Proteins were visualized and the purity estimated by staining the gels with GelCode Blue Stain reagent (Pierce).

2.3.5. Immunoblotting and antibody detection of proteins

The transfer of gel-separated proteins onto a nitrocellulose membrane (BioRad) or PVDF membrane (GE Healthcare) was achieved by using a semi-dry electroblotting apparatus (BioRad) and following the manufacturer's instructions. Western blotting was performed in 25 mM Tris-HCl, 192 mM glycine, 20% methanol, for 30 minutes at 15V. PVDF membranes were used when stripping and reprobing of the same membrane was needed as in Section 2.7.1, the PVDF membrane was pre-soaked in ethanol for 30 seconds before using.

The transferred proteins were detected with appropriate antibodies using the following method. After membranes were incubated with 5% milk (Marvel skimmed milk powder) in western buffer (WB, Table 2-3) for 1 hour at room temperature, they were washed 3 x 10 minutes with WB and incubated with the primary mouse monoclonal antibodies (Table 2-4) in WB containing 1% milk overnight at 4^{o}C. In addition the membranes were blotted for β-actin as a loading control. The filters were then rinsed with 3 washes of WB and incubated with 50 ng/ml HRP-conjugated sheep anti-mouse IgG secondary antibody in 1% milk in WB for 1 hour at room temperature. After final washes with WB (3 x 30 minutes), an enhanced chemiluminescence (ECL) substrate (ECL Plus Western Blotting Detection Reagent, GE Healthcare) was applied in accordance with the manufacturer's specifications and the signal recorded on an X-ray film.

To allow for reprobing for a different protein on PVDF membranes, antibodies were stripped off the membrane by soaking in boiling stripping membrane buffer (Table 2-3) for 5 minutes twice. The membrane was then blocked in 5% milk in WB and incubated with primary and secondary antibodies as above.

2.4 Crystallization trials

His-tag FIII7-12A+B- and FIII8-12A+B- were expressed and purified as described in Section 2.3.1.2 for crystallization studies. The sitting drop vapour diffusion technique was used; in wells of a 96-well plate a Cartesian Robot placed 100 nl sample and 100 nl reservoir buffer in a drop, with 100 µl of reservoir buffer in the well (Oxford Protein Production Facility, Wellcome Trust Centre for Human Genetics). The plates were incubated at both room temperature and 4^{o}C. Commercially available protein crystallization screens (Hampton Research, Aliso Viejo, CA, U.S.A. and Emerald

Biosystem, Bainbridge Island, WA, U.S.A.) with approximately 700 different buffer conditions were used (Table 2-6). Additional optimization screens were used for the preliminary condition of 0.1 M sodium cacodylate pH 6.5, 1.4 M sodium acetate trihydrate for His-FIII7-12A+B-; varying pH, protein to precipitant ratio, percentage of buffer in reservoir and with additional additives.

2.5 Enzyme-linked immunosorbent assays (ELISAs)

2.5.1. Determining protein/integrin coating efficiency

The surface of a 96-well flat-bottom plate (Nunc) was coated with 50 µl of doubling dilutions of the protein of interest in ELISA Buffer (EB, Table 2-3) and incubated overnight at 4^{o}C. After washing the plate 3 times with EB, the uncoated surface was blocked with 5% BSA in EB for 1 hour at 37^{o}C. The washes were repeated and the plate incubated with 50 µl of primary antibody (Table 2-4) in EB containing 1% BSA for 2 hours at 37^{o}C. Following 3 washes with EB, an HRP-conjugated secondary antibody (1:2500 dilution of either HRP-conjugated rabbit anti-goat or HRP-conjugated sheep anti-mouse) was added in 50 µl of EB, 1% BSA, and left for 1 hour at room temperature. The washing step was repeated again and the wells incubated with 100 µl of *o*-Phenylenediamine dihydrochloride substrate (Sigma FAST OPD tablets diluted in distilled H_2O, Sigma) according to the manufacturer's instructions. Colour was allowed to develop for 1 hour before measuring optical density at 450 nm in an MRX Microplate Reader (Dynex Technologies Ltd., Billingshurst, U.K.). Data for all test proteins at each coating concentration was obtained from triplicate wells. Background binding to BSA was subtracted from all test wells.

2.5.2. Integrin-ligand binding assays

To assess ligand binding to the immobilized integrins, 96-well flat-bottomed plates (Nunc) were coated with saturating levels of the integrin in EB and left overnight at 4°C. The plates were then washed three times with EB and blocked with 5% BSA in EB for 1 hour at 37°C. The wells were washed as above, and incubated for 2 hours at 37 °C with the relevant GST-FIII fusion proteins diluted in EB containing 1% BSA. The wells were washed again 3 times with EB, and mouse anti-GST antibody (Table 2-4) in EB containing 1% BSA was added. The plates were incubated for 1 hour at room temperature, the wells washed 3 times with EB, and sheep anti-mouse HRP-conjugated antibody (1:2500 dilution) in EB containing 1% BSA was added and allowed to incubate for 1 hour at room temperature. The wells were washed as above and incubated with OPD substrate as in Section 2.5.1, and the absorbance was measured at 450 nm.

Assays were performed in triplicate, and background antibody binding in the absence of ligand was subtracted from the readings. Non-specific binding of GST fusion proteins to uncoated wells containing BSA only was measured separately for each ligand concentration point and subsequently subtracted from the corresponding values for total binding. Dose-response data from the assays were analyzed by non-linear regression using a sigmoidal curve fit as described previously (Altroff *et al.* 2001), and the apparent dissociation constant (K_D) for binding was calculated from 1-site hyperbolic binding curve fit (Prism version 4, GraphPad Inc.).

2.5.3. Modulation of FN expression in endometrial stromal cells by cytokines and growth factors

An ELISA method was used to investigate the effect of various cytokines and growth factors on fibronectin expression by ESCs. Cells were seeded at 1 x 10^4 cells/well into 96-well flat-bottomed plates (Nunc) and incubated in 10% FCS DMEM at 37^{o}C and 5% CO_2 overnight. The cells were washed with PBS and incubated with 10 ng/ml of cytokine or growth factor (Table 2-5) in 0% or 2% FCS. Control wells were identical to test wells but not treated with any cytokine.

After 48 hours of incubation, cells were washed and treated with 0.02 M NH_4OH, this lyses the cell membrane which remains attached to the matrix, releasing the contents of the cell into the well. The supernatant containing the released protein is transferred to a separate 96-well plate and total protein concentrations measured using the Coomassie Plus assay as described in Section 2.3.3.1.

The ELISA plate containing the remaining matrix was treated with 0.06% H_2O_2 in 40% methanol in PBS to neutralise any peroxidases present, washed 3 times in PBS and blocked with 1% milk in PBS for 30 minutes at 37^{o}C. Excess milk was washed off the plates with PBS. The plate was then incubated with primary antibodies (Table 2-4) to EDIIIA+FN, EDIIIB+FN and total FN, diluted in PBS. Half of the wells were antibody controls and were treated with no primary antibody. The plate was incubated for 1 hour at room temperature and washed 3 times with PBS-0.05% Tween-20 (PBS-T). Biotin-conjugated anti-mouse antibody (0.26 mg/ml) was added to all wells, incubated at room temperature for 1 hour and washed 3 times with PBS-T. The wells were then incubated with HRP-conjugated streptavidin (1 μg/ml) for 1 hour

at room temperature, and the plate washed for a final time with PBS-T and then PBS. The wells were incubated with OPD substrate as in Section 2.5.1 and the reaction was stopped after 20 minutes by 0.5 M H_2SO_4, and absorbance read at 490 nm.

The amount of EDIIIA+FN, EDIIIB+FN and total FN were calculated from FN standard curves (10-3000 ng/ml) and normalised to the amount of total protein in each well. Assays were performed in triplicate, and background antibody binding was subtracted from the readings; both the binding of primary antibody in the absence of cells, and binding in the absence of primary antibody. The minimum detection limit was 30, 50 and 200 ng/ml for total FN, EDIIIA+FN and EDIIIB+FN, respectively. Paired values of control and treated ESCs from each experiment were analyzed using paired, student t-tests (Prism version 4, GraphPad Inc.), differences were considered significant when $P \leq 0.05$. Statistical power was calculated by post hoc power analysis using G*Power (Erdfelder *et al.* 1996).

2.6 Cell adhesion assays

2.6.1. Maintenance and preparation of cells

ESC cells were maintained in appropriately supplemented DMEM as described in Section 2.1.7.2. Prior to cell adhesion assays, the subconfluent monolayer of cells was detached from the flask using trypsin-EDTA. Proteolysis was quickly stopped by the addition of soybean trypsin inhibitor and the cells collected by centrifugation. The ESCs were then washed with PBS, recentrifuged and resuspended in serum-free medium.

2.6.2. Protocols for quantification of cell attachment and spreading

The cell attachment and spreading assays were performed as described previously (Mardon *et al.* 1994) with some modifications. Replicate wells of cell-culture grade 96-well plates (Nunc) were coated with doubling dilutions of purified FIII-GST fusion proteins (Section 2.3.1.1) or full-length FN overnight at 4°C. Uncoated plastic was blocked with 1% BSA. 1 x 10^4 ESCs were seeded into each well in serum-free DMEM and incubated for 2 hours at 37°C and 5% CO_2. Adherent cells were washed gently in pre-warmed PBS and fixed with 4% glutaraldehyde, 4% formaldehyde in PBS for 5 minutes. The wells were filled with PBS, covered with coverslips and viewed by phase contrast microscopy.

To assess cell spreading, in each duplicate well 100 cells were counted and scored for either rounded or spread morphology. Cells that appeared elongated and non-refractile with the nucleus clearly visible were scored as spread. Refractile cells with nucleus not visible were scored as round. Cell attachment was assessed by staining

the adherent cells with 0.1% crystal violet in ethanol for 10 minutes, then solubilizing the dye with methanol for 1 hour and measuring OD_{600} in an MRX Microplate Reader. Background attachment to uncoated, BSA-blocked wells was subtracted from the optical density values for test wells. Spreading and attachment assays were both performed in duplicate in each experiment. Dose-response data from the assays were analyzed by non-linear regression using a sigmoidal curve fit, and the apparent dissociation constant (K_D) for binding was calculated from 1-site hyperbolic binding curve fit (Prism version 4, GraphPad Inc.).

2.7 FAK phosphorylation assays

2.7.1. Extraction and detection of Focal Adhesion Kinase (FAK)

ESCs were grown for 2 hours on cell-culture grade 6-well plates left uncoated or coated overnight with FIII-fusion proteins at a concentration of 100 µg/ml as described in Section 2.6.2, or held in suspension by blocking the surface of the plastic with 1% BSA. The cells seeded at 3.5 x 10^6 cells/well were then washed with pre-warmed PBS and lysed for 20 minutes on ice with 100 µl of ice-cold FAK extraction buffer (Table 2-3). The lysates were collected with a cell scraper (Nunc), transferred to an eppendorf tube and 100 µl of 2x SDS loading buffer (Table 2-3) added. The cell lysates were boiled for 5 minutes, centrifuged for 5 minutes and loaded onto an 8% SDS-PAGE gel in equal volumes (5 µl). This was subjected to electrophoresis and immunoblotting using PVDF membranes (see Section 2.3.5) for the expression of total FAK and phosphorylated FAK. The membranes were first blotted for phospho-FAK using anti-phospho-FAK, stripped and reprobed for FAK using anti-FAK (see Table 2-4 for antibodies). The relative extent of FAK phosphorylation in each sample was estimated by determining the ratio of phosphorylated FAK to total FAK.

2.8 Immunofluorescence detection methods

2.8.1. Immunohistochemistry on tissue sections

Sections from mid- and late- secretory stage human endometrial tissues (Table 2-2) were fixed in cold acetone for 10 minutes at 4°C or with 3% paraformaldehyde in PBS for 10 minutes at room temperature and non-specific IgG-binding sites blocked by incubation in 20% donkey serum for 20 minutes at room temperature. Sections were incubated with primary antibodies (Table 2-4) diluted in 0.1% BSA in PBS containing 10% normal human serum. Control sections were treated with mouse or rabbit IgGs (Beckman Coulter) at the same concentration as the primary antibody. Incubations were performed for one hour at room temperature. Sections were washed in 0.1% BSA in PBS and incubated with 8.3 µg/ml FITC-conjugated donkey anti-mouse IgG or FITC-conjugated donkey anti-rabbit IgG for 45–50 minutes at room temperature. Sections were washed as described above and mounted using Vectashield mountant (Vector Laboratories Ltd, UK), which incorporates the dye 4',6-diamidino-2-phenylindole (DAPI) to allow for visualization of the cell nuclei. Slides were stored in the dark at 4°C.

2.8.2. Immunocytochemistry on cultured cell lines

2.8.2.1 Preparation of samples

Cells to be analysed by immunocytochemistry were prepared as before (Section 2.1.7.2) and grown for 2 hours on sterile BSA-blocked glass coverslips coated overnight with 10 µg/ml of fibronectin or 100 µg/ml of GST-FIII fusion proteins. After incubation, cells were washed twice in pre-warmed PBS and fixed with 3% paraformaldehyde in PBS for 5 minutes at room temperature, followed by incubation

in cytoskeletal permeabilization buffer (Table 2-3) for 5 minutes and blocked in 3% BSA in PBS for 10 minutes.

To assess ECM expression of *in vitro* decidualized ESCs by immunocytochemistry, cells were seeded into glass coverslips in cell-culture grade 4-well plates and prepared as before (Section 2.1.7.3). At 6 days after induction of decidualization, coverslips were fixed and blocked as above but not permeabilized.

2.8.2.2 Staining protocols

Coverslips were incubated with primary antibodies (Table 2-4) diluted in 0.1% BSA in PBS for 1 hour at room temperature, followed by washing in 0.1% BSA in PBS three times. This was followed by incubation with FITC-conjugated anti-mouse IgG or FITC-conjugated anti-rabbit IgG antibody, used at 20 μg/ml in PBS containing 0.1% BSA, for 45 minutes at room temperature in the dark. To visualize polymerized actin, cells were incubated for 1 hour with texas-red phalloidin (200 U/ml). The coverslips were then washed as above and inverted over a drop of Vectashield mounting medium containing DAPI onto glass microscope slides and stored in the dark at 4^{o}C. Mouse IgG substituted for the primary antibody at 10 μg/ml was used as a negative control.

2.9 Cell proliferation assay

2.9.1. Maintenance and preparation of cells

ESC cells maintained as described previously (Section 2.1.7.2) were grown to confluence and serum-starved overnight in serum-free DMEM. The cells were detached using trypsin-EDTA, proteolysis stopped by trypsin inhibitor and the cells collected by centrifugation. The ESCs were then washed with PBS, recentrifuged and resuspended at 1 x 10^5 cells/ml in proliferation medium (phenol-red free DMEM, 2 mM L-glutamine, 0.2% FCS).

2.9.2. Proliferation assays with immobilised fibronectin

Replicate wells of a 96-well plate (Nunc) were coated with 100 μg/ml of GST-FIII fusion protein (Section 2.3.1.1) diluted in PBS overnight at 4^{o}C. Following two washes with PBS, the wells were blocked for at least 1 hour in 0.05% milk in PBS and washed again with PBS. ESCs were seeded at a density of 1 x 10^4 cells/well into each well and cell growth was measured at 24 and 72 hours.

2.9.3. Determining cell growth

The cell proliferation reagent Wst-1 (Roche Applied Science, Burgess Hill, U.K.) was used to assay cell growth. The reagent Wst-1 is cleaved to formazan by mitochondrial dehydrogenases, the amount of formazan formed correlates with the number of metabolically active cells present. Wst-1 was added to the wells at the last hour of incubation at 10 μl/well and absorbance was measured at 450 nm. Assays were performed in triplicate and optical densities were normalised as a percentage of the control where no FN was present. Background measurements in wells where no cells were present were subtracted from the readings.

2.10 *In vitro* blastocyst adhesion model

2.10.1. Human embryo culture

The experiments were performed with ethical approval from OxREC and the Human Fertilisation and Embryology Authority (HFEA), and were carried out by Ms Janet Carver (Nuffield Dept. of Obstetrics and Gynaecology, University of Oxford, Oxford). All the embryos in this study were donated for research with informed consent by couples attending the Oxford Fertility Unit, John Radcliffe Hospital, Oxford. Ovarian stimulation, IVF and embryo culture until day 2 were performed as previously described (Martin *et al.* 1998). Day 2 human embryos were cultured in BlastAssist medium (Medicult, Denmark) until they reached the expanded blastocyst stage (days 5–7).

2.10.2. Embryo attachment assays

Hatched human blastocysts were transferred onto a confluent layer of ESCs on a coverslip in a single well of a 4-well plate, and cultured in 500 µl of serum-free DMEM containing 2.5% HSA as described previously (Carver *et al.* 2003). The co-cultures of embryos and stromal cells were incubated with 50 µM of EDIIIA protein (n=16) for 48 hours and assessed for attachment every 24 hours by gently shaking the culture dish three times for 3 seconds each. Co-cultures of embryos and stromal cells with no EDIIIA added (n=15) were used as controls. Observation was performed after 24 or 48 hours of culture using a Leitz Fluovert FU microscope (Leitz, Germany), and Hoffman modulation contrast images captured using a camera (Photomic Science).

2.10.3. Immunofluorescent labelling of human blastocysts

Coverslip co-cultures of embryo and ESCs, as well as blastocysts cultured on glass coverslips pre-coated with 100 μg/ml of GST-FIII7-12A+B- for 48 hours, were fixed, permeabilized and stained using a modification of the protocol described above for staining of ESC cells (Section 2.8.2). Blastocysts were fixed with 3% paraformaldehyde in PBS for 10 minutes at room temperature, followed by incubation in cytoskeletal permeabilization buffer (Table 2-3) for 10 minutes and finally blocked in 1% BSA in PBS for 10 minutes.

Blastocysts were treated with rabbit anti-human integrin α9 (rabbit polyclonal), mouse anti-human α9β1 (clone Y9A2) and mouse anti-human α4 (clone 44H6) antibodies (Table 2-4), and negative controls were treated with mouse IgG or rabbit IgG. FITC-conjugated donkey anti-mouse IgG and FITC-conjugated donkey anti-rabbit IgG antibodies were used as secondary antibody. Actin was visualized by incubation with Texas Red-conjugated phalloidin. Embryos were mounted in Vectashield containing DAPI.

2.11 Data analysis

2.11.1. General data processing, statistical analysis and molecular graphics

Analysis and graphical representation of numerical data was facilitated by the use of software programs Microsoft Office Excel 2003 and Prism version 4.0 (GraphPad Software, San Diego, CA, U.S.A.). Prism was used primarily for statistical analyses including student t-tests, error handling, K_D determinations, data normalization and data processing such as nonlinear regression analysis and curve fitting. Statistical

power was calculated by post hoc power analysis using G*Power Version 3.0.3 (Erdfelder *et al.* 1996).

All experimental data presented in this thesis are either given at the originally assessed value or represented as arithmetic means of a number of determinations, together with positive and/or negative values of the standard error of the mean (S.E.M.).

Graphical manipulation of protein crystallographic data was achieved with the program RasMol, version 2.7.3 (R. Sayle, Glaxo Wellcome Research & Development, Stevenage, U.K.). Atomic coordinates were retrieved from the Protein Data Bank (Brookhaven National Laboratory, Upton, NY, U.S.A.).

2.11.2. Densitometric quantification of immunoblotting

ECL signals recorded on X-ray film during immunoblotting experiments were quantified by digitalizing the images by scanning and determining the density of the bands with the software program Bio Image Intelligent Quantifier, version 2.1 (Bio Image, Crewe, U.K.).

2.11.3. Image capturing and analysis

Immunofluorescent staining of cells prepared as described in Section 2.8 and 2.10.3 was viewed using a Leica DMRBE microscope (Leica, U.K.). Image capture and analysis was achieved by the use of Openlab image capture and manipulation software (Improvision Ltd., UK). Images were captured using equal exposure times for each ECM component in each individual experiment in Chapter 3 and for each blastocyst in Chapter 5.

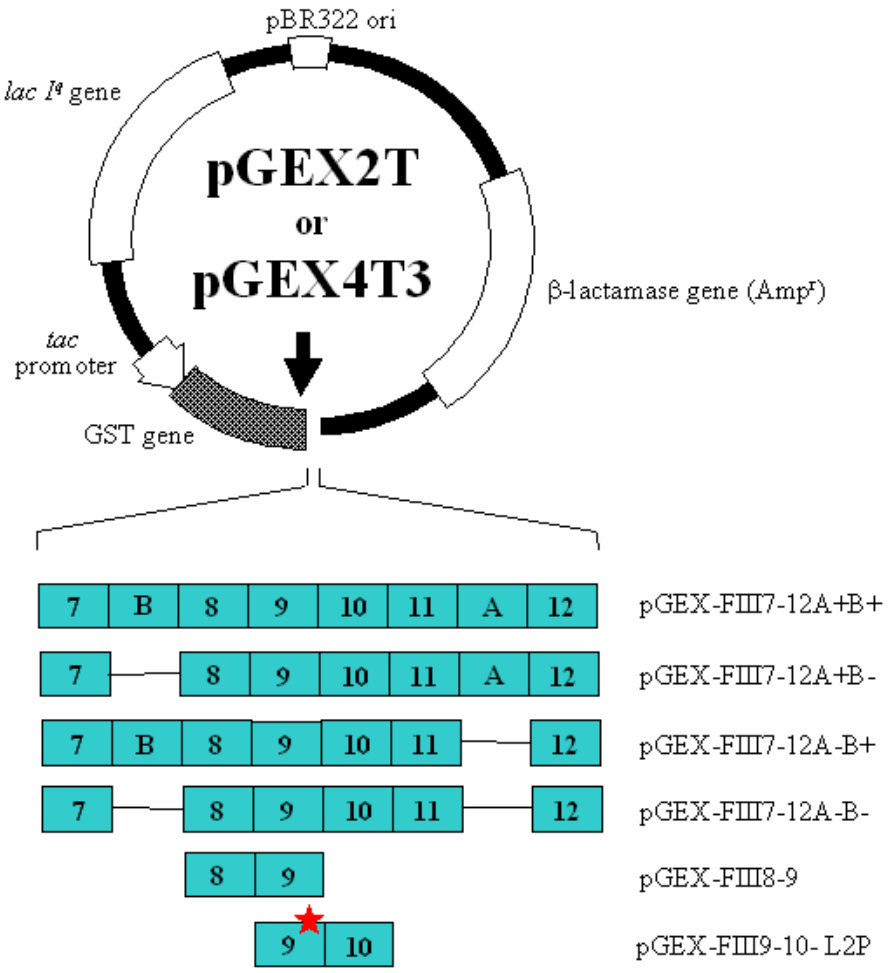

Figure 2-1 Diagram of pGEX constructs used for the expression of FIII proteins.

Blue colour stands for regions encoding intact FIII domains, red star for point mutation. Black arrow denotes thrombin cleavage site. Red star denotes L2P mutation: Leu1408 to Pro substitution in FIII9 which confers better conformational stability and functional activity (van der Walle *et al.* 2002).

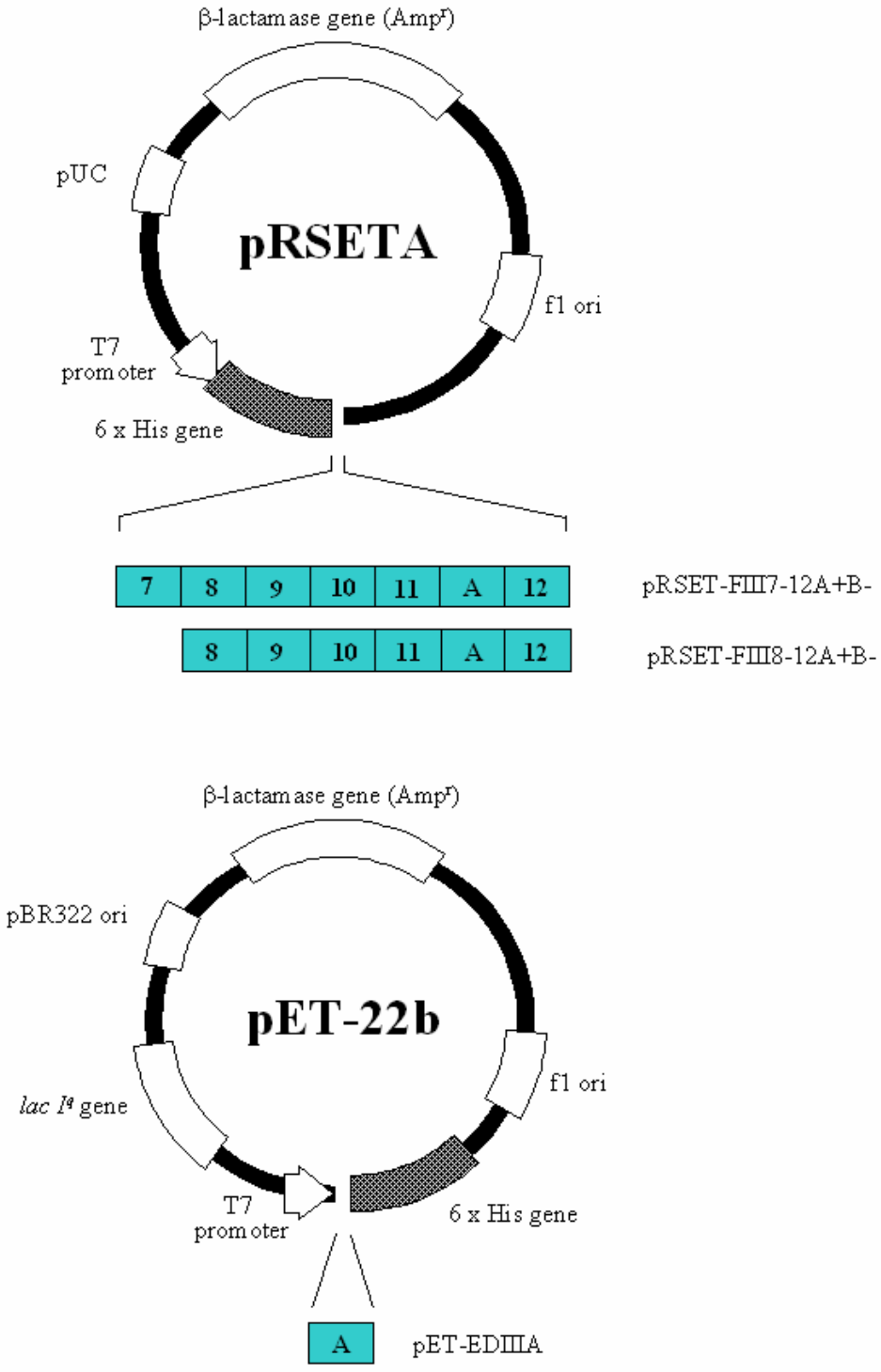

Figure 2-2 Diagram of pRSET and pET constructs used for the expression of FIII proteins, blue colour stands for regions encoding intact FIII domains.

Cells	Age	Parity	Reason for surgery	Day from LMP
629S	48	3+4	TAH for mennorhagia	21
706S	32	3+0	Pipelle biopsy from hysteroscopy	22
778S	36	4+0	Laparoscopy/sterilization	21
862S	40	1+3	Benign ovarian cysts	22
890S	35	3+1	Laparoscopy/sterilization	20
984S	41	0+0	Fibroids	21

Table 2-1 Details of ESCs used

Tissue	Age	Parity	Reason for surgery	Day from LMP
317	47	5+1	TAH for menorhagia	25
592	54	3+1	TAH for menorhagia	21

Table 2-2 Details of endometrial tissues used as controls for immunohistochemical staining.

Buffer name	Composition
DNA loading buffer (6x)	0.25 % bromophenol blue, 0.25 % xylene cyanol FF, 30% glycerol in water
TAE buffer (50x)	2 M Tris acetate, 0.2 M EDTA pH 8.0
Cell lysis buffer	50 mM NaF, 1 mM EDTA, 50 mM Tris-HCl pH 8, 150 mM NaCl, 1 mM Na_3VO_4, 1 mM EGTA, 1% Triton X-100, 1 cOmplete protease inhibitor cocktail tablet (Roche) in water
FAK extraction buffer	2% SDS, 1 mM EDTA, 1 mM EGTA, protease inhibitor cocktail, phosphatase inhibitor cocktail 1, phosphatase inhibitor cocktail 2 (all three cocktails from Roche), in water
Permeabilization buffer	10 mmol/l HEPES, pH 7.4, 200 mmol/l sucrose, 3 mmol/l $MgCl_2$, 50 mmol/l NaCl, 0.5% Triton X-100, 0.2% NaN_3 in PBS
Thrombin cleavage buffer	2.5 mM $CaCl_2$, 150 mM NaCl, 50 mM Tris-HCl pH 7.5
Lysis buffer	50 mM NaH_2PO_4, 300 mM NaCl, 10mM Imidazole, pH 8 in water, 0.2 µm filtered
Wash buffer	50 mM NaH_2PO_4, 300 mM NaCl, 20 mM Imidazole, pH 8 in water, 0.2 µm filtered
Elution buffer	50 mM NaH_2PO_4, 300 mM NaCl, 250 mM Imidazole, pH 8 in water, 0.2 µm filtered
Phosphate-buffered saline (PBS)	phosphate-buffered saline from PBS tablets (Oxoid Ltd., Basingstoke, U.K.)
Integrin storage buffer	150 mM NaCl, 50 mM Tris, pH 7.4, 1 mM $MnCl_2$, 0.1 mM $MgCl_2$, 0.1 mM $CaCl_2$, 30 mM octyl-β-glucoside
Tris-buffered saline (TBS)	150 mM NaCl, 25 mM Tris, pH 7.4
Integrin purification buffers A-E	
Buffer A	TBS, 1 mM PMSF
Buffer B	TBS, 2% Triton X-100, 1 mM PMSF, 10 µg/ml leupeptin
Buffer C	TBS, 1 mM $CaCl_2$, 0.1% Triton X-100
Buffer D	TBS, 1 mM $CaCl_2$, 1 mM $MgCl_2$
Buffer E	10 mM NaOAc, pH 3.1 with glacial, 1 mM $MgCl_2$, 1 mM $CaCl_2$, 30 mM octyl-β-glucoside
Protein loading buffer (6x)	350 mM Tris-HCl pH6.8, 10% SDS, 35% Glycerol, 5% β-mercaptoethanol, 0.05% bromophenol blue, in water
Western buffer (WB)	PBS, 0.05% Tween 20
ELISA buffer (EB)	25 mM Tris-HCl, pH 7.4, 150 mM NaCl, 1 mM $MnCl_2$, 0.1 mM $MgCl_2$, 0.1 mM $CaCl_2$
SDS loading buffer (2x)	100mM Tris-HCl, pH 6.8, 4% SDS, 20% glycerol, 0.1% bromophenol blue, 10% β-mercaptoethanol
Membrane stripping buffer	50 mM glycine, 0.5 M NaCl, 0.1% Triton X-100, 2% SDS, pH 2.4, in water
Cytoskeletal permeabilization buffer	10 mM HEPES pH 7.4, 200 mM sucrose, 3 mM $MgCl_2$, 50 mM NaCl, 0.5% Triton X-100, 0.2% Sodium Azide

Table 2-3 Composition of buffers used.

Application	Antigen	Host Organism and Isotype	Clone	Source*	Dilution	Concentration (µg/ml)
Immunocytochemistry						
	EDIIIA+FN	mouse IgG1	IST9	OB	1:50	supernatant
	EDIIIB+FN	mouse IgG1	BC-1	gift (Carnemolla 1992)	Neat	supernatant
	Total FN	mouse IgG1	IST4	S	1:100	ascites fluid
	Collagen type I	mouse IgG1	5D8-G9	A	1:100	10
	Collagen type IV	mouse IgG1	COL-94	S	1:500	ascites fluid
	Vitronectin	mouse IgG1	BV2	C	1:20	5
	Vitronectin	mouse IgG2b	342603	R	1:100	10
	Laminin γ1	mouse IgG1	LN 82-13	I	1:200	10
	Vinculin	mouse IgG1	VIN-11-5	S	1:100	ascites fluid
	Tenascin-C	mouse IgG1	T2H5	ST	1:100	10
	Paxillin	mouse IgG1	349	BD	1:25	10
	Integrin α5	mouse IgG1	SAM-1	ST	1:100	10
	Integrin αvβ3	mouse IgG1	23C6	ST	1:100	10
Immunohistochemistry						
	Integrin α4	mouse IgG1	44H6	ST	1:100	10
	Integrin α9	rabbit	polyclonal	gift from D.Sheppard	1:100	ascites fluid
	Integrin α9β1	mouse IgG1	Y9A2	C	1:100	10
	Cytokeratin	mouse IgG1	CY-90	S	1:5	ascites fluid
	Laminin γ1	mouse IgG1	LN 82-13	I	1:100	20
	Collagen type I	mouse IgG1	5D8-G9	A	1:100	10
	Vitronectin	mouse IgG1	BV2	C	1:10	10
Immunoblotting						
	EDIIIA+FN	mouse IgG1	IST9	OB	1:200	supernatant
	Total FN	mouse IgG1	IST4	S	1:500	ascites fluid
	Collagen type I	mouse IgG1	5D8-G9	A	1:500	2
	Collagen type IV	mouse IgG1	COL-94	S	1:1000	ascites fluid
	Vitronectin	mouse IgG1	BV2	C	1:200	5
	Laminin γ1	mouse IgG1	LN82-13	I	1:1000	2
	Tenascin-C	mouse IgG1	T2H5	ST	1:500	2
	total FAK	mouse IgG1	77	BD	1:1000	0.25
	phospho-FAK (pY397)	mouse IgG1	61172	BD	1:500	0.5
	β-actin	mouse IgG1	ab8226	A	1:15000	0.067
ELISA						
	integrin α5β1	goat	polyclonal	C	1:1000	goat antisera
	integrin αvβ3	mouse IgG1	23C6	ST	1:1000	1
	GST	mouse IgG1	GST2	S	1:2000	ascites fluid
	EDIIIA+FN	mouse IgG1	IST9	OB	1:200	supernatant
	Total FN (human)	mouse IgG1	3E3	C	1:2000	0.5
	EDIIIB+FN	mouse IgG1	BC-1	gift	1:50	supernatant

Table 2-4 Details of primary antibodies used. *Supplying companies and institutions are abbreviated as follows: C, Chemicon Inc.; I, Invitrogen Life Technologies; S, Sigma-Aldrich; OB, Oxford Biotechnology; ST, Serotec; BD, Beckton Dickinson Biosciences, A; Abcam, R; R&D Systems.

Cytokine or Growth factor	Abbreviation
EGF superfamily	
Epidermal growth factor	EGF
Heparin binding epidermal growth factor	HB-EGF
IL-6 superfamily	
Interleukin-11	IL-11
Leukemia inhibitory factor	LIF
Proinflammatory cytokines	
Interleukin 1β	IL-1β
Tumour necrosis factor α	TNFα
Basic fibroblast growth factor	bFGF
Transforming growth factor β1	TGFβ

Table 2-5 Cytokines and Growth Factors used in FN ELISAs

Plate	Reference	Commercial Protein Crystallization Screen
Block 1	A1-D12	Hampton Research Crystal Screen
	E1-H12	Hampton Research Crystal Screen II
Block 2	A1-D12	Emerald Biosciences Wizard I
	E1-H12	Emerald Biosciences Wizard II
Block 3	A1-D12	Hampton Research PEG/Ion Screen
	E1-F12	Hampton Research Grid Screen PEG 6000
	G1-H12	Hampton Research Grid Screen Ammonium Sulphate
Block 4	A1-D12	Hampton Research Natrix
	E1-H12	Hampton Research Crystal Screen Cryo
Block 5	A1-B12	Hampton Research Grid Screen PEG/LiCl
	C1-D12	Hampton Research Grid Screen NaCl
	E1-F12	Hampton Research Grid Screen MPD
	G1-H12	Hampton Research Quik Screen (Na/K Phosphate)
Block I	A1-H12	Hampton Index Screen
Block SRX	A1-H12	Hampton Salt RX Screen

Table 2-6 Commercial protein crystallization screens used.

Chapter 3

Synthesis and Remodelling of ECM during *in vitro* decidualization of human endometrial stromal cells

3.1 Introduction

During the secretory phase of the menstrual cycle, the endometrial stroma undergoes pre-decidualization in preparation for potential embryo implantation. This process involves remodelling of the stromal ECM and endometrial stromal cell proliferation and differentiation to a distinct morphological and secretory phenotype, with coordinated expression of cellular products including PRL and IGFBP-1. During pregnancy, decidualization extends throughout the endometrial stroma to form a dense cellular matrix, the decidua, which regulates trophoblast invasion and provides mechanical support, protection and nourishment for the embryo (Finn 1971; Lala *et al.* 1984; Graham *et al.* 1992).

The constitutive and cycle-dependent expression of ECM proteins are well established in the human endometrium (Aplin *et al.* 1988; Beliard *et al.* 1997). Immunolocalisation of ECM components in first trimester human decidual tissue has shown that the ECM composition is different to that of non-pregnant endometrium. The pericellular distribution of basement membrane components CNIV and LN may restrict motility of decidual cells, and interstitial components FN, CNI, CNIII and CNV become less tightly packed (Aplin *et al.* 1988), perhaps to allow for the

morphological changes that occur during decidualization, and to prepare the tissue for potential implantation and subsequent trophoblast invasion into the decidua.

Previous *in vitro* decidualization studies have suggested that FAs and the cytoskeleton are disrupted during the process. Vinculin is redistributed from focal contacts in decidualized ESCs (Maruyama *et al.* 1999), and cytochalasin D which destabilizes the actin cytoskeleton accelerated cAMP-induced decidualization (Ihnatovych *et al.* 2007), suggesting that the regulation of cytoskeletal dynamics may be important for decidualization.

The factors that modulate ECM synthesis during ECM remodelling of decidualization are not known. In this chapter an *in vitro* model system for human ESC decidualization was utilized to investigate changes in the production of ECM components and FA proteins during this process.

3.2 Results

3.2.1. Endometrial stromal cells undergo decidualization in response to cAMP after six days

Human ESCs can be induced to undergo *in vitro* decidualization in response to the cAMP analogue 8-Br-cAMP (Tang *et al.* 1993; Mizuno *et al.* 1998), a membrane-permeable long-acting derivative of cAMP, it is an activator of cyclic AMP-dependent protein kinase (PKA), but is resistant to degradation by cAMP phosphodiesterase, and elicits a much more rapid response in decidualization than observed with progesterone and estrogen.

Human ESCs were cultured for three days to confluence before being induced to decidualize with 0.5 mM 8-Br-cAMP at day 0. After a further six days of culture the ESCs displayed similar morphological and biochemical changes to those observed *in vivo*, the elongated fibroblast-like ESCs became larger and rounder as decidualization progressed (Figure 3-1), and secretion of the biochemical marker PRL reached maximal levels after six days (Figure 3-2)(Tang *et al.* 1993). Measurements of PRL confirmed that ESCs treated with cAMP for six days (day 6 +cAMP) had undergone *in vitro* decidualization. Levels remained low in the culture supernatants of ESCs in the absence of cAMP (day 6 –cAMP).

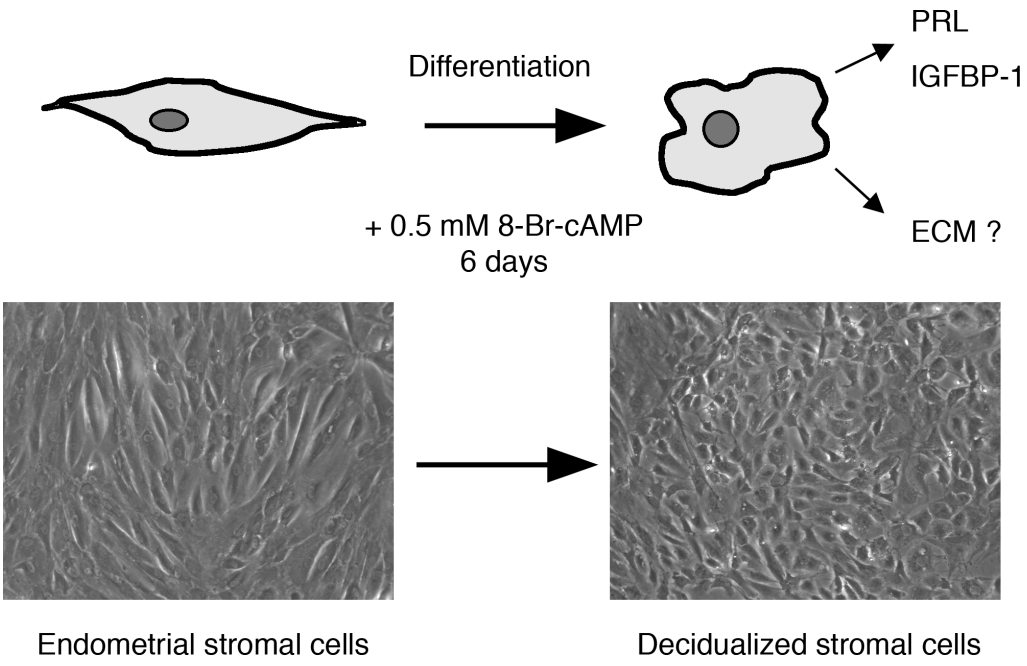

Figure 3-1 *In vitro* model for decidualization of human ESCs with 0.5 mM cAMP for six days.

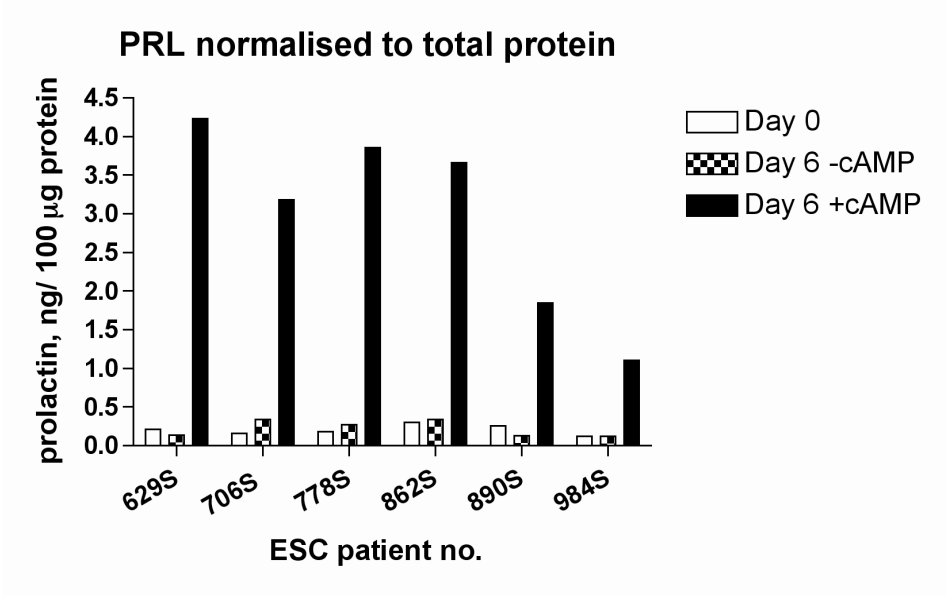

Figure 3-2 PRL measurements normalized to total protein levels from ESCs at day 0, day 6 with no cAMP and day 6 with cAMP. Bars are single PRL measurements from culture supernatants of each ESC number (n=1).

The ESCs at day 0 before cAMP induction, and at day 6 with and without cAMP treatment were assessed by immunostaining for the presence of ECM components CNI, CNIV, LN, VN, TN, FN, EDIIIA+FN and EDIIIB+FN, as well as for the FA

proteins vinculin and paxillin which additionally required cell permeabilization for intracellular localization.

Changes in levels of LN, VN, EDIIIA+FN, EDIIIB+FN, total FN and TN were further quantified by immunoblotting cell lysates of ESCs at day 0 and day 6 with and without cAMP, from at least three independent ESC cell numbers. Therefore immunofluorescence detected levels of protein in the stromal cell ECM as the ESCs were not permeabilized, whereas the immunoblotting carried out under reducing conditions assessed protein abundance in cells, as total cell lysates of ESCs were used. A number of different exposure times were taken for each immunoblot to ensure that they were not over-exposed. However, this was difficult as the signals for day 6 +cAMP cell lysates were considerably weaker than that of day 6 –cAMP, with equal amounts of total protein being loaded into each well.

3.2.2. Levels of ECM components collagen types I and IV, laminin, and vitronectin are not altered during *in vitro* decidualization of ESCs

Immunostaining of ESCs indicated no marked differences in the level and distribution of CNI (Figure 3-3, Appendix I) and CNIV (Figure 3-4, Appendix II) during cAMP-induced decidualization. The distribution of CNIV was pericellular around ESCs and levels appear to be lower in day 6 +cAMP ESCs relative to day 6 –cAMP ESCs, but only in one observed ESC patient number (Figure 3-4 b, Appendix II i-k).

There were no differences in the levels of ECM components LN and VN between decidualized and non-decidualized ESCs, as observed visually and shown quantitatively by immunoblotting. The anti-laminin antibody clone LN82-13 (Table 2-4) detects the LN γ1 fragment, which is found in most of the LN isoforms (ten of fifteen). Similar to CNIV, LN was distributed pericellularly around ESCs in both day 6 cells with and without cAMP (Figure 3-5, Appendix III). Immunoblotting demonstrates no difference in LN levels on in vitro decidualization, as the levels were not statistically significant between day 6 –cAMP and day 6 +cAMP ESCs (Figure 3-6, P = 0.135). The distribution of VN was unclear from the immunostaining using the anti-VN antibody clone BV2 (Figure 3-7 b, Appendix IV a-f), but immunostaining using a different antibody clone 342603 which is functional for immunofluorescence (Figure 3-7 a, Appendix IV g-k), and immunoblotting indicated no difference in VN production between day 6 –cAMP and day 6 +cAMP ESCs (Figure 3-8, $P = 0.662$).

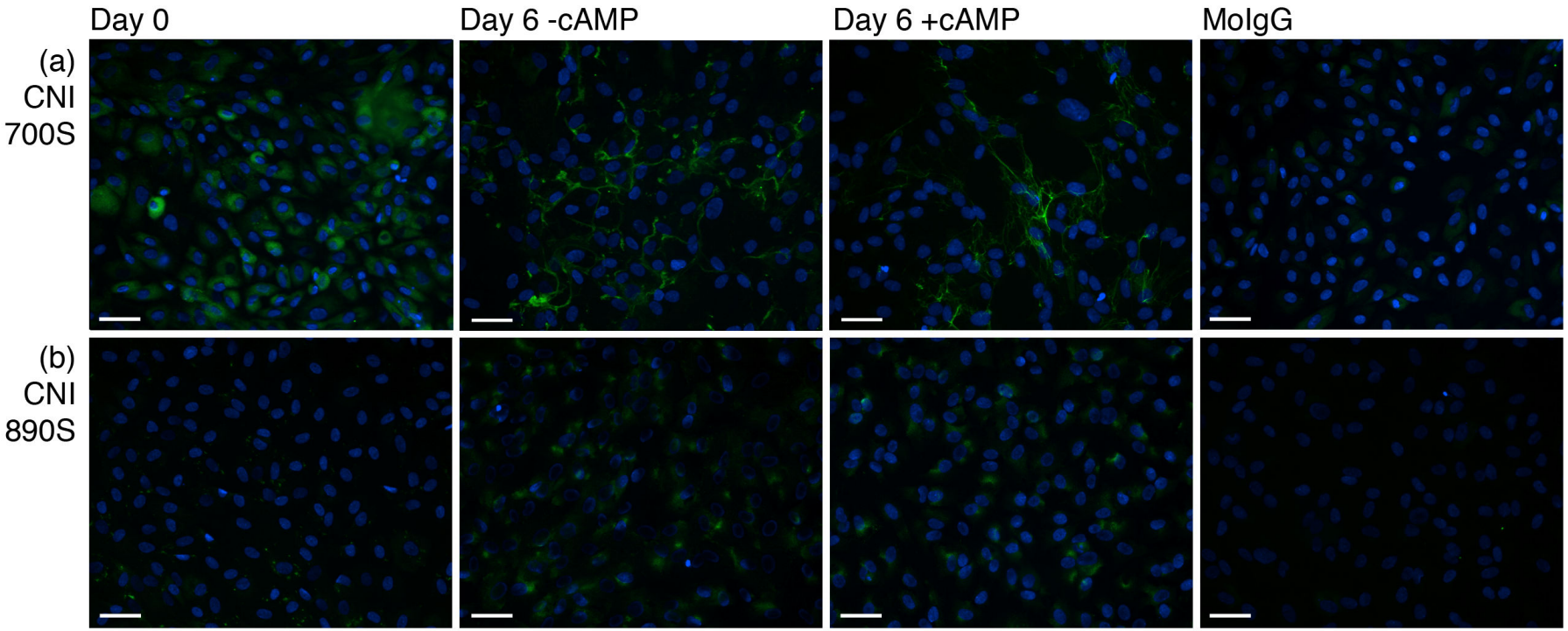

Figure 3-3 Immunofluorescence staining for CNI (a, b) produced by ESCs at day 0, day 6 and day 6 with cAMP, from two independent ESC cell numbers. CNI is in green and nuclei are in blue, images were captured using an equal exposure time, scale bars are 50 μm. See Appendix I for immunofluorescence staining of CNI in additional ESC cell numbers and at different magnifications.

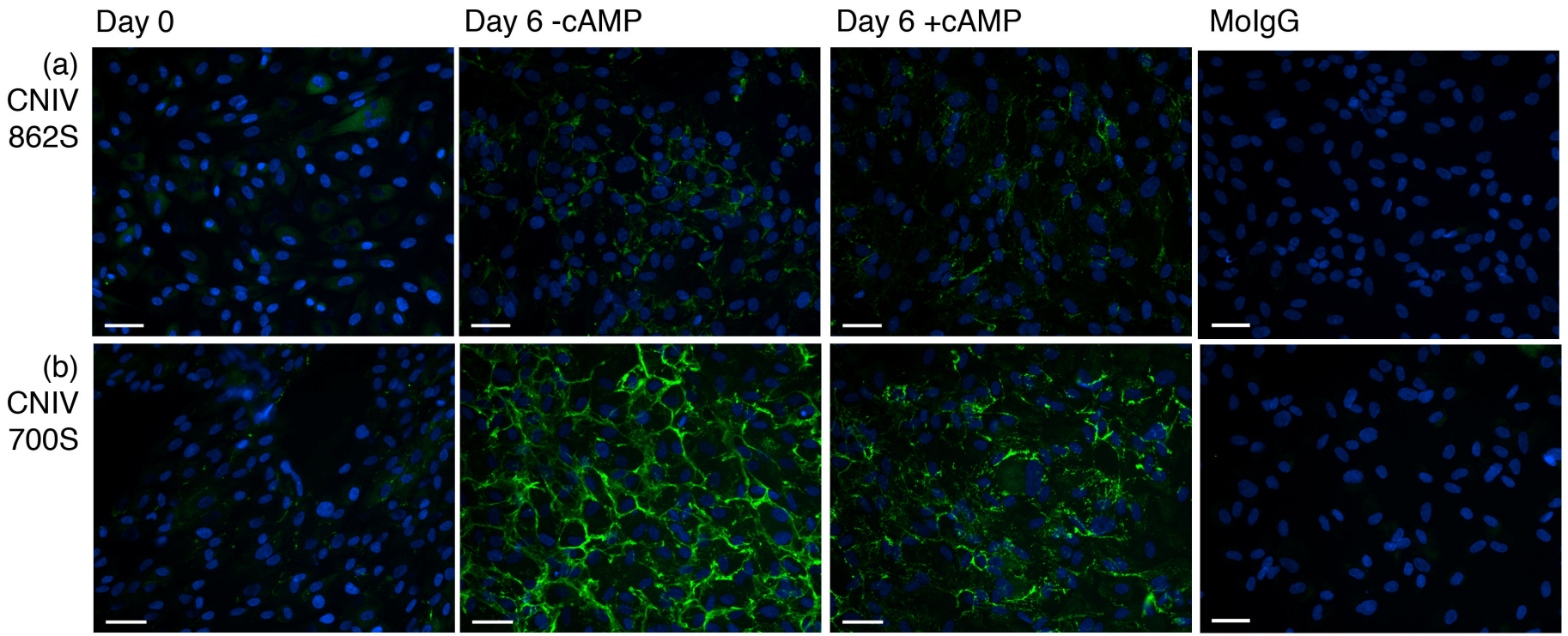

Figure 3-4 Immunofluorescence staining for CNIV (a, b) produced by ESCs at day 0, day 6 and day 6 with cAMP, from two independent ESC cell numbers. CNIV is in green and nuclei are in blue, images were captured using an equal exposure time, scale bars are 50 □m. See Appendix II for immunofluorescence staining of CNIV in additional ESC cell numbers and at different magnifications.

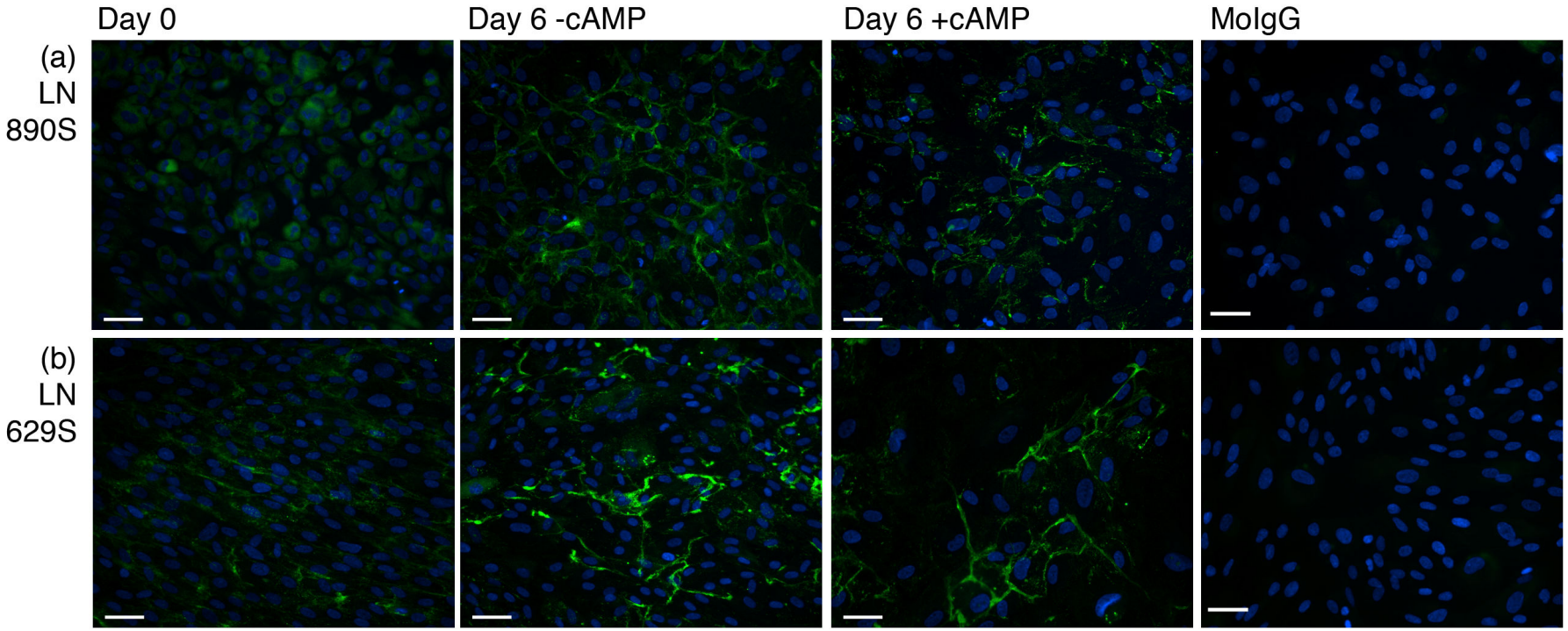

Figure 3-5 Immunofluorescence staining for LN (a, b) produced by ESCs at day 0, day 6 and day 6 with cAMP, from two independent ESC cell numbers. LN is in green and nuclei are in blue, images were captured using an equal exposure time, scale bars are 50 □m. The anti-LN antibody clone LN82-13 detects the laminin γ1 fragment, which is found in LN isoforms LN1-4. See Appendix III for immunofluorescence staining of LN in additional ESC cell numbers and at different magnifications.

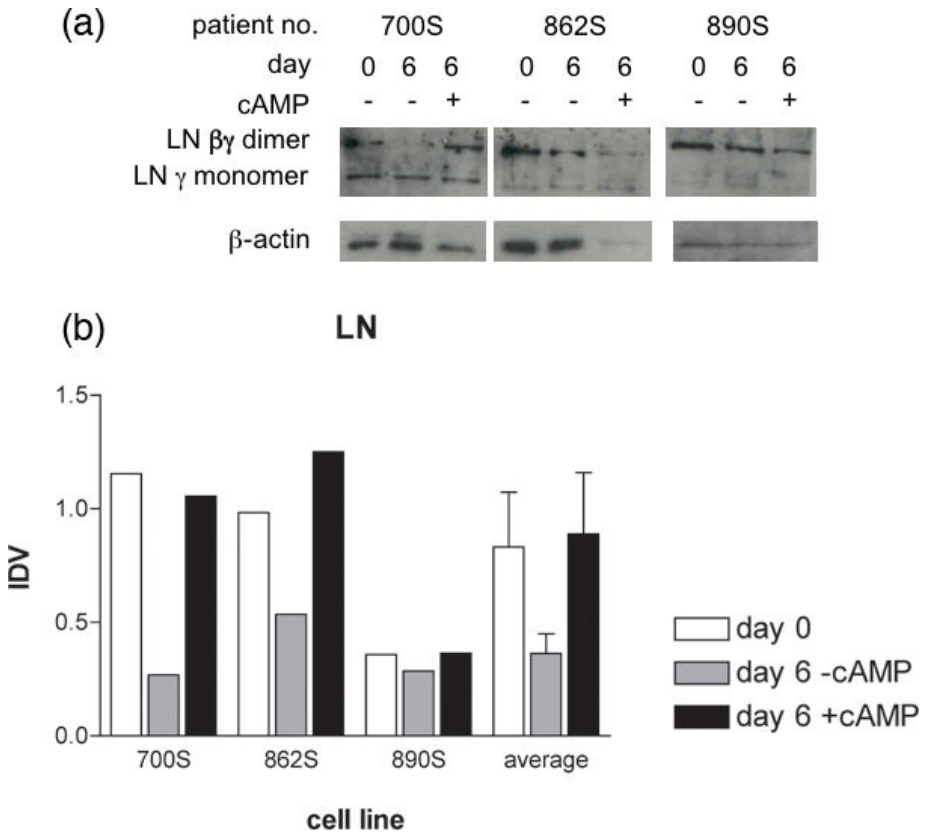

Figure 3-6 Immunoblots (a) and densitometry measurements (b) for LN in cell lysates of ESCs at day 0, day 6 and day 6 with cAMP, from three independent ESC cell numbers (n=3). 10 μg of total protein was loaded onto each lane of the gel, under reducing conditions. IDV = integrated density value, normalised to β-actin. Mean of three ESC patient cell numbers (n = 3) are shown as bars representing mean ± S.E.M. (average).

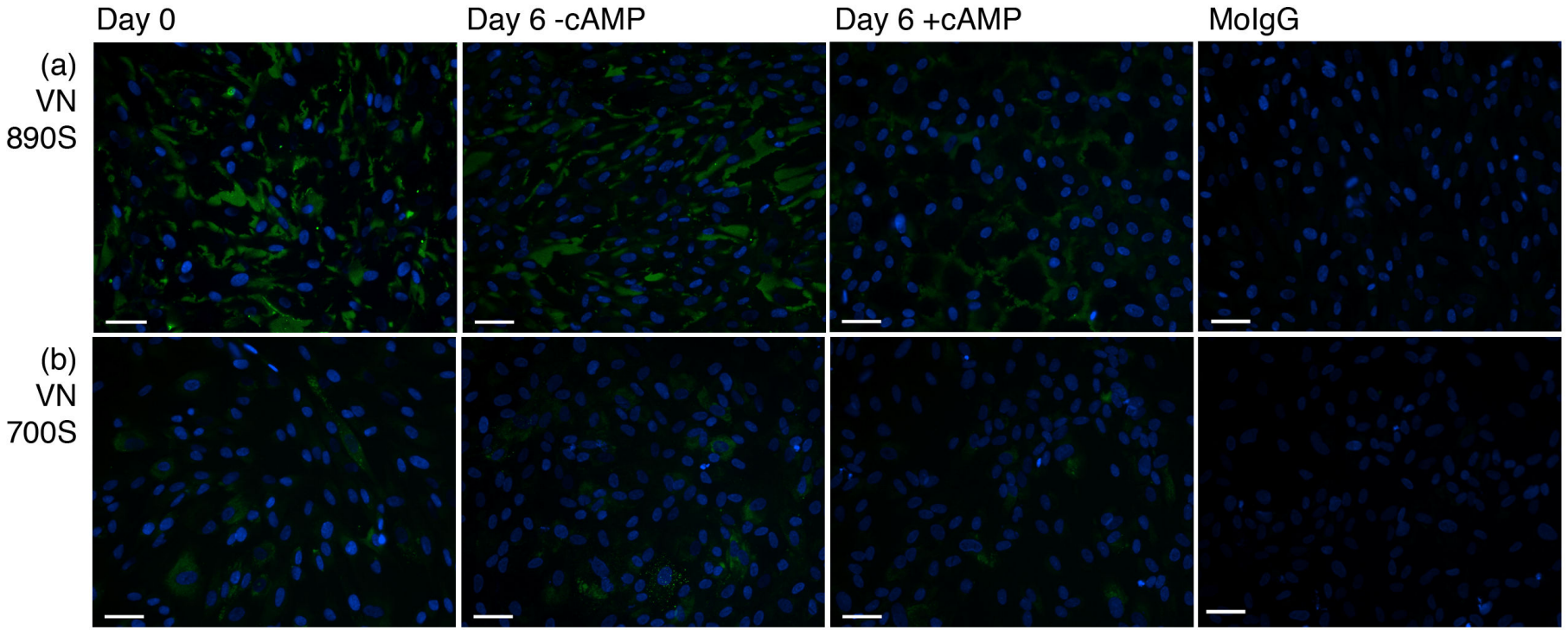

Figure 3-7 Immunofluorescence staining for VN (a, b) produced by ESCs at day 0, day 6 and day 6 with cAMP, from two independent ESC cell numbers, using anti-VN antibodies clone (a) 342603 and (b) BV2. VN is in green and nuclei are in blue, images were captured using an equal exposure time, scale bars are 50 μm. See **Appendix IV** for immunofluorescence staining of VN in additional ESC cell numbers and at different magnifications.

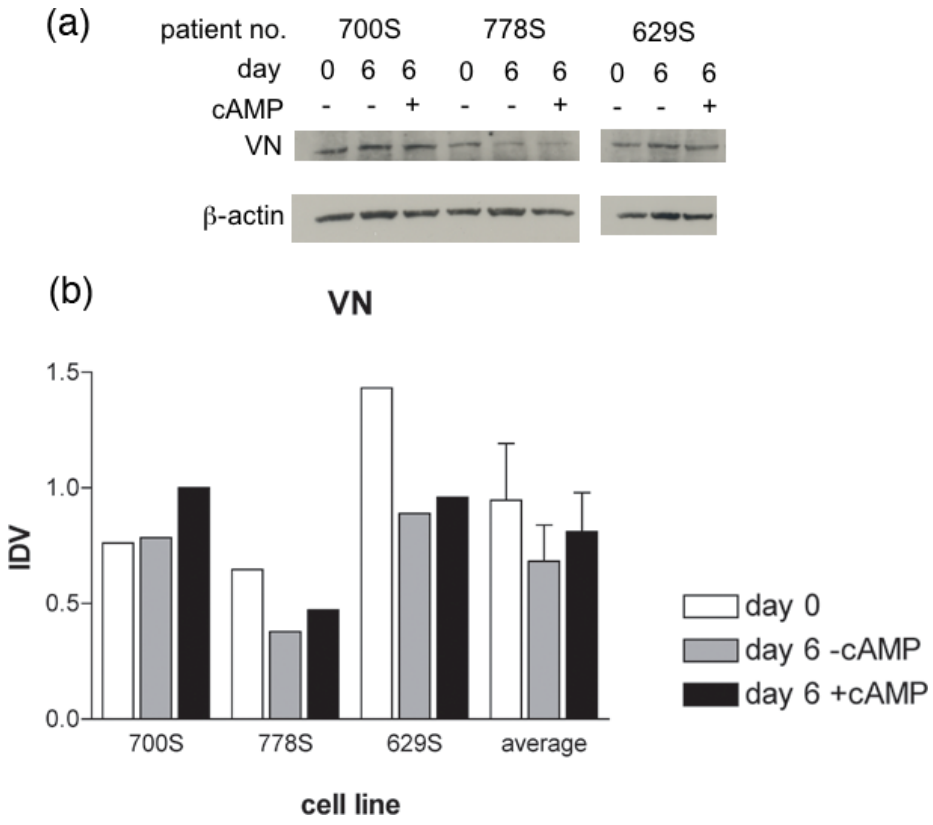

Figure 3-8 Immunoblots (a) and densitometry measurements (b) for VN in cell lysates of ESCs at day 0, day 6 and day 6 with cAMP, in three different patient ESC numbers (n=3). 10 μg of total protein was loaded onto each lane of the gel, under reducing conditions. IDV = integrated density value, normalised to β-actin. Mean of three ESC patient cell numbers (n = 3) are shown as bars representing mean ± S.E.M. (average).

3.2.3. Levels of TN, FN, EDIIIA+FN and EDIIIB+FN are modulated during *in vitro* decidualization of ESCs

The levels of TN were reduced upon decidualization in vitro, as observed visually in decidualized ESCs relative to non-induced cells in one ESC cell number (890S, Figure 3-9 a, Appendix V a-d), but this decrease was not apparent in the immunostaining of two other ESC cell numbers (700S and 629S, Figure 3-9 b, Appendix V e-h). Further quantification by immunoblotting of cell lysates from the three ESC cell numbers demonstrate that the difference in TN levels between day 6 – cAMP and day +cAMP to be statistically significant (Figure 3-10, P = 0.013), there is a lack of increase in TN levels upon decidualization in vitro. This difference in observation could be due to immunostaining detecting TN in the ECM as cells were not permeabilized, whereas immunoblotting will measure TN in the ECM and cells as total cell lysates were used. The anti-TN antibody clone T2H5 used detects the TN-C isoform, which has been shown to be expressed by endometrial stromal cells (Vollmer et al. 1997).

The production of total FN (Figure 3-11,Appendix VI) and its alternatively spliced variants EDIIIA+FN (Figure 3-12, Appendix VII) and EDIIIB+FN (Figure 3-13, Appendix VIII) was also decreased upon decidualization in vitro, as observed visually in day 6 +cAMP relative to day 6 -cAMP. This was confirmed quantitatively by immunoblotting (Figure 3-14 a) and densitometry measurements for total FN (Figure 3-14 b, P = 0.0131) and EDIIIA+FN (Figure 3-14 c, P = 0.0042) demonstrated the decrease in levels to be statistically significant between day 6 and day 6 +cAMP ESCs. The antibodies used to detect FN do not detect bovine FN, so detect only FN that has been synthesised and deposited by ESCs and not incorporated from the FCS.

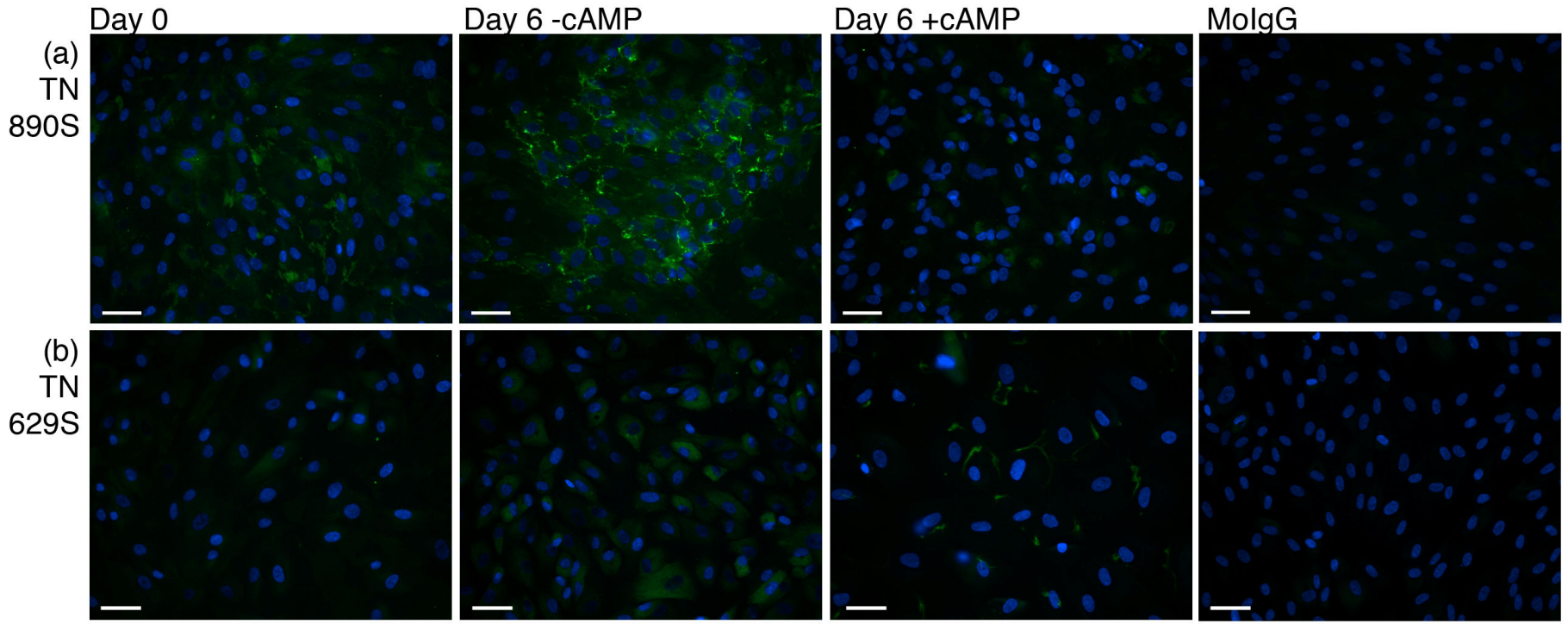

Figure 3-9 Immunofluorescence staining for TN produced by ESCs at day 0, day 6 and day 6 with cAMP, from two independent ESC cell numbers. TN is in green and nuclei in blue, images were captured using an equal exposure time, scale bars are 50 μm. See Appendix V for immunofluorescence staining of TN in additional ESC cell numbers and at different magnifications.

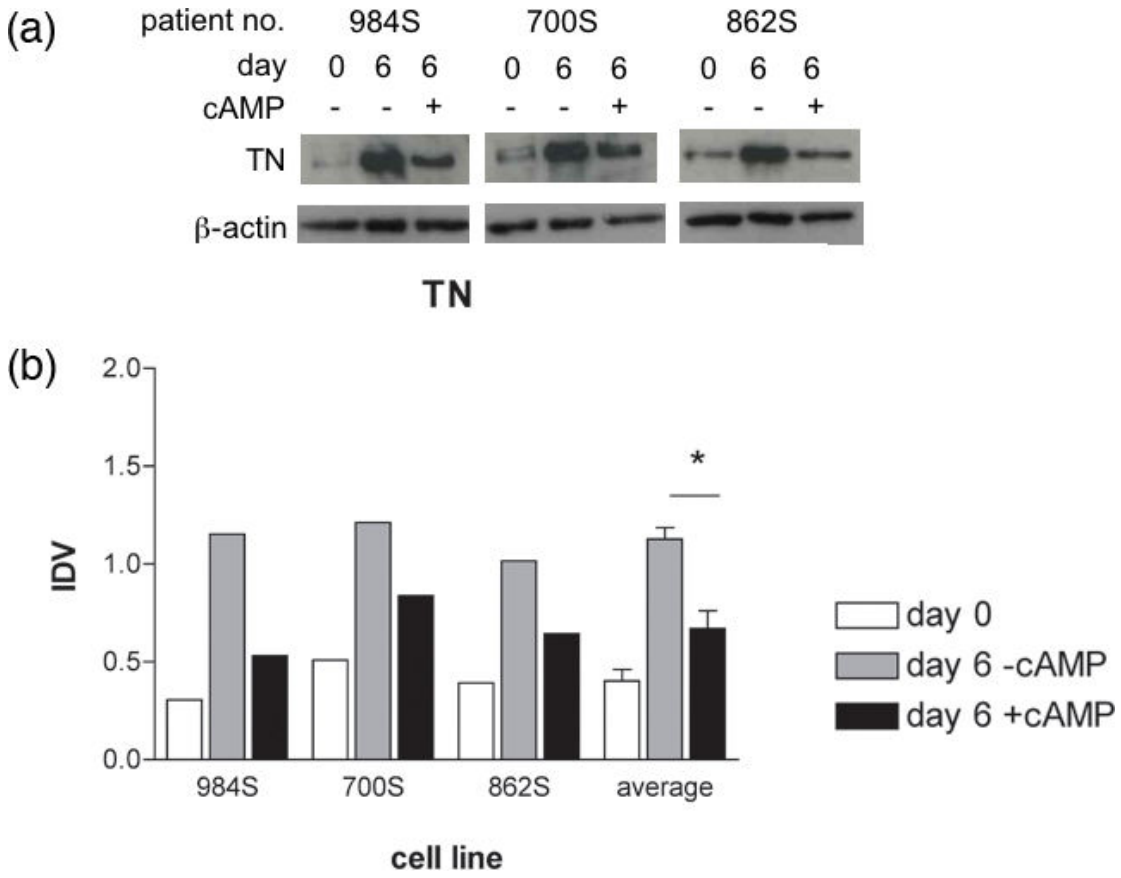

Figure 3-10 Immunoblots (a) and densitometry measurements (b) for TN in cell lysates of ESCs at day 0, day 6 and day 6 with cAMP, from three independent cell numbers (n=3). 10 µg of total protein was loaded onto each lane of the gel, under reducing conditions. IDV = integrated density value, normalised to β-actin. Mean of three ESC patient cell numbers (n = 3) are shown as bars representing mean ± S.E.M. (average), data were analyzed using student t-tests, differences between day 6 ESCs with and without cAMP were considered significant when $P \leq 0.05$ (*).

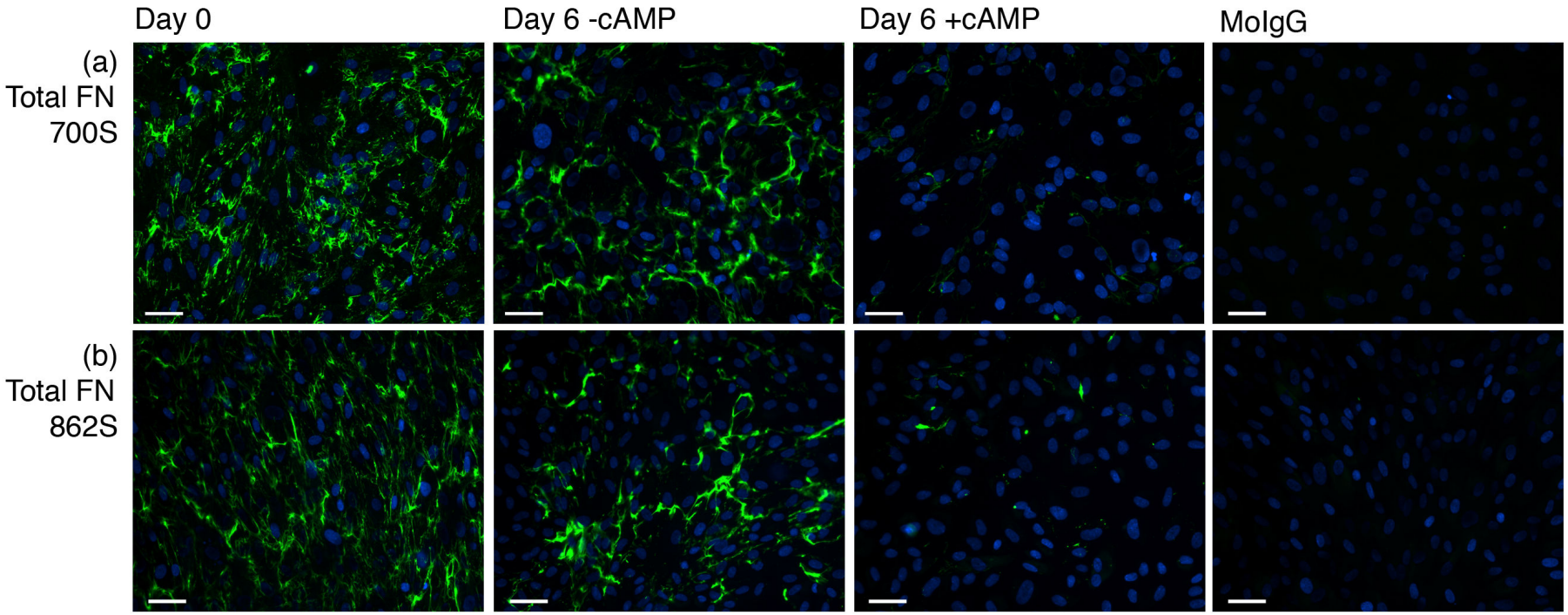

Figure 3-11 Immunofluorescence staining for total FN produced by ESCs at day 0, day 6 and day 6 with cAMP, from two independent ESC cell numbers. FNs are in green and nuclei are in blue, images were captured using an equal exposure time, scale bars are 50 μm. See Appendix VI for immunofluorescence staining of FN in additional ESC cell numbers and at different magnifications.

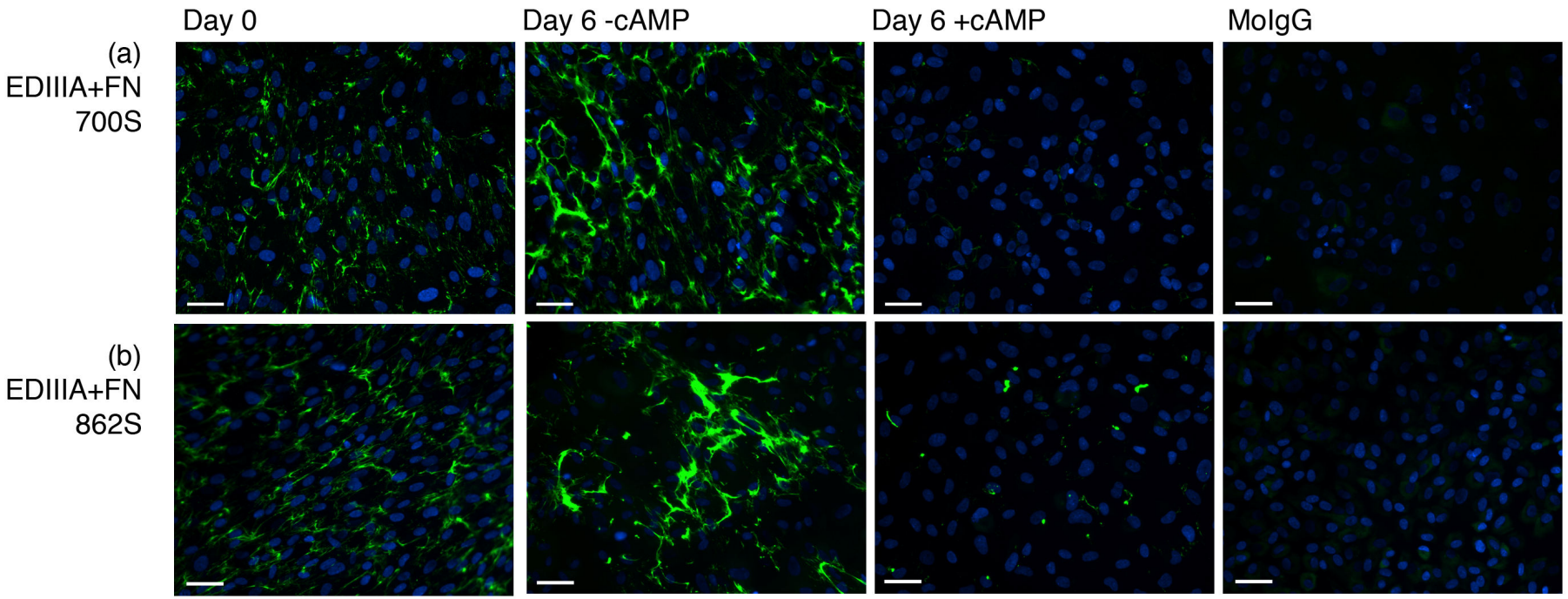

Figure 3-12 Immunofluorescence staining for EDIIIA+FN (a, b) produced by ESCs at day 0, day 6 and day 6 with cAMP, from two independent ESC cell numbers. FNs are in green and nuclei are in blue, images were captured using an equal exposure time, scale bars are 50 μm. See Appendix VII for immunofluorescence staining of LN in additional ESC cell numbers and at different magnifications.

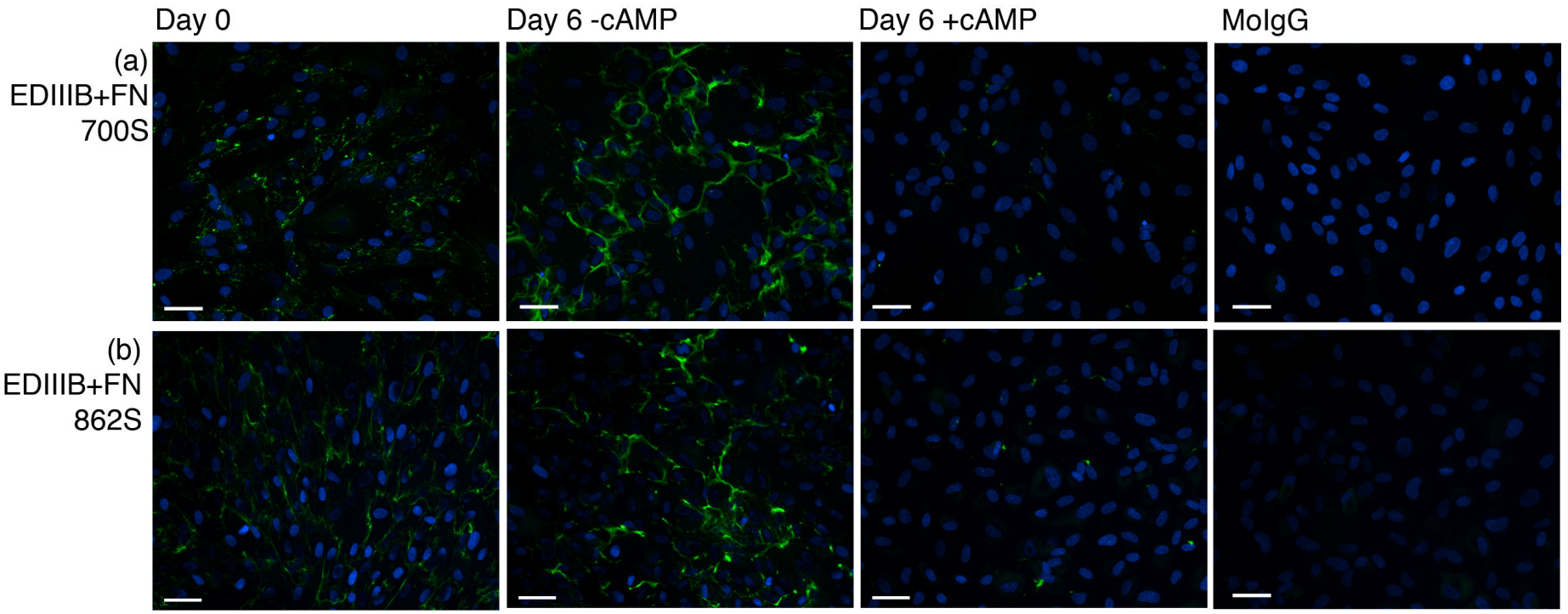

Figure 3-13 Immunofluorescence staining for EDIIIB+FN (a, b) produced by ESCs at day 0, day 6 and day 6 with cAMP, from two independent ESC cell numbers. FNs are in green and nuclei are in blue, images were captured using an equal exposure time, scale bars are 50 μm. See Appendix VIII for immunofluorescence staining of EDIIIB+FN in additional ESC cell numbers and at different magnifications.

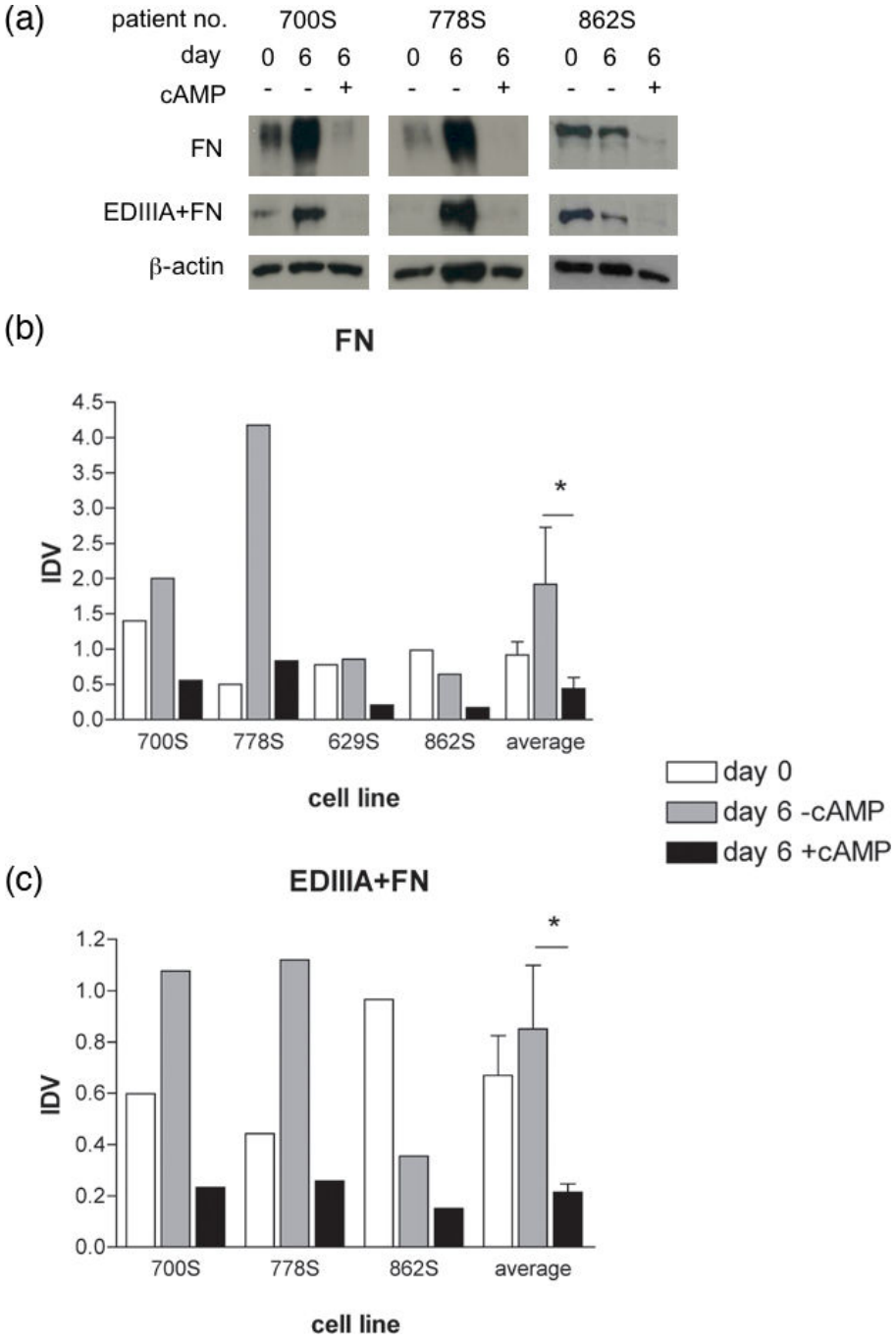

Figure 3-14 Immunoblots (a) and densitometry measurements (b, c) for FN and EDIIIA+FN in cell lysates of ESCs at day 0, day 6 and day 6 with cAMP, from three independent ESC cell numbers (n=3). 10 μg of total protein was loaded onto each lane, IDV = integrated density value, normalised to β-actin. Mean of three ESC patient cell numbers (n = 3) are shown as bars representing mean ± S.E.M. (average), data were analyzed using student t-tests, differences between day 6 ESCs with and without cAMP were considered significant when $P \leq 0.05$ (*).

3.2.4. Levels of focal adhesion proteins vinculin and paxillin appear to be reduced in response to *in vitro* decidualization of ESCs

The cytoskeletal proteins vinculin and paxillin were localized at focal adhesions in ESCs (Figure 3-15, Appendix IX and Figure 3-16, Appendix X). During *in vitro* decidualization, levels of both FA proteins appear to be reduced as their staining intensities at day 6 +cAMP were less than that of day 6 –cAMP ESCs. This difference was more evident at a higher magnification (Figure 3-17, Appendix IX c and d), and could be a result of the decreased total protein levels during *in vitro* decidualization, or redistribution from focal contacts as observed previously in the cAMP-induced decidualization of human uterine fibroblasts (Ihnatovych *et al.* 2007). Further quantification of vinculin and paxillin expression by immunoblotting is needed. Immunostaining of actin filaments also demonstrates the morphological changes of ESCs during *in vitro* decidualization, the fibroblast-like ESCs at day 0 and day 6 –cAMP become larger rounder decidualized ESCs at day 6 with cAMP, which was most evident in Figure 3-15b. It has been previously demonstrated that the production of α-smooth muscle actin to be decreased and β-actin levels remain the same during cAMP-induced decidualization of human uterine fibroblasts (Ihnatovych *et al.* 2007), thus β-actin was used as a reasonable loading control.

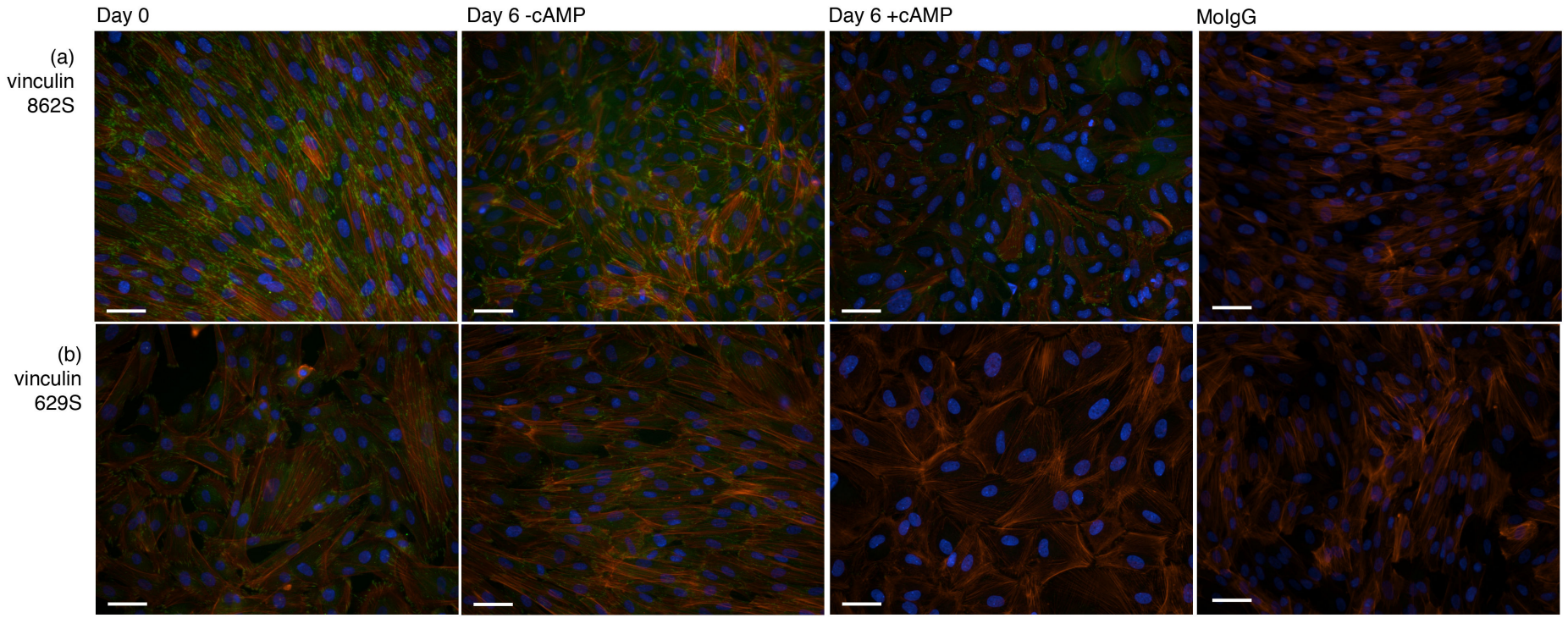

Figure 3-15 Immunofluorescence staining for vinculin produced by ESCs, at day 0, day 6 and day 6 with cAMP. Vinculin is in green, actin in red and nucleus in blue, images were captured using an equal exposure time, scale bars are 50 μm, two independent ESC cell numbers are shown. See Appendix IX for immunofluorescence staining of vinculin in additional ESC cell numbers and at different magnifications.

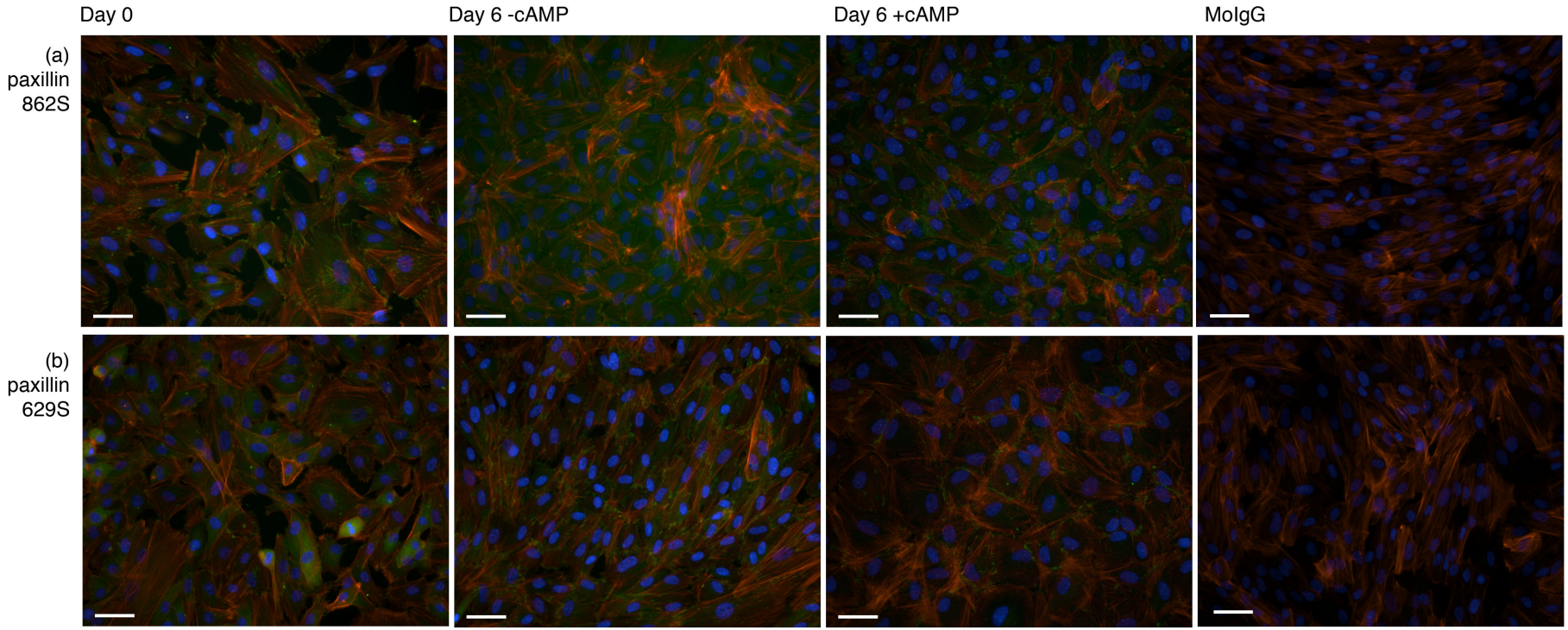

Figure 3-16 Immunofluorescence staining for paxillin (a, b) produced by ESCs at day 0, day 6 and day 6 with cAMP. FA proteins are in green, actin in red and nucleus in blue, images were captured using an equal exposure time, scale bars are 50 μm, two independent ESC cell numbers are shown. See Appendix X for immunofluorescence staining of paxillin in additional ESC cell numbers and magnifications.

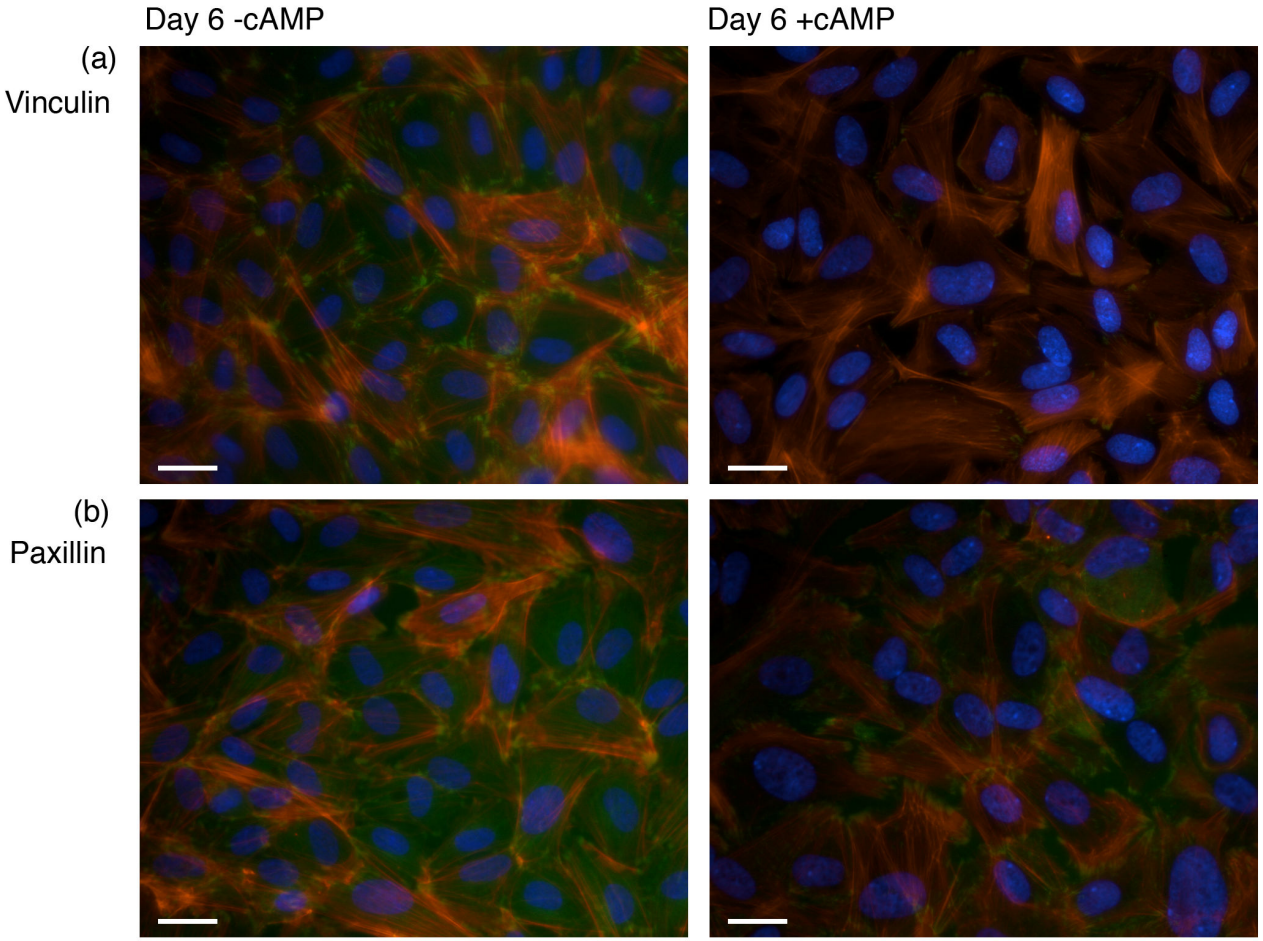

Figure 3-17 Immunofluorescence staining for (a) vinculin and (b) paxillin produced by ESCs at day 6 and day 6 +cAMP. FA proteins are in green, actin in red and nucleus in blue, images were captured using an equal exposure time, scale bars are 25 μm.

3.3 Discussion

The endometrial stroma undergoes extensive differentiation in response to steroid hormones in preparation for potential embryo implantation. Here we have used an *in vitro* model for decidualization to investigate the changes that occur in the endometrial stromal ECM during decidualization, as alterations in the ECM will have implications on decidual function. ESCs induced with 8-Br-cAMP display the most rapid and strongest induction of PRL synthesis, as compared with other inducers of *in vitro* decidualization including progesterone, medroxyprogesterone acetate (MPA) and prostaglandin E_2 (Mizuno *et al.* 1998), and display the morphological and biochemical changes characteristic of decidualization *in vivo*. However, the induction of decidual markers by cAMP is transient, and the model does not reflect *in vivo* conditions as the ESCs are cultured in isolation and lack interactions with other endometrial cellular components such as epithelial cells, endothelial cells and immunological cells, which may modulate endometrial function.

There was a certain degree of variation in PRL levels between the different ESC cell numbers (Figure 3-2). This was minimized by using cells isolated at day 20-22 from LMP (Table 2-1), but there are differences in the passage number and degree of confluency of ESCs used, and biological variation between patients, such as the older age of some patients may have affected results. Also, the ESCs were grown for three days in culture to reach confluence before being induced with cAMP at day 0, this pre-confluent stage may result in the selective growth of a subset of cells, resulting in variations in PRL and ECM output.

At six days after cAMP treatment, the levels of ECM components of *in vitro* decidualized ESCs displayed a number of differences relative to non-decidualized ESCs mainly in FNs and TN, there were no significant alterations in the production of CNI, CNIV, LN and VN. A pericellular distribution of basement membrane proteins CNIV and LN (Figure 3-4 b, Figure 3-5) was observed as shown previously (Iwahashi *et al.* 1996) in fully decidualized stroma. There was an increase in CNI and CNIV expression in previous studies of first trimester decidual tissue, but this was not seen in the current immunostaining of *in vitro* decidualized ESCs (Figure 3-3 and Figure 3-4).

Immunostaining of non-decidualized and decidualized ESCs showed no major differences in levels of LN (Figure 3-5) and VN (Figure 3-7). The expression of LN has previously been shown to increase during progesterone-induced *in vitro* decidualization of ESCs (Brar *et al.* 1995). Further quantification of LN levels by immunoblotting of cell lysates, normalized to total protein levels (Figure 3-6) suggests no modulations in the protein abundance of LN in the ESCs upon *in vitro* decidualization.

The levels of total FN, EDIIIA+FN and EDIIIB+FN produced by ESCs were altered during *in vitro* decidualization, as observed visually in the reduced staining intensities in day 6 +cAMP ESCs compared to day 6 -cAMP cells (Figure 3-11, Figure 3-12 and Figure 3-13). Immunoblotting of ESC cell lysates demonstrate quantitatively the differences in the protein abundance of FN and EDIIIA+FN between ESCs at day 6 with and without cAMP to be statistically significant (Figure 3-14). The levels of EDIIIA+FN and FN appear to be less at day 6 +cAMP relative to day 0, but this could

be due to the levels of FN being normalized to total protein levels. For example, if the increase in total protein was greater than the increase in FN levels, the amount of FN present when normalized to total protein levels would appear to decrease. The lack of an increase in FN production may be the result of ECM remodelling during decidualization, or inhibition of FN expression by cAMP as seen in ovarian follicles (Bermath *et al.* 1990).

In previous studies, expression of FN and LN persists in the endometrial stroma of first trimester decidua, becoming less tightly packed and distributed pericellularly in the human decidua (Aplin *et al.* 1988; Burrows *et al.* 1995). In the current cAMP-induced model of *in vitro* decidualization, levels of FN decreased on decidualization of ESCs. Perhaps the present model resembles the pre-decidualization reaction that occurs in the secretory stage of the menstrual cycle and early stages of implantation, whereas the earlier immunolocalization studies are of first trimester decidua in the later stages of decidualization. More recently, it was observed that FN expression is decreased in ESCs induced to decidualize with hCG and progesterone, supporting our observation of reduced FN levels during decidualization (Kayisli *et al.* 2005).

Over the six days of the experiment the levels of TN increased but less so when the cells were treated with cAMP (Figure 3-10). Expression of TN is generally restricted to embryonic development and tissue remodelling processes in adults (Harrington et al. 1999; Sedele et al. 2002). In the endometrium TN displays spatial and temporal regulation; its adhesion-modulatory properties (Orend *et al.* 2000) together with its localization in the stroma adjacent to the glandular epithelium at the secretory phase of the menstrual cycle suggests TN may facilitate embryo penetration and tissue

remodelling processes of decidualization. It may achieve this by disrupting uterine cell adhesion to the underlying basal lamina (Julian *et al.* 1994), and by the loosening of stromal contacts with ECM components (Chiquet-Ehrismann 1991).

The observed modulations in FN and TN levels of the decidualized stromal cell ECM could be due to proteolytic breakdown by MMPs. Our unpublished results have shown expression of MMPs-7, 8, 14 and 15 mRNA by ESCs to be up-regulated in this cAMP-induced *in vitro* decidualization model. These MMPs all act on FN, whilst MMP-14 and 15 can degrade both FN and TN, their upregulation during *in* vitro decidualization could result in the reduced FN and TN levels in the endometrial stromal ECM.

It must be noted the differences between the two approaches, immunostaining will detect ECM proteins deposited by ESCs in the ECM as cells were not permeabilized, and immunoblotting of cell lysates will detect total protein content, both intracellular and deposited in the ECM. There are difficulties involved in the staining of structural proteins of the ECM due to the variability in their deposition, and in immunoblotting which requires the total solubilization of protein, resulting in only large differences being detected by these methods. An alternative approach would have been to investigate changes in gene expression in ESCs during *in vitro* decidualization by RT-PCR analysis, but as we are interested in the functional protein being produced by ESCs, immunofluorescence and immunoblotting were used to assess protein levels.

There are limitations in the use of cell culture models, one of them being the generation of oxidative stress in cell culture conditions (Halliwell 2003), resulting in

the production of reactive oxygen species (ROS), leading to cell apoptosis and protein modifications. The ECM is susceptible to oxidation, affecting its adhesive properties and susceptibility to degradation (Ahmed *et al.* 2003), and ROS may have a role in increasing ECM synthesis as has been demonstrated in other cell types (Ha *et al.* 2003). These may influence ECM synthesis and deposition by ESCs in the *in vitro* decidualization model, which has also been suggested to have anti-oxidative properties, as ESCs are extremely resistant to oxidative stress-induced apoptosis upon cAMP/protesterone-induced decidualization (Brosens *et al.* 2006). In the endometrium, expression of ROS and superoxide dismutases (SOD) which scavenges these superoxide radicals are increased in ESCs from the proliferative to secretory phase, and in decidualized ESCs in the decidua of early pregnancy. ESCs undergoing *in vitro* decidualization induced by E_2 and MPA also increased expression of SOD (Sugino 2007). These suggest possible roles for oxidative stress and SOD in the regulation of endometrial function and decidualization, ROS have been suggested to have proliferative effects on ESCs (Foyouzi *et al.* 2004), and SOD may protect ESCs from oxidative stress for decidualization by scavenging oxidative radicals generated. Therefore, the presence of oxidative stress in the cell culture may reflect similar conditions in the endometrium.

In summary, the results suggest that levels FNs and TN produced by ESCs to be modulated upon decidualization *in vitro*. The modified composition of the decidualized stromal cell ECM is likely to modulate cell behaviour, perhaps to allow for differentiation during decidualization. The observed decrease in levels of both cell-adhesive FNs and adhesion-modulatory TNs may provide a balance in the regulation of cell adhesive properties of the endometrial stromal ECM, to regulate

cell-ECM interactions and associated cellular processes in the endometrial stroma. The observed ECM remodelling may alter the stromal ECM to allow for potential implantation, breakdown of ECM may facilitate cell migration and embryo invasion through the endometrial stroma during implantation. The degradation of ECM will also release ECM-sequestered cytokines and growth factors, which will have further implications for decidual function.

Endometrial function and decidualization are under the control of steroid hormones, the action of which is mediated by locally acting cytokines and growth factors. The effect of cAMP during *in vitro* decidualization may be mediated by cytokines and growth factors, Chapter 4 will investigate their effect on the production of FN and its splice variants EDIIIA and EDIIIB by human ESCs. Currently the biological functions of EDIIIA+FN and EDIIIB+FN are unclear, their functional roles are further investigated in Chapter 6.

Chapter 4

Modulation of FN levels in endometrial stromal cells by endometrial cytokines and growth factors

4.1 Introduction

It is well established that endometrial function is under the overall control of steroid hormones, the actions of which are mediated locally by cytokines and growth factors. These are secreted by uterine glands, stromal fibroblasts, decidual cells and trophoblasts. They can act separately or in concert on trophoblasts, endometrial epithelium and stroma to contribute to the events of implantation, including the initial blastocyst adhesion and attachment to the endometrium, decidualization of the stroma and the invasion process.

Chapter 3 described a reduction in the levels of FN and its alternative splice variants EDIIIA and EDIIIB during cAMP-induced *in vitro* decidualization of ESCs. Since *in vitro* decidualization is controlled locally by cytokines and growth factors, the effect of endometrial cytokines and growth factors on FN production by ESCs was investigated using an ELISA as described in Section 2.5.3.

Using this assay, we assessed the effects of individual cytokines and growth factors on FN deposition. The ESCs were cultured in either 0% FCS to minimize the effects of serum, and also in 2% FCS for more physiological conditions. An ELISA using 96-well plates was chosen as the assay format, to allow for the screening of numerous

cytokines or growth factors (Table 2-5). The antibodies used to detect FN do not detect bovine FN, so detect only FN that has been synthesised and deposited by the ESCs and not incorporated from the FCS. Because the ESCs were cultured in the absence of or in minimal serum, it was not feasible to keep the cells in culture for a long period of time. Therefore the FN production was assessed after forty-eight hours of treatment, it has previously been shown that ESCs produce and deposit FN in the ECM within two hours after being seeded on tissue culture plates. The absence of serum in the culture media may contribute to the generation of oxidative stress, as serum contains anti-oxidant enzymes such as catalase and superoxide dismutase, this may result in the generation of ROS and affect the amount of FN produced by ESCs, the role of ROS in increased ECM synthesis has been demonstrated in other cell types (Ha *et al.* 2003). As mentioned in Section 3.3, oxidative stress and SOD may have roles in the regulation of endometrial function and decidualization, with ROS suggested to have proliferative effects on ESCs (Foyouzi *et al.* 2004), the presence of oxidative stress in cell culture may reflect similar conditions in the endometrium.

The levels of total FN, EDIIIA+FN and EDIIIB+FN were measured forty-eight hours after treatment with cytokines and growth factors (Table 2-5), and normalized to total protein levels in each replicate well. The measurements were then quantified using a standard curve with FIII7-12A+B+ as the standard, which is presumed to be adsorbed at random to the plastic and so should be constant between experiments. A new standard curve was generated for each experiment.

4.2 Results

4.2.1. Effect of the EGF family of growth factors on FN levels

The levels of total FN and its splice variants EDIIIA and EDIIIB by ESCs were not altered in response to EGF (Figure 4-1) or HBEGF (Figure 4-2) at both serum levels.

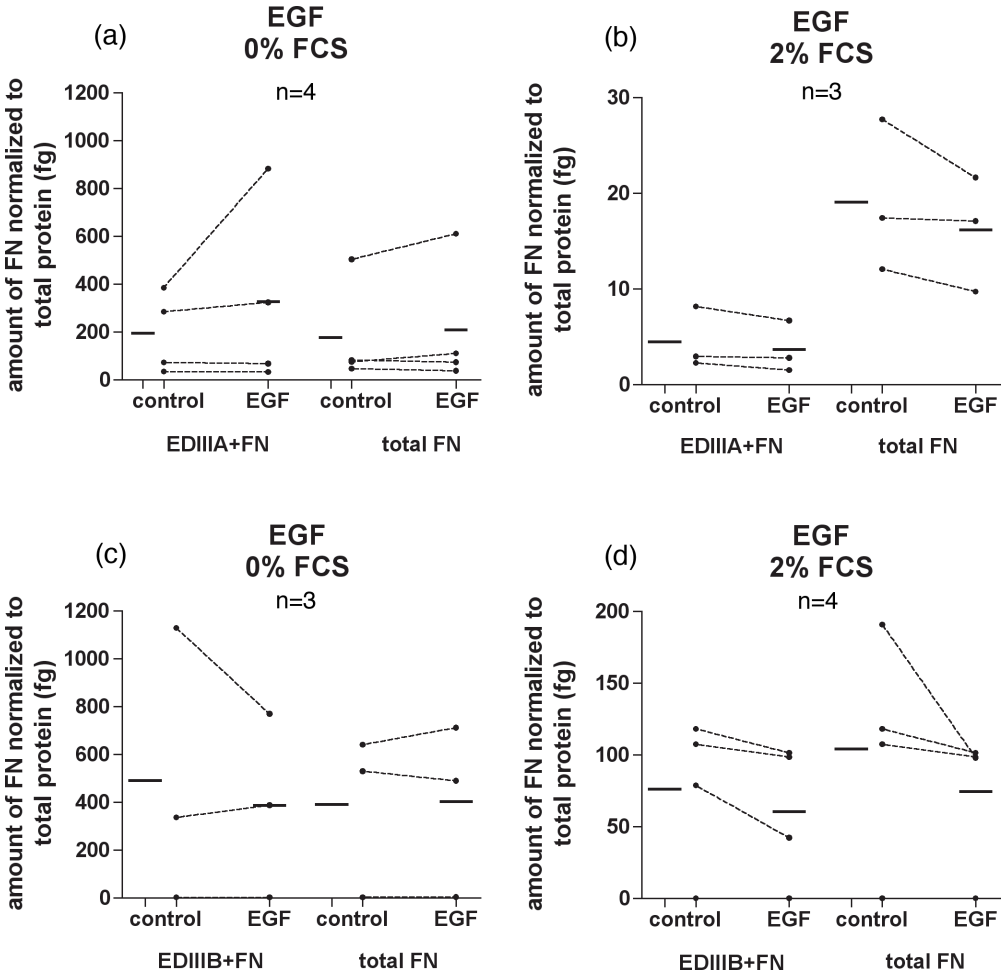

Figure 4-1 Effect of EGF (10ng/ml) on levels of (a) EDIIIA+FN and total FN 0% FCS, (b) EDIIIA+FN and total FN in 2% FCS, (c) EDIIIB+FN and total FN in 0% FCS and (d) EDIIIB+FN and total FN in 2% FCS, produced by ESCs and normalized to total protein levels. Data points represent mean of triplicate measurements in each of several (n) independent experiments using different ESC cell numbers. Solid horizontal lines represent the mean of these means, note: the horizontal line for controls are slightly left of the data points. In the control, ESCs were not treated with any cytokine or growth factor. Paired values of control and treated ESCs from each experiment are connected by dotted lines, and analyzed using paired, student t-tests, differences were considered significant when $P \leq 0.05$ (*).

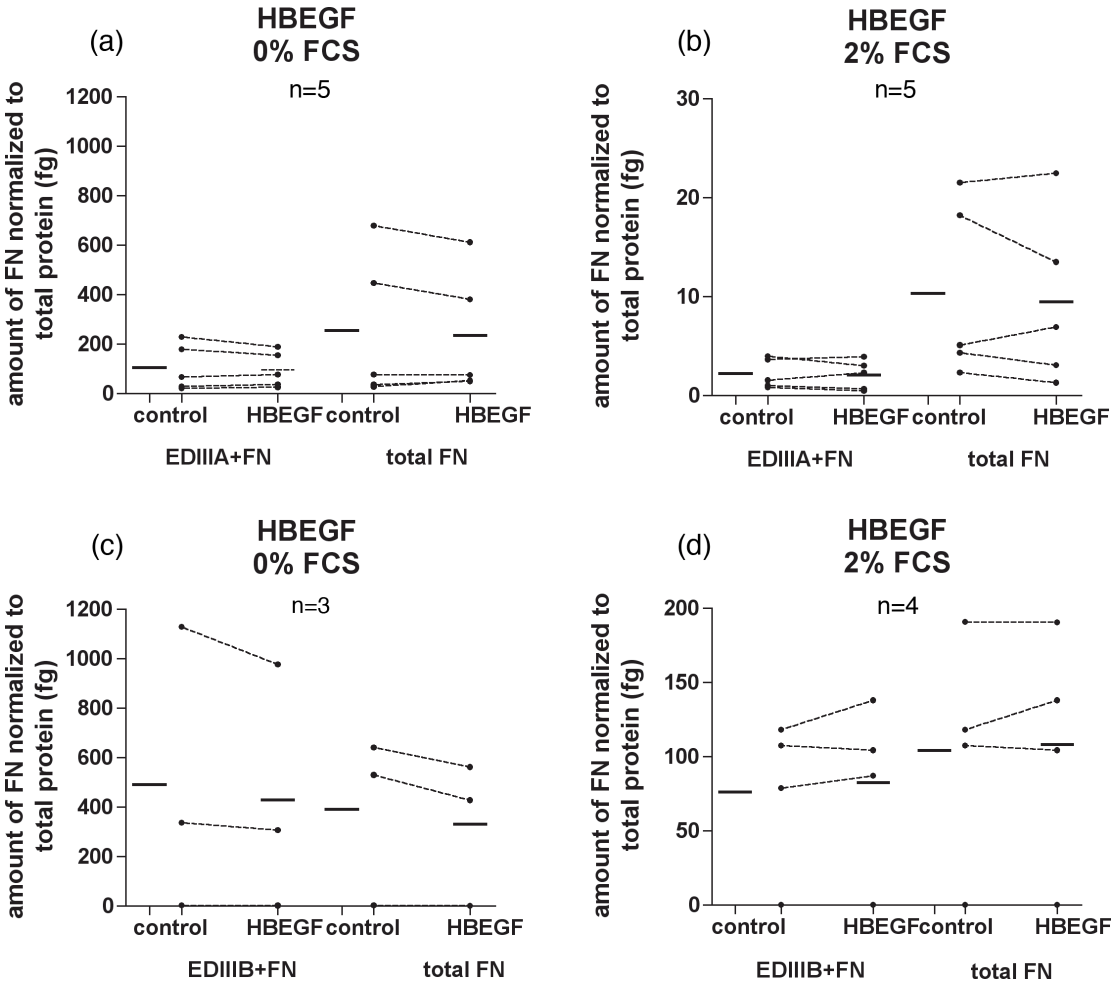

Figure 4-2 Effect of HBEGF (10ng/ml) on levels of (a) EDIIIA+FN and total FN 0% FCS, (b) EDIIIA+FN and total FN in 2% FCS, (c) EDIIIB+FN and total FN in 0% FCS and (d) EDIIIB+FN and total FN in 2% FCS, produced by ESCs and normalized to total protein levels. Data points represent mean of triplicate measurements in each of several (n) independent experiments using different ESC cell numbers. Solid horizontal lines represent the mean of these means, note: the horizontal line for controls are slightly left of the data points. In the control, ESCs were not treated with any cytokine or growth factor. Paired values of control and treated ESCs from each experiment are connected by dotted lines, and analyzed using paired, student t-tests, differences were considered significant when $P \leq 0.05$ (*).

4.2.2. Effect of the IL-6 superfamily of cytokines on FN levels

Treatment of ESCs with LIF (Figure 4-3) or IL-11 (Figure 4-4) had no effect on levels of total FN, EDIIIA+FN or EDIIIB+FN produced.

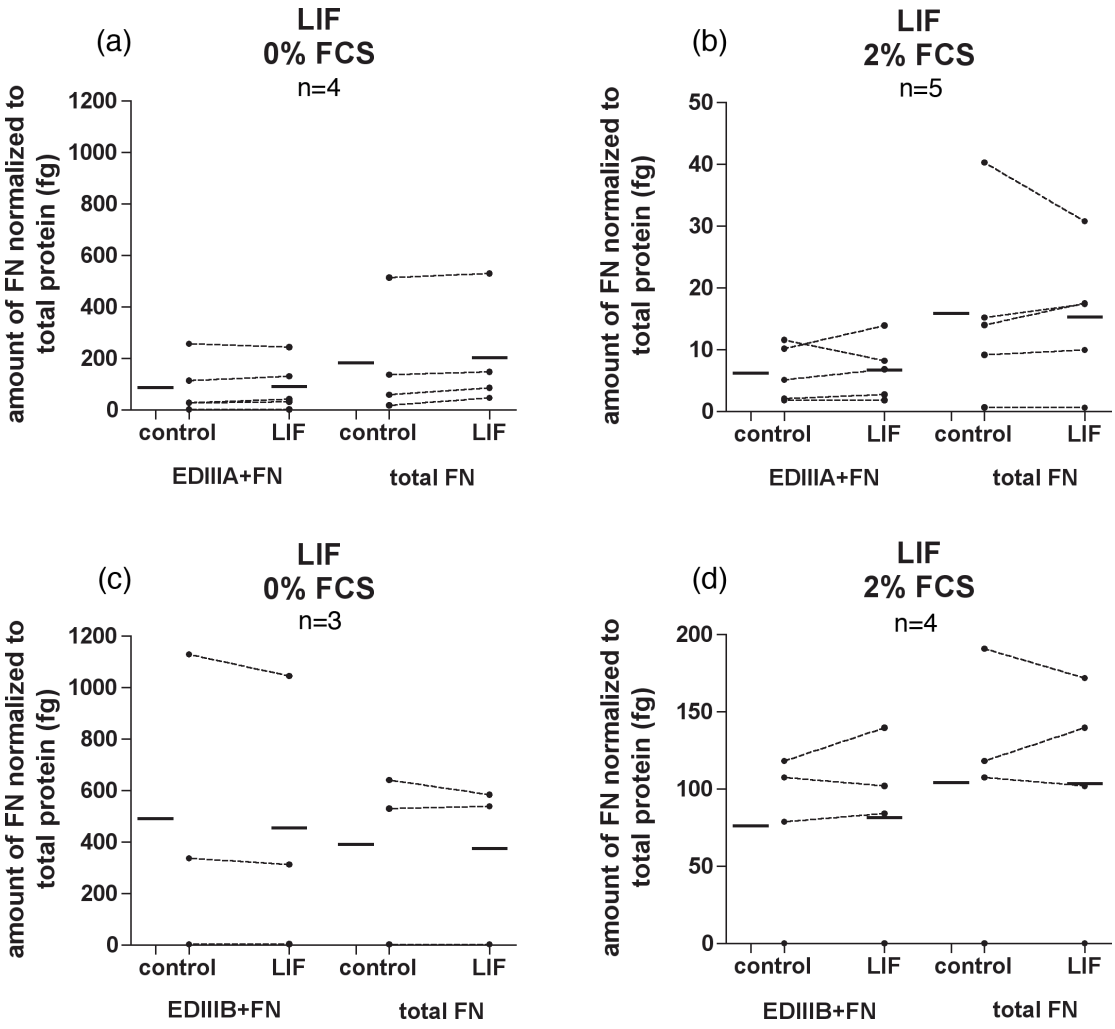

Figure 4-3 Effect of LIF (10ng/ml) on levels of (a) EDIIIA+FN and total FN 0% FCS, (b) EDIIIA+FN and total FN in 2% FCS, (c) EDIIIB+FN and total FN in 0% FCS and (d) EDIIIB+FN and total FN in 2% FCS, produced by ESCs and normalized to total protein levels. Data points represent mean of triplicate measurements in each of several (n) independent experiments using different ESC cell numbers. Solid horizontal lines represent the mean of these means, note: the horizontal line for controls are slightly left of the data points. In the control, ESCs were not treated with any cytokine or growth factor. Paired values of control and treated ESCs from each experiment are connected by dotted lines, and analyzed using paired, student t-tests, differences were considered significant when $P \leq 0.05$ (*).

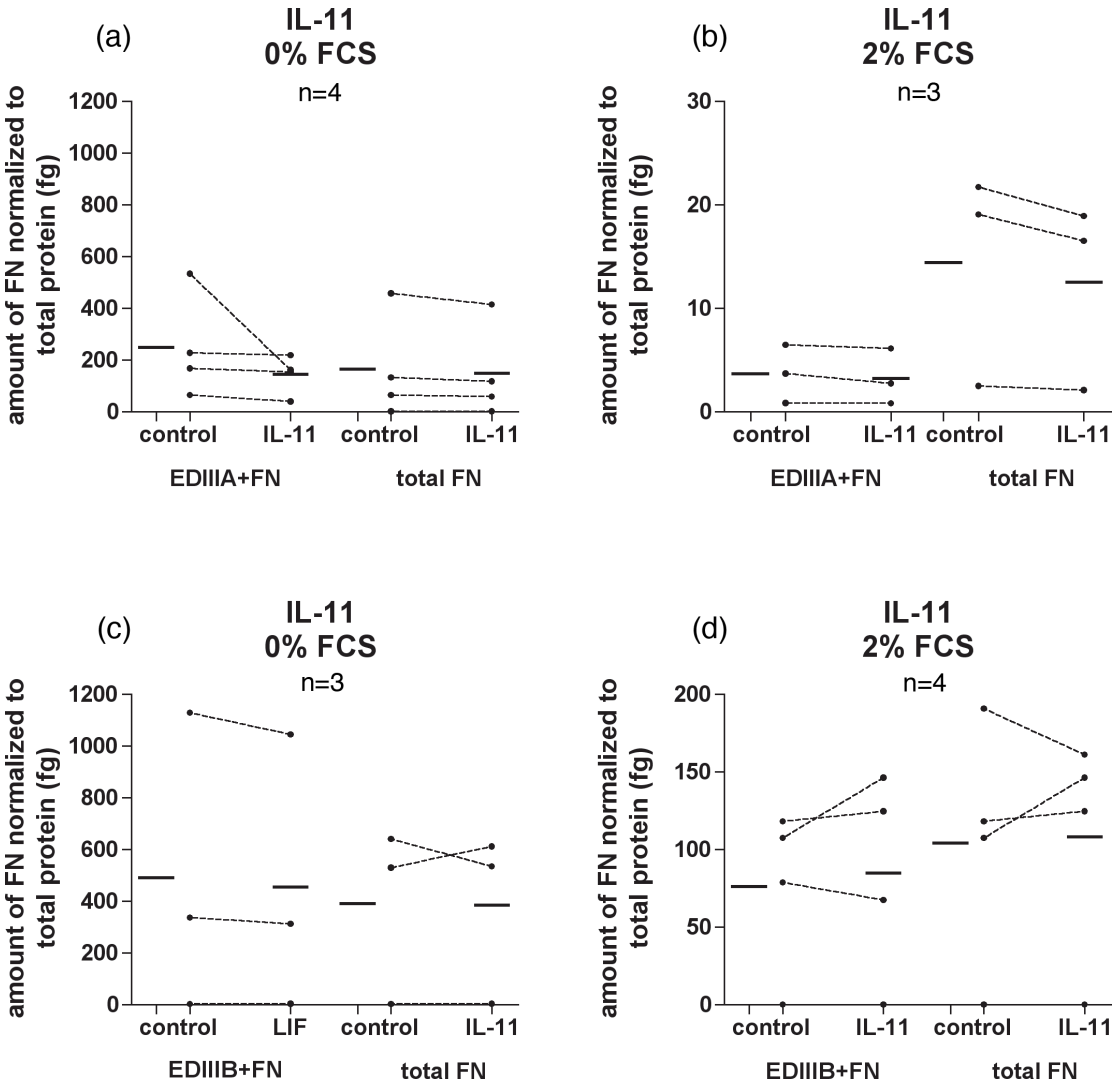

Figure 4-4 Effect of IL-11 (10ng/ml) on levels of (a) EDIIIA+FN and total FN in 0% FCS, (b) EDIIIA+FN and total FN in 2% FCS, (c) EDIIIB+FN and total FN in 0% FCS and (d) EDIIIB+FN and total FN in 2% FCS, produced by ESCs and normalized to total protein levels. Data points represent mean of triplicate measurements in each of several (n) independent experiments using different ESC cell numbers. Solid horizontal lines represent the mean of these means, note: the horizontal line for controls are slightly left of the data points. In the control, ESCs were not treated with any cytokine or growth factor. Paired values of control and treated ESCs from each experiment are connected by dotted lines, and analyzed using paired, student t-tests, differences were considered significant when $P \leq 0.05$ (*).

4.2.3. Effect of IL-1β on FN levels

The production of EDIIIA+FN, EDIIIB+FN and total FN by ESCs appear to be decreased in response to IL-1β relative to the control ESCs (Figure 4-5), but the differences were not statistically significant.

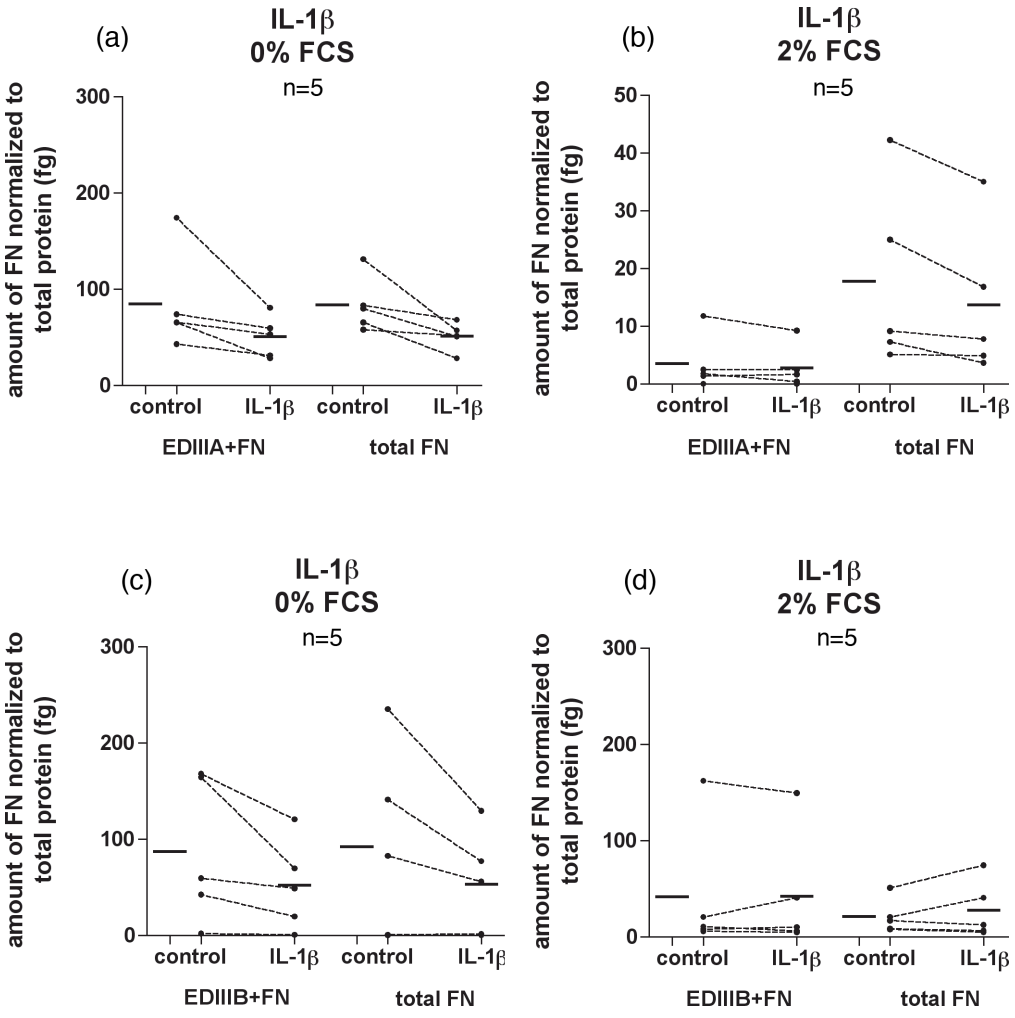

Figure 4-5 Effect of IL-1β (10ng/ml) on levels of (a) EDIIIA+FN and total FN in 0% FCS, (b) EDIIIA+FN and total FN in 2% FCS, (c) EDIIIB+FN and total FN in 0% FCS and (d) EDIIIB+FN and total FN in 2% FCS, produced by ESCs and normalized to total protein levels. Data points represent mean of triplicate measurements in each of several (n) independent experiments using different ESC cell numbers. Solid horizontal lines represent the mean of these means, note: the line for controls are slightly left of the data points. In the control, ESCs were not treated with any cytokine or growth factor. Paired values of control and treated ESCs from each experiment are connected by dotted lines, and analyzed using paired, student t-tests, differences were considered significant when $P \leq 0.05$ (*).

4.2.4. Levels of FN are decreased in response to TNFα in 0% serum

The levels of EDIIIA+FN, EDIIIB+FN and total FN produced by ESCs appear to decrease in response to TNFα (Figure 4-6), but the differences were only statistically significant for total FN levels at 0% serum levels ($P = 0.0204$, Figure 4-6a).

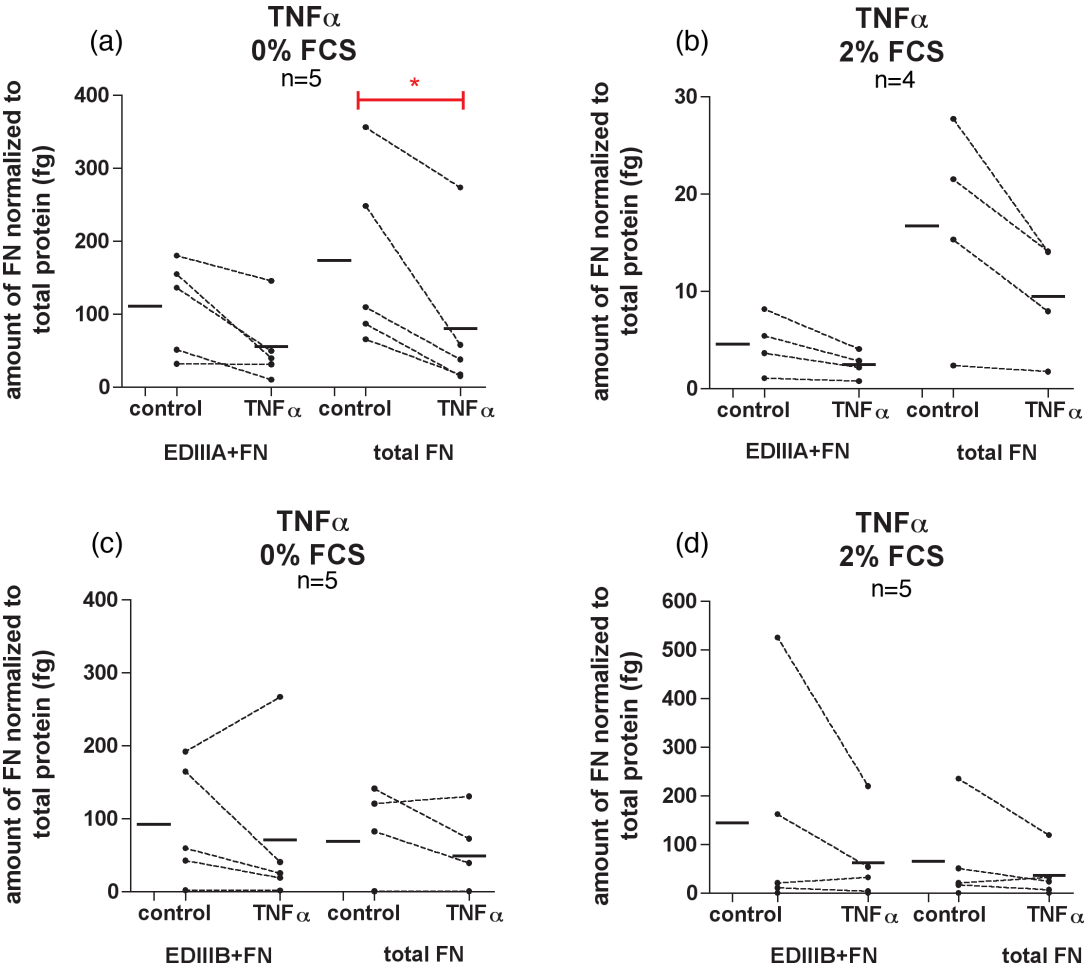

Figure 4-6 Effect of TNFα (10ng/ml) on levels of (a) EDIIIA+FN and total FN in 0% FCS, (b) EDIIIA+FN and total FN in 2% FCS, (c) EDIIIB+FN and total FN in 0% FCS and (d) EDIIIB+FN and total FN in 2% FCS, produced by ESCs and normalized to total protein levels. Data points represent mean of triplicate measurements in each (n) independent experiment using different ESC cell numbers. Solid horizontal lines represent the mean of these means, note: the horizontal line for controls are slightly left of the data points. In the control, ESCs were not treated with any cytokine or growth factor. Paired values of control and treated ESCs from each experiment are connected by dotted lines, and analyzed using paired, student t-tests, differences were considered significant when $P \leq 0.05$ (*).

4.2.5. Effect of bFGF on FN levels

The levels of FN secreted by ESCs were not modulated in response to bFGF at 0% and 2% FCS (Figure 4-7).

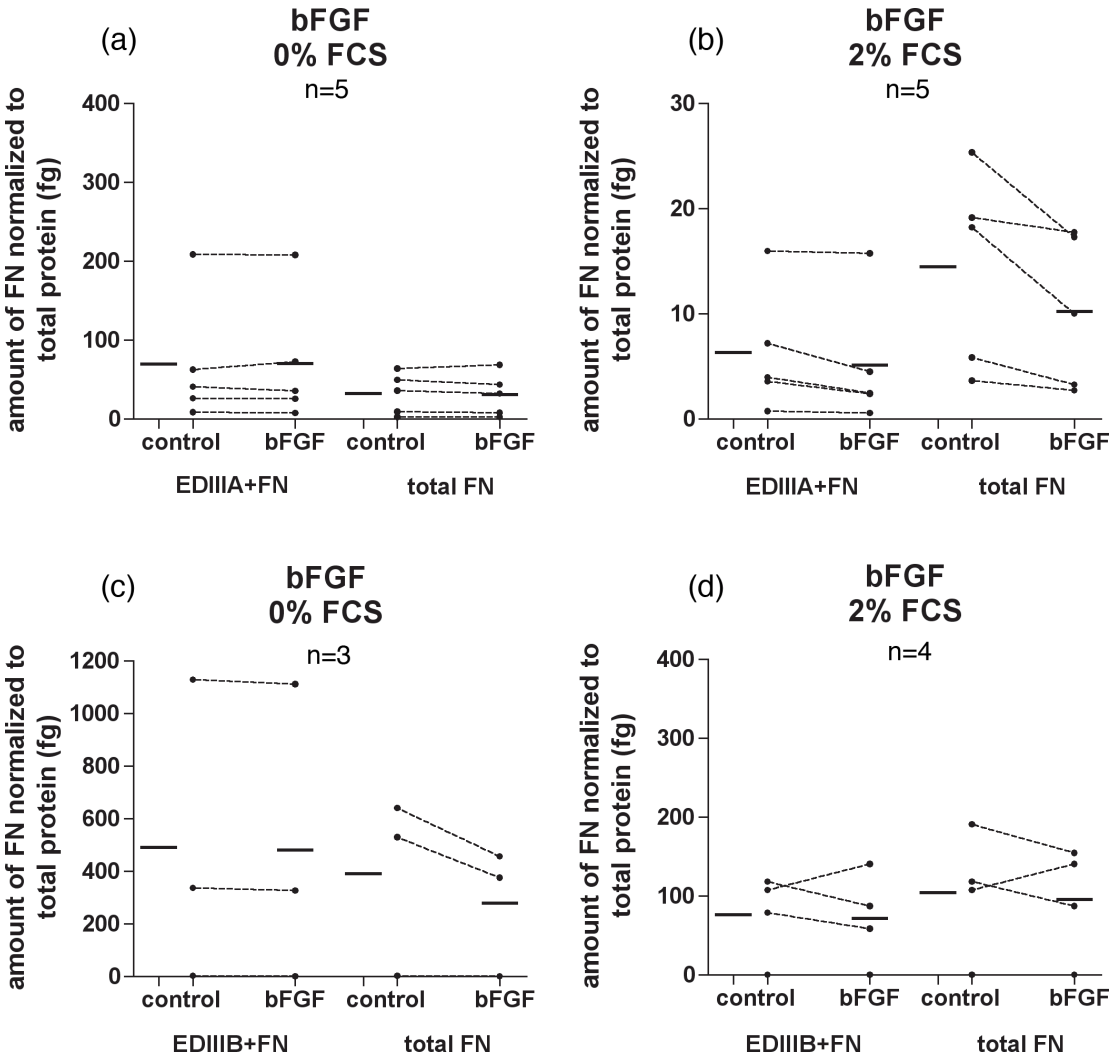

Figure 4-7 Effect of bFGF (10ng/ml) on levels of (a) EDIIIA+FN and total FN in 0% FCS, (b) EDIIIA+FN and total FN in 2% FCS, (c) EDIIIB+FN and total FN in 0% FCS and (d) EDIIIB+FN and total FN in 2% FCS, produced by ESCs and normalized to total protein levels. Data points represent mean of triplicate measurements in each of several (n) independent experiments using different ESC cell numbers. Solid horizontal lines represent the mean of these means, note: the horizontal line for controls are slightly left of data points. In the control, ESCs were not treated with cytokine or growth factor. Paired values of control and treated ESCs from each experiment are connected by dotted lines, and analyzed using paired, student t-tests, differences were considered significant when $P \leq 0.05$ (*).

4.2.6. Effect of TGFβ on FN levels

The levels of EDIIIA+FN, EDIIIB+FN and total FN produced by ESCs displayed an upward trend in response to TGFβ in 2% FCS (Figure 4-8 b, d), but the differences were not statistically significant.

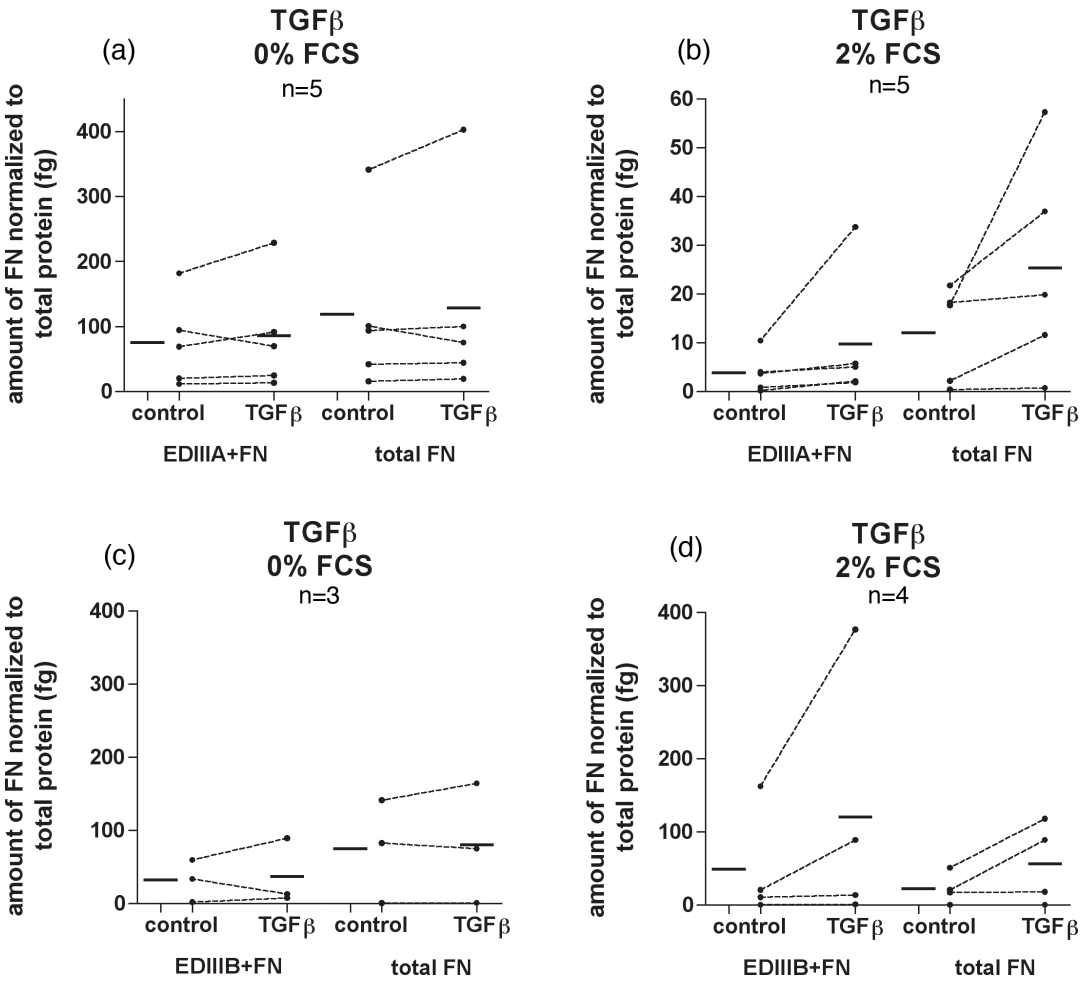

Figure 4-8 Effect of TGFβ (10ng/ml) on levels of (a) EDIIIA+FN and total FN in 0% FCS, (b) EDIIIA+FN and total FN in 2% FCS, (c) EDIIIB+FN and total FN in 0% FCS and (d) EDIIIB+FN and total FN in 2% FCS, produced by ESCs and normalized to total protein levels. Data points represent mean of triplicate measurements in each of several (n) independent experiments using different ESC cell numbers. Solid horizontal lines represent the mean of these means, note: the horizontal line for controls are slightly left of the data points. In the control, ESCs were not treated with any cytokine or growth factor. Paired values of control and treated ESCs from each experiment are connected by dotted lines, and analyzed using paired, student t-tests, differences were considered significant when $P \leq 0.05$ (*).

4.3 Discussion

The menstrual cycle stage-dependent expression of FN in the endometrium is well established, however the factors influencing the production of FN and its splice variants are unclear. In Chapter 3 it was shown that levels of FN, EDIIIA+FN and EDIIIB+FN are reduced during *in vitro* decidualization of ESCs. The data presented in this chapter demonstrate that the levels of FN and its variants produced by ESCs in culture are only modulated in response to TNFα, but not other cytokines and growth factors known to be local mediators of the steroid hormone control of endometrial function.

The ESCs were assessed for FN production forty-eight hours after treatment with cytokine or growth factor. It has been previously shown that ESCs begin to deposit FN in the ECM at two hours after being seeded onto tissue culture plates, therefore we would expect to observe the effects of the cytokine or growth factor on FN production by ESCs after forty-eight hours of culture. But if the cytokines and growth factors require a longer period of time to exert their effects on FN deposition, then we would require more than forty-eight hours of culture to see any significant modulations in FN levels.

It would have been useful to have carried out the ELISA on cells treated with and without cAMP for six days as in the *in vitro* decidualization model (Chapter 3), as a control to demonstrate that a similar reduction in FN production could be detected by the different assay format of the ELISA. We have used non-decidualized ESCs in this chapter and subsequent chapters as they secrete abundant FN in the matrix, and

have functions in the proliferation and tissue remodelling processes necessary for, and prior to, implantation.

Here, the ESC monolayers were treated with NH_4OH to lyse cell membranes and total protein measured in the cell contents released, to which the FN measurements were normalised. The amount of FN was then detected in the remaining ECM attached to the cell membranes or under the cells, in the subcellular matrix. Therefore the amount of deposited FN measured by the ELISA will differ to the total FN content measured by immunoblotting, as a proportion of FN will be removed in the lysing step of the ELISA. This may be a reason why no significant differences were detected in FN production in response to cytokines and growth factors by the ELISA. To demonstrate that FN was still present in the ECM of ESCs after treatment with NH_4OH, ESC monolayers treated with and without NH_4OH were detected for FN by immunofluorescence (Figure 4-9). Another approach could have been to analyse gene expression by RT-PCR, which would provide quantitative changes, but as we are interested in the functional protein, only immunofluorescence, immunoblotting and an ELISA were used to detect changes in protein levels.

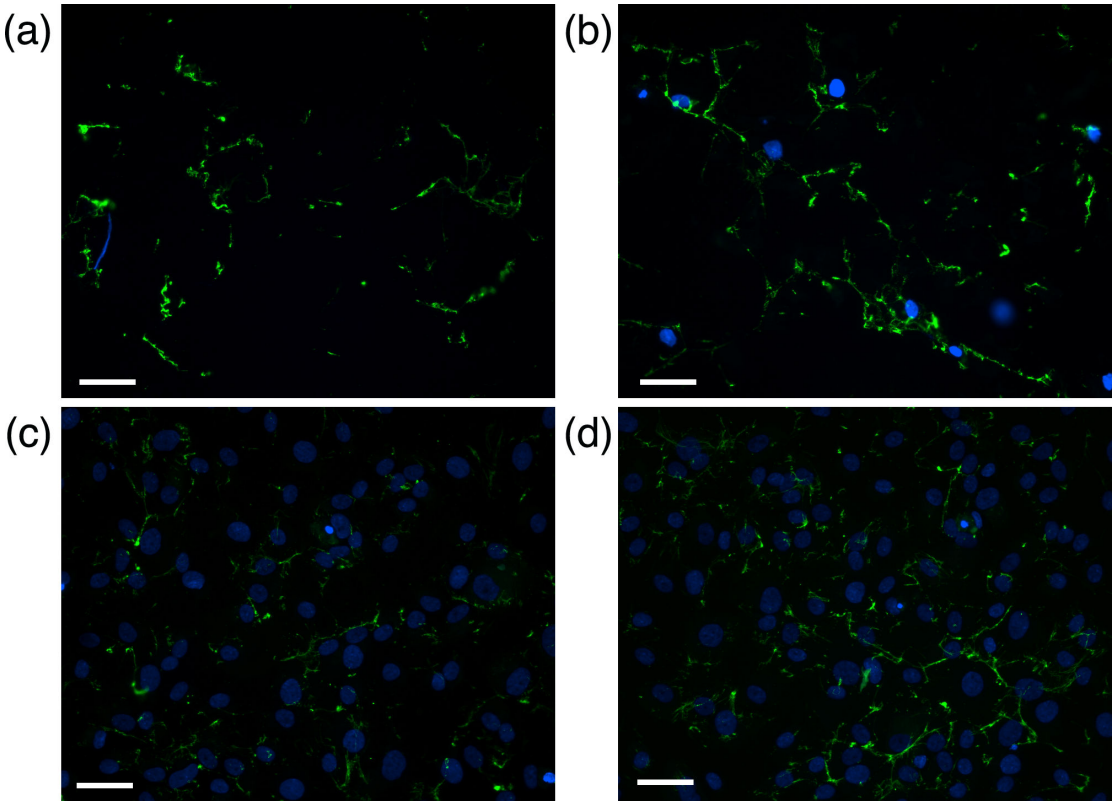

Figure 4-9 Immunofluorescence staining for total FN produced by ESCs (778S) detected by the anti-FN clone IST4 (Table 2-4), which does not detect bovine FN. FNs are in green and nuclei are in blue, images were captured using an equal exposure time, scale bars are 50 μm. ESCs were seeded and cultured for six days in 10% FCS before treatment with 0.02 M NH_4OH (a, b) or with PBS (c, d).

The amount of FN deposited by ESCs appeared to decrease in response to the proinflammatory cytokines IL-1β (Figure 4-5) and TNFα (Figure 4-6), but these differences were only statistically significant for total FN levels in response to TNFα in serum-free conditions ($P = 0.0204$, Figure 4-6 a). The reduced levels of FN could be due to degradation mediated by FN-degrading enzymes induced by IL-1β and TNFα. These stimulated MMP-1, 3 and 9 and downregulated TIMP-1 and 3 expression by ESCs, and also induced expression of components of the uPA/PA-I cascade by ESCs (Rawdanowicz *et al.* 1994; Huang *et al.* 1998; Singer *et al.* 1999; Chung *et al.* 2001; Braundmeier *et al.* 2006).

The lack of effect on FN production by most of the cytokines and growth factors could be the result of biological variation between different patient ESC cell numbers, differences in day from LMP of cell isolation, the passage number and degree of confluency of ESCs used. Another possible reason is that more than one cytokine and growth factor is required to modulate FN production by ESCs. In previous studies, cytokines including IL-1α, EGF, PDGF-BB and TNFα displayed additive effects in their stimulation of MMPs by endometrial fibroblasts (Singer *et al.* 1999).

The other cytokines and growth factors used in this experiment, EGF, HB-EGF, LIF and IL-11 did not influence FN deposition in the ECM (Figure 4-1, Figure 4-2, Figure 4-3, Figure 4-4). The levels of FN appeared to increase in response to TGFβ (Figure 4-8), but the difference was not statistically significant. TGFβ is known to induce FN expression in many cell types including EECs and ESCs (Luo *et al.* 2004), and can promote EDIIIA splicing in cultured normal skin fibroblasts (Borsi *et al.* 1990).

In summary, the levels of FN produced by ESCs and deposited in the ECM were decreased in response to TNFα in serum-free conditions, but no modulations in EDIIIA+FN and EDIIIB+FN levels were seen in response to the other cytokines and growth factors at both 0% and 2% serum. To further investigate the role of the FN alternative splice variant EDIIIA, in the next chapters we will assess its role in human blastocyst adhesion and in modulating the functional properties of FN.

Chapter 5

The function of EDIIIA+FN in blastocyst adhesion

5.1 Introduction

Implantation involves the apposition and attachment of the blastocyst to the LE, penetration of the LE and invasion of the blastocyst into the endometrial stroma. Contact of the adhesion-competent blastocyst with the basement membrane and decidual ECM activates integrin signalling and trafficking, resulting in strong trophoblast adhesion and differentiation of the trophoblast to an invasive phenotype (Rout *et al.* 2004). This allows the blastocyst to invade and migrate through the basement membrane to infiltrate the stroma. We have previously shown that FN and its alternatively spliced variants EDIIIA+FN and EDIIIB+FN are localised in the human endometrial stroma adjacent to the LE at the time of implantation and are particularly abundant in the epithelial basement membrane (Figure 5-1), these experiments were performed previously by Ms Janet Carver, Nuffield Dept. of Obstetrics and Gynaecology (unpublished data). This suggests a role for FN and its splice variants in supporting blastocyst attachment and activation of signals such as integrin trafficking required for subsequent invasion into the stroma.

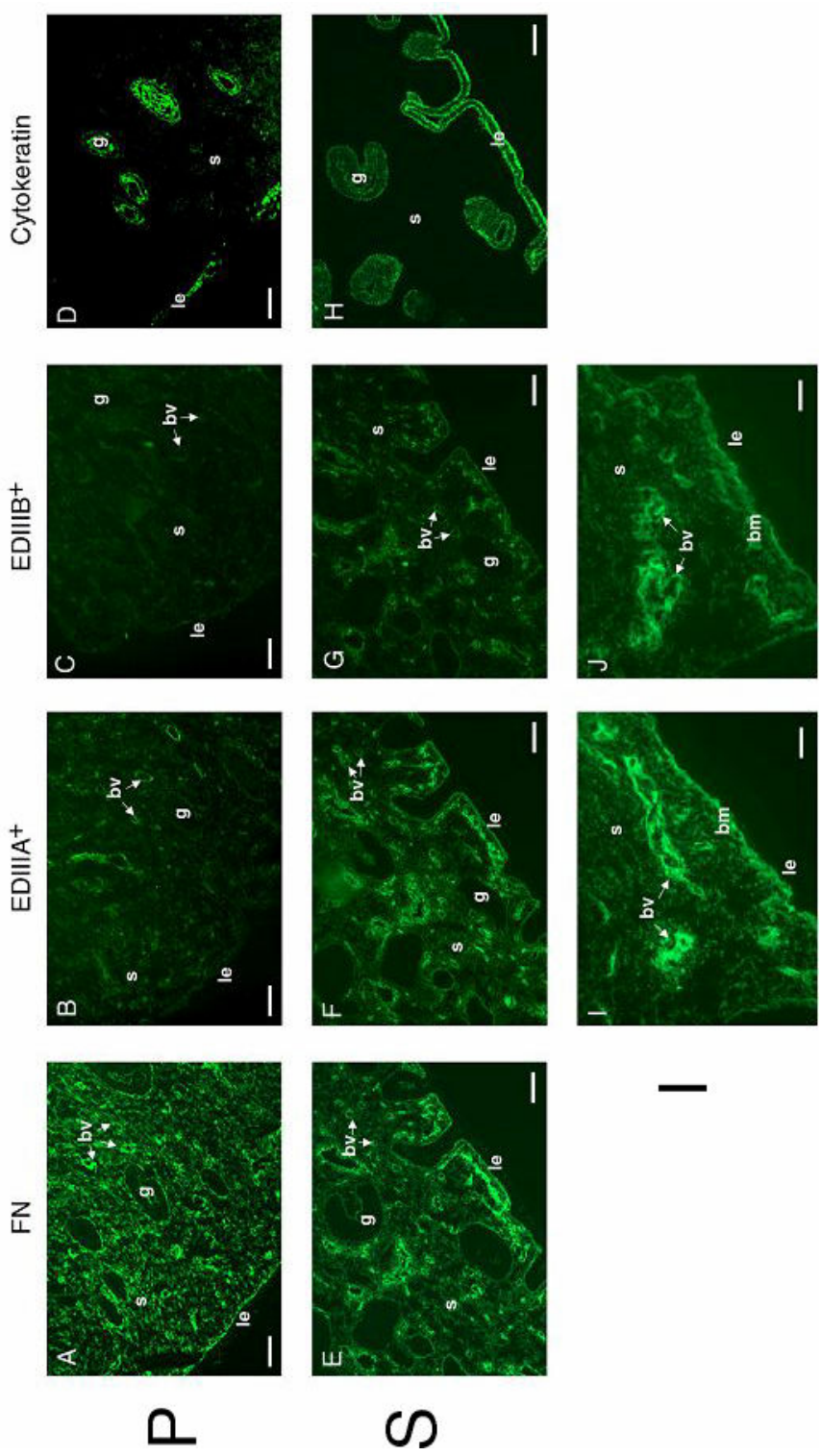

Figure 5-1 Immunohistochemical staining for FN, EDIIIA+FN, EDIIIB+FN and cytokeratin (shown in green) in endometrial sections from the proliferative (P), secretory (S) or window of implantation (I) stages of the menstrual cycle. bm: basement membrane; bv: blood vessels; le: luminal epithelium; g: glands; s: stroma; scale bars are 100 μm; carried out previously by Ms Janet Carver (Nuffield Dept. of Obstetrics and Gynaecology, University of Oxford).

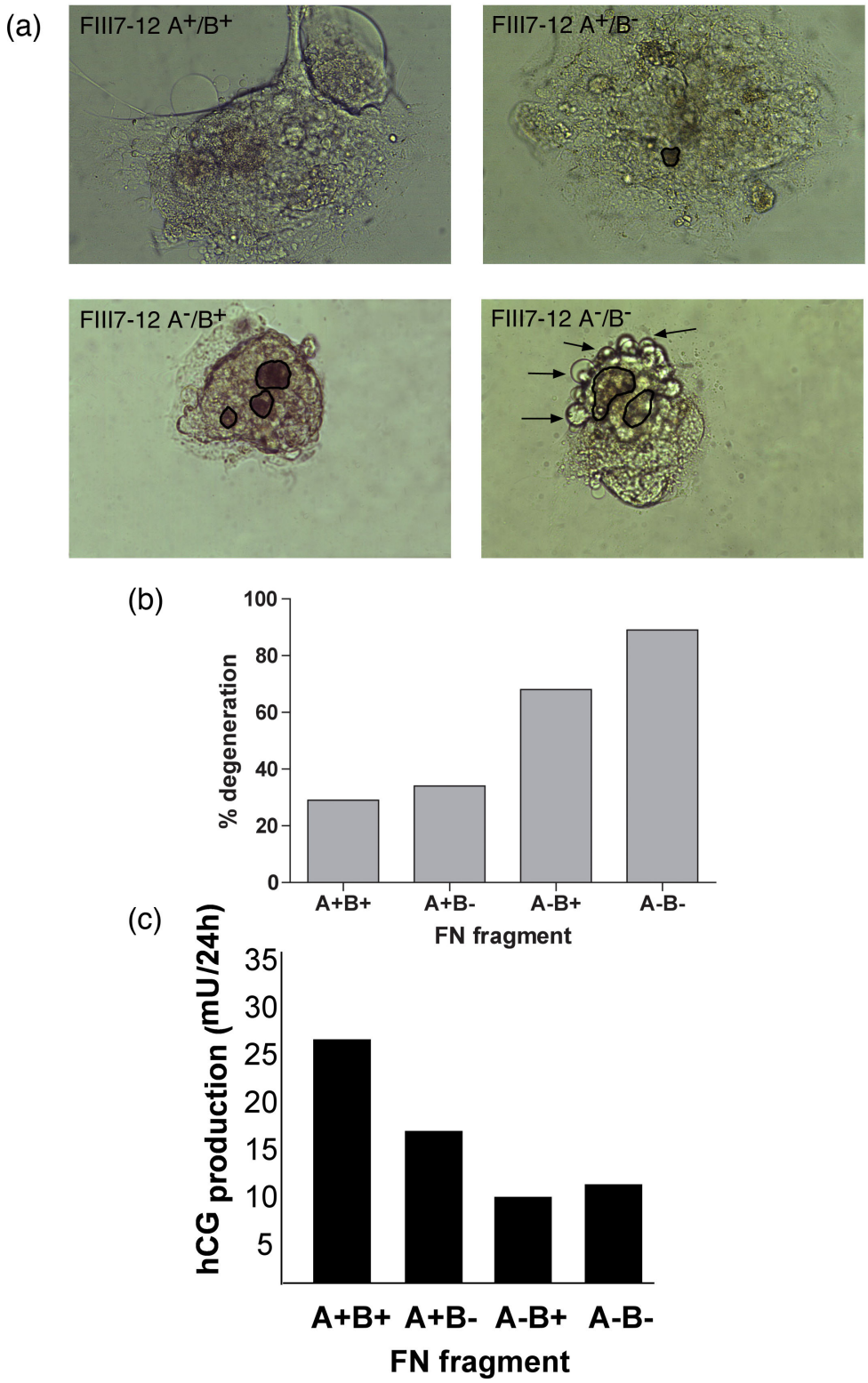

Figure 5-2 Blastocysts cultured on FN fragments with and without EDIIIA and/or EDIIIB; (a) those cultured on FIII7-12A+B+ exhibited strong attachment and spreading, but collapsed and degenerated on FIII7-12A-B-; blastocysts were also assessed for % degeneration (b) and hCG production (c); carried out previously by Dr Karen Martin (Nuffield Dept. of Obstetrics and Gynaecology, University of Oxford, unpublished data).

The role of EDIIIA/B+FN in implantation was previously tested using a blastocyst attachment assay (Carver *et al.* 2003). Blastocysts were cultured on surfaces coated with FN fragments spanning FIII domains 7-12 with and without EDIIIA and/or EDIIIB. The blastocysts cultured on FIII7-12A+B+ expanded with strong attachment and spreading, but collapsed and degenerated when plated on FIII7-12A-B- (Figure 5-2a). Blastocysts cultured on FIII7-12A-B- had a greater percentage of degeneration and lower expression of hCG, a measure of embryo well-being, relative to those cultured on FIII7-12A+B+ (Figure 5-2 b, c). Therefore EDIIIA and EDIIIB were suggested to have functions in the process of trophoblast adhesion. These experiments were performed previously by Dr Karen Martin, Nuffield Dept. of Obstetrics and Gynaecology (unpublished data). The role of EDIIIA in supporting blastocyst attachment was investigated using an *in vitro* blastocyst implantation model, in which blastocysts are co-cultured with ESCs in the presence of recombinant EDIIIA protein (Figure 5-3).

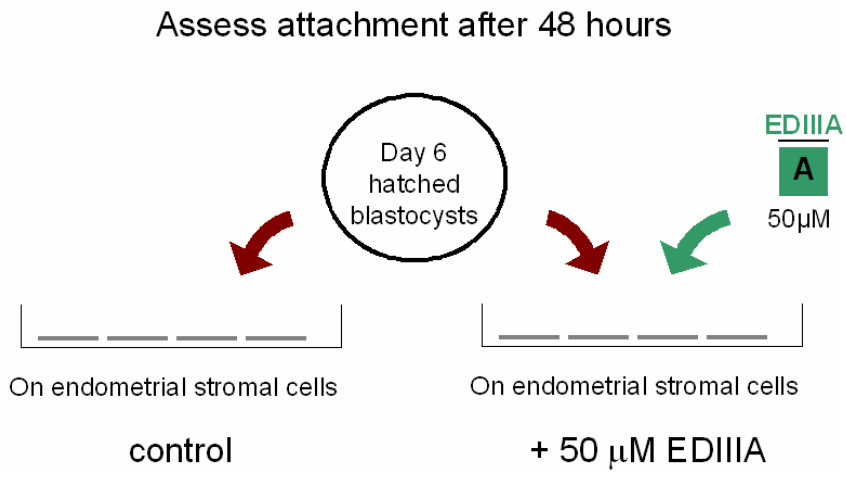

Figure 5-3 Schematic diagram of *in vitro* blastocyst implantation assay; day 6 hatched blastocysts were co-cultured on confluent monolayers of human ESCs and recombinant EDIIIA protein (final concentration 50 µM) for 48 hours. Control blastocysts were co-cultured with endometrial stromal cells with no EDIIIA added. Blastocysts were assessed for attachment and phase-contrast images captured at 24 and/or 48 hours of co-culture.

The EDIIIA domain is a ligand for the α4 and α9 subset of integrins (Liao *et al.* 2002). The α4 integrin subunit has been localized in mouse oocytes, peri-implantation and post-implantation embryos (Basak *et al.* 2002; Lu *et al.* 2002), but has only been studied and identified in human oocytes (Campbell *et al.* 1995). The expression of integrin subunits α4 and α9 by human blastocysts in the *in vitro* implantation model was investigated (Figure 5-4). All work which involved manipulation of human blastocysts in this chapter was carried out by Ms Janet Carver, Nuffield Dept. of Obstetrics and Gynaecology.

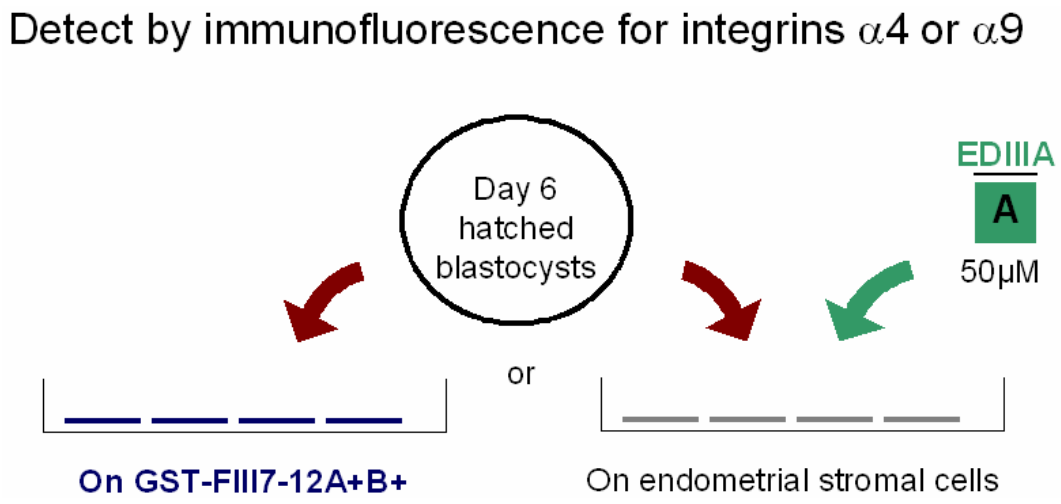

Figure 5-4 Schematic diagram of *in vitro* blastocyst implantation assay; day 6 hatched blastocysts were co-cultured on surfaces pre-coated with GST-FIII7-12A+B- or on confluent monolayers of human ESCs and recombinant EDIIIA protein (final concentration 50 μM) for 48 hours. The expression of integrin subunits α4 and α9 in the attached blastocysts were assessed by immunofluorescence after 48 hours of co-culture.

5.2 Results

5.2.1. Expression and purification of His-EDIIIA

The recombinant EDIIIA protein was expressed with a 6xHis-tag to allow for affinity purification by Ni-NTA and by FPLC size-exclusion chromatography (Superdex 200 HR 10/30) as described in Section 2.3.1.1 (Figure 5-5). The FPLC peaks labelled A2 and B2 (Figure 5-5a) were pooled as they gave a band at ~20 kDa on reducing SDS-PAGE gels (Figure 5-5b and Figure 5-6a). The other peaks including A1, B1, A3 and B3 contained contaminants as shown by the reducing 15% SDS-PAGE (Figure 5-5b) and so were not pooled for further concentration. The pooled fractions A2 and B2 were detected as a single band by immunoblotting using the anti-EDIIIA antibody IST9 (Figure 5-6b) at approximately 20 kDa, which was different from the expected molecular weight of 11 kDa. This difference in the size of bands of His-EDIIIA observed in SDS-PAGE gels was observed previously (Saito *et al.* 1999) and could be due to differences in migration in the SDS-PAGE gel depending on the percentage of gel used.

Mass spectrometry analysis (Figure 5-7) of the His-EDIIIA protein confirmed that the sample is of molecular weight 11288.0 Da, which is different to the expected molecular weight of 11328.3 Da. This difference of 40 Da could be the result of errors in machine calibration and a noisy sample. The mass spectrometry analysis was of a newer batch of EDIIIA (Batch#2- 11/2007) than that used in the blastocyst attachment experiments in Chapter 5 (Batch#1- 12/2005, Figure 5-5, Figure 5-6), 4-12% gradient reducing SDS-PAGE of both batches of EDIIIA confirms that they were the same protein (Figure 5-8a lanes 1 and 2), with a molecular weight of

approximately 11 kDa. The immunoblot of the Batch #2 EDIIIA (Figure 5-8b lane 3), detected using the anti-EDIIIA antibody IST9 confirms that the His-EDIIIA had a molecular weight of approximately 11 kDa. Also loaded on this immunoblot are GST-FIII 7-12A-B+ and GST-FIII7-12 A-B- (Figure 5-8b lanes 4 and 5) and GST-FIII 7-12 A+B+ (Figure 5-8b lane 6) as negative and positive controls, respectively, for the anti-EDIIIA antibody IST9.

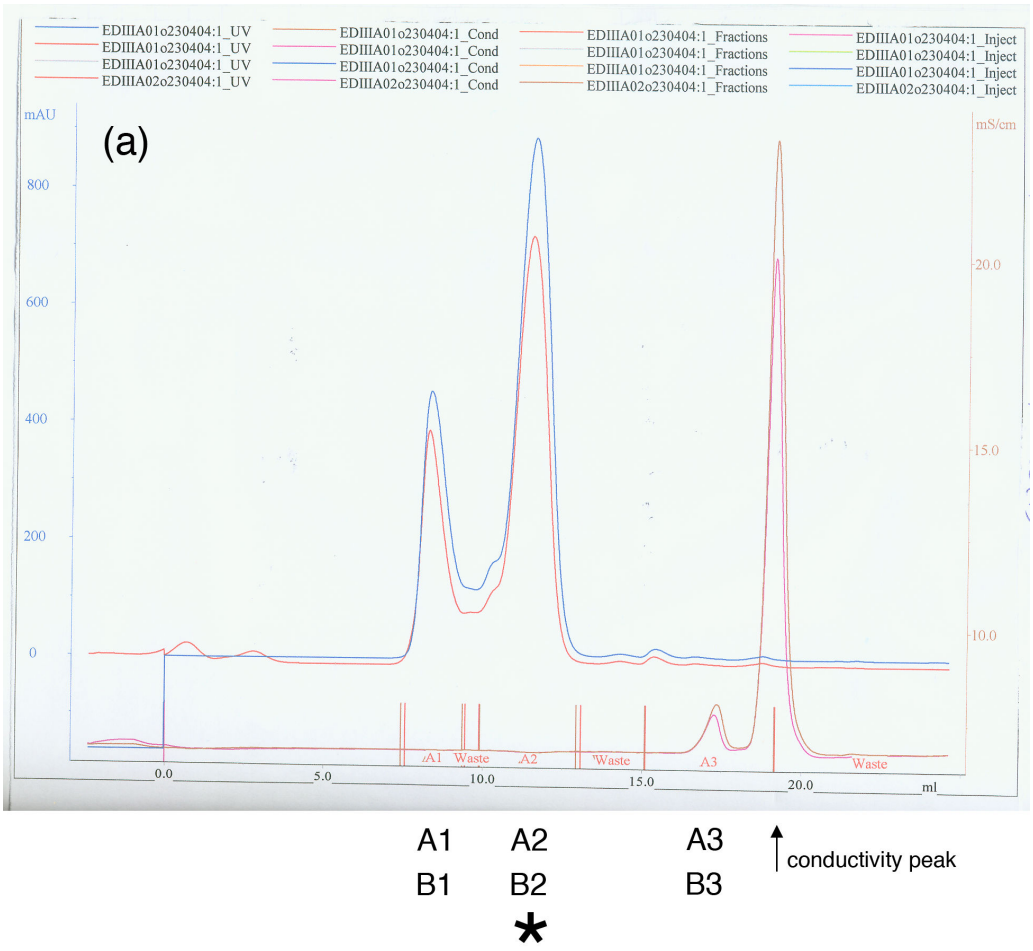

Figure 5-5 Protein purification by FPLC size exclusion chromatography (Superdex 200) (a) FPLC elution profile for the purification of His-EDIIIA (Batch#1), asterix (*) denotes the eluted fractions (A2 and B2) that was pooled for further concentration. (b) 15% reducing SDS-PAGE of FPLC fractions, Mw ladder = molecular weight ladder in kDa.

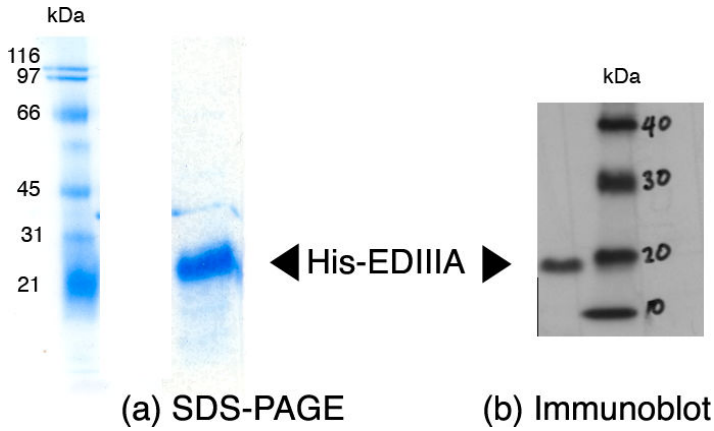

Figure 5-6 (a) 15% reducing SDS-PAGE gel and (b) immunoblot of the expressed and purified His-EDIIIA (Batch#1), using the anti-EDIIIA antibody, IST9 as described in Section 2.3.5 and Table 2-4.

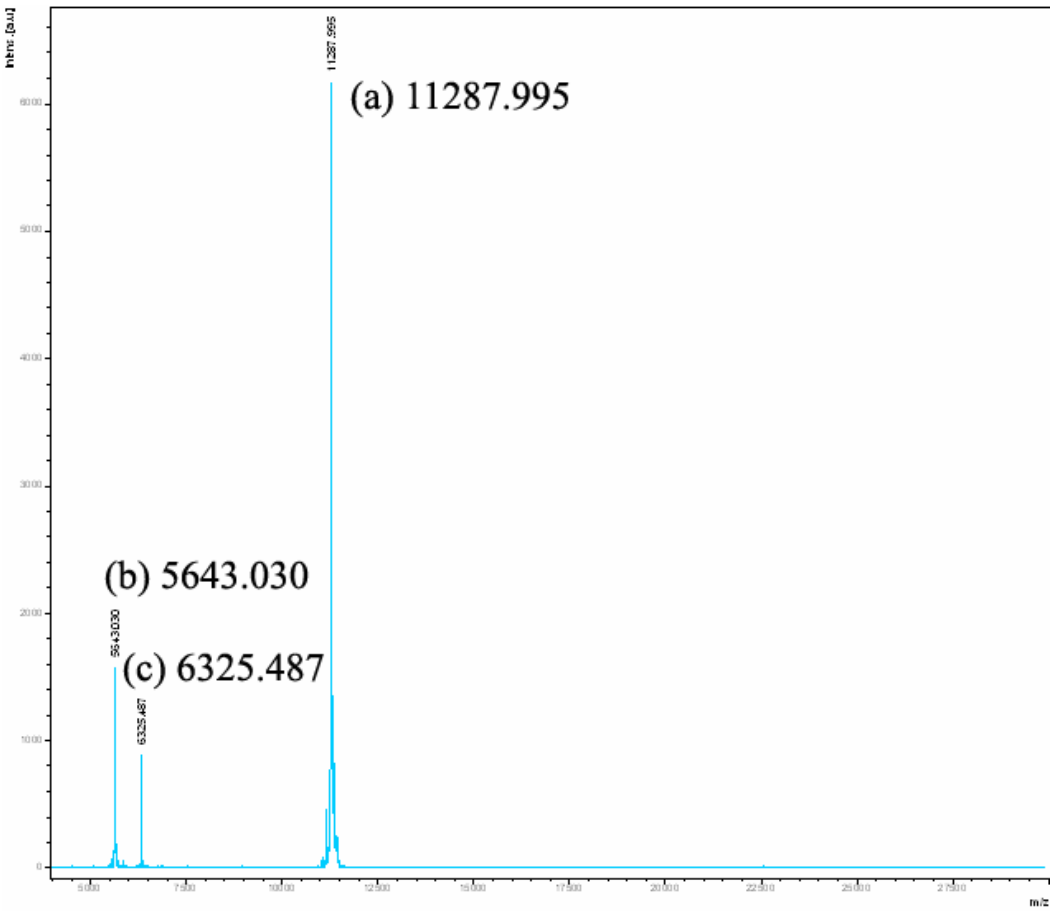

Figure 5-7 Electrospray Ionisation Mass Spectral analysis (ESI-MS) profile of the expressed and purified His-EDIIIA (Batch#2), carried out by Dr Katalin di Gleria, Weatherall Institute of Molecular Medicine, Oxford. The experimental determined value of 11288.0 Da differs to the expected molecular weight of 11328.3 Da, possibly due to errors in machine calibration or noisy sample. SDS-PAGE and immunoblotting provided evidence for the identity of the His-EDIIIA protein (Figure 5-8).

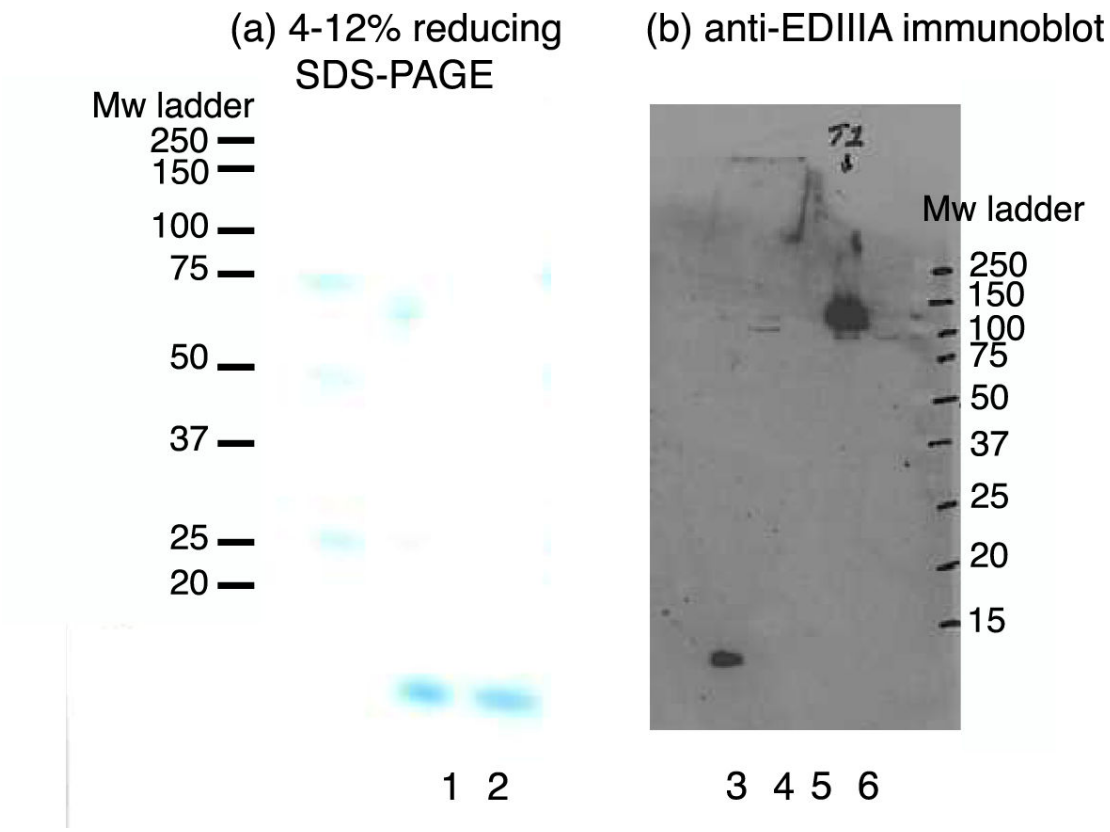

Figure 5-8 (a) 4-12% gradient, reducing SDS-PAGE gel of His-EDIIIA from Batch#1 (lane 1) and Batch #2 (lane 2), demonstrating that both batches of His-EDIIIA had approximate molecular weights of 10 kDa. (b) Immunoblot from 10% reducing SDS-PAGE gel of the expressed and purified His-EDIIIA (Batch#2, lane 3), using the anti-EDIIIA antibody IST9 as described in Section 2.3.5 and Table 2-4. Lane 4 is GST-FIII7-12A-B+, lane 5 is GST-FIII7-12A-B- and lane 6 is GST-FIII7-12A+B+. Mw ladder = molecular weight ladder in kDa. Carried out by Mrs Céline Jones (Nuffield Dept. of Obstetrics and Gynaecology, University of Oxford).

5.2.2. EDIIIA had no effect on human blastocyst adhesion and trophoblast outgrowth

There were no significant differences in the number of attached blastocysts in the presence of 50 μM recombinant EDIIIA protein relative to control blastocysts (Table

5-1)(Figure 5-9). Fourteen of the sixteen attached blastocysts cultured with EDIIIA attached to the ESCs and all sixteen of the control blastocysts were attached. Of the attached blastocysts, eight of the fourteen in the presence of EDIIIA exhibited trophoblast spreading and outgrowth onto the stromal cell layer, and six of the sixteen attached control blastocysts exhibited trophoblast spreading and outgrowth. Recombinant EDIIIA had no effect on blastocyst spreading and extent of trophoblast outgrowth and invasion into the endometrial stromal cell layer.

	No. of embryos	attached	loosely attached	not attached	outgrowth
+ 50 µM EDIIIA	14	10	4	2	8
control	16	8	8	0	6

Table 5-1 No. of blastocysts attached, loosely attached and not attached after forty eight hours of co-culture with ESCs and with/without 50 µM EDIIIA; attached blastocysts were assessed for outgrowths. Attachment was assessed by gently shaking the culture dish three times for three seconds each; blastocysts which were initially attached but later detached were scored as loosely attached, whilst those that remain attached were scored as attached. Carried out by Ms Janet Carver (Nuffield Dept. of Obstetrics and Gynaecology, University of Oxford).

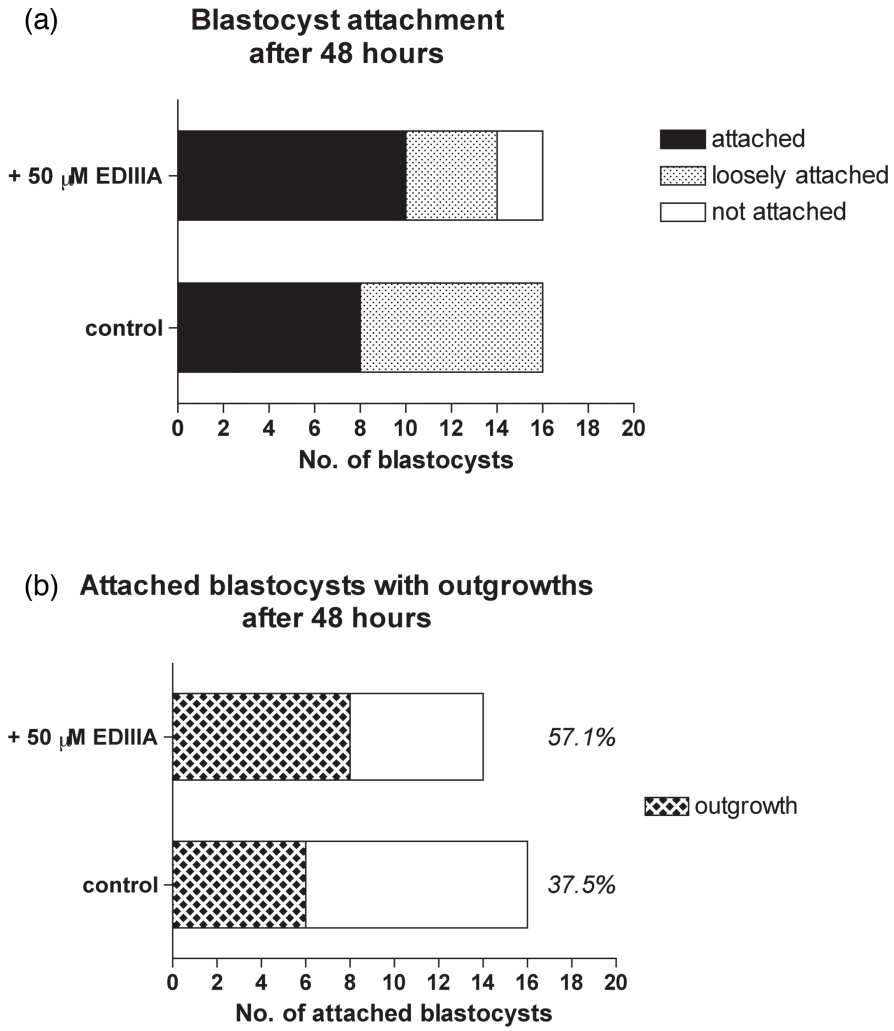

Figure 5-9 (a) Number of blastocysts attached, loosely attached and not attached after 48 hours of co-culture with ESCs and with/without 50 μM EDIIIA. (b) Blastocysts attached after 48 hours of co-culture with ESCs with/without 50 μM EDIIIA were assessed for outgrowths. Carried out by Ms Janet Carver (Nuffield Dept. of Obstetrics and Gynaecology, University of Oxford).

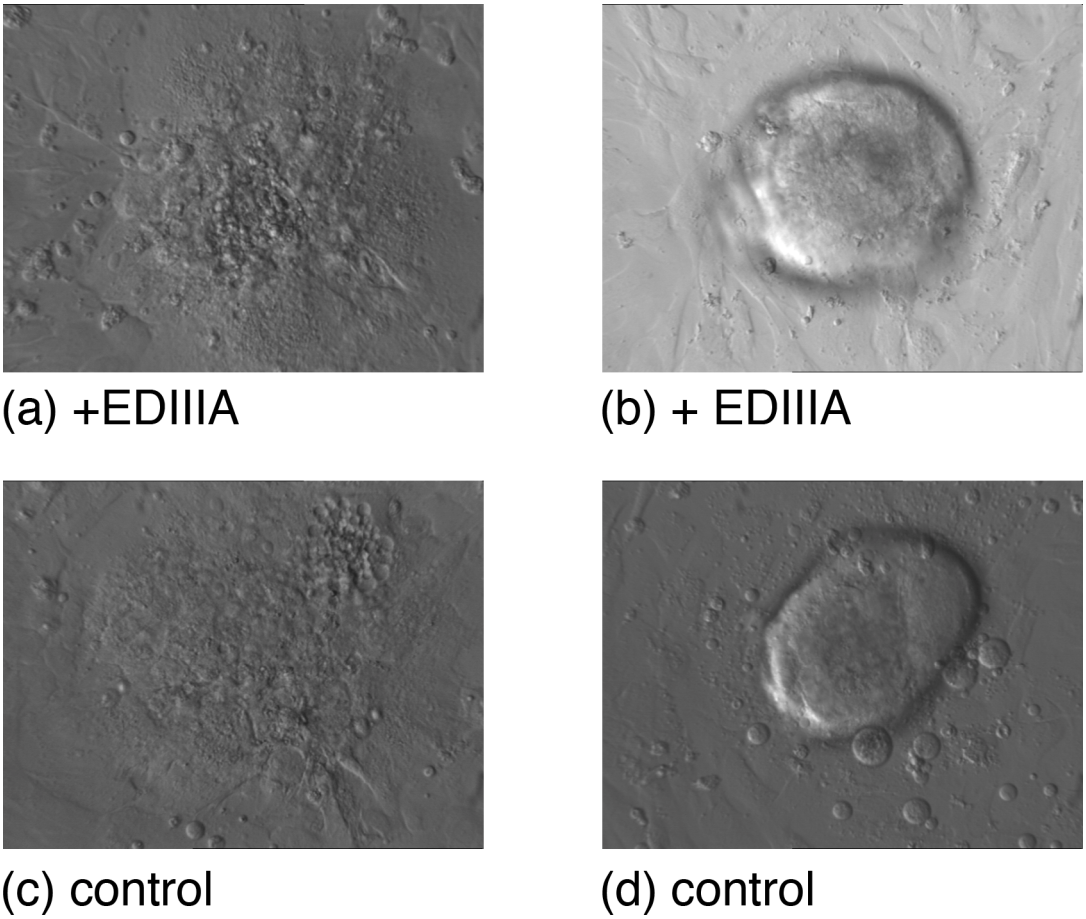

Figure 5-10 Phase contrast images of attached blastocysts exhibiting spreading and outgrowth on the endometrial stromal cell layer (a, c) and blastocysts that stayed round and displayed no outgrowths (b, d), in both control and with 50 μM EDIIIA added. Carried out by Ms Janet Carver (Nuffield Dept. of Obstetrics and Gynaecology, University of Oxford).

5.2.3. Integrin subunits α4 and α9 are expressed by post-implantation human blastocysts

Blastocysts attached onto coverslips coated with FIII7-12A+B+ (Figure 5-12) and onto ESCs (Figure 5-13) showed localization of the α9 integrin subunit in the ICM of both blastocysts (Figure 5-12 a, b, g and h, Figure 5-13 a and b). Staining for α9 was barely detectable in trophoblast outgrowths of both attached blastocysts, as indicated by the lack of α9 immunostaining in the areas marked for trophoblast outgrowths (Figure 5-12 a, b, i and j, Figure 5-13 a, b, f and g). A control blastocyst attached on a monolayer of ESCs (Figure 5-12 c, d, k and l) was treated with rabbit IgG at the same concentration as the primary antibody as a negative control. Phase contrast images of the embryos (Figure 5-12 e and Figure 5-13 c) are included to show the cell density and morphology of the embryo. The α9 subunit has previously been shown to be widely expressed in muscles (Palmer *et al.* 1993). Immunostaining of human myometrium sections using the anti-α9 antibody (Figure 5-11) was carried out to demonstrate that the antibody was functional for immunostaining. The tissue sections were fixed with acetone (Figure 5-11 a, b, d) as routinely used in immunohistochemical staining and also with 3% paraformaldehyde (Figure 5-11c) which was used to fix the blastocysts for immunostaining.

The α4 integrin subunit was expressed in blastocysts attached onto ESCs (Figure 5-14 and Figure 5-15). However, as the location of the ICM of these two embryos was not clear from the pictures, it is uncertain whether integrin α4 is expressed in the ICM. Punctate staining of α4 was detected in some trophoblast outgrowths (Figure 5-14 h-I and Figure 5-15 g-h), but not others (Figure 5-14 f-g), and intense α4 staining was observed in a single embryo cell in the trophoblast outgrowths (Figure 5-15 i-j). This

increase in integrin α4 expression could be due to the trophoblast cell undergoing differentiation to an invasive phenotype, as α4β1-mediated cell adhesion has been shown to result in increased cell migration (Liu et al. 2002) which could contribute to its invasive potential. In the control blastocysts treated with mouse IgG (Figure 5-15 k-l) there was also some FITC staining, though it is not localised in foci as it is in the blastocysts treated with the mouse anti-α4 antibody, suggesting that α4 staining is specific in the blastocysts attached onto ESCs. The anti-α4 antibody has been shown to be functional in immunostaining (Heij *et al.* 1998). Phase contrast images (Figure 5-14 c and Figure 5-15 c and d) show the cell density and morphology of the embryo.

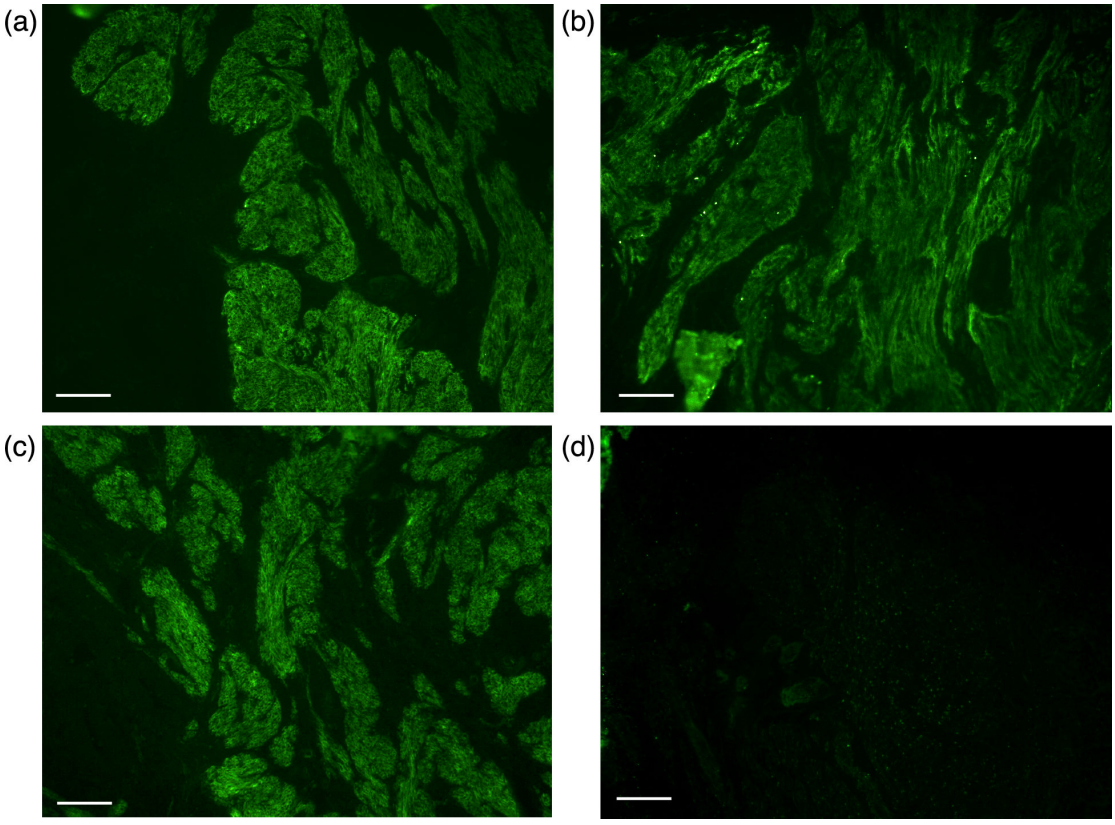

Figure 5-11 Immunohistochemical staining for integrin α9 subunit (a, b, c, in green) in myometrium tissue sections from two different ESC patient cell numbers (a: 317, b: 592, c: 317, d: 317) using the rabbit anti-α9 antibody (Table 2-4), (d) a control myometrium tissue section was treated with rabbit IgG at the same concentration as the primary antibody, scale bars are 50 µm. Sections (a), (b) and (d) were fixed with cold acetone, and section (c) was fixed with 3% paraformaldehyde as in the immunostaining protocol for blastocysts.

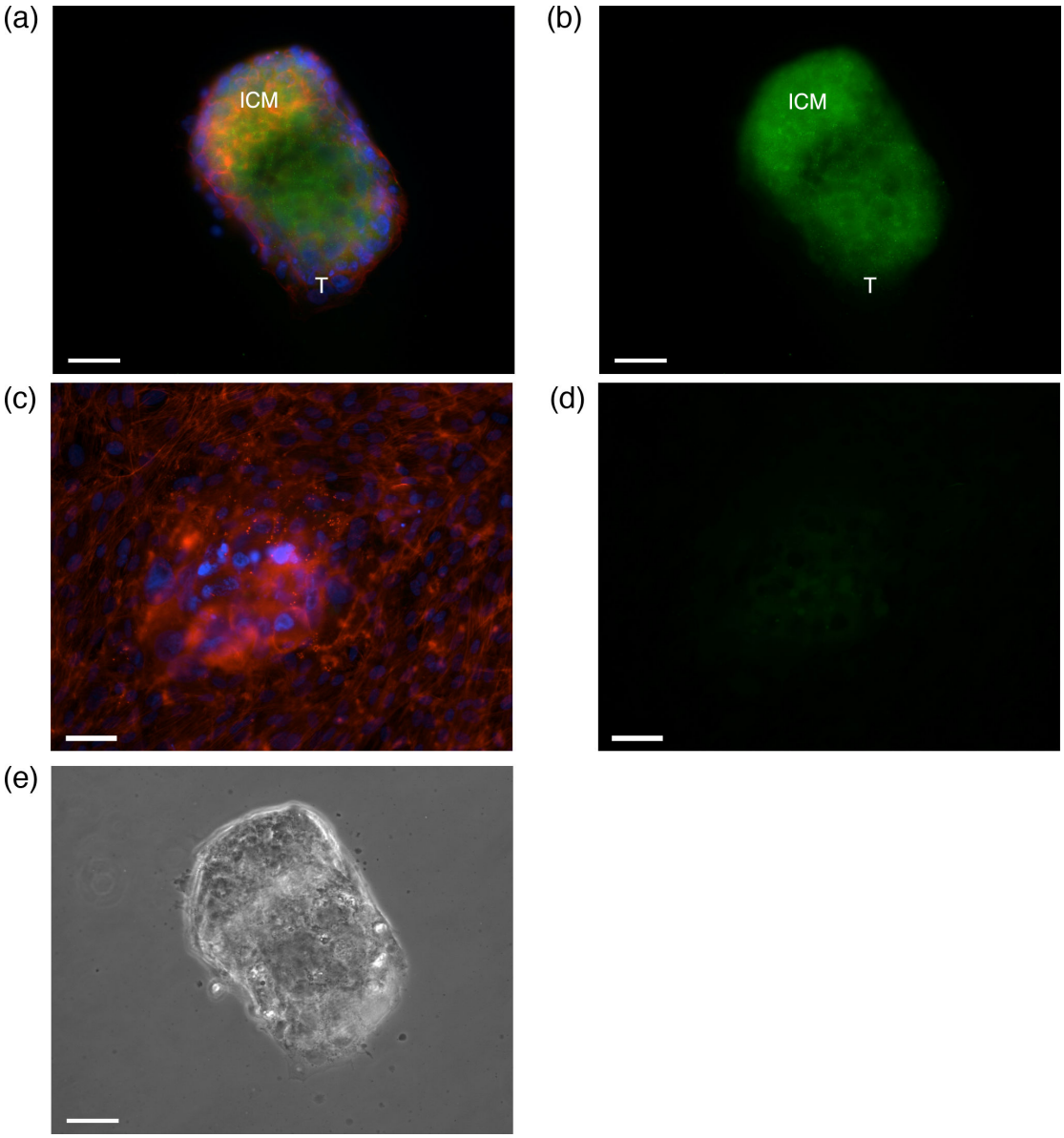

Figure 5-12 Blastocyst attached on a coverslip coated with FIII7-12 A+B+ (a, b and e) after culture for 48 hours; detected by immunofluorescence (a, b) for integrin α9 (green), actin (red) and nucleus (blue), orange denotes co-localization of integrin α9 with actin. (e) is a phase contrast image of the embryo. A control blastocyst attached on a monolayer of ESCs (c and d) was treated with rabbit IgG at the same concentration as the primary antibody. Images are of the base of the attached embryo and shown as an overlay of all three components (a and c) and individual images of the green FITC staining of the same blastocyst shown in (b and d). ICM: inner cell mass, T: trophoblast outgrowth, also indicated by arrows. Scale bars = 50 μm. See next page for higher magnification images of the same embryo. Carried out by Ms Janet Carver (Nuffield Dept. of Obstetrics and Gynaecology, University of Oxford).

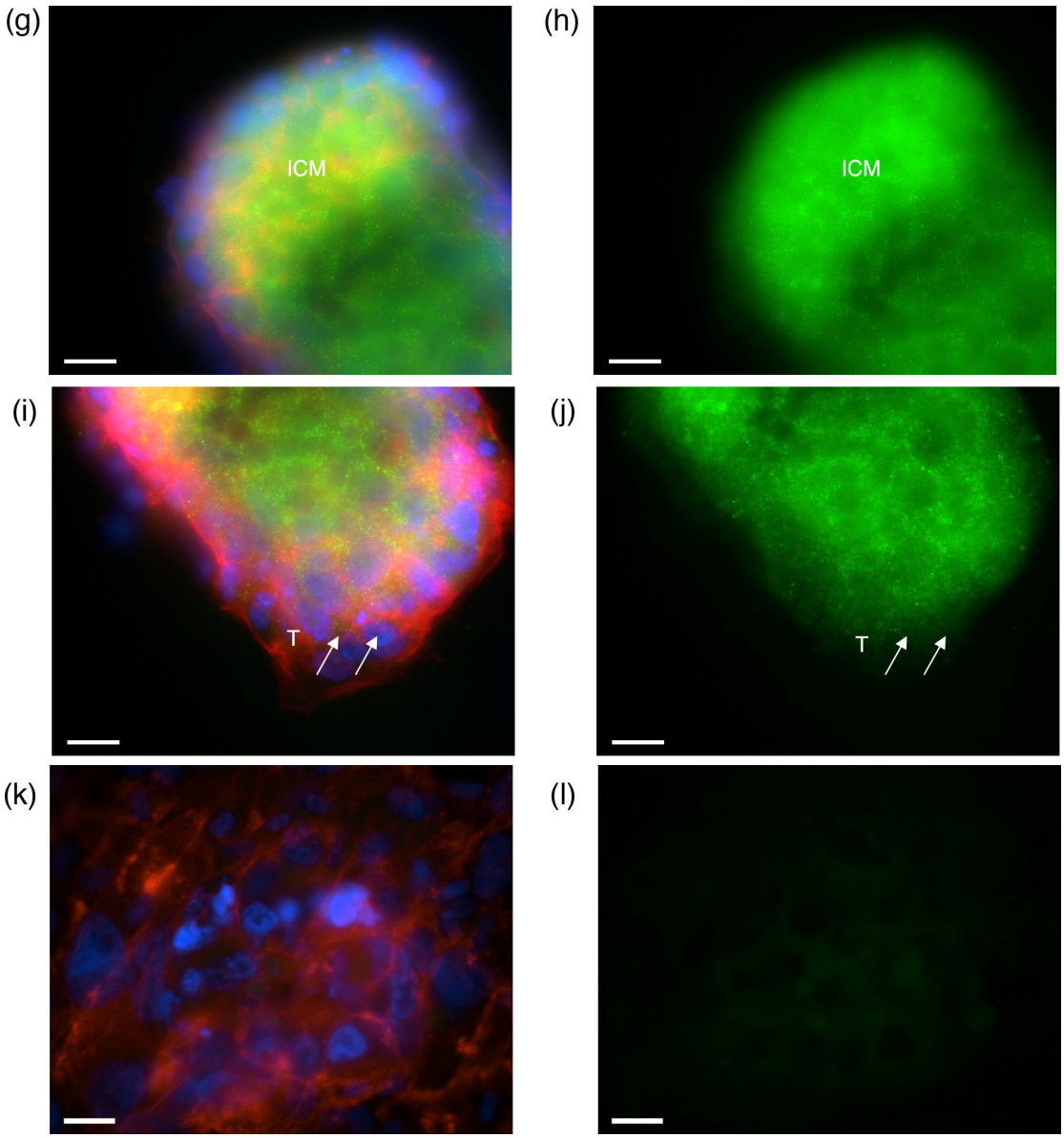

Figure 5-12 Blastocyst attached on a coverslip coated with FIII7-12 A+B+ (g-j) after culture for 48 hours; detected by immunofluorescence for integrin α9 (green), actin (red) and nucleus (blue), orange denotes co-localization of integrin α9 with actin. A control blastocyst attached on a monolayer of ESCs (k and l) was treated with rabbit IgG at the same concentration as the primary antibody. Images are of the base of the attached embryo and shown as an overlay of all three components (g, i and k) and individual images of the green FITC staining of the same blastocyst shown in (h, j and l). ICM: inner cell mass, T: trophoblast outgrowth, also indicated by arrows. Scale bars = 25 µm. See previous page for lower magnification images. Carried out by Ms Janet Carver (Nuffield Dept. of Obstetrics and Gynaecology, University of Oxford).

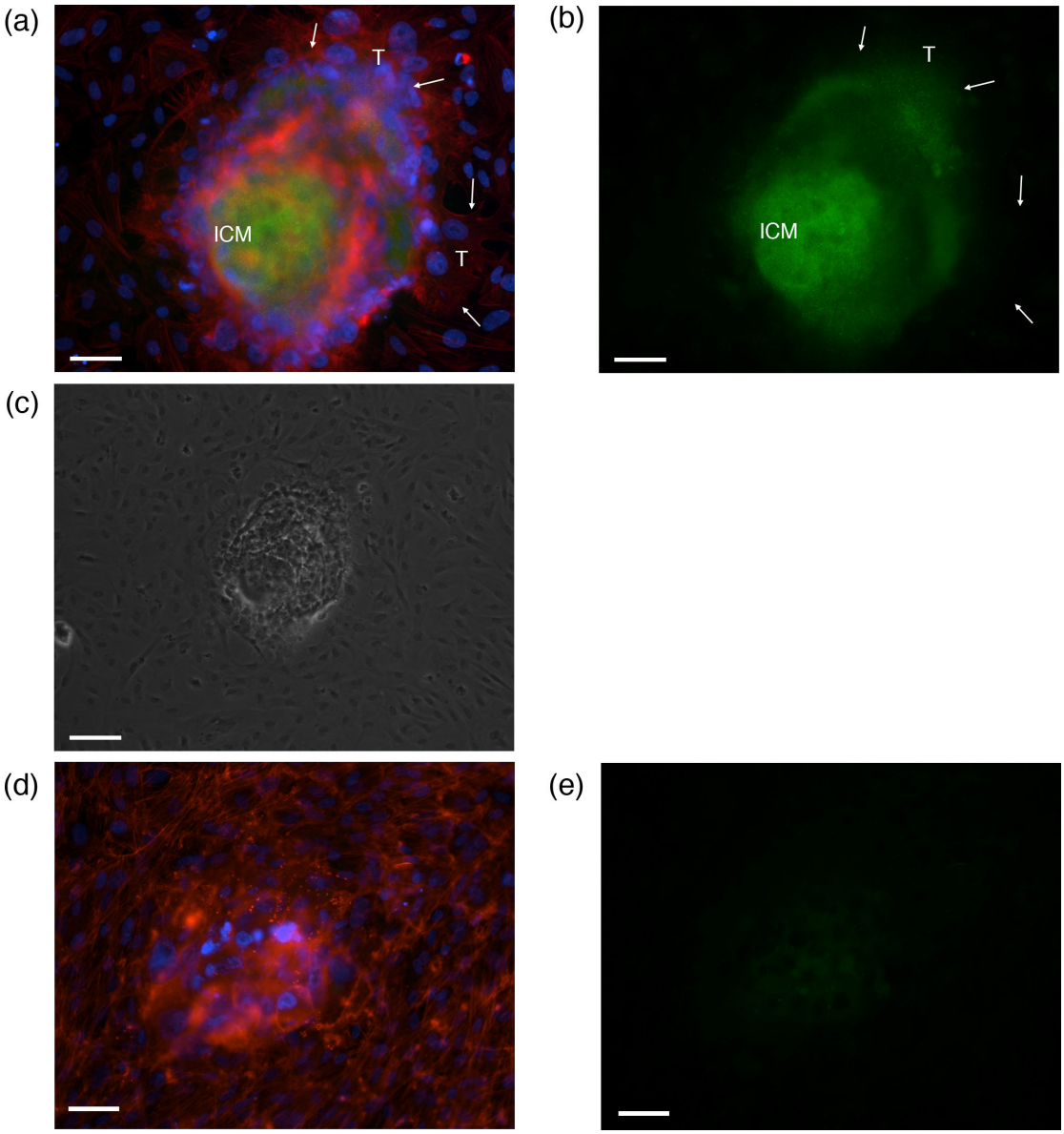

Figure 5-13 Blastocyst attached on ESCs in the presence of 50 µM EDIIIA (a-c) after culture for 48 hours; detected by immunofluorescence for integrin α9 (green), actin (red) and nucleus (blue). Orange denotes co-localization of integrin α9 with actin. (c) is a phase contrast image of the embryo. A control blastocyst attached on a monolayer of ESCs (d, e) was treated with rabbit IgG at the same concentration as the primary antibody. Images are of the base of the attached embryo and shown as an overlay of all three components (a, d) and individual images of green FITC staining of the same blastocyst shown in (b, e). ICM: inner cell mass, T: trophoblast outgrowth, also indicated by arrows. Scale bars: (a, b, d, e) = 50 µm; (c) = 100 µm. See next page for higher magnification images of the same embryo. Carried out by Ms Janet Carver (Nuffield Dept. of Obstetrics and Gynaecology, University of Oxford).

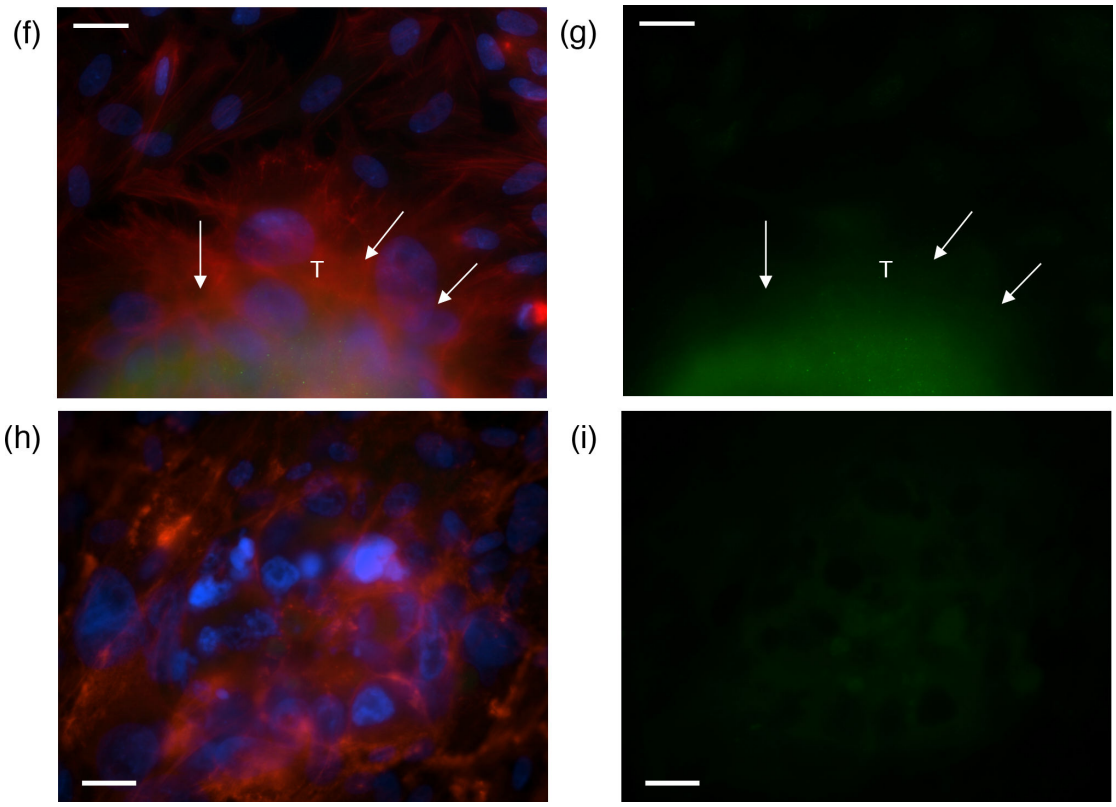

Figure 5-13 Blastocyst attached on ESCs in the presence of 50 μM EDIIIA (f-g) after culture for 48 hours; detected by immunofluorescence for integrin α9 (green), actin (red) and nucleus (blue). Orange denotes co-localization of integrin α9 with actin. A control blastocyst attached on a monolayer of ESCs (h, i) was treated with rabbit IgG at the same concentration as the primary antibody. Images are of the base of the attached embryo and shown as an overlay of all three components (f, h) and individual images of green FITC staining of the same blastocyst shown in (g, i). ICM: inner cell mass, T: trophoblast outgrowth, also indicated by arrows. Scale bars = 25 μm. See previous page for lower magnification images of the same embryo. Carried out by Ms Janet Carver (Nuffield Dept. of Obstetrics and Gynaecology, University of Oxford).

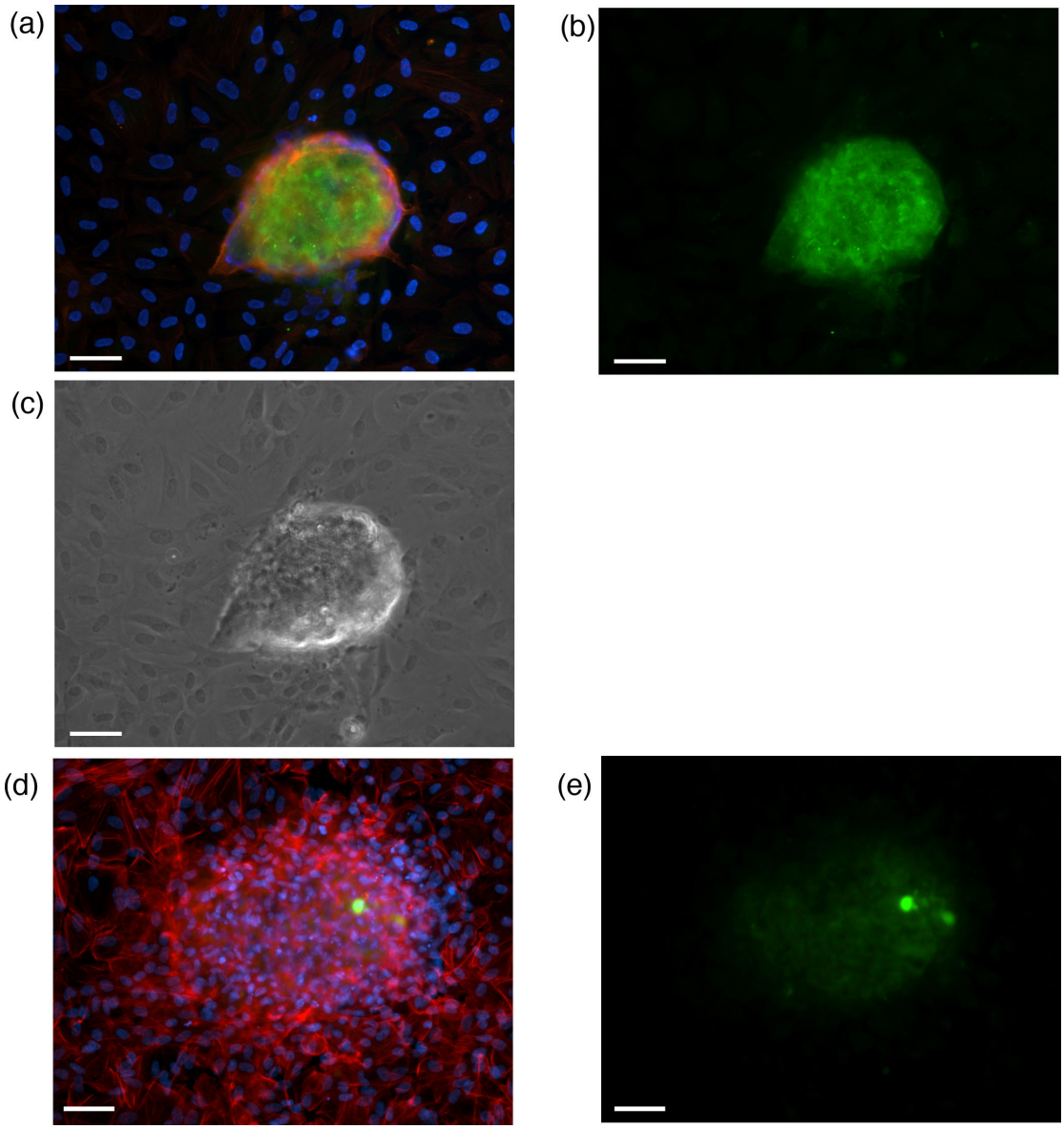

Figure 5-14 Blastocyst attached on ESCs in the presence of 50 μM EDIIIA (a-c) after culture for 48 hours; detected by immunofluorescence for integrin α4 (green), actin (red) and nucleus (blue). Orange denotes co-localization of integrin α4 with actin. (c) is a phase contrast image of the embryo. A control blastocyst attached on a monolayer of ESCs (d, e) was treated with mouse IgG at the same concentration as the primary antibody. Images are of the base of the attached embryo and shown as an overlay of all three components (a, d) and individual images of the green FITC staining of the same blastocyst shown in (b, e). (a) Exposure for actin is adjusted so to prevent over-exposure of actin within the blastocyst, therefore actin present in ESCs is not as apparent. ICM: inner cell mass, T: trophoblast outgrowth, also indicated by arrows. Scale bars = 50 μm. See next page for higher magnification images of the same embryo. Carried out by Ms Janet Carver (Nuffield Dept. of Obstetrics and Gynaecology, University of Oxford).

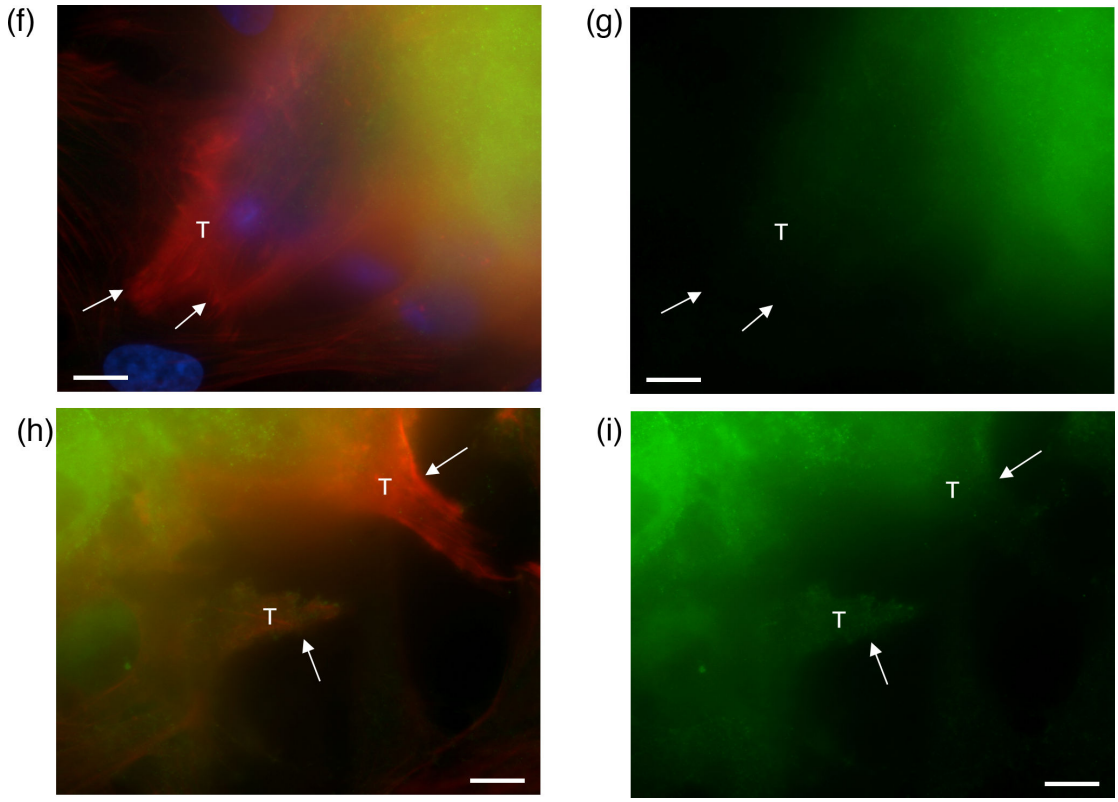

Figure 5-14 Blastocyst attached on ESCs in the presence of 50 µM EDIIIA (f-i) after culture for 48 hours; detected by immunofluorescence for integrin α4 (green), actin (red) and nucleus (blue). Orange denotes co-localization of integrin α4 with actin. A control blastocyst attached on a monolayer of ESCs (Figure 5-15 k, i) was treated with mouse IgG at the same concentration as the primary antibody. Images are of the base of the attached embryo and shown as an overlay of all three components (f, h) and individual images of the green FITC staining of the same blastocyst shown in (g, i). Exposure for actin is adjusted so to prevent over-exposure of actin within the blastocyst, therefore actin present in ESCs are not as apparent. ICM: inner cell mass, T: trophoblast outgrowth, also indicated by arrows. Scale bars = 10 µm. See previous page for lower magnification images of the same embryo. Carried out by Ms Janet Carver (Nuffield Dept. of Obstetrics and Gynaecology, University of Oxford).

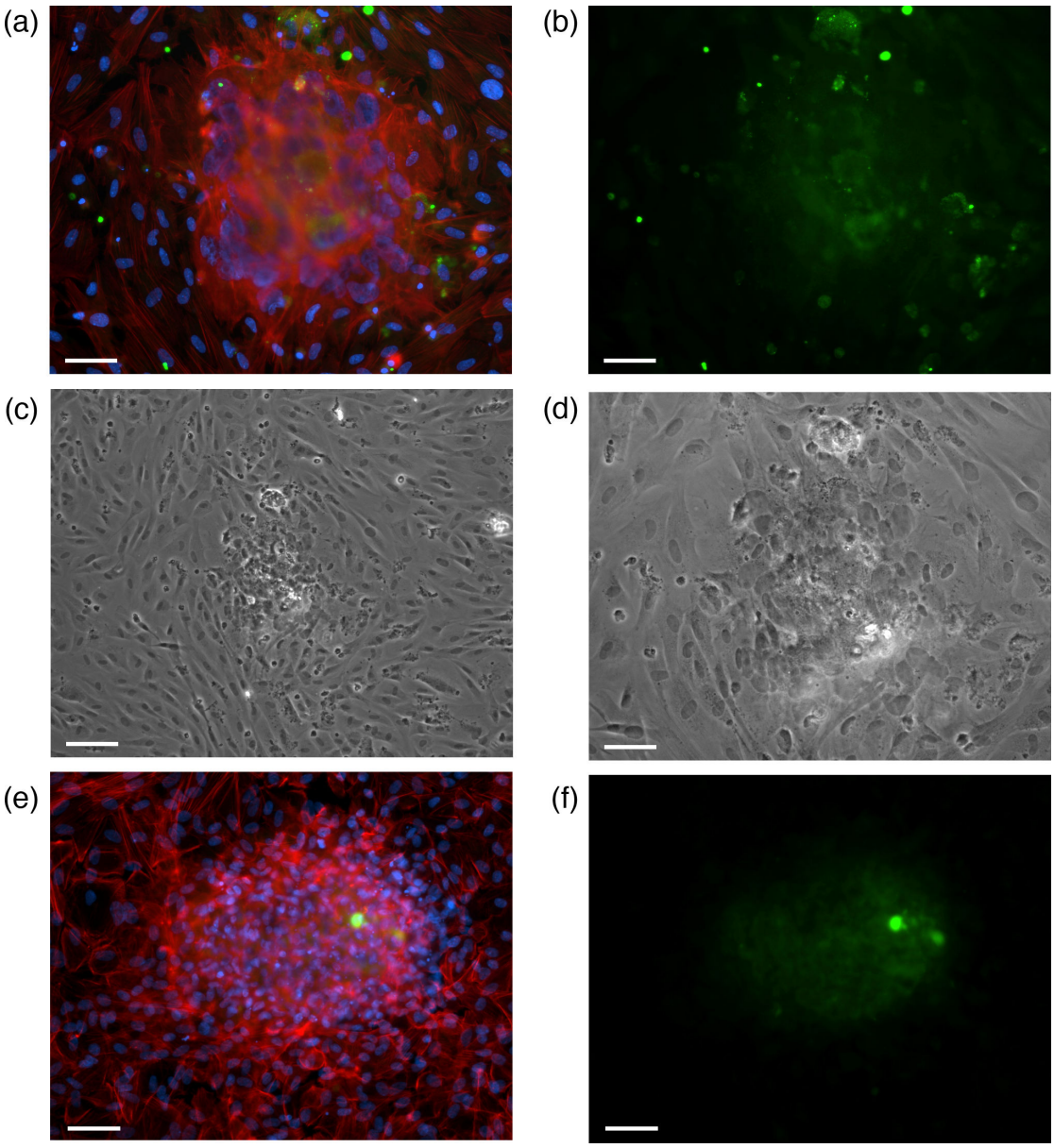

Figure 5-15 Blastocyst attached on ESCs (a-d) after culture for 48 hours; detected by immunofluorescence for integrin α4 (green), actin (red) and nucleus (blue). Orange denotes co-localization of integrin α4 with actin. (c, d) are phase contrast images of the embryo. A control blastocyst attached on a monolayer of ESCs (e, f) was treated with mouse IgG at the same concentration as the primary antibody. Images are of the base of the attached embryo and shown as an overlay of all three components (a, e) and individual images of the green FITC staining of the same blastocyst shown in (b, f). ICM: inner cell mass, T: trophoblast outgrowth, also indicated by arrows. Scale bars: (a, b, d, e, f) = 50 µm; (c) = 100 µm. See next page for higher magnification images of the same embryo. Carried out by Ms Janet Carver (Nuffield Dept. of Obstetrics and Gynaecology, University of Oxford).

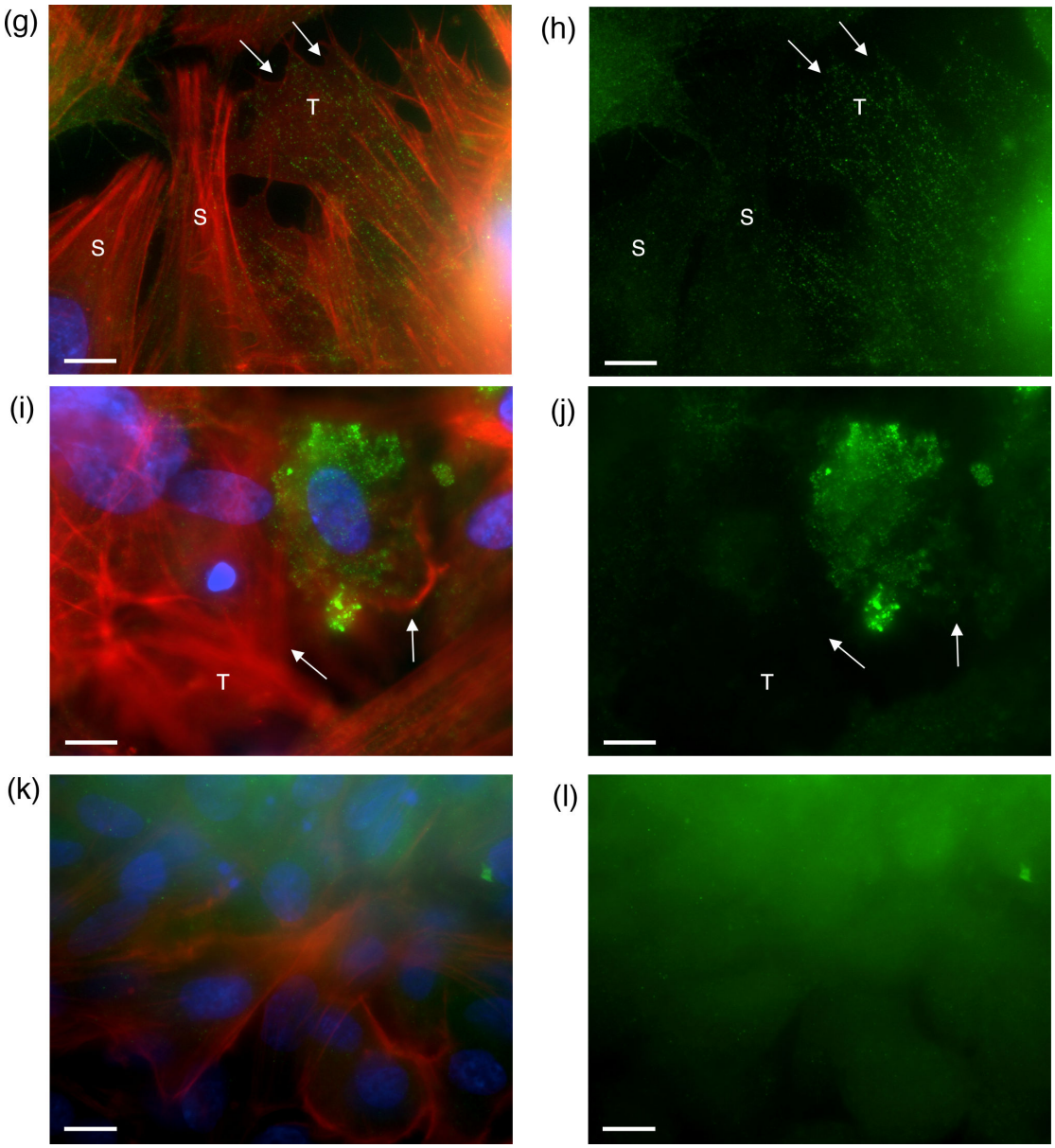

Figure 5-15 Blastocyst attached on ESCs (g-j) after culture for 48 hours; detected by immunofluorescence for integrin α4 (green), actin (red) and nucleus (blue). Orange denotes co-localization of integrin α4 with actin. A control blastocyst attached on a monolayer of ESCs (k, i) was treated with mouse IgG at the same concentration as the primary antibody. Images are of the base of the attached embryo and shown as an overlay of all three components (g, i, k) and individual images of the green FITC staining of the same blastocyst shown in (h, j, i). ICM: inner cell mass, T: trophoblast outgrowth, also indicated by arrows. Scale bars = 10 µm. See previous page for lower magnification images of the same embryo. Carried out by Ms Janet Carver (Nuffield Dept. of Obstetrics and Gynaecology, University of Oxford).

5.3 Discussion

Alternative splicing of FN is regulated in a tissue-specific and developmental manner (Peters *et al.* 1996). Expression of EDIIIA and EDIIIB in the endometrial stroma adjacent to the luminal epithelium and epithelial basement membrane at the time of implantation (Figure 5-1) suggests possible roles in implantation.

The purified recombinant protein was confirmed to be His-EDIIIA, as SDS-PAGE (Figure 5-8a) and mass spectrometry (Figure 5-7) confirmed its molecular weight to be 11 kDa and it could be detected by immunoblotting using the anti-EDIIIA antibody IST9 (Figure 5-8b). The addition of recombinant EDIIIA to the blastocyst-stromal cell co-culture had no inhibitory effect on blastocyst attachment and its ability to form outgrowths onto the stromal cell layer (Figure 5-9). These results suggest that the EDIIIA domain itself does not directly mediate blastocyst attachment. Alternatively, the conformation of the individual EDIIIA domain could be different from when EDIIIA is part of the FN molecule, thereby exposing or masking integrin binding sites in the presence of neighbouring FIII domains in the FN molecule. For example, MMP-9 expression in chondrocytes can be induced by recombinant EDIIIA protein, but not by cellular fibronectin containing EDIIIA (Saito *et al.* 1999). This provides a feasible explanation as to why treatment with recombinant EDIIIA did not affect blastocyst attachment, since EDIIIA+FN in the endometrial stroma may possess different integrin binding properties.

It has been shown that the attachment reaction between the trophoblast and LE is mediated by numerous complementary surface molecules, including mucins, HSPG, lectins, the trophinin-tastin-cystin complex, HB-EGF and its receptors and integrins

(Aoki *et al.* 2000; Kimber *et al.* 2000). Altering the potential interaction of EDIIIA+FN with the blastocyst may not significantly affect blastocyst attachment as the process may also be mediated by many different molecules in the stroma.

The EDIIIA segment has been identified to bind to integrins α4β1 and α9β1 (Liao *et al.* 2002). Here, we have shown that the integrin subunits α4 and α9 are potentially expressed by blastocysts attached onto ESCs, raising the possibility that endometrial stromal EDIIIA+FN could interact with the blastocyst via these integrin receptors. As α4β1- and α9β1-mediated cell adhesion results in increased cell migration (Young *et al.* 2001; Liu *et al.* 2002), ligation of α4β1 and α9β1 in the blastocyst with EDIIIA may modulate blastocyst migration and invasion into the stroma.

The EDIIIA domain may influence cellular processes other than attachment, such as invasion and migration by inducing expression of MMPs as shown in synovial cells (Saito *et al.* 1999). The EDIIIA domain can also interact with TLR-4, a signalling receptor that is stimulated by LPS to induce expression of genes involved in inflammatory responses, such as pro-inflammatory cytokines IL-8, IL-6, IL-1β and TNFα, and MMPs (Saito *et al.* 1999; Okamura *et al.* 2001; Gondokaryono *et al.* 2007). The expression of TLR-4 has been demonstrated in ESCs and EECs (Hirata *et al.* 2005), first trimester trophoblast cells (Abrahams *et al.* 2004), but has not yet been identified in human embryos. In future studies, the expression of TLR-4 by the blastocyst and potential interactions with endometrial stromal EDIIIA+FN could be investigated. The ability of endometrial stromal EDIIIA+FN to induce inflammatory responses in ESCs on TLR-4 ligation could also be tested, by culturing ESCs on EDIIIA+FN and assessing the secretion of pro-inflammatory cytokines such as IL-1β

and TNFα, and if any observed effects could be reversed by neutralizing antibodies to TLR-4.

As well as providing an additional interaction site in the FN molecule, inclusion of the EDIIIA domain in FN of the endometrial stroma may modify the conformation of the FN molecule, including accessibility of the cell-adhesive RGD motif, to modulate functional properties of FN such as cell adhesion and migration; this will be further investigated in Chapter 6.

Chapter 6

Structural and functional roles of EDIIIA and EDIIIB inclusion in FN

6.1 Introduction

FNs can mediate cell adhesion via interaction with integrin receptors to regulate cellular activities including cell migration, proliferation and differentiation. Expression of FN splice variants are regulated in a tissue-specific and developmental manner (Peters *et al.* 1996), but their precise biological functions are unclear. There is conflicting evidence as to how EDIIIA and EDIIIB can modulate cell adhesive properties of FN, and it was suggested that inclusion of the alternatively spliced domains induces conformational change in the FN molecule and not by providing additional cell-interaction sites (Hashimoto-Uoshima *et al.* 1997; Manabe *et al.* 1997).

The insertion of the EDIIIA domain has been proposed to alter the global conformation of the FN molecule, the N-terminal two-thirds of the FN molecule (N-terminal through FIII11) could rotate up to 180^{o} relative to the C-terminal one-third, FIII12 through the C-terminus (Manabe *et al.* 1997). Previously, it has been demonstrated that adjacent FIII modules are interconnected with rotations along the long axis of the FN molecule, with highly variable tilt and rotation angles between adjacent domains (Leahy *et al.* 1996). A particularly small rotation between FIII9 and FIII10 with the RGD motif of FIII10 and the PHSRN synergistic sequence of FIII9 on the same face creates a binding site for integrins. The insertion of EDIIIA or

EDIIIB may cause the FN molecule to shift and alter interdomain angles and orientations. Integrin specificity has been shown to be determined by the FIII9-10 interdomain tilt (Altroff *et al.* 2004), therefore insertion of EDIIIA or EDIIIB could alter FN conformation and accessibility of the RGD motif to integrins.

The effects of EDIIIA and EDIIIB inclusion on the functional properties of FN, such as integrin binding, FAK activation and endometrial stromal cell adhesion and proliferation were investigated. Preliminary structural studies were carried out to elucidate how EDIIIA inclusion affects the structure and conformation of the FN molecule, including crystallization studies of recombinant FN fragments containing the EDIIIA domain.

6.2 Results

6.2.1. Expression and purification of recombinant fibronectin fragments

Recombinant FN fragments were expressed using prokaryotic gene expression systems. FN modules produced in *E.coli* assume a stable conformation and do not seem to have reduced functionality due to the lack of glycosylation (Olden *et al.* 1979). The FN fragments FIII7-12A+B+, FIII7-12A+B-, FIII7-12A-B+, FIII7-12A-B- and FIII9'10 were expressed as GST-FIII fusion proteins (Figure 6-1 a). GST has been shown to be functionally inert and does not influence the activity of the FIII domains (Mardon *et al.* 1994). Also, as GST can dimerise there will be increased function because the recombinant proteins are presented as dimers. Recombinant FN fragments spanning FIII7 to FIII12 were used as they span just the FIII domains where EDIIIA and EDIIIB are inserted into the FN molecule, and include the RGD motif of FIII10 and PHSRN synergistic sequence of FIII9. The GST-fusion proteins were purified by affinity purification over Glutathione-Sepharose and by FPLC size-exclusion chromatography (Superdex 200 HR 10/30) as described in Section 2.3.1.1.

In the FPLC purification of GST-FIII7-12A+B+ (A+B+, Figure 6-3), fractions A1 and A2 were pooled for further concentration as they were detected as a single band in the reducing 12% SDS-PAGE near the expected molecular weight of 105 kDa. Two fractions were collected probably as a result of slightly different conformations of the protein present in the non-reducing conditions of the FPLC column, which then gave a single band under the reducing conditions of the 12% SDS-PAGE. In the FPLC elution profile of GST-FIII7-12A+B- (A+B-, Figure 6-4), only fractions A1

and A2 were pooled as they were detected as single bands near the expected molecular weight of 96 kDa on the 12% SDS-PAGE gel. Fraction A3 contained a lower molecular weight contaminant. In the purification of GST-FIII7-12A-B+ and GST-FIII7-12A-B- (A-B+ and A-B-, Figure 6-5), the fractions eluted at 10 ml were collected as in the previous FPLC purifications of A+B+ and A+B-. The fraction eluted at ~18 ml did not contain the protein of interest (SDS-PAGE not shown).

The purified GST-fusion proteins migrated on the reducing 12% SDS-PAGE gels as single bands (Figure 6-1 b) and were more than 90% pure, displaying slightly different molecular weights as expected, due to differences in mobilities of fibrous proteins and molecular weight markers in the SDS-PAGE gel. All four GST-fusion FIII7-12 proteins were detected by the anti-FN antibody by immunoblotting (Figure 6-2 a). Their molecular weights were not clear on the immunoblots due to large amounts of sample loaded onto the gels. The GST-fusion FIII7-12 proteins did not run precisely at the expected molecular weights, but the relative difference between them is as expected. It can be seen that the sizes of A-B+ was larger than A-B-, and A+B+ was larger than A+B- as expected. However, the A+B+ fragment could be detected by the anti-EDIIIA+FN antibody (Figure 6-2 b lane 8), but not the A+B- fragment (Figure 6-2 b lane 9), though the same A+B- fragment but with a His-tag instead of the GST-tag could be detected by the anti-EDIIIA+FN antibody (Figure 6-6 and Figure 6-8a, b). So perhaps the absence of the anti-EDIIIA signal for the GST-FIII7-12A+B+ in the immunoblot (Figure 6-2 b lane 9) could be the result of an experimental error such as non-uniform transfer of protein from the gel to membrane or non-uniform incubation of the membrane with antibody, or because of steric hindrance of the large (26kDa) GST tag.

For structural studies, the FN fragments FIII7-12A+B- and FIII8-12A+B- were expressed with a 6xHis-tag (Figure 6-7a) to allow for affinity purification by Ni-NTA as described in Section 2.3.1.2. The purified proteins migrated on reducing 12% SDS-PAGE gels as single bands (Figure 6-7b) and were detected by immunoblotting using the anti-EDIIIA antibody IST9 (Figure 6-8). The proteins were more than 90% pure, displaying slightly different molecular weights as expected, due to differences in mobilities of fibrous proteins and molecular weight markers in the SDS-PAGE gel.

Their molecular weights were investigated by mass spectrometry (Figure 6-10), the mass spectrometry profiles appear to be quite dirty with a lot of minor peaks, though both His-FIII7-12A+B- and His-FIII8-12A+B- could be detected as single bands by reducing 12% SDS-PAGE (Figure 6-7b) and immunoblotting (Figure 6-8). The experimental determined values of 70956 Da and 60781 Da for His-FIII7-12A+B- and His-FIII8-12A+B- were different to their expected molecular weights of 70850 Da and 60795 Da. These differences could be the result of errors in machine calibration and a noisy sample.

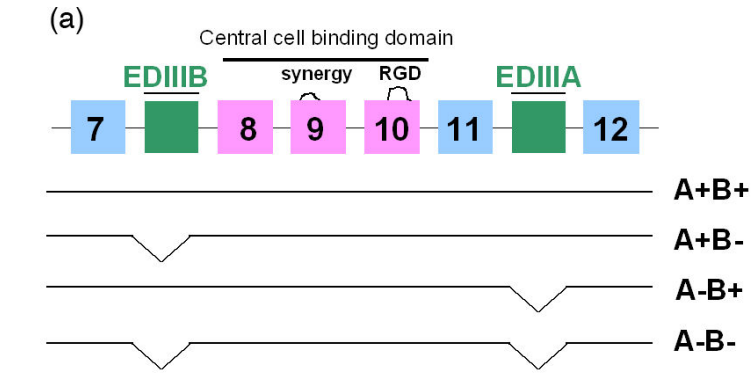

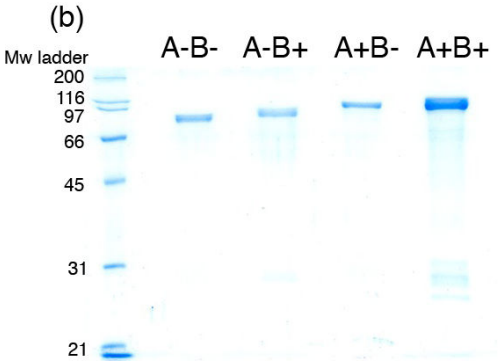

FIII 7-12 fragment	Expected molecular weights (kDa)
A+B+	105
A+B-	95.7
A-B+	95.5
A-B-	85.8

Figure 6-1 (a) Diagram of FIII7-12 domains expressed as GST-FIII fusion proteins, (b) 12% reducing SDS-PAGE gel and expected molecular weights of purified GST fusion proteins; FIII 7-12 A+B+ (A+B+, 105kDa), FIII 7-12 A+B- (A+B-, 95.7kDa), FIII 7-12 A-B+ (A-B+, 95.5kDa), FIII 7-12 A-B- (A-B-, 85.8kDa). Mw ladder = molecular weight ladder in kDa.

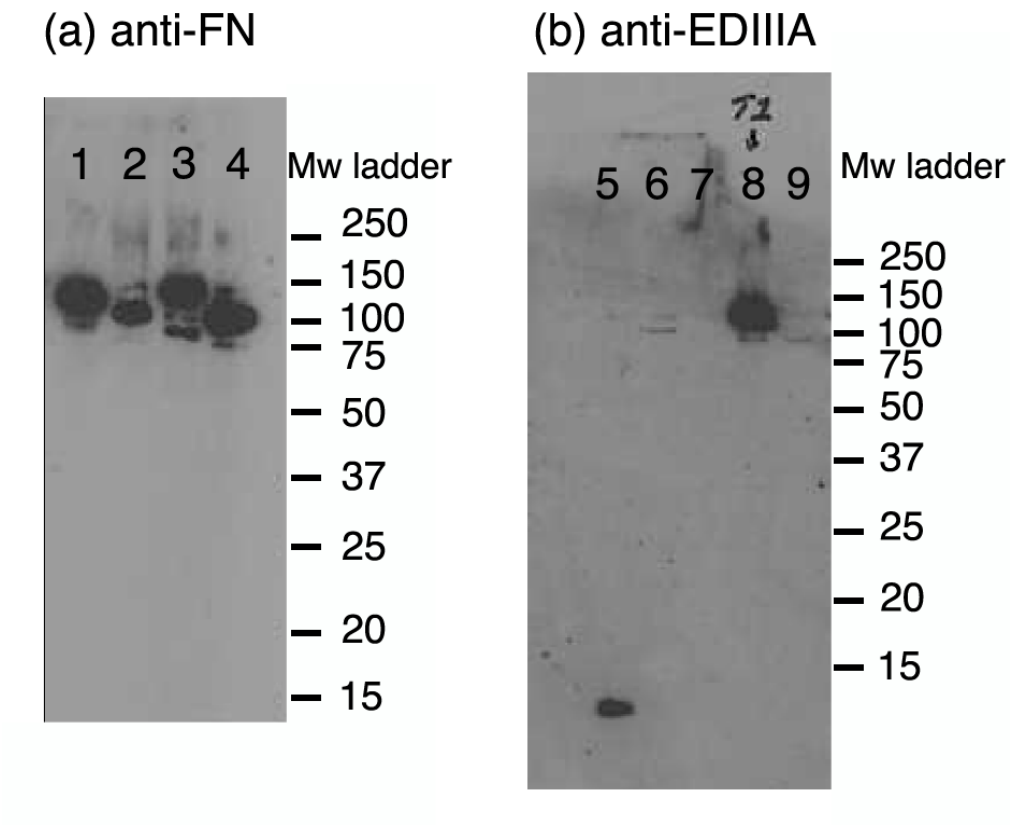

Figure 6-2 Immunoblots of purified GST- FIII7-12 fusion proteins (Table 6-1) detected using (a) anti-total FN (clone 3E3) and (b) anti-EDIIIA+FN (clone IST9), from a 10 % SDS-PAGE gel. Mw ladder = molecular weight ladder in kDa, carried out by Mrs Céline Jones (Nuffield Dept. of Obstetrics and Gynaecology, University of Oxford).

Lane	GST-FIII 7-12 fusion protein	Expected molecular weight (kDa)
1	FIII 7-12 A-B+	95.5
2	FIII 7-12 A-B-	85.8
3	FIII 7-12 A+B+	105
4	FIII 7-12 A+B-	95.7
5	His-EDIIIA	11.5
6	FIII 7-12 A-B+	95.5
7	FIII 7-12 A-B-	85.8
8	FIII 7-12 A+B+	105
9	FIII 7-12 A+B-	95.7

Table 6-1 Purified GST-FN fusion proteins and His-EDIIIA loaded on immunoblots in Figure 6-2

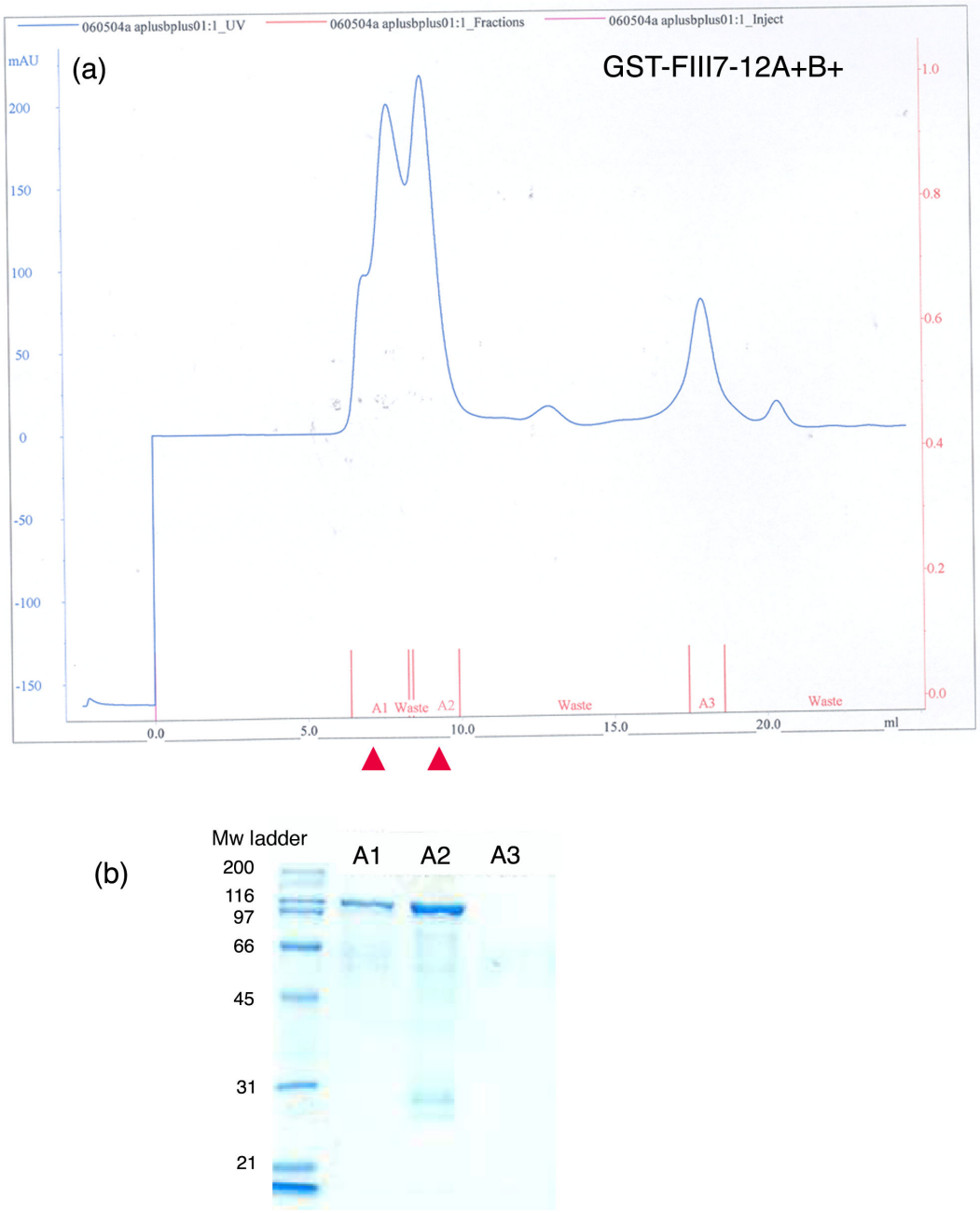

Figure 6-3 Protein purification by FPLC size exclusion chromatography (Superdex 200) (a) FPLC elution profile for the purification of GST-FIII7-12A+B+, the red triangle denotes the eluted fractions that were pooled (A1 and A2), (b) 12%, reducing SDS-PAGE of the eluted fractions. Mw ladder = molecular weight ladder in kDa.

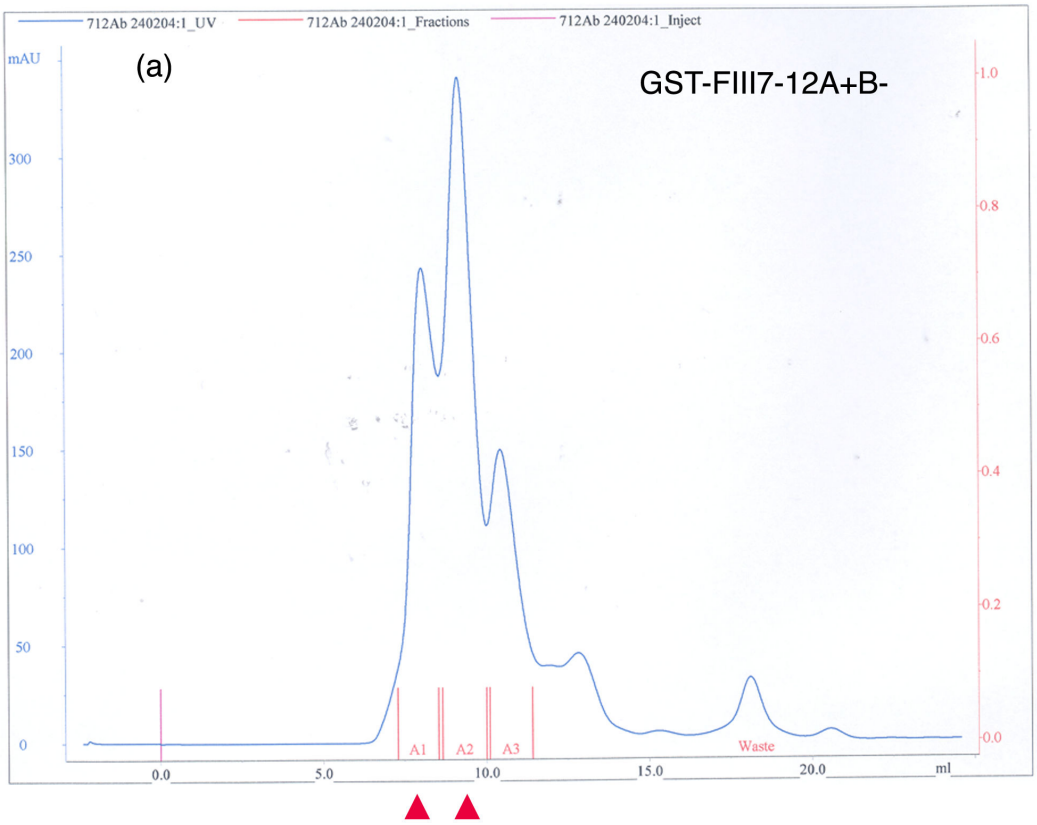

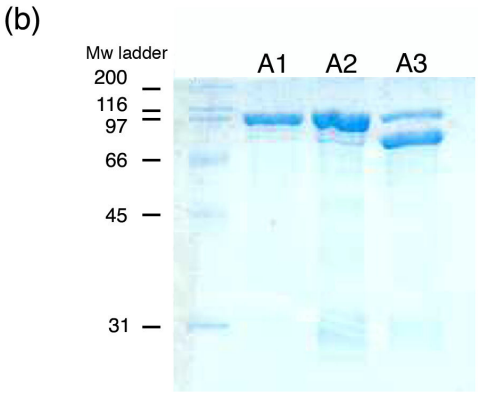

Figure 6-4 Protein purification by FPLC size exclusion chromatography (Superdex 200) (a) FPLC elution profile for the purification of GST-FIII7-12A+B-, the red triangle denotes the eluted fractions that were pooled for further concentration (A1 and A2), (b) 12%, reducing SDS-PAGE of the eluted fractions. Mw ladder = molecular weight ladder in kDa.

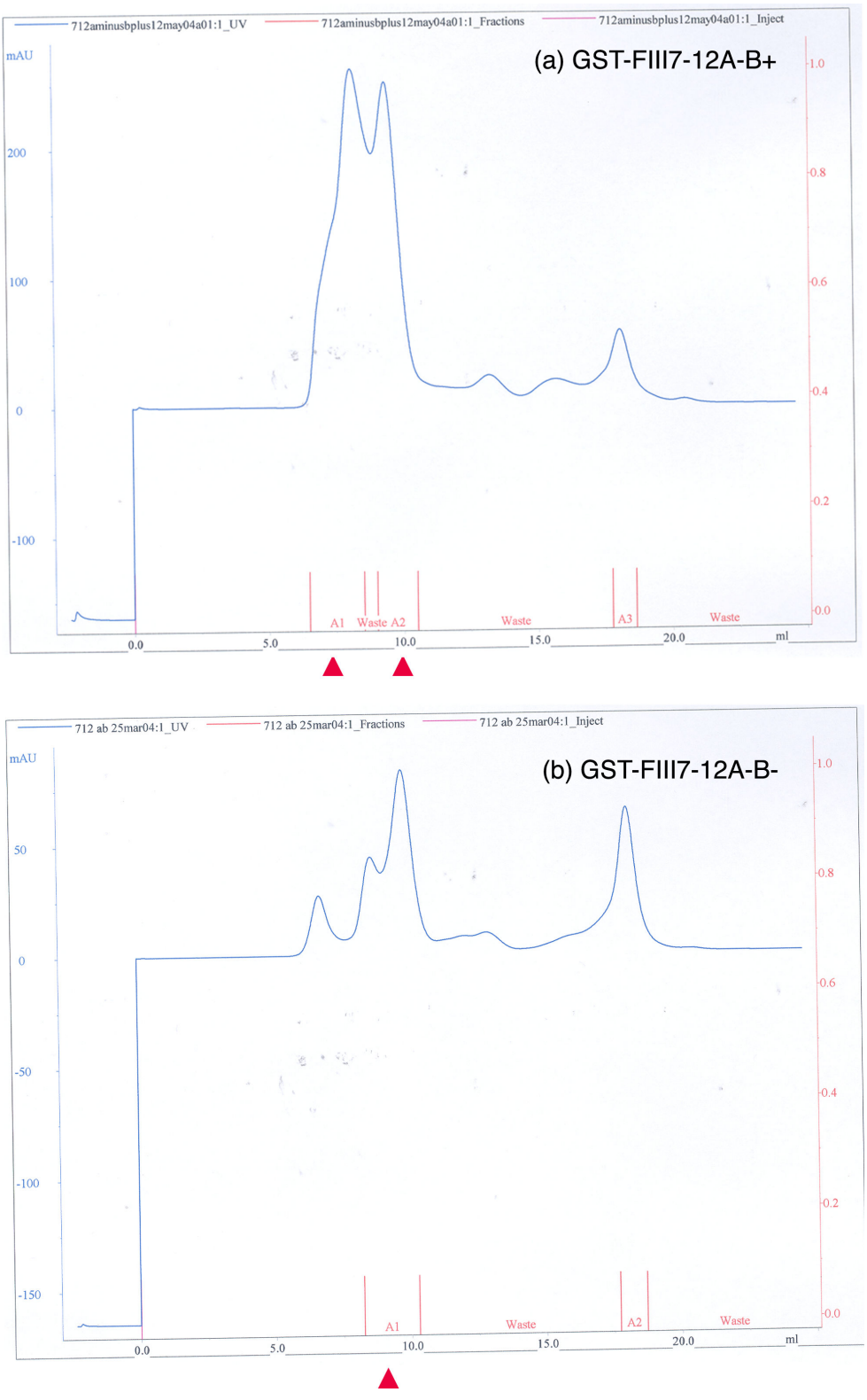

Figure 6-5 Protein purification by FPLC size exclusion chromatography (Superdex 200). FPLC elution profile for the purification of (a) GST-FIII7-12A-B+ and (b) GST-FIII7-12A-B-, red triangle denotes the eluted fraction that was pooled for further concentration.

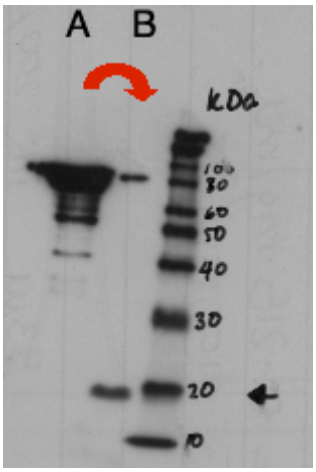

Figure 6-6 Immunoblot of purified His-FIII7-12 A+B- (A, expected Mw 70.9 kDa) and His-EDIIIA (B, expected Mw 11.5 kDa), detected using anti-EDIIIA (clone IST9) from a reducing 12 % SDS-PAGE gel. The red arrow indicates His-FIII7-12 A+B- that 'leaked' into the next lane on the gel.

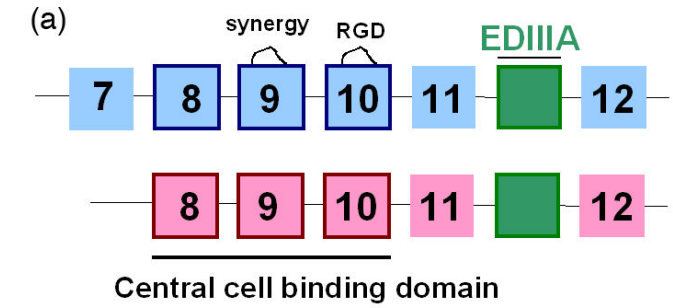

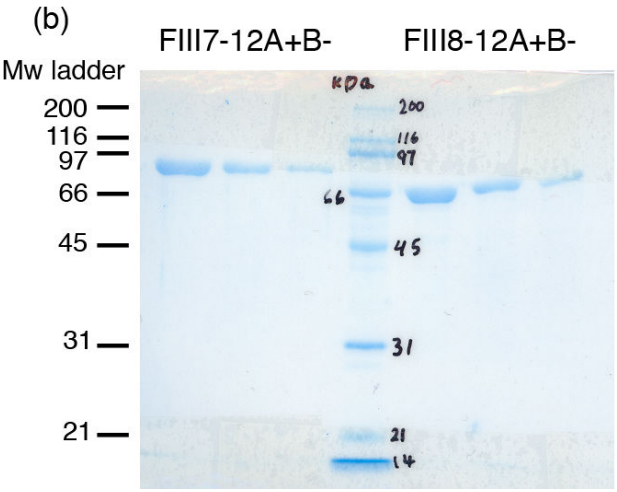

His-FIII fragment	Expected molecular weight (kDa)
FIII7-12A+B-	70.9
FIII8-12A+B-	60.8

Figure 6-7 (a) FIII domains expressed as His-tag proteins, (b) reducing 12% SDS-PAGE gel and expected molecular weights of purified His-FIII 7-12 A+B- (70.9kDa) and His-FIII 8-12 A+ (60.8kDa). Mw ladder = molecular weight ladder in kDa.

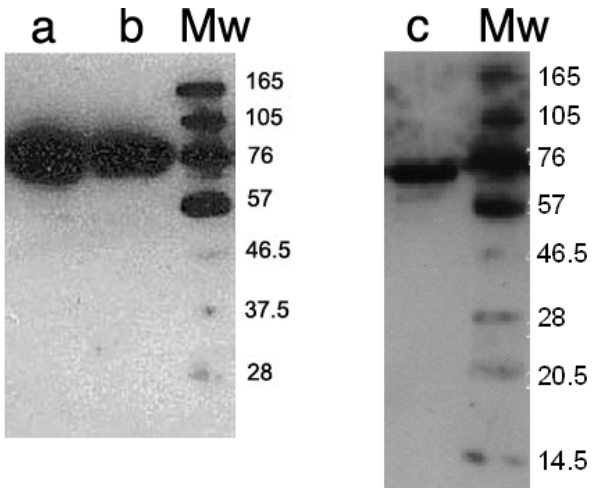

Figure 6-8 Immunoblots of purified His-FIII7-12 A+B- (a and b, expected Mw 70.0 kDa) and His-FIII8-12 A+B- (c, expected Mw 60.8 kDa) detected using anti-EDIIIA+FN (clone IST9) from a reducing 12 % SDS-PAGE gel. Mw ladder = molecular weight ladder in kDa.

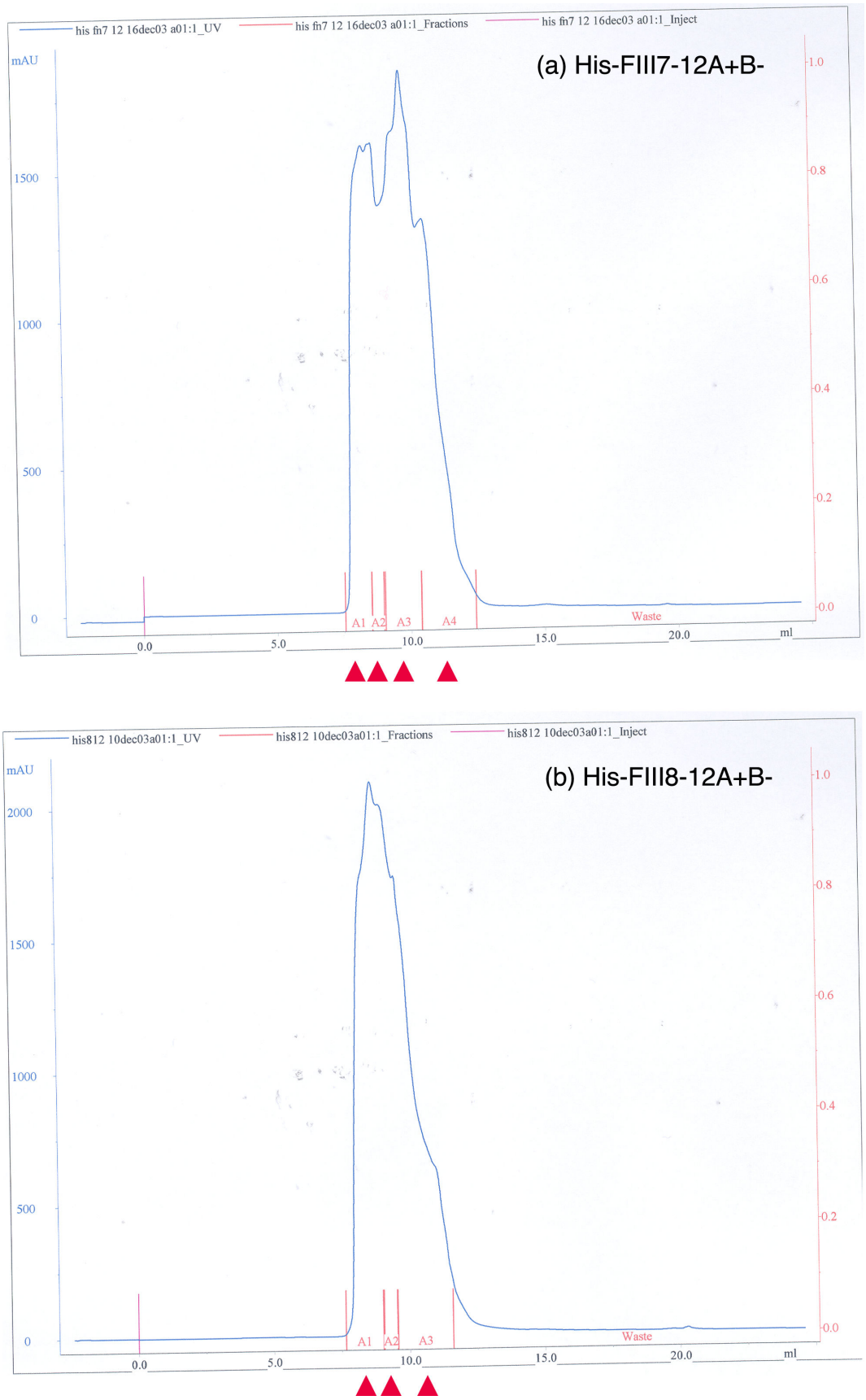

Figure 6-9 FPLC elution profile for the purification of (a) His-FIII7-12A+B- and (b) His-FIII8-12A+B-, red triangle denotes the eluted fraction that was pooled for further concentration.

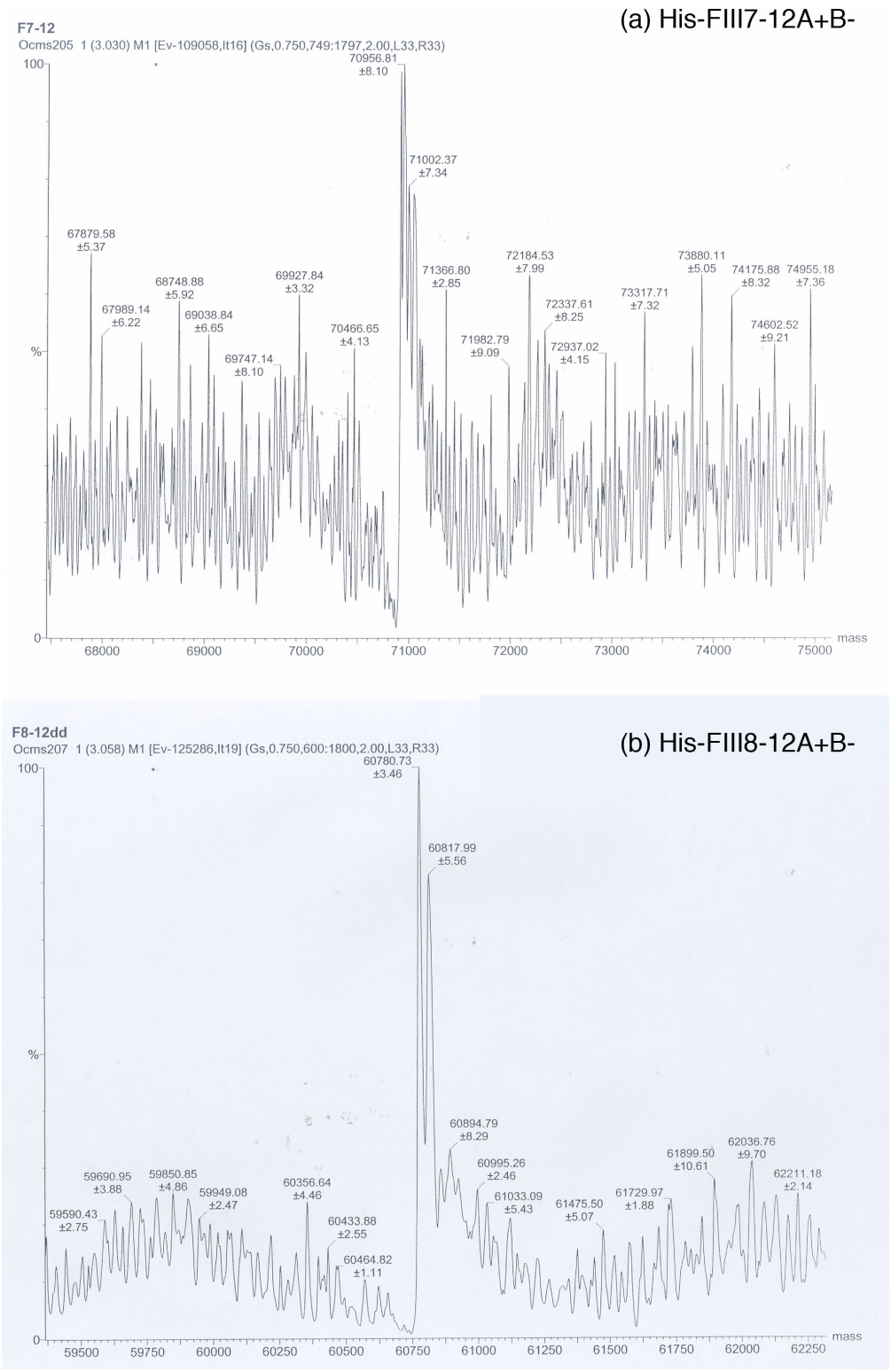

Figure 6-10 ESI-MS profile for (a) His-FIII7-12A+B-, expected molecular weight 70850 Da and (b) His-FIII8-12A+B-, expected molecular weight 60795 Da, carried out by Dr Katalin di Gleria, Weatherall Institute of Molecular Medicine, Oxford. These differ to experimentally determined mass values of 70956 Da for His-FIII7-12A+B- and 60781 Da for His-FIII8-12A+B-, SDS-PAGE and immunoblotting provided evidence for the identities of the proteins (Figure 6-7, Figure 6-8).

6.2.2. EDIIIA and EDIIIB does not modulate cell adhesive activities of FIII7-12

Endometrial stromal cell attachment was assessed by culturing ESCs on serial dilutions of recombinant GST-FIII7-12A±B± fusion proteins (See Section 2.6.2, Figure 6-12), the same batch of recombinant proteins were used in the cell attachment and spreading experiments. The GST-fusion proteins were coated at the starting saturating concentration of 100 µg/ml, which was approximately 1000 nM for each of the GST-fusion proteins. The fusion proteins exhibited similar binding capacities to plastic as assessed by ELISA using an anti-GST antibody (Section 2.5.1, Figure 6-11). Previous studies have shown that FN produced endogenously by ESCs are detected on the cell surface two hours after plating (Altroff 1999). As cell adhesion was assessed two hours after the ESCs were plated, the observed cell adhesion should be mediated by the recombinant GST-FIII7-12A±B± fusion proteins and not by the FN produced by ESCs. The ability of the recombinant GST-FIII7-12A±B± fusion proteins to induce secondary changes in cell morphology was tested by quantifying the proportion of spread cells on the FN-coated surfaces (See Section 2.6.2, Figure 6-13).

All four GST-FIII7-12A±B± fusion proteins supported the attachment, spreading and growth of ESCs. Cell attachment and spreading on all four fragments reached saturating levels near 100 nM (Figure 6-12 and Figure 6-13), replicate values from each of six independent experiment (n=6) has been plotted in a log scale to allow results at lower concentrations to be seen more clearly. Taking into account the variation between the different ESCs due to biological variation and factors such as the passage and number of ESCs used, their incubation times, concentrations of

proteins and substrates used, cell attachment measurements from each of the six individual experiments were normalized with the maximum OD value in each data set as 100, and expressed as a percentage of maximum attachment. The mean was then taken from the means of each individual experiment and plotted (Figure 6-14). No significant differences were observed between the cell attachment and spreading properties of the GST-FIII7-12A±B± fusion proteins.

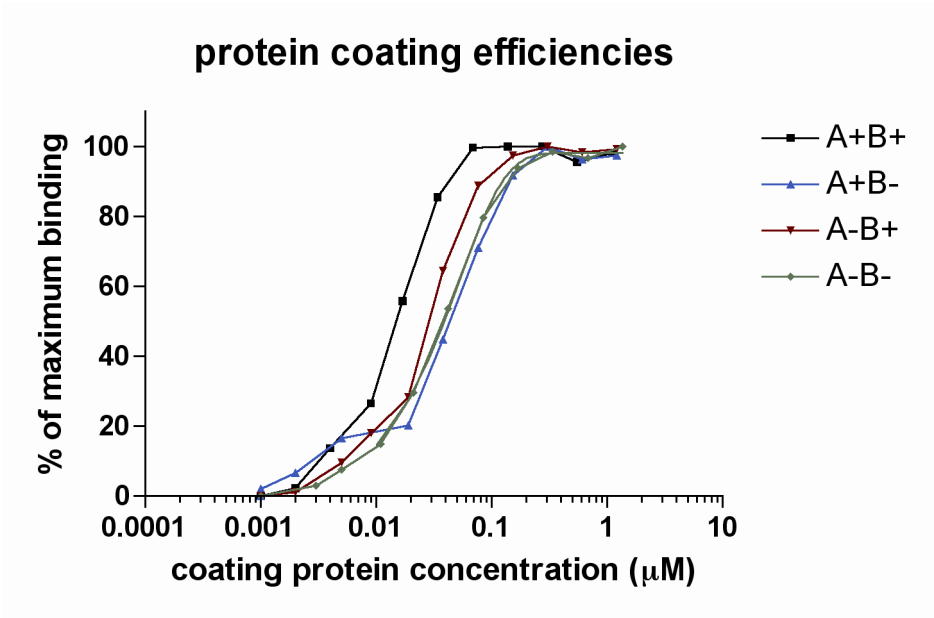

Figure 6-11 Plastic coating efficiencies of GST-FIII7-12A±B± fusion proteins. Binding to polystyrene surface was quantified by ELISA using an anti-GST antibody (See Section 2.5.1). Data points are means from replicate values in one independent experiment (n=1), represented as % of maximum binding and plotted on a log scale.

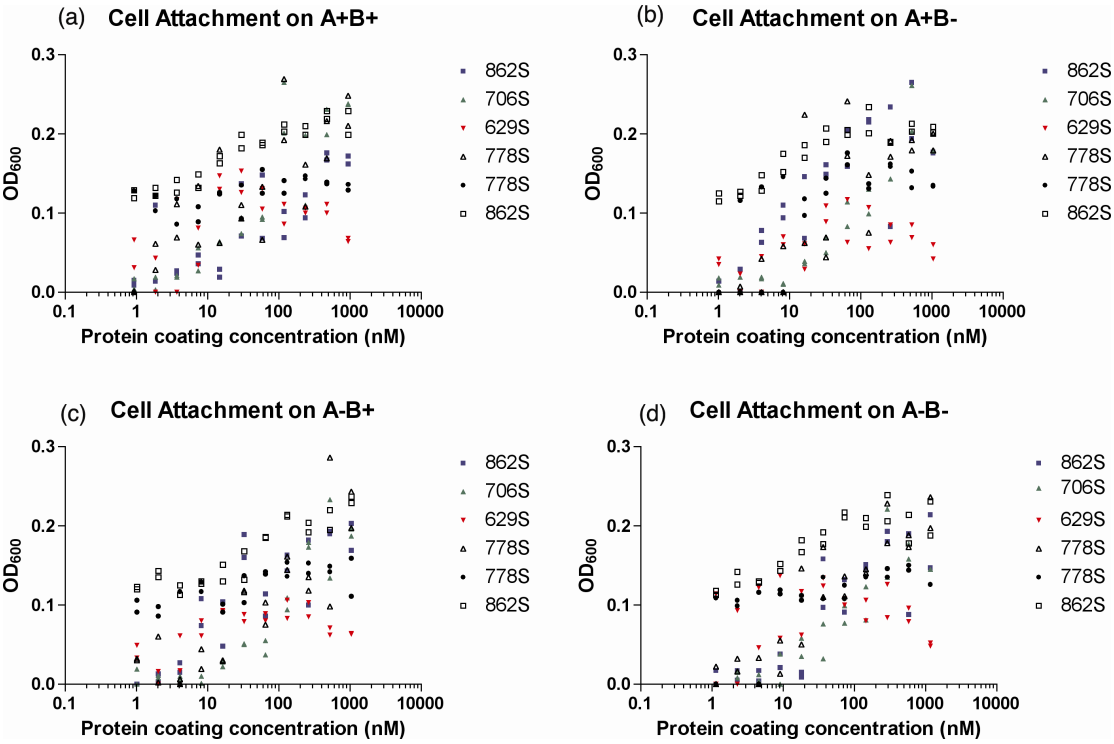

Figure 6-12 OD values for cell attachment of ESCs on (a) GST-FIII7-12A+B+, (b) GST-FIII7-12A+B-, (c) GST-FIII7-12A-B+ and (d) GST-FIII7-12A-B-. Attachment assays were performed in duplicate in six independent experiments (n = 6); data points are replicate OD_{600} measurements of each ESC patient cell number at each coating protein concentration and plotted on a log scale.

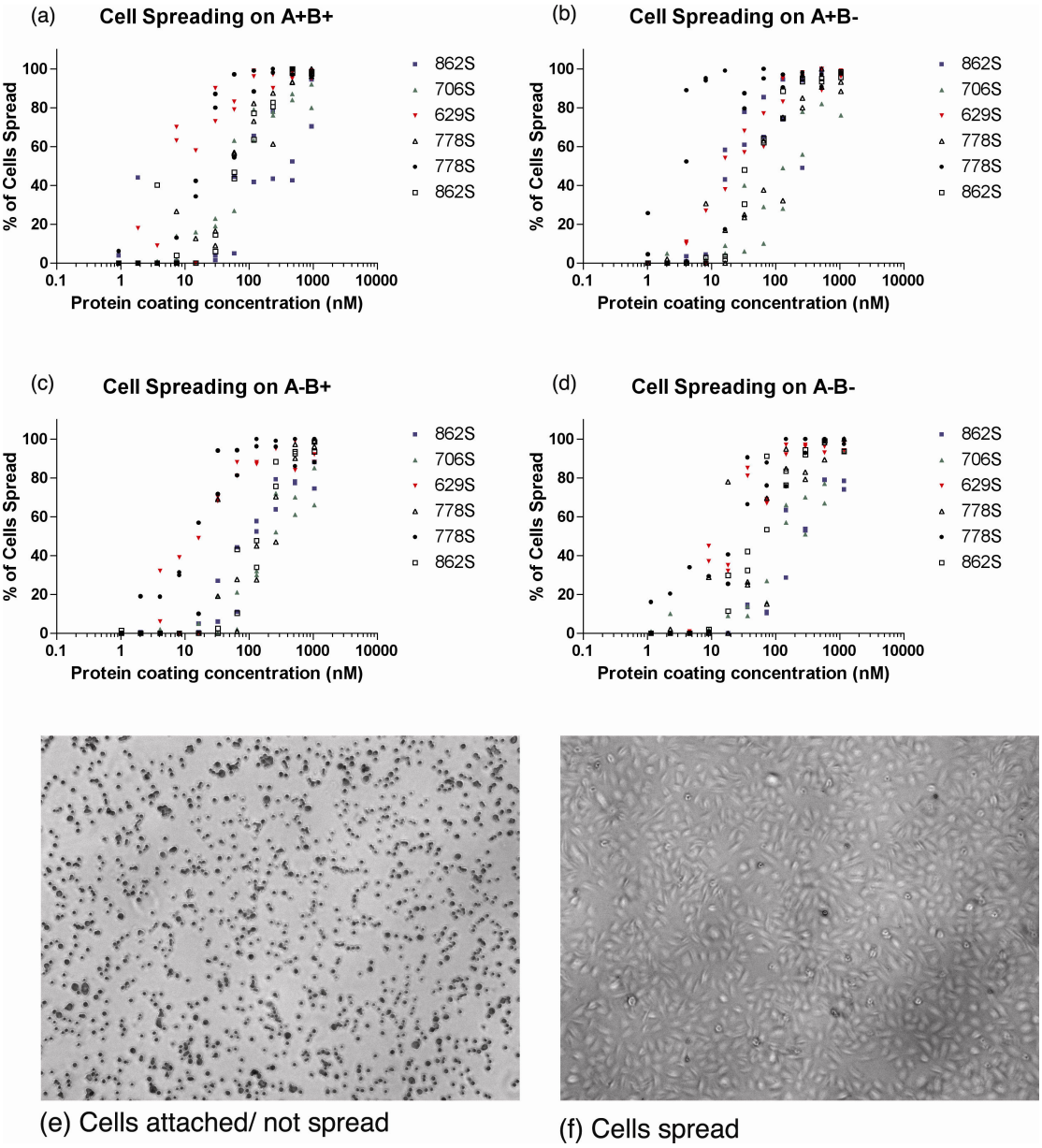

Figure 6-13 (a-d) Cell spreading activities of ESCs on GST·FIII7-12A±B± fragments. Spreading assays were performed in duplicate in six independent experiments (n = 6); data points are replicate measurements of each ESC patient cell number at each coating protein concentration, plotted on a log scale. Morphology of cells scored as spread or non-spread; spread cells were elongated and non-refractile with the nucleus clearly visible (f), non-spread cells were refractile with nucleus not visible (e).

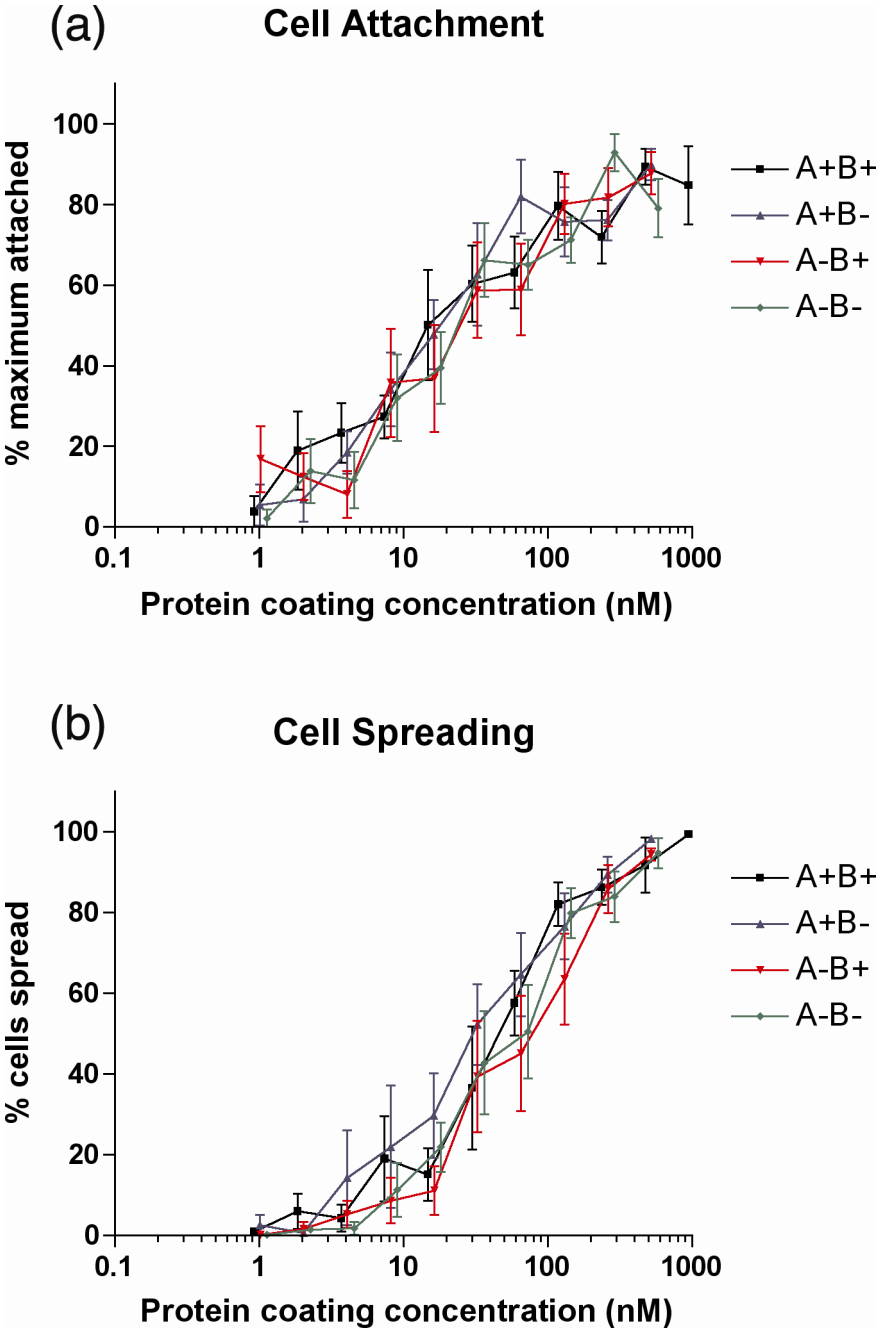

Figure 6-14 Normalized (a) Cell attachment and (b) cell spreading activities of ESCs on GST-FIII7-12A±B± fragments. Cell attachment and spreading assays were performed in duplicate in six independent experiments (n = 6), data points are means ± SEM of six independent duplicate determinations, plotted on a log scale. Results are expressed as percentage of cells spread or percentage of maximum attachment in each data set, as described previously (van der Walle *et al.* 2002) and (Mardon *et al.* 1994).

6.2.3. Inclusion of EDIIIA decreases binding affinity to integrin α5β1

The effect of EDIIIA and EDIIIB inclusion on FIII7-12 binding to integrins α5β1 (Figure 6-18 a, c) and αvβ3 (Figure 6-18 b, d) was evaluated. An ELISA was used to assess binding of GST-FIII7-12A±B± fusion proteins to immobilized integrins (Section 2.5.2). The same batch of integrin α5β1, integrin αvβ3 and each of the recombinant GST-FIII7-12A±B± fusion proteins was used in these integrin binding experiments. Integrins were purified from placental tissue together with Mrs Céline Jones (Nuffield Dept. of Obstetrics and Gynaecology, University of Oxford) as described in Section 2.3.2. Their coating efficiencies were determined by ELISA (Figure 6-15, Section 2.5.1). Saturating levels of the integrins were used to coat the plastic surfaces to ensure equal concentrations of integrin used in each experiment. An alternative experimental set-up would have been to plate the ligands onto the plastic surfaces, and then to measure the amount of integrin bound to the immobilized ligands. However, this was not used as it was easier to detect bound GST-tagged ligands using anti-GST antibody, and also immobilizing ligand onto surfaces may affect its conformation and function. It would be useful to also carry out the alternative experimental set-up as a comparison, since in the cell adhesion and proliferation assays the ligands were immobilized onto plates (Sections 6.2.2 and 6.2.6).

Binding of all four GST-FIII7-12A±B± fragments and FIII9'10 was detected on integrins α5β1 and αvβ3 (Figure 6-16). Here, the data points are duplicate OD_{600} measurements from each of three (for α5β1, n=3) or two (for αvβ3, n=2) independent experiments. Due to variations between each independent experiment resulting from

factors such as incubation times, concentrations of proteins and substrates used, the data were normalized with the maximum OD value in each data set set as 100. The mean was then taken from the means of each individual experiment, this was analyzed by non-linear regression using a sigmoidal curve fit as described previously (Altroff *et al.* 2001) (Figure 6-17).

Dose-response curves were plotted for binding to α5β1 (Figure 6-18 c) and αvβ3 (Figure 6-18 d) and the apparent dissociation constant (K_D), the ligand concentration at the midpoint of the dose response curves was calculated as an indication, but not an absolute measurement of binding affinity (Figure 6-19), as reported previously (Altroff *et al.* 2001).

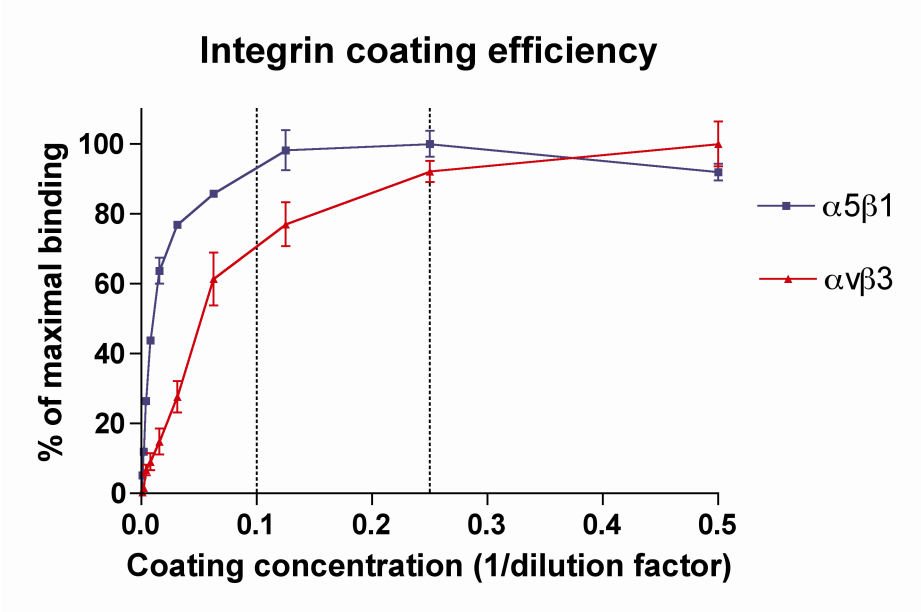

Figure 6-15 Coating efficiencies for integrins α5β1 and αvβ3 purified from human placental tissues determined by ELISA, in this one batch of integrin preparation α5β1 was used at 1 in 10 dilution and αvβ3 used at 1 in 4 dilution for saturating coating efficiencies. Data points are means of replicate measurements in one experiment (n=1). Integrins were purified from placental tissue together with Mrs Céline Jones (Nuffield Dept. of Obstetrics and Gynaecology, University of Oxford).

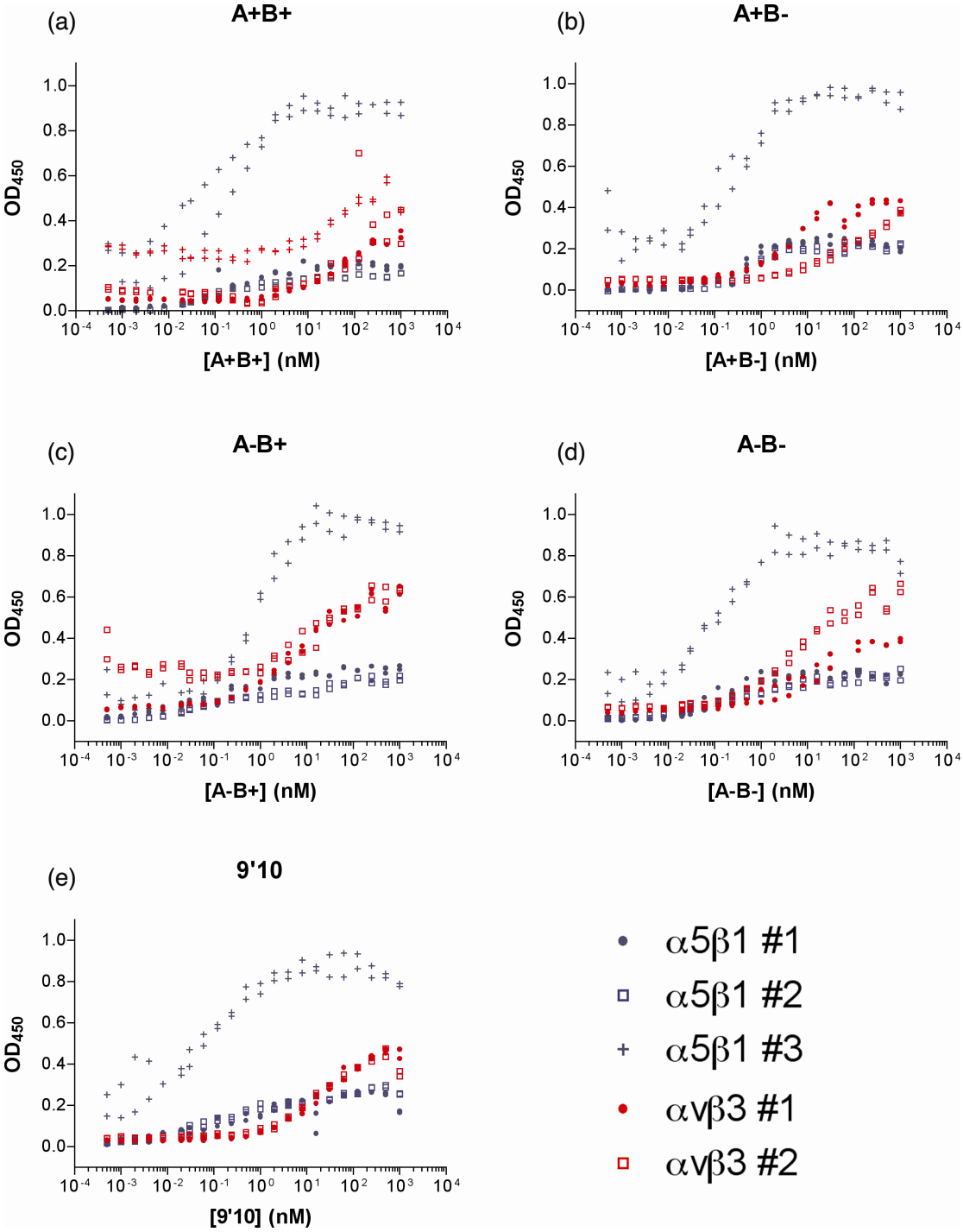

Figure 6-16 Dose-response data for the binding of recombinant GST·FIII 7-12A±B± fragments; (a) A+B+, (b) A+B-, (c) A-B+, (d) A-B- to purified integrin α5β1 and αvβ3. (e) A modified FIII9-10 construct (9'10), which incorporates a Leu[1408]→Pro substitution in FIII9 that confers better conformational stability and functional activity (van der Walle *et al.* 2002) was used as a control. Data points are duplicate OD_{600} measurements from each of three (for α5β1, n=3) or two (for αvβ3, n=2) independent experiments, background antibody binding and non-specific binding of ligand was subtracted from the readings.

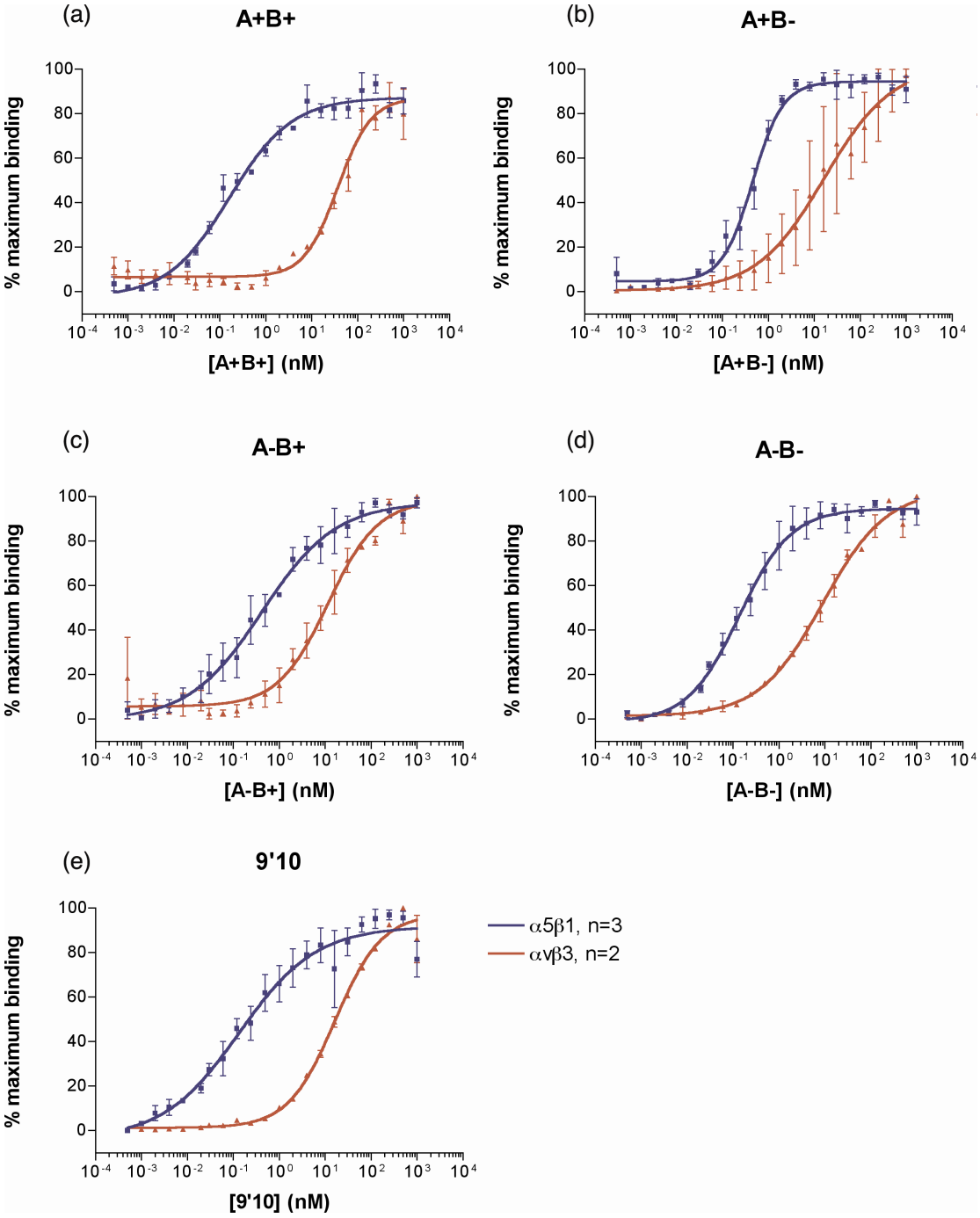

Figure 6-17 Normalized dose-response data for the binding of recombinant GST·FIII 7-12A±B± fragments; (a) A+B+, (b) A+B-, (c) A-B+, (d) A-B- and (e) 9'10 to surface-immobilized integrin α5β1 and αvβ3. Data points are the means ± SEM from three (for α5β1, n=3) or two (for αvβ3, n=2) independent experiments. Dose-response data from the assays were analyzed by non-linear regression using a sigmoidal curve fit as described previously (Altroff *et al.* 2001).

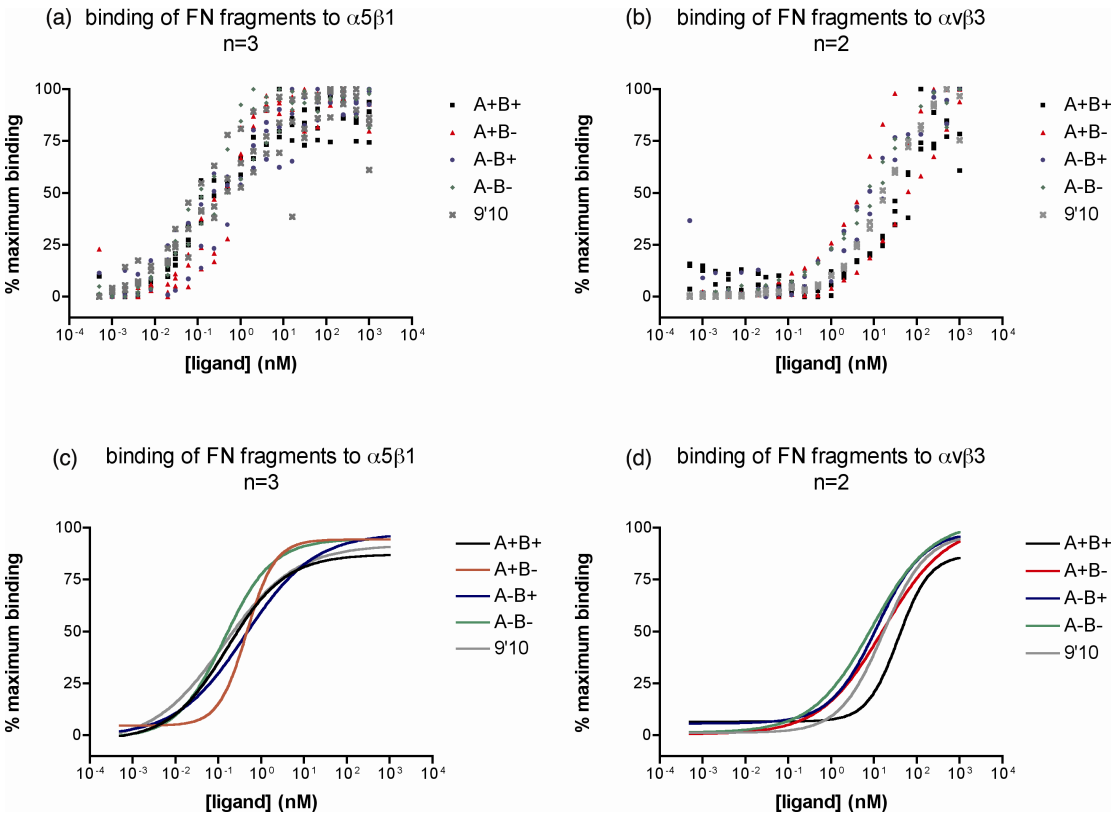

Figure 6-18 Normalized dose-response data for the binding of recombinant GST·FIII 7-12A±B± and 9'10 fragments to surface-immobilized integrin α5β1 (a, c) and αvβ3 (b, d). Assay results are expressed as means from each of three (for α5β1, n=3, a) or two (for αvβ3, n=2, b) independent experiments. Dose-response data was analyzed by non-linear regression using a sigmoidal curve fit for α5β1 (c) and αvβ3 (d) as described previously (Altroff *et al.* 2001).

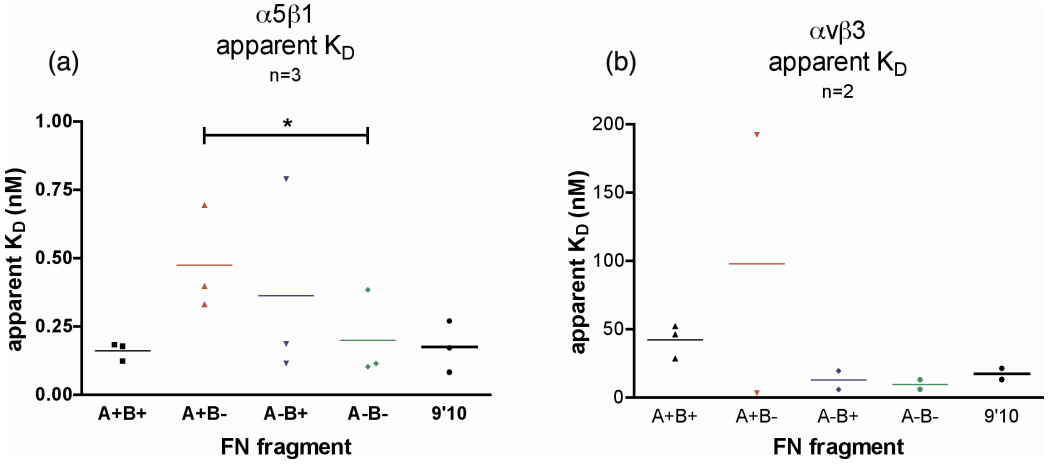

Figure 6-19 Apparent K_D values of GST-FIII 7-12A±B± binding to immobilized integrins α5β1 and αvβ3 calculated from the dose-response curves (Figure 6-18 c and d), from three (n=3, for α5β1) or two (n=2, for αvβ3) independent experiments. Data were analyzed using student t-tests, differences were considered significant when $P \leq 0.05$ (*).

α5β1 apparent K_D values (nM)

	A+B+	A+B-	A-B+	A-B-	9'10
	0.178	0.398	0.187	0.114	0.270
	0.124	0.695	0.115	0.385	0.172
	0.184	0.332	0.789	0.103	0.083
mean	0.162	0.475	0.364	0.201	0.175
std. error	0.019	0.112	0.214	0.092	0.054
n	3	3	3	3	3

αvβ3 apparent K_D values (nM)

	A+B+	A+B-	A-B+	A-B-	9'10
	52.5	3.41	6.15	13.1	21.4
	46.2	192	19.8	6.06	13.3
	28.7				
mean	42.5	97.9	13.0	9.59	17.4
std. error	7.11	94.5	6.82	3.54	4.08
n	3	2	2	2	2

Table 6-2 Apparent K_D values of GST-FIII 7-12A±B± binding to immobilized integrins α5β1 and αvβ3 calculated from the dose-response curves (Figure 6-18 c and d), from three (n=3, for α5β1) or two (n=2, for αvβ3) independent experiments.

The four recombinant GST-FIII7-12A±B± fragments and the 9'10 control appear to bind to integrin α5β1 with a greater affinity than to integrin αvβ3, as observed in the binding curves (Figure 6-17) and in the lower apparent K_D values (Figure 6-19, Table 6-2), this could be due to differences in the quality of integrin purified from the placental tissues. The apparent K_D of binding to α5β1 (Figure 6-19 a) was observed to increase on inclusion of EDIIIA, rising from 0.201 nM for A-B- to 0.475 nM for A+B- ($P = 0.0076$). This decrease in binding affinity to α5β1 was not observed when EDIIIB or both EDIIIA and EDIIIB domains were inserted into the FN fragment. No significant changes in the apparent K_D of binding to αvβ3 was observed, more experiments are required as only two independent experiments have been carried out, this was difficult as there were practical limitations in the purification of integrins. It must noted that as only single preps of integrins and substrates were used in these integrin binding experiments, therefore the results shown including the determination of apparent K_D are only preliminary observations.

6.2.4. Inclusion of EDIIIA and EDIIIB does not modulate FAK phosphorylation

Focal adhesion kinase (FAK) is one of the most prominent protein kinases to be phosphorylated in response to integrin engagement and cell attachment on plasma FN (Burridge et al. 1992; Guan et al. 1992). Phosphorylation of FAK was used as a marker for adhesion-dependent signal propagation, to see if the observed effects of EDIIIA and EDIIIB on cell adhesion and integrin binding also apply for FAK phosphorylation. ESCs were plated on GST-FIII7-12A±B± fusion proteins as described in Section 6.2.2 and levels of FAK and phosphorylated FAK (phosphotyrosine) measured after two hours from cell lysates as described in Section 2.7.1. The same batch of GST-FIII7-12A±B± fusion proteins were used in the FAK phosphorylation experiments. A time-course experiment revealed that FAK phosphorylation was maximal at two hours after the cells were plated (Figure 6-20).

The production of FAK and phosphorylated FAK (pFAK) was measured in three independent immunoblots (Figure 6-21) in each of three ESC patient cell numbers (n=3). The ratio of phosphorylated FAK to total FAK (pFAK/FAK) was calculated by dividing the densitometry measurement of each pFAK signal by that of FAK on the same immunoblot which had been stripped and reprobed. Densitometry measurements from three immunoblots in each of three ESC cell numbers are shown in Figure 6-22 and the means of each ESC cell number shown in Figure 6-23. Densitometry measurements from the immunoblots demonstrated no differences in the pFAK/FAK ratio between the GST-FIII7-12A±B± fusion proteins. The phosphorylation and activation of FAK in ESCs was not modulated by the inclusion of EDIIIA and EDIIIB in the FN fragments.

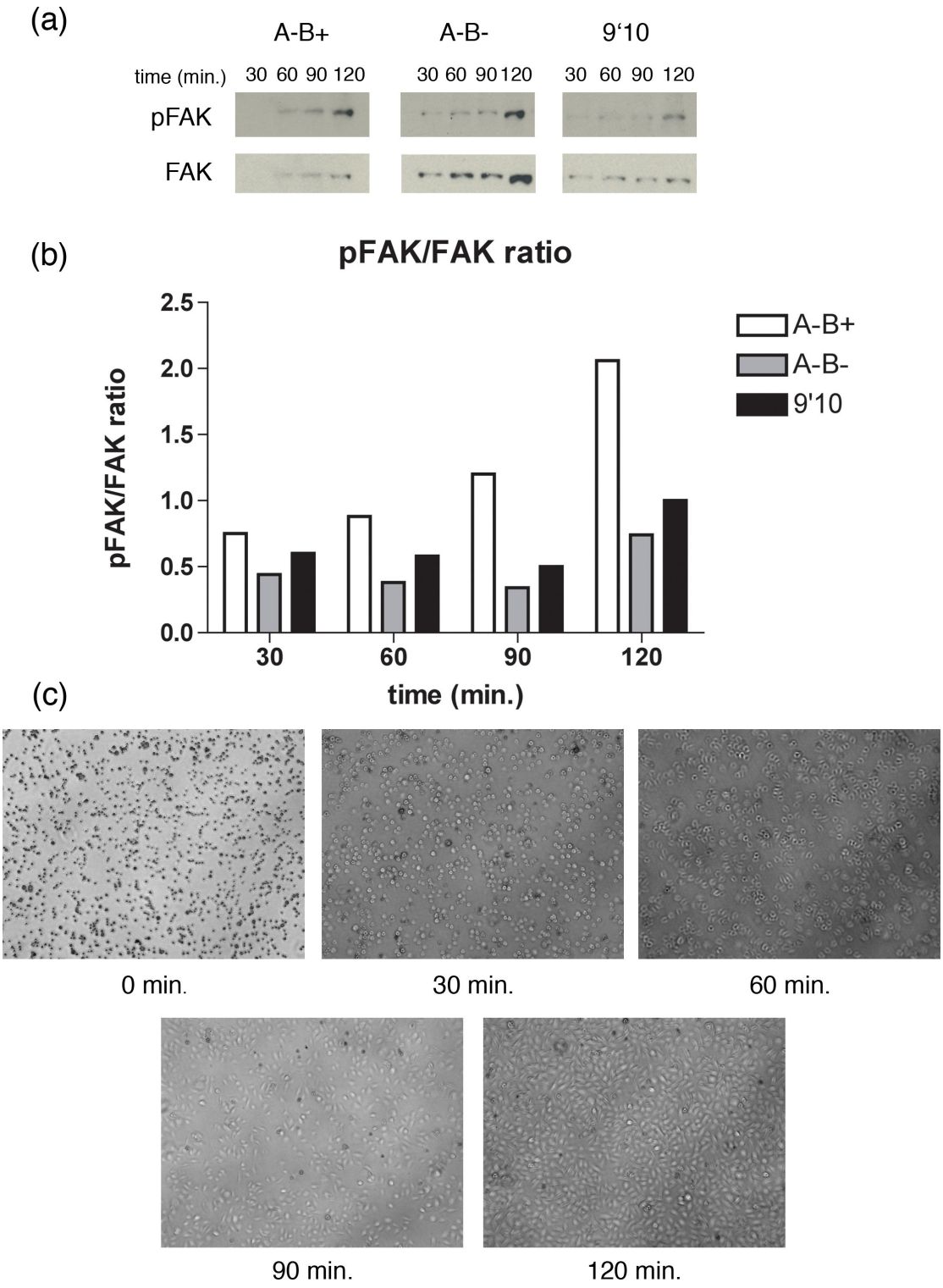

Figure 6-20 Time-course of FAK activation in ESCs cultured on GST-FIII7-12 A-B+, GST-FIII7-12 A-B- and FIII 9'10. Immunoblots (a) and densitometry measurements (b) are displayed as a ratio of pFAK/FAK, and cell morphologies (c) of ESCs plated on GST-FIII7-12A-B- at 30, 60, 90 and 120 min, carried out for one ESC cell number in one immunoblot (n=1)

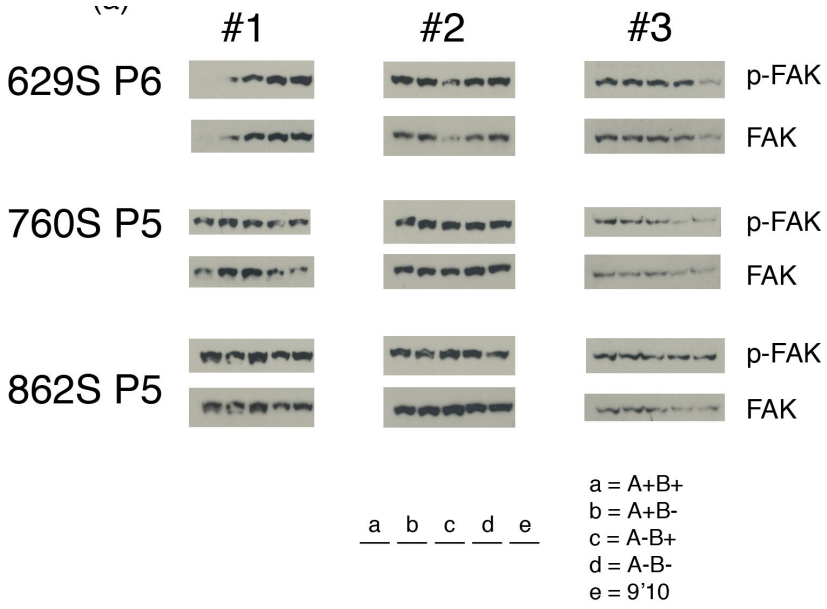

Figure 6-21 Immunoblots of FAK and phosphorylated-FAK (pFAK) produced by ESCs cultured for two hours on GST-FIII7-12 A±B±, in three different ESC patient cell numbers and repeated in three independent immunoblots (n = 3).

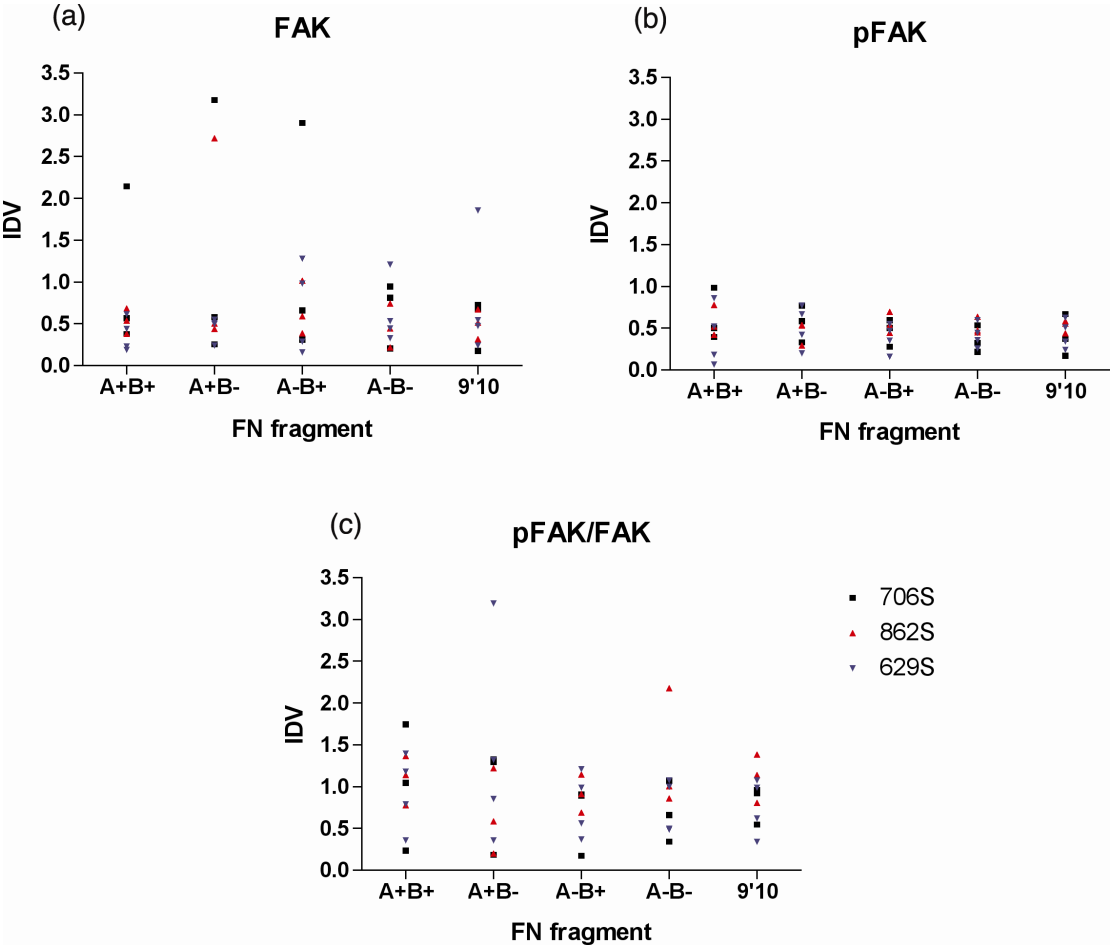

Figure 6-22 Densitometry measurements from immunoblots (Figure 6-21) of FAK (a) and pFAK (b) production by ESCs cultured for two hours on GST-FIII7-12 A±B± and GST-FIII9'10, in three different ESC patient cell numbers (n = 3), repeated in three independent immunoblots. The pFAK/FAK ratio (c) was calculated by dividing each replicate signal of pFAK by that of FAK on the same immunoblot which had been stripped and reprobed. IDV = integrated density value, normalised to β-actin. Data points are triplicate values from each of three ESC patient cell numbers.

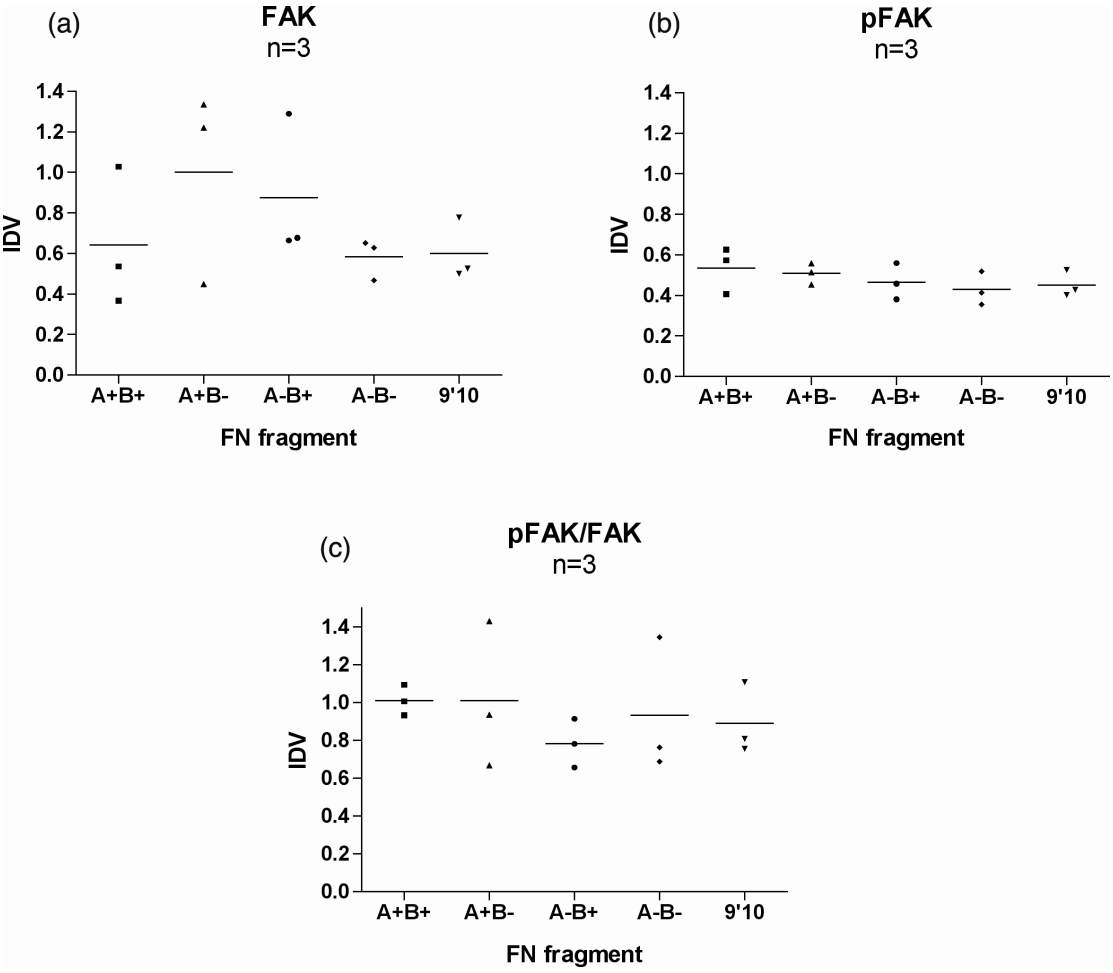

Figure 6-23 Densitometry measurements from immunoblots (Figure 6-21) of FAK and phosphorylated-FAK (pFAK) production by ESCs cultured for two hours on GST-FIII7-12 A±B± and GST-FIII9'10, in three different ESC patient cell numbers (n = 3), repeated in three independent immunoblots. The pFAK/FAK ratio was calculated by dividing each replicate signal of pFAK by that of FAK on the same immunoblot which had been stripped and reprobed. IDV = integrated density value, normalised to β-actin. Data points are the means of triplicate values from each of three ESC patient cell numbers. Horizontal lines are the mean of the means from each of three ESC patient cell numbers

6.2.5. ESCs adhered to FIII7-12A±B± display spread morphologies with formation of actin stress fibres and focal adhesions.

Immunocytochemistry was used to visualize actin stress fibres and the formation of focal adhesion complexes, in order to determine any adhesion-driven morphological changes in ESCs adhered to immobilised FIII7-12A±B± and full-length FN. Vinculin was used as a marker protein for an assembled focal adhesion complex. All four recombinant FIII7-12A±B± proteins supported the formation of actin stress fibres, which terminated in the vinculin-positive focal complexes to produce orange-yellow colocalization signals (Figure 6-24).

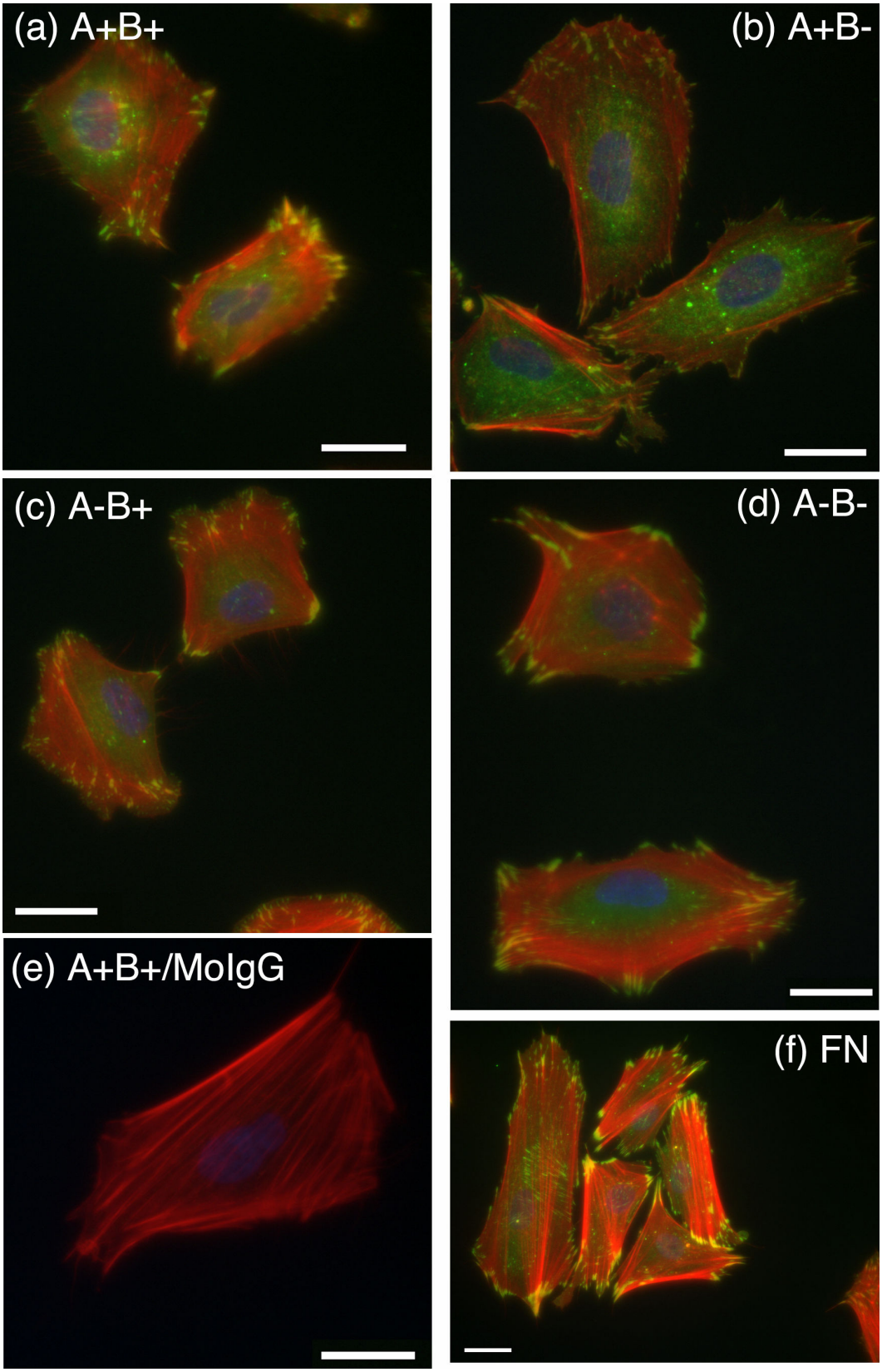

Figure 6-24 Immunofluorescence staining for actin (red) and vinculin (green) in ESCs adhering to (a, e) GST-FIII7-12A+B+, (b) GST-FIII7-12A+B-, (c) GST-FIII7-12A-B+, (d) GST-FIII7-12A-B- or (f) full-length FN, (e) ESCs were treated with moIgG as a negative control . Scale bars are 25 μm.

6.2.6. EDIIIA and EDIIIB does not modulate proliferative capacities of ESCs

The upregulation of EDIIIA+FN and EDIIIB+FN production in cells of high proliferative potential have suggested possible roles in promoting cell proliferation (Manabe *et al.* 1999). ESCs were cultured on surfaces coated with GST-FIII7-12A±B± fusion proteins as described in Section 6.2.2, and cell growth assessed using the cell proliferation reagent Wst1 at 24 and 72 hours as described in Section 2.9. The same batch of GST-FIII7-12A±B± fusion proteins were used in all the cell proliferation experiments.

Cell growth are plotted as triplicate values from each of four different ESC cell numbers showing ESC growth on GST-FIII7-12A±B± fusion proteins measured at twenty-four (Figure 6-25) and seventy-two (Figure 6-26) hours. There was a considerable amount of variation between the ESCs due to biological variation and factors such as number of cells used, incubation times, protein and substrate concentrations as described in Section 6.2.2. Therefore the measurements were normalized with the maximal OD value in each data set being 100.

The mean ESC growth on GST-FIII7-12A±B± fusion proteins at twenty-four and seventy-two hours are shown in Figure 6-27. The inclusion of EDIIIA and/or EDIIIB in the FIII7-12 fragment did not modulate proliferative capacities in ESCs, as cell proliferation were not significantly different between increasing concentrations of FIII7-12A+B+, FIII7-12A+B-, FIII7-12A-B+ and FIII7-12A-B- after both twenty-four and seventy-two hours of incubation (Figure 6-25, Figure 6-26 and Figure 6-27).

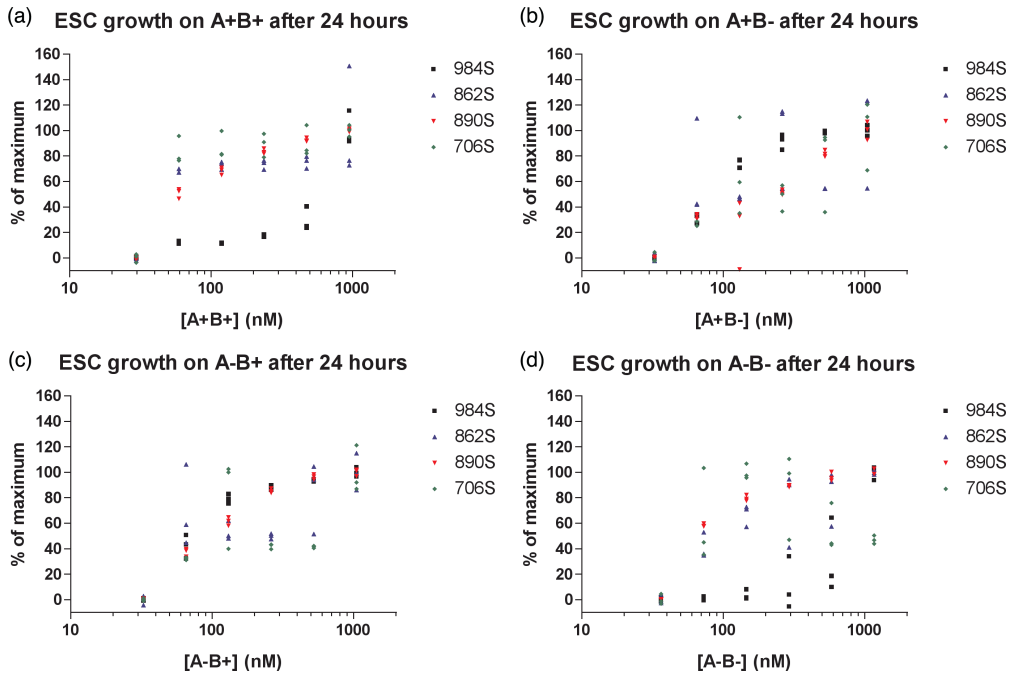

Figure 6-25 ESC growth after 24 h incubation in response to increasing concentrations of immobilized FIII7-12A±B±. Assays were performed in triplicate in each of four independent experiments using different ESC patient numbers (n = 4). Data points are replicate values from each experiment, expressed as a percentage of the maximal OD values in each data set and plotted on a log scale.

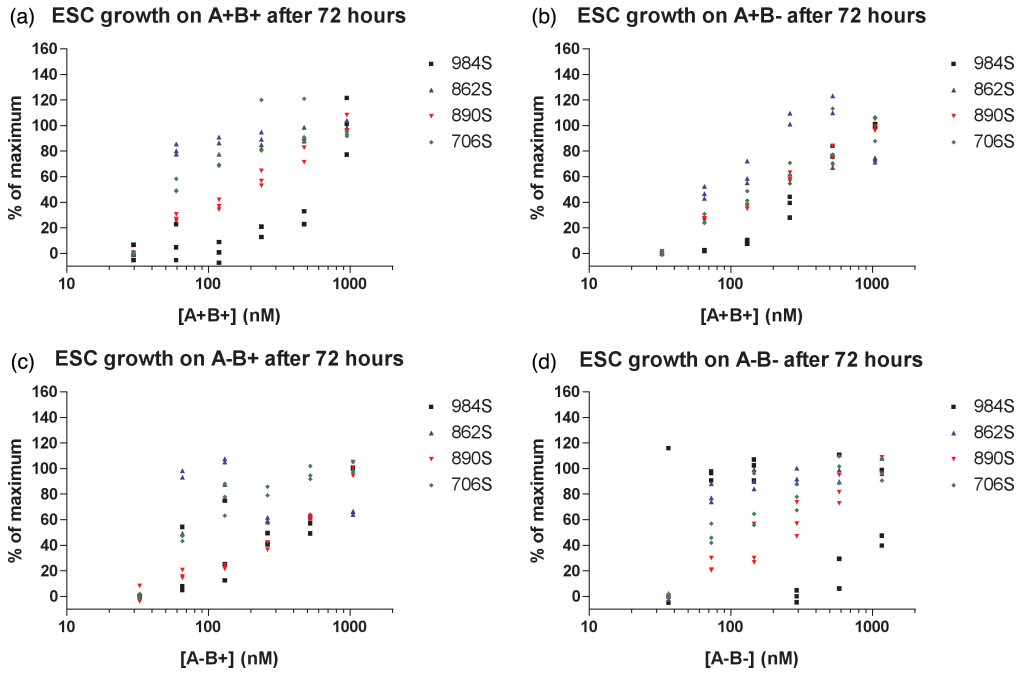

Figure 6-26 ESC growth after 72 h incubation in response to increasing concentrations of immobilized FIII7-12A±B±. Assays were performed in triplicate in each of four independent experiments using different ESC patient numbers (n = 4). Data points are replicate values from each experiment, expressed as a percentage of the maximal OD values in each data set and plotted on a log scale.

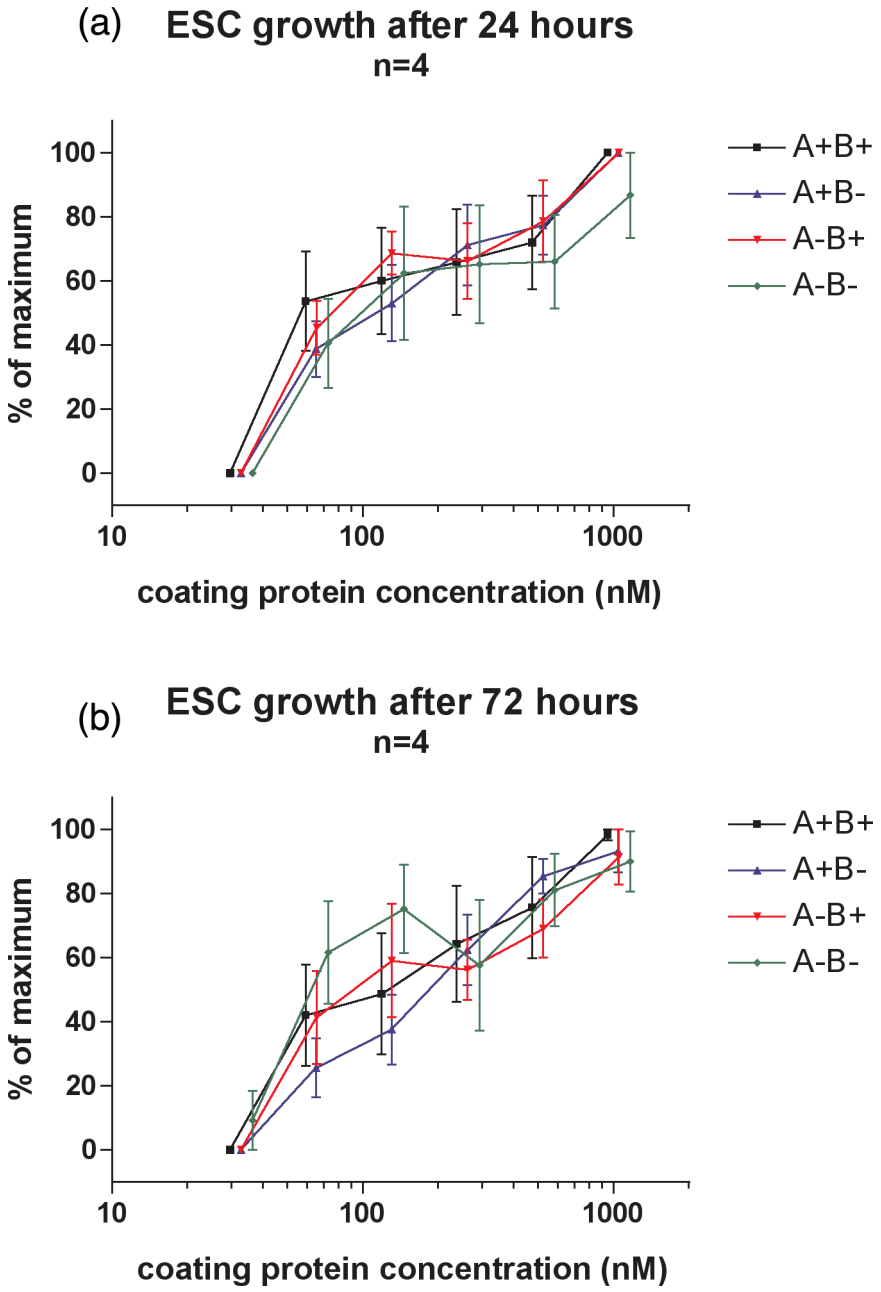

Figure 6-27 ESC growth after (a) 24 h and (b) 72 h incubation in response to increasing concentrations of immobilized FIII7-12A±B±. Data points are means ± SEM from four independent experiments (n = 4). Assays were performed in triplicate in each of four independent experiments using different ESC patient numbers (n = 4), normalized with the maximal OD values in each data set as 100 and plotted on a log scale.

6.2.7. Structural studies

We attempted to crystallize the His-FIII7-12A+B- and His-FIII8-12A+ fragments (Figure 6-7) for x-ray diffraction studies, in order to elucidate the structural role of EDIIIA inclusion in the FN molecule. The FIII7-12A+B- fragment was used as it spans the FIII7-12 domains where EDIIIA and EDIIIB are inserted and include the RGD motif of FIII10 and PHSRN synergistic sequence of FIII9. The FIII8-12A+ fragment also contain EDIIIA and the RGD and synergistic motifs, but not FIII7 and the EDIIIB domain which is inserted between FIII7 and FIII8, minimizing any effects FIII7 might exert in the absence of EDIIIB. Commercially available protein crystallization screens were used with approximately seven hundred different buffer conditions, the crystallization trials were set-up using a Cartesian Robot (Oxford Protein Production Facility, Wellcome Trust Centre for Human Genetics, Oxford). A few small crystals appeared initially for FIII7-12A+B- (data not shown), and additional optimization screens were carried out with the preliminary condition of 0.1 M sodium cacodylate pH 6.5 and 1.4 M sodium acetate tryhydrate; varying pH, protein to precipitant ratios, percentage of buffer in the reservoir and the presence of additives (Figure 6-28). These optimization screens produced a number of flower-shaped and rod-shaped crystals, but diffracted poorly. Small needles were obtained for FIII8-12A+B- with the crystallization screens (Figure 6-29); optimization screens were set-up for the condition 0.1 M HEPES pH 7.5, 0.1 M NaCl and 1.6 M ammonium sulphate, forming small needles again, and on additive screening only a small hexagonal salt crystal was formed with L-cysteine (data not shown).

Cryo-electron microscopy of the FIII7-12A+B- fragment in complex with recombinant α5β1 integrin was performed by Mr Gregor Hofmann, Dept. of

Biochemistry, University of Oxford, the α5β1 integrin was provided by Mrs Céline Jones, Nuffield Dept. of Obstetrics and Gynaecology, University of Oxford. The resolution of images obtained in preliminary experiments was poor, possibly due to the flexibility of seven FIII domains in the FIII7-12 fragment and further repetition will be needed.

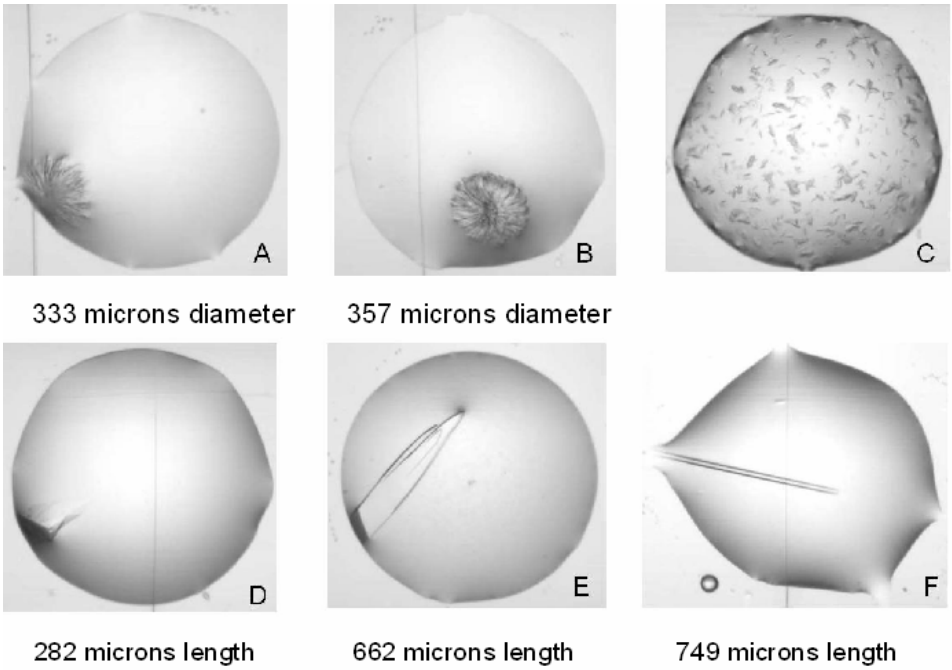

0.1M Sodium Cacodylate pH 6.5, 1.4M Sodium Acetate tryhydrate

	% buffer	protein : precipitant	pH	additive
A	85	1:1	<6.5	-
B	85	2:1	<6.5	-
C	100	1:2	6.5	-
D	85	1:2	<6.5	
E	85	2:1	6.5	
F	100	1:1	6.5	0.25% v/v dichloromethane

Figure 6-28 Crystallization trials for His-FIII7-12A+B-; optimization of the preliminary condition of 0.1 M Sodium Cacodylate pH 6.5, 1.4 M Sodium Acetate tryhydrate.

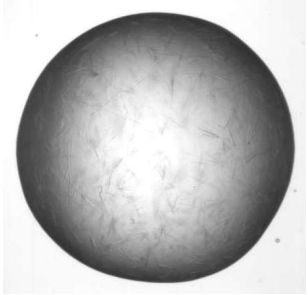

Figure 6-29 Small needles were obtained for His-FIII8-12A+ with 0.1 M HEPES pH 7.5, 0.1 M NaCl and 1.6 M ammonium sulphate.

6.3 Discussion

The expression of EDIIIA+FN and EDIIIB+FN in the endometrial stroma at the time of implantation suggests a role for these alternatively spliced domains in decidualization and implantation. The identity of the expressed and purified recombinant FN fragments GST-FIII7-12A±B± was confirmed by SDS-PAGE (Figure 6-1) and immunoblotting (Figure 6-2). The recombinant FN fragments GST-FIII7-12A±B± were used to investigate the influence of EDIIIA and EDIIIB on functional properties of FN, including cell adhesion, integrin binding, FAK phosphorylation and cell proliferation. Their coating efficiencies on plastic surfaces was confirmed by an ELISA (), it appears that GST-FIII7-12A+B+ had a greater binding affinity to the plastics more strongly than the other fragments, but only one experiment was carried out for one batch of recombinant proteins purified.

The inclusion of EDIIIA decreased the binding affinity of the FIII7-12 fragment for α5β1, whilst the presence of either EDIIIA or EDIIIB did not alter binding affinities to αvβ3. In cell adhesion assays neither EDIIIA nor EDIIIB modulated the cell spreading and attachment properties of FIII7-12, and the inclusion of either domains in FIII7-12 did not alter FAK activation in attached ESCs. The lack of difference in cell adhesion and FAK phosphorylation exerted by the FIII7-12 fragments could be due to variation between the different ESC cell numbers as described in the previous chapters. This was minimized by using cells isolated at day 20-22 from LMP (Table 2-1), but there were differences in the passage number and degree of confluency of ESCs used, and biological variation between patients.

Results of the FAK phosphorylation assay should correlate with the cell adhesion assay, as both are influenced by integrin responses following the initial recognition event in cell adhesion, including integrin clustering and integrin-mediated signalling, affecting ligand binding affinity. Also, FAK integrates inputs from a variety of cell surface-associated receptors, including integrins, G protein linked receptors, and growth factor receptors. The integrin binding assay only reflects requirements for the initial ligand binding event to one particular integrin.

Discrepancies between the cell adhesion and FAK phosphorylation experiments and the integrin binding ELISA data could also be due to differences in the assay formats used. Cell adhesion and FAK phosphorylation assays were carried out with captured FN ligands, whereas immobilized integrin and soluble FN fragments were used in the ELISAs. The immobilization to the plastic surfaces may impose conformational constraints on the FN ligands which are not present in the integrin binding assay.

Previous studies have indicated conflicting roles of EDIIIA and EDIIIB in supporting cell attachment and spreading, the EDIIIB domain promoted cell attachment and spreading using FIII7-12 fragments, while EDIIIA had a negative effect (Hashimoto-Uoshima *et al.* 1997). In another study using the larger FIII2-14 fragment, EDIIIA enhanced cell attachment and spreading irrespective of EDIIIB (Manabe *et al.* 1997). The insertion of EDIIIA but not EDIIIB into full-length FN promoted FN-induced cell proliferation, but cell adhesion on this recombinant FN had no effect on FAK activation (Manabe *et al.* 1999). The results of our study suggest EDIIIA and EDIIIB inclusion in FIII7-12 to have no effect on ESC proliferation, FAK phosphorylation and ESC cell adhesion. These discrepancies could be due to differences in cell type

and size of FN fragment used. The presence of the IIICS domain in the larger FIII2-14 fragment and other domains present in full-length FN are not present in the FIII7-12 fragments used in our study.

In our study using FIII7-12 fragments, the inclusion of EDIIIA decreased binding affinity for α5β1; FIII7-12A+B- had a lower binding affinity to α5β1 relative to FIII7-12A-B-. This disagrees with the previous results where EDIIIA augments α5β1 binding affinity (Manabe 1997), where α5β1 was reconstituted into liposomes and binding to immobilised FN fragments was assessed, whereas in our assay soluble FN fragments and immobilised integrins were used, the different assay formats may explain the differences in the role of EDIIIA on integrin binding as discussed above.

The alternatively spliced domains were proposed to exert their effects via alterations in the global conformation of FN and not by providing additional integrin interaction sites (Hashimoto-Uoshima *et al.* 1997; Manabe *et al.* 1997). In their study the individual EDIIIA or EDIIIB domains did not have adhesive properties, and cell adhesion to EDIIIA+FN or EDIIIB+FN was not inhibited by the individual domains or by monoclonal antibodies directed against them. Therefore the inclusion of EDIIIA in the FIII2-14 fragment was proposed to alter the global conformation of FN by increasing integrin accessibility to the CCBD, as EDIIIA inclusion enhanced cell attachment and spreading, and binding to integrins α5β1 and αvβ3 (Manabe *et al.* 1997).

The hypothesis that EDIIIA and EDIIIB induce changes in the global conformation of FN is further supported by the observation that cellular FN containing EDIIIA and/or

EDIIIB are much less soluble than plasma FN under physiological buffer conditions (Yamada *et al.* 1977). This difference in solubility could be due to differences in global conformation of EDIIIA+FN that may increase exposure of hydrophobic and/or charged surfaces of the FN molecule. In addition, the inclusion of EDIIIB in a β-galactose-FN fusion protein unmasked cryptic sequences, supporting the hypothesis that EDIIIB inclusion could modify the FN conformation (Carnemolla *et al.* 1992). In addition, the recent crystal structure of FIII8-B+ indicates a small interface between domains FIII8 and EDIIIB, forming a unique acidic groove which could be a potential protein-protein interaction site (Bencharit *et al.* 2007).

To investigate if EDIIIA inclusion modifies the global conformation of FN, crystallization trials and cryo-EM experiments were set-up to determine the structures of FN fragments FIII7-12A+B- and FIII8-12A+B-, however, the crystals produced diffracted poorly and cryo-EM images were of poor resolution. These difficulties in structural determination could be due to conformational flexibility between FIII domains (Lombardo *et al.* 1996), the high degree of molecular flexibility between the seven FIII domains of FIII7-12A+ may affect the crystallization process to produce crystals that diffract poorly and failed to form ordered crystals.

In previous structural studies, FN was demonstrated to be a long, thin flexible strand by EM (Engel *et al.* 1981; Erickson *et al.* 1981), and the FIII7-10 crystal structure suggested the molecule to be extended and rod-like with highly variable tilt and rotation angles between adjacent FIII domains (Leahy *et al.* 1996). The inclusion of EDIIIA may alter conformation of the RGD sequence by modification of linked neighbouring modules FIII11 and FIII12 (Ffrench-Constant 1995), by readjusting

intermodular rotations and tilts, which could in turn alter the conformation of their neighbouring modules including the RGD-containing loop of FIII10.

Another model suggests a globular arrangement of FIII modules in FN (Litvinovich *et al.* 1995), the flexibility between linked modules allows formation of numerous molecular conformations of FN, with proposed stabilizing interactions between FIII7 and FIII10, and between FIII7 and FIII9. These could be disrupted by alternative splicing on inclusion of domains EDIIIA or EDIIIB, altering the supertertiary structure of the central region of FN and its interaction with other molecules such as integrins.

In summary, inclusion of the EDIIIA domain in the FIII7-12 fragment decreased binding affinity to integrin α5β1 but not αvβ3. The presence of either or both domains in the FIII7-12 fragment did not confer additional cell attachment and spreading properties, FAK phosphorylation or proliferative capacities of ESCs. The inclusion of EDIIIA may modulate integrin binding affinities by providing additional interaction sites, this could be investigated by addition of the recombinant EDIIIA domain or monoclonal antibodies to EDIIIA as inhibitors in the integrin binding assay. The inclusion of EDIIIA may also modulate conformation of the FN molecule, including access to integrin binding sites. We attempted to elucidate this by the crystallization of His-FIII7-12A+B- and His-FIII8-12A+ fragments for x-ray diffraction studies.

The recombinant FIII7-12A±B± fragments used in this chapter were all assumed to be of a stable conformation, they all bound to plastic surfaces with similar coating

efficiencies (Figure 6-11), and were functional in mediating cell adhesion of ESCs (Figure 6-14) and in binding to integrins α5β1 and αvβ3 (Figure 6-18). Further experiments can be carried out to determine the conformational flexibilities and stabilities of recombinant FIII7-12A±B± fragments, to investigate if inclusion of EDIIIA and EDIIIB could alter the conformational flexibility of the FN molecule. These include equilibrium denaturation experiments to investigate unfolding of the FIII7-12A±B± fragments, and NMR studies which would require smaller FN fragments.

Chapter 7

General discussion and future directions

7.1 Overview of data presented in this thesis

Implantation failure remains an unsolved problem in reproductive medicine and is considered to be the major cause of infertility in otherwise healthy women. This thesis aimed to test the hypothesis that the tightly regulated modulation of ECM components is required for implantation of the human embryo.

During *in vitro* decidualization, a decrease in the production of TN, FN, EDIIIA+FN and EDIIIB+FN by ESCs was demonstrated. This modified ECM composition is likely to have consequences on the behaviour of ESCs, as a result of changes in integrin signalling and the downstream effects modulating cellular processes including cell adhesion, migration, proliferation and differentiation. The decreased synthesis of ECM proteins may allow for the loosening of stromal ECM required for differentiation during decidualization, and may facilitate trophoblast invasion into the endometrial stroma.

The production of FN by ESCs was decreased in response to the proinflammatory cytokine TNFα, which has previously been shown to induce MMP secretion by ESCs, including MMPs-3 and 9 which can degrade FN (Rawdanowicz *et al.* 1994; Huang *et al.* 1998; Singer *et al.* 1999), suggesting the TNFα-induced reduction in ESC FN levels may be mediated by MMPs.

Recombinant EDIIIA protein had no effect on blastocyst attachment and invasion onto ESCs. This may be due to EDIIIA not being the sole mediator of attachment on ESCs, or that its conformation differs to that when inserted in the FN molecule, to expose different interaction sites in the endometrial stromal ECM. In addition to providing an additional binding site for integrins α4β1 and α9β1 (Liao *et al.* 2002), EDIIIA inclusion may alter the global conformation of FN, hence these effects would not be affected by addition of recombinant EDIIIA protein. Blastocysts attached to ESCs displayed some positive staining for integrin subunits α4 and α9, suggesting that the blastocyst could interact with EDIIIA/B+ in the endometrial stromal ECM via these integrins. However, staining for these two integrin subunits has not been detected in the majority of trophoblast outgrowths, it is unclear if they play any role in the blastocyst attachment and invasion processes.

The inclusion of EDIIIA reduced binding affinities of FIII7-12 to integrin α5β1, and cell attachment and spreading properties, FAK phosphorylation and cell proliferation of ESCs were not altered by EDIIIA and EDIIIB.

In the structural studies performed with FIII7-12A+B- fragments, the crystals produced diffracted poorly and cryo-EM images were of poor resolution, which could be due to the conformational flexibility between FIII domains (Lombardo *et al.* 1996). The molecular flexibility between the seven FIII domains of FIII7-12A+ could result in the difficulties in structural determination.

7.2 Wider implications

The development of uterine receptivity may involve the modulation and redistribution of ECM molecules, including EDIIIA+FN and EDIIIB+FN which are present in the ECM adjacent to the luminal epithelium at the time of implantation. Previous observations have indicated the ability of EDIIIA/B+FN fragments to support blastocyst attachment and trophoblast outgrowth, which suggests a role for EDIIIA and EDIIIB. However, in the experiments performed here, recombinant EDIIIA did not have any effect on blastocyst attachment and outgrowth onto ESCs in an *in vitro* blastocyst implantation model.

The observed decrease in FN and TN levels produced by ESCs during *in vitro* decidualization may result from proteolytic degradation by MMPs. The cleavage and release of FN and TN fragments may induce further cellular responses via interaction with cell surface receptors, to modulate proliferation, migration and protease activation (Turpeenniemi et al. 1995; Saito et al. 1999). For example, EDIIIA can induce MMP expression and interact with TLR-4 to induce proinflammatory response (Saito *et al.* 1999; Okamura *et al.* 2001), and the alternatively spliced domain of TN, TNfnA-D stimulates cell migration and focal adhesion disassembly (Chung *et al.* 1996). The degradation of ECM would also release ECM-sequestered cytokines and growth factors, making them bioavailable to induce further cellular responses.

Functional assays suggest EDIIIA inclusion to have negative effects on binding affinities of FIII7-12 fragments to integrin α5β1 in endometrial stroma cells. Cell-cell and cell-ECM adhesions need to be disconnected and reformed in order for cells to

undergo differentiation during decidualization. The EDIIIA domain may facilitate the decidualization process by decreasing binding interactions of ESCs with the ECM.

Therefore it is hypothesized that in addition to supporting blastocyst attachment, EDIIIA+FN may have a role in promoting decidualization by decreasing cell-ECM interactions in the endometrial stroma. This disassembly in adhesions may assist in ESC differentiation and ECM remodelling. As decidualization proceeds, as demonstrated by the diminished synthesis of FNs and TN in the *in vitro* decidualization model, and decrease in ESC FN levels in response to the endometrial cytokine TNFα, the looser stromal ECM may assist in invasion of the embryo during implantation. The degradation of FNs will release FN fragments including the EDIIIA and EDIIIB domains which may induce further cellular effects such as induction of MMP expression (Saito *et al.* 1999).

7.3 Limitations

There were a number of experimental limitations encountered in this thesis, including the physiological relevance of using cell culture systems. The ESCs maintained in monolayer cultures lack many interactions that are present in the tissue *in vivo*. These include interactions with other endometrial cellular components such as epithelial cells, endothelial cells, immunological cells or myometrium, which may play a role in endometrial function. However, the use of *in vitro* systems provides an alternative that overcomes limitations of studying complex biological processes *in vivo* such as those encountered during the time of implantation. *In vitro* approaches allow the study and manipulation of specific cell types in a defined cellular environment.

For example, in the *in vitro* decidualization model the cAMP analogue 8-Br-cAMP was used to activate the PKA pathway and induce decidualization in ESCs. This allows the study of decidualization in ESCs in response to an increase in intracellular cAMP levels, but may not reflect *in vivo* conditions, where the endometrial stroma is under the influence of progesterone and factors that bind to GPCRs to produce cAMP, and can also interact with additional cellular components of the endometrium.

In the *in vitro* blastocyst implantation assay, a major limitation was the quality of blastocysts, as the embryos used are donated for research after the best quality embryos are used in IVF treatment. In the ELISAs used to investigate effects of cytokines and growth factors on FN production by ESCs, serum-free conditions were used to study individual effects of the cytokines and growth factors without the influence of serum in culture media. However, 2% serum was also used for more physiological conditions, as additional factors in serum may have synergistic effects with cytokines and growth factors, or influence FN production by ESCs themselves.

It must also be taken into consideration the differences in cell-matrix interactions between 2D cell cultures, 3D matrices and tissue environments *in vivo*. Fibroblasts in 3D matrices can form 3D-matrix adhesions which differ from focal and fibrillar adhesions formed on 2D substrates. For example, in fibroblasts cultured on 2D substrates such as FN, tyrosine-phosphorylated FAK and tyrosine-phosphorylated paxillin are co-localized to focal adhesions with integrin α51. Whereas in 3D-matrix interactions, FAK and paxillin are co-localized to the 3D-matrix adhesions with α5β1 along with phospho-paxillin, but phospho-FAK was absent. The 3D-matrix interactions also display enhanced biological activities including cell migration and

proliferation, with a restricted integrin usage to only α5β1. These differences in structure, localization and function may indicate 3D-matrix adhesions to be more biologically relevant than adhesions formed in 2D cell cultures (Cukierman *et al.* 2001).

7.4 Future studies

A number of questions remain to be answered concerning the roles of the FN alternatively spliced domains EDIIIA and EDIIIB in the endometrium during decidualization and embryo implantation. Firstly, it is not yet elucidated how inclusion of EDIIIA and EDIIIB in the FN molecule enhances its ability to support blastocyst attachment and spreading. Recombinant EDIIIA had no significant effect on blastocyst attachment on ESCs. Other approaches to probe the role of EDIIIA include the silencing of EDIIIA+FN expression in ESCs using RNA interference and assessing their subsequent capacity to support blastocyst attachment.

Further confirmation of expression of integrins α4β1 and α9β1 in the blastocyst by immunostaining is required to confirm whether they mediate interactions with EDIIIA in the stromal ECM. Integrin binding assays using FIII7-12A±B± fragments and integrins α4β1 and α9β1, possibly purified from placental tissue, could demonstrate how EDIIIA and EDIIIB inclusion modulates FN binding to these integrins.

Since recombinant EDIIIA can induce the expression of MMPs-1, 3, and 9 in synovial cells (Saito *et al.* 1999), its influence on MMP expression by ESCs and the embryo could be assessed. Such an induction of MMPs could degrade the stromal ECM, to assist in ESC differentiation and ECM remodelling during decidualization,

the looser stromal ECM may also facilitate the invasion process during embryo implantation. Also involved in the invasion process is cell migration, the role of EDIIIA and EDIIIB in inducing cell migration of ESCs has been previously investigated, EDIIIA/B+FN in matrigel had no effect on the migration of ESCs.

Alternative approaches to study the structural basis of EDIIIA and EDIIIB inclusion on FN functional properties are required. Further repetition of the preliminary cryo-EM studies of FIII7-12A+B- with α5β1 could be carried out. The recent crystal structure of FIII8-B+ indicates a small interface between domains FIII8 and EDIIIB, forming a unique acidic groove which could be a protein-protein interaction site (Bencharit *et al.* 2007). Similarly, short FN fragments of two to three FIII domains such as FIII11-12A+ could be used in crystallization trials; these would overcome our difficulties in structural determination of the longer FN fragments caused by molecular flexibilities between FIII domains. But the effects seen in the shorter FN fragments may not be representative if EDIIIA or EDIIIB inclusion were to alter the global conformation of FN. Also, ideally we would want to see how their insertion affects the RGD and synergistic motif in FIII9 and FIII10, which may not be present if shorter FN fragments were to be used in structural studies.

References

Abrahams, V. M., P. Bole-Aldo, et al. (2004). "Divergent Trophoblast Responses to Bacterial Products Mediated by TLRs." J Immunol **173**(7): 4286-4296.

Achache, H. and A. Revel (2006). "Endometrial receptivity markers, the journey to successful embryo implantation." Hum Reprod Update: dml004.

Adair, B. D., J.-P. Xiong, et al. (2005). "Three-dimensional EM structure of the ectodomain of integrin aVb3 in a complex with fibronectin." J. Cell Biol. **168**(7): 1109-1118.

Adamson, E. D. (1993). "Activities of growth factors in preimplantation embryos." Journal of Cellular Biochemistry **53**(4): 280-287.

Ahmed, S., A. Adamidis, et al. (2003). "Dexamethasone attenuates oxidation of extracellular matrix proteins by human monocytes." Experimental and Molecular Pathology **75**(2): 137-143.

Akiyama, S. K., S. Aota, et al. (1995). "Function and receptor specificity of a minimal 20 kilodalton cell adhesive fragment of fibronectin." Cell Adhesion and Communication **3**(1): 13-25.

Akiyama, S. K., S. S. Yamada, et al. (1989). "Analysis of fibronectin receptor function with monoclonal antibodies: roles in cell adhesion, migration, matrix assembly, and cytoskeletal organization." J. Cell Biol. **109**(2): 863-875.

Albers, A., M. Thie, et al. (1995). "Differential expression and localization of integrins and CD44 in the membrane domains of human uterine epithelial cells during the menstrual cycle." Acta Anat (Basel) **153**(1): 12-9.

Alberts, B., A. Johnson, et al. (2002). Molecular Biology of the Cell. New York, Garland Science.

Alexander, W. S. (2002). "Suppressors of cytokine signalling (SOCS) in the immune system " Nature Reviews Immunology **2**(6): 410-416.

Ali, I. U. and T. Hunter (1981). "Structural comparison of fibronectins from normal and transformed cells." J. Biol. Chem. **256**(14): 7671-7677.

Altroff, H. (1999). The role of FIII domains of human fibronectin in cell adhesion. Nuffield Department of Obstetrics and Gynaecology. Oxford, U.K., University of Oxford. **D.Phil.:** 152.

Altroff, H., R. Schlinkert, et al. (2004). "Interdomain Tilt Angle Determines Integrin-dependent Function of the Ninth and Tenth FIII Domains of Human Fibronectin." J. Biol. Chem. **279**(53): 55995-56003.

Altroff, H., C. F. van der Walle, et al. (2001). "The Eighth FIII Domain of Human Fibronectin Promotes Integrin alpha 5beta 1 Binding via Stabilization of the Ninth FIII Domain." J. Biol. Chem. **276**(42): 38885-38892.

Annes, J. P., J. S. Munger, et al. (2003). "Making sense of latent TGF{beta} activation." J Cell Sci **116**(2): 217-224.

Aoki, R. and M. N. Fukada (2000). "Recent molecular approaches to elucidate the mechanism of embryo implantation: trophinin, bystin, and tastin as molecules involved in the initial attachment of blastocysts to the uterus in humans." Semin Reprod Med **18**(3): 265-71.

Aplin, A. E., A. Howe, et al. (1998). "Signal Transduction and Signal Modulation by Cell Adhesion Receptors: The Role of Integrins, Cadherins, Immunoglobulin-Cell Adhesion Molecules, and Selectins." Pharmacol Rev **50**(2): 197-264.

Aplin, J., A. Charlton, et al. (1988). "An immunohistochemical study of human endometrial extracellular matrix during the menstrual cycle and first trimester of pregnancy." Cell and Tissue Research **253**(1): 231-40.

Aplin, J. D. (1997). "Adhesion molecules in implantation." Rev Reprod **2**(2): 84-93.

Aplin, J. D., N. A. Hey, et al. (1998). "Human endometrial MUC1 carries keratan sulphate: characteristic glycoforms in the luminal epithelium at receptivity." Glycobiology **8**: 269 - 276.

Apparao, K. B. C., M. J. Murray, et al. (2001). "Osteopontin and Its Receptor αvβ3 Integrin Are Coexpressed in the Human Endometrium during the Menstrual Cycle But Regulated Differentially." J Clin Endocrinol Metab **86**(10): 4991-5000.

Argraves, W. S., S. Suzuki, et al. (1987). "Amino acid sequence of the human fibronectin receptor." J. Cell Biol. **105**(3): 1183-1190.

Arici, A., O. Engin, et al. (1995). "Modulation of leukemia inhibitory factor gene expression and protein biosynthesis in human endometrium." J Clin Endocrinol Metab **80**(6): 1908-1915.

Armant, D. R. (1991). "Cell interactions with laminin and its proteolytic fragments during outgrowth of mouse primary trophoblast cells." Biol Reprod **45**(5): 664-672.

Armant, D. R. (2005). "Blastocysts don't go it alone. Extrinsic signals fine-tune the intrinsic developmental program of trophoblast cells." Developmental Biology **280**(2): 260-280.

Armant, D. R., H. A. Kaplan, et al. (1986). "Fibronectin and laminin promote in vitro attachment and outgrowth of mouse blastocysts." Developmental Biology **116**(2): 519-523.

Armant, D. R., H. A. Kaplan, et al. (1986). "The Effect of Hexapeptides on Attachment and Outgrowth of Mouse Blastocysts Cultured in vitro: Evidence for the Involvement of the Cell Recognition Tripeptide Arg-Gly-Asp." PNAS **83**(18): 6751-6755.

Arnaout, M. A., B. Mahalingam, et al. (2005). "Integrin structure, allostery, and bidirectional signaling." Annual Review of Cell and Developmental Biology **21**(1): 381-410.

Askari, J. A., D. J. Thornton, et al. (2007). "The alternatively spliced type III connecting segment of fibronectin is a zinc-binding module." Matrix Biology **26**(6): 485-493.

Atalay, G., F. Cardoso, et al. (2003). "Novel therapeutic strategies targeting the epidermal growth factor receptor (EGFR) family and its downstream effectors in breast cancer." Ann Oncol **14**(9): 1346-1363.

Ayscough, K. R. and S. J. Winder (2004). "Two billion years of actin " EMBO Reports **5**(10): 947-52.

Bankers-Fulbright, J. L., K. R. Kalli, et al. (1996). "Interleukin-1 signal transduction." Life Sciences **59**(2): 61-83.

Basak, S., R. Dhar, et al. (2002). "Steroids Modulate the Expression of α4 Integrin in Mouse Blastocysts and Uterus During Implantation." Biol Reprod **66**(6): 1784-1789.

Beliard, A., J. Donnez, et al. (1997). "Localization of laminin, fibronectin, E-cadherin, and integrins in endometrium and endometriosis." Fertility and Sterility **67**(2): 266-272.

Bencharit, S., C. B. Cui, et al. (2007). "Structural Insights into Fibronectin Type III Domain-mediated Signaling." Journal of Molecular Biology **367**(2): 303-309.

Bentin-Ley, U., A. Sjogren, et al. (1999). "Presence of uterine pinopodes at the embryo-endometrial interface during human implantation in vitro." Hum Reprod **14**: 515 - 520.

Bergh, P. A. and D. Navot (1992). "The impact of embryonic development and endometrial maturity on the timing of implantation." Fertil Steril **58**: 537 - 42.

Bermath, V. A., A. F. Muro, et al. (1990). "Cyclic AMP inhibits fibronectin gene expression in a newly developed granulosa cell line by a mechanism that suppresses cAMP-responsive element-dependent transcriptional activation." J. Biol. Chem. **265**(30): 18219-18226.

Bigonnesse, F., Y. Labelle, et al. (2001). "Triphasic expression of interleukin-1 receptor type I in human endometrium throughout the menstrual cycle of fertile women and women with unexplained infertility." Fertility and Sterility **75**(1): 79-87.

Bischof, P. and A. Campana (2000). "Molecular mediators of implantation." Best Practice & Research Clinical Obstetrics & Gynaecology **14**(5): 801-814.

Bischof, P., A. Meisser, et al. (1998). "Involvement of trophoblast in embryo implantation: regulation by paracrine factors." Journal of Reproductive Immunology **39**(1-2): 167-177.

Blaustein, M., F. Pelisch, et al. (2004). "Mammary Epithelial-Mesenchymal Interaction Regulates Fibronectin Alternative Splicing via Phosphatidylinositol 3-Kinase." J. Biol. Chem. **279**(20): 21029-21037.

Blaustein, M., F. Pelisch, et al. (2005). "Concerted regulation of nuclear and cytoplasmic activities of SR proteins by AKT." Nat Struct Mol Biol **12**(12): 1037-1044.

Bloor, D. J., A. D. Metcalfe, et al. (2002). "Expression of cell adhesion molecules during human preimplantation embryo development." Mol. Hum. Reprod. **8**(3): 237-245.

Borsi, L., B. Carnemolla, et al. (1987). "Monoclonal antibodies in the analysis of fibronectin isoforms generated by alternative splicing of mRNA precursors in normal and transformed human cells." J. Cell Biol. **104**(3): 595-600.

Borsi, L., P. Castellani, et al. (1990). "Transforming growth factor-[beta] regulates the splicing pattern of fibronectin messenger RNA precursor." FEBS Letters **261**(1): 175-178.

Borthwick, J. M., D. S. Charnock-Jones, et al. (2003). "Determination of the transcript profile of human endometrium." Mol Hum Reprod **9**: 19 - 33.

Bourdoulous, S., G. Orend, et al. (1998). "Fibronectin Matrix Regulates Activation of RHO and CDC42 GTPases and Cell Cycle Progression." J. Cell Biol. **143**(1): 267-276.

Bowditch, R., M. Hariharan, et al. (1994). "Identification of a novel integrin binding site in fibronectin. Differential utilization by beta 3 integrins." J. Biol. Chem. **269**(14): 10856-10863.

Bowen, J. A. and J. S. Hunt (2000). "The Role of Integrins in Reproduction." Proc Soc Exp Biol Med **223**(4): 331-343.

Brar, A., Frank GR, et al. (1995). "Laminin decreases PRL and IGFBP-1 expression during in vitro decidualization of human endometrial stromal cells." J Cell Physiol. **163**(1): 30-7.

Brar, A. K., S. Handwerger, et al. (2001). "Gene induction and categorical reprogramming during in vitro human endometrial fibroblast decidualization." Physiol. Genomics **7**(2): 135-148.

Braundmeier, A. G. and R. A. Nowak (2006). "Cytokines Regulate Matrix Metalloproteinases in Human Uterine Endometrial Fibroblast Cells Through a Mechanism That Does Not Involve Increases in Extracellular Matrix Metalloproteinase Inducer." American Journal of Reproductive Immunology **56**(3): 201-214.

Brooks, P. C., S. Stromblad, et al. (1996). "Localization of Matrix Metalloproteinase MMP-2 to the Surface of Invasive Cells by Interaction with Integrin [alpha]v[beta]3." Cell **85**(5): 683-693.

Brosens, J. J. and B. Gellersen (2006). "Death or survival - progesterone-dependent cell fate decisions in the human endometrial stroma." J Mol Endocrinol **36**(3): 389-398.

Brown, L. F., B. Berse, et al. (1992). "Expression and distribution of osteopontin in human tissues: widespread association with luminal epithelial surfaces." Mol Biol Cell **3**(10): 1169-80.

Bruner, K. L., W. H. Rodgers, et al. (1995). "Transforming Growth Factor β Mediates the Progesterone Suppression of an Epithelial Metalloproteinase by Adjacent Stroma in the Human Endometrium." PNAS **92**(16): 7362-7366.

Burridge, K. and M. Chrzanowska-Wodnicka (1996). "Focal adhesions, contractility, and signaling." Annual Review of Cell and Developmental Biology **12**(1): 463-519.

Burridge, K., C. E. Turner, et al. (1992). "Tyrosine phosphorylation of paxillin and pp125FAK accompanies cell adhesion to extracellular matrix: a role in cytoskeletal assembly." J. Cell Biol. **119**(4): 893-903.

Burrows, T. D., A. King, et al. (1995). "The Role of Integrins in Adhesion of Decidual NK Cells to Extracellular Matrix and Decidual Stromal Cells." Cellular Immunology **166**(1): 53.

Bush, M. R., J. M. Mele, et al. (1998). "Evidence of Juxtacrine Signaling for Transforming Growth Factor {alpha} inHuman Endometrium." Biol Reprod **59**(6): 1522-1529.

Calderwood, D. A., S. J. Shattil, et al. (2000). "Integrins and Actin Filaments: Reciprocal Regulation of Cell Adhesion and Signaling." J. Biol. Chem. **275**(30): 22607-22610.

Campbell, S., H. Swann, et al. (1995). "Cell adhesion molecules on the oocyte and preimplantation human embryo." Hum. Reprod. **10**(6): 1571-1578.

Canty, E. G. and K. E. Kadler (2005). "Procollagen trafficking, processing and fibrillogenesis." J Cell Sci **118**(7): 1341-1353.

Carnemolla, B., A. Leprini, et al. (1992). "The inclusion of the type III repeat ED-B in the fibronectin molecule generates conformational modifications that unmask a cryptic sequence [published erratum appears in J Biol Chem 1993 Apr 5;268(10):7602]." J. Biol. Chem. **267**(34): 24689-24692.

Carson, D. D., E. Lagow, et al. (2002). "Changes in gene expression during the early to mid-luteal (receptive phase) transition in human endometrium detected by high-density microarray screening." Mol. Hum. Reprod. **8**(9): 871-879.

Carson, D. D., J.-P. Tang, et al. (1988). "Collagens support embryo attachment and outgrowth in vitro: Effects of the Arg-Gly-Asp sequence." Developmental Biology **127**(2): 368-375.

Carver, J., K. Martin, et al. (2003). "An in-vitro model for stromal invasion during implantation of the human blastocyst." Hum. Reprod. **18**(2): 283-290.

Castellani, P., G. Viale, et al. (1994). "The fibronectin isoform containing the ED-B oncofetal domain: a marker of angiogenesis." International Journal of Cancer **59**(5): 612-8.

Charnock-Jones, D., A. Sharkey, et al. (1994). "Leukaemia inhibitory factor mRNA concentration peaks in human endometrium at the time of implantation and the blastocyst contains mRNA for the receptor at this time." J Reprod Fertil **101**(2): 421-426.

Chegini, N., Y. Zhao, et al. (1994). "Human uterine tissue throughout the menstrual cycle expresses transforming growth factor-beta 1 (TGF beta 1), TGF beta 2, TGF beta 3, and TGF beta type II receptor messenger ribonucleic acid and protein and contains [125I]TGF beta 1-binding sites." Endocrinology **135**(1): 439-449.

Chen, J., T. Maeda, et al. (1996). "Distinct structural requirements for interaction of the integrins alpha 5 beta 1, alpha v beta 5, and alpha v beta 6 with the central cell binding domain in fibronectin." Cell Adhesion and Communication **4**(4-5): 237-50.

Chen, L. B., A. Murray, et al. (1978). "Studies on intercellular LETS glycoprotein matrices." Cell **14**(2): 377-391.

Chia, C. M., R. M. Winston, et al. (1995). "EGF, TGF-alpha and EGFR expression in human preimplantation embryos." Development **121**(2): 299-307.

Chiquet-Ehrismann, R. (1991). "Anti-adhesive molecules of the extracellular matrix." Current Opinion in Cell Biology **3**(5): 800-804.

Chiquet-Ehrismann, R. (2004). "Tenascins." The International Journal of Biochemistry & Cell Biology **36**(6): 986-990.

Chobotova, K., I. Spyropoulou, et al. (2002). "Heparin-binding epidermal growth factor and its receptor ErbB4 mediate implantation of the human blastocyst." Mechanisms of Development **119**(2): 137-144.

Chung, C. Y., J. E. Murphy-Ullrich, et al. (1996). "Mitogenesis, cell migration, and loss of focal adhesions induced by tenascin-C interacting with its cell surface receptor, annexin II." Mol. Biol. Cell **7**(6): 883-892.

Chung, H.-W., Y. Wen, et al. (2001). "Interleukin-1{beta} Regulates Urokinase Plasminogen Activator (u-PA), u-PA Receptor, Soluble u-PA Receptor, and Plasminogen Activator Inhibitor-1 Messenger Ribonucleic Acid Expression in Cultured Human Endometrial Stromal Cells." J Clin Endocrinol Metab **86**(3): 1332-1340.

Church, H. J., L. M. Vicovac, et al. (1996). "Laminins 2 and 4 are expressed by human decidual cells." Lab Invest **74**: 21 - 32.

Clark, E. A. and J. S. Brugge (1995). "Integrins and signal transduction pathways: the road taken." Science **268**(5208): 233-239.

Clark, R. A. F., J.-Q. An, et al. (2003). "Fibroblast Migration on Fibronectin Requires Three Distinct Functional Domains." **121**(4): 695-705.

Colognato, H. and P. D. Yurchenco (2000). "Form and function: The laminin family of heterotrimers." Developmental Dynamics **218**(2): 213-234.

Coutifaris, C. (1999). Osteopontin in human endometrium: a role in endometrial receptivity and embryo implantation? Embryo Implantation: Molecular, Cellular and Clinical Aspects. D. D. Carson. New York, Springer Verlag**:** 141-8.

Cukierman, E., R. Pankov, et al. (2001). "Taking Cell-Matrix Adhesions to the Third Dimension." Science **294**(5547): 1708-1712.

Cullinan, E. B., S. J. Abbondanzo, et al. (1996). "Leukemia inhibitory factor (LIF) and LIF receptor expression in human endometrium suggests a potential autocrine/paracrine function in regulating embryo implantation." PNAS **93**(7): 3115-3120.

Daly, D., I. Maslar, et al. (1983). "Prolactin production during in vitro decidualization of proliferative endometrium." Am J Obstet Gynaecol. **145**(6): 672.

Damsky, C. H., C. Librach, et al. (1994). "Integrin switching regulates normal trophoblast invasion." Development **120**(12): 3657-3666.

Das, S., X. Wang, et al. (1994). "Heparin-binding EGF-like growth factor gene is induced in the mouse uterus temporally by the blastocyst solely at the site of its apposition: a possible ligand for interaction with blastocyst EGF-receptor in implantation." Development **120**(5): 1071-1083.

Das, S. K., N. Das, et al. (1997). "Expression of Betacellulin and Epiregulin Genes in the Mouse Uterus Temporally by the Blastocyst Solely at the Site of Its Apposition Is Coincident with the "Window" of Implantation." Developmental Biology **190**(2): 178-190.

De los Santos, M. J., A. Mercader, et al. (1996). "Role of endometrial factors in regulating secretion of components of the immunoreactive human embryonic interleukin-1 system during embryonic development." Biol Reprod **54**(3): 563-574.

de los Santos, M. J., A. Mercader, et al. (2003). "Implantation Rates after Two, Three, or Five Days of Embryo Culture." Placenta **24**(Supplement 2): S13-S19.

Dimitriadis, E., L. A. Salamonsen, et al. (2000). "Expression of interleukin-11 during the human menstrual cycle: coincidence with stromal cell decidualization and relationship to leukaemia inhibitory factor and prolactin." Mol. Hum. Reprod. **6**(10): 907-914.

Dimitriadis, E., C. Stoikos, et al. (2006). "Interleukin 11 Signaling Components Signal Transducer and Activator of Transcription 3 (STAT3) and Suppressor of Cytokine Signaling 3 (SOCS3) Regulate Human Endometrial Stromal Cell Differentiation." Endocrinology **147**(8): 3809-3817.

Dimitriadis, E., C. A. White, et al. (2005). "Cytokines, chemokines and growth factors in endometrium related to implantation." Hum Reprod Update **11**(6): 613-630.

Dinarello, C. A. (1997). "Interleukin-1." Cytokine & Growth Factor Reviews **8**(4): 253-265.

Djouad, F. and C. Jorgenssen (2007). "Microenvironment changes during mesenchymal stem cell differentiation towards chondrocytes." Arthritis Research & Therapy **9**: R33.

Dosiou, C. and L. C. Giudice (2005). "Natural Killer Cells in Pregnancy and Recurrent Pregnancy Loss: Endocrine and Immunologic Perspectives." Endocr Rev **26**(1): 44-62.

Engel, J. (1992). "Laminins and other strange proteins." Biochemistry **31**(44): 10643-51.

Engel, J., E. Odermatt, et al. (1981). "Shapes, domain organizations and flexibility of laminin and fibronectin, two multifunctional proteins of the extracellular matrix." Journal of Molecular Biology **150**(1): 97-120.

Erdfelder, E., F. Faul, et al. (1996). "GPOWER: A general power analysis program." Behavior Research Methods, Instruments, & Computers **28**(1): 1-11.

Erickson, H. and N. Carrell (1983). "Fibronectin in extended and compact conformations. Electron microscopy and sedimentation analysis." J. Biol. Chem. **258**(23): 14539-14544.

Erickson, H. P., N. Carrell, et al. (1981). "Fibronectin molecule visualized in electron microscopy: a long, thin, flexible strand." J. Cell Biol. **91**(3): 673-678.

Fattorusso, R., M. Pellecchia, et al. (1999). "NMR structure of the human oncofoetal fibronectin ED-B domain, a specific marker for angiogenesis." Structure with Folding & Design **7**(4): 381-390.

Feinberg, R. F., H. J. Kliman, et al. (1994). "Transforming growth factor-beta stimulates trophoblast oncofetal fibronectin synthesis in vitro: implications for trophoblast implantation in vivo." J Clin Endocrinol Metab **78**(5): 1241-1248.

Fernandez-Shaw, S., S. C. Shorter, et al. (1992). "Isolation and purification of human endometrial stromal and glandular cells using immunomagnetic microspheres." Hum. Reprod. **7**(2): 156-161.

Ffrench-Constant, C. (1995). "Alternative Splicing of Fibronectin--Many Different Proteins but Few Different Functions." Experimental Cell Research **221**(2): 261-271.

Ffrench-Constant, C., L. Van de Water, et al. (1989). "Reappearance of an embryonic pattern of fibronectin splicing during wound healing in the adult rat." J. Cell Biol. **109**(2): 903-914.

Finn, C. A. (1971). "The biology of decidual cells." Advances in reproductive physiology **5**: 1-26.

Folkman, J. and M. Klagsbrun (1987). "Angiogenic factors." Science **235**(4787): 442-447.

Foyouzi, N., M. Berkkanoglu, et al. (2004). "Effects of oxidants and antioxidants on proliferation of endometrial stromal cells." Fertility and Sterility **82**(Supplement 3): 1019-1022.

Frank, G., A. Brar, et al. (1995). "Interleukin-1 beta and the endometrium: an inhibitor of stromal cell differentiation and possible autoregulator of decidualization in humans." Biol Reprod **52**(1): 184-191.

Fraser, I. S. (1990). "Mechanisms of endometrial bleeding." Reprod Fertil Dev. **2**(2): 193-8.

Friesel, R., W. H. Burgess, et al. (1989). "Heparin-binding growth factor 1 stimulates tyrosine phosphorylation in NIH 3T3 cells." Mol. Cell. Biol. **9**(5): 1857-1865.

Fujimoto, J., S. Ichigo, et al. (1996). "Alteration of E-cadherin alpha- and beta-catenin mRNA expression in human uterine endometrium during the menstrual cycle." Gynecol Endocrinol **10**: 187 - 191.

Fukuda, M. N., T. Sato, et al. (1995). "Trophinin and tastin, a novel cell adhesion molecule complex with potential involvement in embryo implantation." Genes Devel **9**: 1199 - 1210.

Gellersen, B. and J. Brosens (2003). "Cyclic AMP and progesterone receptor cross-talk in human endometrium: a decidualizing affair." J Endocrinol **178**(3): 357-372.

George, E. L., E. N. Georges-Labouesse, et al. (1993). "Defects in mesoderm, neural tube and vascular development in mouse embryos lacking fibronectin." Development **119**(4): 1079-1091.

Giancotti, F. G. (1997). "Integrin signaling: specificity and control of cell survival and cell cycle progression." Current Opinion in Cell Biology **9**(5): 691-700.

Gibori, G., B. Kalison, et al. (1984). "Endocrine role of the decidual tissue: decidual luteotropin regulation of luteal adenylyl cyclase activity, luteinizing hormone receptors, and steroidogenesis." Endocrinology **115**(3): 1157-1163.

Giudice, L. C. (2004). "Microarray Expression Profiling Reveals Candidate Genes for Human Uterine Receptivity." American Journal of PharmacoGenomics **4**: 299-312.

Godkin, J. D. and J. J. Dore (1998). "Transforming growth factor beta and the endometrium." Rev Reprod **3**(1): 1-6.

Gondokaryono, S. P., H. Ushio, et al. (2007). "The extra domain A of fibronectin stimulates murine mast cells via Toll-like receptor 4." J Leukoc Biol: jlb.1206730.

Gospodarowicz, D., N. Ferrara, et al. (1987). "Structural characterization and biological functions of fibroblast growth factor." Endocrine Reviews **8**(2): 95-114.

Graham, C. and P. Lala (1992). "Mechanisms of placental invasion of the uterus and their control." Biochem Cell Biol **70**(10-11): 867-74.

Graham, C. H., I. Connelly, et al. (1994). "Resistance of Malignant Trophoblast Cells to both the Anti-proliferative and Anti-invasive Effects of Transforming Growth Factor-[beta]." Experimental Cell Research **214**(1): 93-99.

Grant, R. P., C. Spitzfaden, et al. (1997). "Structural Requirements for Biological Activity of the Ninth and Tenth FIII Domains of Human Fibronectin." J. Biol. Chem. **272**(10): 6159-6166.

Grosskinsky, C. M., C. W. Yowell, et al. (1996). "Modulation of integrin expression in endometrial stromal cells in vitro." J Clin Endocrinol Metab **81**(6): 2047-2054.

Guan, J.-L. and D. Shalloway (1992). "Regulation of focal adhesion-associated protein tyrosine kinase by both cellular adhesion and oncogenic transformation." Nature **358**(6388): 690-692.

Ha, H. and H. B. Lee (2003). "Reactive Oxygen Species and Matrix Remodeling in Diabetic Kidney." J Am Soc Nephrol **14**(90003): S246-249.

Haas, T. A. and E. F. Plow (1994). "Integrin-ligand interactions: a year in review." Current Opinion in Cell Biology **6**(5): 656-662.

Halliwell, B. (2003). "Oxidative stress in cell culture: an under-appreciated problem?" FEBS Letters **540**(1-3): 3-6.

Hambartsoumian, E. (1998). "Endometrial leukemia inhibitory factor (LIF) as a possible cause of unexplained infertility and multiple failures of implantation." American Journal of Reproductive Immunology **39**(2): 137-43.

Hamilton, G. S., J. J. Lysiak, et al. (1998). "Autocrine-Paracrine Regulation of Human Trophoblast Invasiveness by Insulin-like Growth Factor (IGF)-II and IGF-Binding Protein (IGFBP)-1." Experimental Cell Research **244**(1): 147-156.

Hanashi, H. and Y. Nakamura (2003). "Physiologic Role of Decidual β1 Integrin and Focal Adhesion Kinase in Embryonic Implantation." Endocrine Journal **50**(2): 189-198.

Hansard, L. J., B. E. Healy-Gardner, et al. (1997). "Human endometrial transforming growth factor-alpha: A transmembrane, surface epithelial protein that transiently disappears during the midsecretory phase of the menstrual cycle." Journal of the Society for Gynecologic Investigation **4**(3): 160-166.

Harrington, D. J., B. A. Lessey, et al. (1999). "Tenascin is differentially expressed in endometrium and endometriosis." The Journal of Pathology **187**(2): 242-248.

Hashimoto-Uoshima, M., Y. Yan, et al. (1997). "The alternatively spliced domains EIIIB and EIIIA of human fibronectin affect cell adhesion and spreading." J Cell Sci **110**(18): 2271-2280.

Hayman, E. G., M. D. Pierschbacher, et al. (1983). "Serum Spreading Factor (Vitronectin) is Present at the Cell Surface and in Tissues." PNAS **80**(13): 4003-4007.

Heij, E. L., R. W. A. M. Kuijpers, et al. (1998). "Adhesion molecules in iris biopsy specimens from patients with uveitis." Br J Ophthalmol **82**(4): 432-437.

Heinrich, P. C., I. Behrmann, et al. (2003). "Principles of interleukin (IL)-6-type cytokine signalling and its regulation." Biochemical Journal **374**: 1-20.

Hey, N. A., R. A. Graham, et al. (1994). "The polymorphic epithelial mucin MUC1 in human endometrium is regulated with maximal expression in the implantation phase." J Clin Endocrinol Metab **78**: 337 - 342.

Hey, N. A., T. C. Li, et al. (1995). "MUC1 in secretory phase endometrium: expression in precisely dated biopsies and flushings from normal and recurrent miscarriage patients." Hum Reprod **10**: 2555 - 2662.

Hirata, T., Y. Osuga, et al. (2005). "Evidence for the Presence of Toll-Like Receptor 4 System in the Human Endometrium." J Clin Endocrinol Metab **90**(1): 548-556.

Hofmann, G. E., M. R. Drews, et al. (1992). "Epidermal growth factor and its receptor in human implantation trophoblast: immunohistochemical evidence for autocrine/paracrine function." J Clin Endocrinol Metab **74**(5): 981-988.

Hofmann, G. E., R. T. Scott, Jr., et al. (1991). "Immunohistochemical localization of epidermal growth factor in human endometrium, decidua, and placenta." J Clin Endocrinol Metab **73**(4): 882-887.

Huang, H.-Y., Y. Wen, et al. (1998). "Cytokine-Mediated Regulation of 92-Kilodalton Type IV Collagenase, Tissue Inhibitor of Metalloproteinase-1 (TIMP-1), and TIMP-3 Messenger Ribonucleic Acid Expression in Human Endometrial Stromal Cells." J Clin Endocrinol Metab **83**(5): 1721-1729.

Huang, J. R., L. Tseng, et al. (1987). "Regulation of prolactin production by progestin, estrogen, and relaxin in human endometrial stromal cells." Endocrinology **121**(6): 2011-2017.

Hulmes, D. J. S. (2002). "Building Collagen Molecules, Fibrils, and Suprafibrillar Structures." Journal of Structural Biology **137**(1-2): 2-10.

Humphries, M. J. (2000). "Integrin Structure." Biochem Soc Transac **28**: 311-339.

Hynes, R. O. (1990). Fibronectin. New York, Springer-Verlag.

Hynes, R. O. (1992). "Integrins: Versatility, modulation, and signaling in cell adhesion." Cell **69**(1): 11-25.

Hynes, R. O. (2002). "Integrins: Bidirectional, Allosteric Signaling Machines." Cell **110**(6): 673-687.

Idriss, H. T. and J. H. Naismith (2000). "TNF-alpha and the TNF receptor superfamily: Structure-function relationship(s)." Microscopy Research and Technique **50**(3): 184-195.

Ihnatovych, I., W. Hu, et al. (2007). "Increased Phosphorylation of Myosin Light Chain Prevents in Vitro Decidualization." Endocrinology **148**(7): 3176-3184.

Inoue, J.-i., T. Ishida, et al. (2000). "Tumor Necrosis Factor Receptor-Associated Factor (TRAF) Family: Adapter Proteins That Mediate Cytokine Signaling." Experimental Cell Research **254**(1): 14-24.

Inoue, T., H. Kanzaki, et al. (1994). "Tumour necrosis factor alpha inhibits in-vitro decidualization of human endometrial stromal cells." Hum. Reprod. **9**(12): 2411-2417.

Irving, J. A. and P. K. Lala (1995). "Functional Role of Cell Surface Integrins on Human Trophoblast Cell Migration: Regulation by TGF-[beta], IGF-II, and IGFBP-1." Experimental Cell Research **217**(2): 419-427.

Iwahashi, M., Y. Muragaki, et al. (1996). "Alterations in distribution and composition of the extracellular matrix during decidualization of the human endometrium." J Reprod Fertil **108**(1): 147-155.

Jahn, E., I. Classen-Linke, et al. (1995). "Expression of gap junction connexins in the human endometrium throughout the menstrual cycle." Hum. Reprod. **10**(10): 2666-2670.

Jarnagin, W. R., D. C. Rockey, et al. (1994). "Expression of variant fibronectins in wound healing: cellular source and biological activity of the EIIIA segment in rat hepatic fibrogenesis." J. Cell Biol. **127**(6): 2037-2048.

Jokhi, P. P., A. King, et al. (1994). "Screening for cytokine messenger ribonucleic acids in purified human decidual lymphocyte populations by the reverse-transcriptase polymerase chain reaction." J Immunol **153**(10): 4427-4435.

Jones, P. L. and F. S. Jones (2000). "Tenascin-C in development and disease: gene regulation and cell function." Matrix Biology **19**(7): 581-596.

Julian, J., R. Chiquet-Ehrismann, et al. (1994). "Tenascin is induced at implantation sites in the mouse uterus and interferes with epithelial cell adhesion." Development **120**(3): 661-671.

Kao, L. C., S. Tulac, et al. (2002). "Global Gene Profiling in Human Endometrium during the Window of Implantation." Endocrinology **143**(6): 2119-2138.

Kariya, M., H. Kanzaki, et al. (1991). "Interleukin-1 inhibits in vitro decidualization of human endometrial stromal cells." J Clin Endocrinol Metab **73**(6): 1170-1174.

Karpovich, N., K. Chobotova, et al. (2003). "Expression and function of interleukin-11 and its receptor {alpha} in the human endometrium." Mol. Hum. Reprod. **9**(2): 75-80.

Kauma, S. W., D. Matt, et al. (1990). "Interleukin-1β, human leukocyte antigen HLA-DRα, and transforming growth factor-β expression in endometrium, placenta, and placental membranes." Am J Obstet Gynaecol. **163**(5 I): 1430-1437.

Kayisli, U. A., E. T. Korgun, et al. (2005). "Expression of integrin alpha5 and integrin beta4 and their extracellular ligands fibronectin and laminin in human decidua during early pregnancy and its sex steroid-mediated regulation." Acta Histochemica **107**(3): 173.

Kim, J. J., R. C. Jaffe, et al. (1999). "Insulin-Like Growth Factor Binding Protein-1 Expression in Baboon Endometrial Stromal Cells: Regulation by Filamentous Actin and Requirement for de Novo Protein Synthesis." Endocrinology **140**(2): 997-1004.

Kimber, S. J. and C. Spanswick (2000). "Blastocyst implantation: the adhesion cascade." Seminars in Cell & Developmental Biology **11**(2): 77-92.

Kisalus, L., J. Herr, et al. (1987). "Immunolocalization of extracellular matrix proteins and collagen synthesis in first-trimester human decidua." Anatomical Record **218**(4): 402-15.

Kliman, H. J. (2000). "Uteroplacental Blood Flow : The Story of Decidualization, Menstruation, and Trophoblast Invasion." Am J Pathol **157**(6): 1759-1768.

Koopman, L. A., H. D. Kopcow, et al. (2003). "Human Decidual Natural Killer Cells Are a Unique NK Cell Subset with Immunomodulatory Potential." J. Exp. Med. **198**(8): 1201-1212.

Kornblihtt, A., K. Umezawa, et al. (1985). "Primary structure of human fibronectin: differential splicing may generate at least 10 polypeptides from a single gene." EMBO J. **4**(7): 1755-1759.

Kreis, T. and R. Vale (1999). Guidebook to the Extracellular Matrix, Anchor, and Adhesion Proteins, Oxford University Press.

Krussel, J. S., C. Simon, et al. (1998). "Expression of interleukin-1 system mRNA in single blastomeres from human preimplantation embryos." Human Reproduction (Oxford, England) **13**(8): 2206-2211.

Laemmli, U. K. (1970). "Cleavage of Structural Proteins during the Assembly of the Head of Bacteriophage T4." Nature **227**(5259): 680-685.

Lala, P., M. Kearns, et al. (1984). "Cells of the fetomaternal interface: their role in the maintenance of viviparous pregnancy." American Journal of Anatomy **170**(3): 501-17.

Lange-Mutschler, J. (1986). "Acylated fibronectin: a new type of posttranslational modification of cellular fibronectin." FEBS Letters **201**(2): 210-214.

Lash, G. E., H. A. Otun, et al. (2005). "Inhibition of Trophoblast Cell Invasion by TGFB1, 2, and 3 Is Associated with a Decrease in Active Proteases." Biol Reprod **73**(2): 374-381.

Leach, R. E., R. Khalifa, et al. (1999). "Multiple Roles for Heparin-Binding Epidermal Growth Factor-Like Growth Factor Are Suggested by Its Cell-Specific Expression during the Human Endometrial Cycle and Early Placentation." J Clin Endocrinol Metab **84**(9): 3355-3363.

Leahy, D. J., I. Aukhil, et al. (1996). "2.0 Å Crystal Structure of a Four-Domain Segment of Human Fibronectin Encompassing the RGD Loop and Synergy Region." Cell **84**(1): 155-164.

Ledee-Bataille, N., G. Lapree-Delage, et al. (2002). "Concentration of leukaemia inhibitory factor (LIF) in uterine flushing fluid is highly predictive of embryo implantation." Hum. Reprod. **17**(1): 213-218.

Lessey, B. A. (1994). "Further characterization of endometrial integrins during the menstrual cycle and in pregnancy." Fertil Steril **62**(3): 497-506.

Lessey, B. A., L. Damjanovich, et al. (1992). "Integrin adhesion molecules in the human endometrium. Correlation with the normal and abnormal menstrual cycle." J. Clin. Invest. **90**(1): 188-195.

Lessey, B. A., A. O. Ilesanmi, et al. (1996). "Luminal and glandular endometrial epithelium express integrins differentially throughout the menstrual cycle: implications for implantation, contraception and infertility." Am. J. Reprod. Immunol. **35**: 195-204.

Li, R. H. and L. Z. Zhuang (1997). "The effects of growth factors on human normal placental cytotrophoblast cell proliferation." Hum. Reprod. **12**(4): 830-834.

Liao, Y.-F., P. J. Gotwals, et al. (2002). "The EIIIA Segment of Fibronectin Is a Ligand for Integrins alpha 9beta 1 and alpha 4beta 1 Providing a Novel Mechanism for Regulating Cell Adhesion by Alternative Splicing." J. Biol. Chem. **277**(17): 14467-14474.

Librach, C. L., Z. Werb, et al. (1991). "92-kD type IV collagenase mediates invasion of human cytotrophoblasts." J. Cell Biol. **113**(2): 437-449.

Lim, H., L. Ma, et al. (1999). "Hoxa-10 Regulates Uterine Stromal Cell Responsiveness to Progesterone during Implantation and Decidualization in the Mouse." Mol Endocrinol **13**(6): 1005-1017.

Litvinovich, S. V. and K. C. Ingham (1995). "Interactions Between Type III Domains in the 110 kDa Cell-binding Fragment of Fibronectin." Journal of Molecular Biology **248**(3): 611-626.

Liu, S., W. B. Kiosses, et al. (2002). "A Fragment of Paxillin Binds the alpha 4 Integrin Cytoplasmic Domain (Tail) and Selectively Inhibits alpha 4-Mediated Cell Migration." J. Biol. Chem. **277**(23): 20887-20894.

llic, D. k., Y. Furuta, et al. (1995). "Reduced cell motility and enhanced focal adhesion contact formation in cells from FAK-deficient mice." Nature **377**(6549): 539-544.

Locksley, R. M., N. Killeen, et al. (2001). "The TNF and TNF Receptor Superfamilies: Integrating Mammalian Biology." Cell **104**(4): 487-501.

Lodish, H., A. Berk, et al. (2000). Molecular Cell Biology. New York, W. H. FREEMAN.

Lombardo, A., Y. Wang, et al. (1996). "Conformational flexibility and crystallization of tandemly linked type III modules of human fibronectin." Protein Sci **5**(9): 1934-1938.

Lu, D. P., L. Tian, et al. (2002). "Regulation of cellular adhesion molecule expression in murine oocytes, peri-implantation and post-implantation embryos." Cell Research **12**(5-6): 373-83.

Luo, B.-H., C. V. Carman, et al. (2007). "Structural Basis of Integrin Regulation and Signaling." Annual Review of Immunology **25**(1): 619-647.

Luo, B.-H. and T. A. Springer (2006). "Integrin structures and conformational signaling." Current Opinion in Cell Biology **18**(5): 579-586.

Luo, X., L. Ding, et al. (2004). "Gonadotropin-releasing hormone and TGF-β activate MAP kinase and differentially regulate fibronectin expression in endometrial epithelial and stromal cells." Am J Physiol Endocrinol Metab **287**(5): E991-1001.

Magnuson, V., M. Young, et al. (1991). "The alternative splicing of fibronectin pre-mRNA is altered during aging and in response to growth factors." J. Biol. Chem. **266**(22): 14654-14662.

Main, A. L., T. S. Harvey, et al. (1992). "The three-dimensional structure of the tenth type III module of fibronectin: An insight into RGD-mediated interactions." Cell **71**(4): 671-678.

Manabe, R.-i., N. Oh-e, et al. (1997). "Modulation of Cell-adhesive Activity of Fibronectin by the Alternatively Spliced EDA Segment." J. Cell Biol. **139**(1): 295-307.

Manabe, R.-i., N. Oh-e, et al. (1999). "Alternatively Spliced EDA Segment Regulates Fibronectin-dependent Cell Cycle Progression and Mitogenic Signal Transduction." J. Biol. Chem. **274**(9): 5919-5924.

Mardon, H. J. and K. E. Grant (1994). "The role of the ninth and tenth type III domains of human fibronectin in cell adhesion." FEBS Letters **340**(3): 197-201.

Martin, K., D. Barlow, et al. (1998). "Heparin-binding epidermal growth factor significantly improves human blastocyst development and hatching in serum-free medium." Hum. Reprod. **13**(6): 1645-1652.

Maruyama, T., Y. Yoshimura, et al. (1999). "Tyrosine Phosphorylation and Subcellular Localization of Focal Adhesion Proteins during in Vitro

Decidualization of Human Endometrial Stromal Cells." Endocrinology **140**(12): 5982-5990.

Massague, J. and A. Pandiella (1993). "Membrane-Anchored Growth Factors." Annual Review of Biochemistry **62**(1): 515-541.

McKay, N. G., D. J. Hunter, et al. (1994). "Regulation of Alternative Splicing of the Fibronectin IIICS Domain by Cytokines." Biochemical and Biophysical Research Communications **199**(2): 1005-1011.

Meisser, A., D. Chardonnens, et al. (1999). "Effects of tumour necrosis factor-alpha, interleukin-1 alpha, macrophage colony stimulating factor and transforming growth factor beta on trophoblastic matrix metalloproteinases." Molecular Human Reproduction **5**(3): 252-260.

Meseguer, M., J. D. Aplin, et al. (2001). "Human endometrial mucin MUC1 is up-regulated by progesterone and down-regulated in vitro by the human blastocyst." Biol Reprod **64**: 590 - 601.

Midwood, K. S. and J. E. Schwarzbauer (2002). "Tenascin-C Modulates Matrix Contraction via Focal Adhesion Kinase- and Rho-mediated Signaling Pathways." Mol. Biol. Cell **13**(10): 3601-3613.

Miner, J. H. and P. D. Yurchenco (2004). "Laminin functions in tissue morphogenesis " Annual Review of Cell and Developmental Biology **20**(1): 255-284.

Mirkin, S., M. Arslan, et al. (2005). "In search of candidate genes critically expressed in the human endometrium during the window of implantation." Hum. Reprod. **20**(8): 2104-2117.

Mizuno, K., T. Tanaka, et al. (1998). "Establishment and characterization of in vitro decidualization in normal human endometrial stromal cells." Osaka City Med J. **44**(1): 105-15.

Moller, B., C. Rasmussen, et al. (2001). "Expression of the angiogenic growth factors VEGF, FGF-2, EGF and their receptors in normal human endometrium during the menstrual cycle." Mol. Hum. Reprod. **7**(1): 65-72.

Mould, A. P., S. K. Akiyama, et al. (1996). "The inhibitory anti-beta1 integrin monoclonal antibody 13 recognizes an epitope that is attenuated by ligand occupancy. Evidence for allosteric inhibition of integrin function." Journal Of Biological Chemistry **271**(34): 20365-74.

Mould, A. P., L. A. Wheldon, et al. (1990). "Affinity chromatographic isolation of the melanoma adhesion receptor for the IIICS region of fibronectin and its identification as the integrin alpha 4 beta 1." J. Biol. Chem. **265**(7): 4020-4024.

Moustakas, A., K. Pardali, et al. (2002). "Mechanisms of TGF-[beta] signaling in regulation of cell growth and differentiation." Immunology Letters **82**(1-2): 85-91.

Muro, A. F., A. K. Chauhan, et al. (2003). "Regulated splicing of the fibronectin EDA exon is essential for proper skin wound healing and normal lifespan." J. Cell Biol. **162**(1): 149-160.

Murphy, G., S. Atkinson, et al. (1992). "The Role of Plasmhogen Activators in the Regulation of Connective Tissue Metalloproteinasesa." Annals of the New York Academy of Sciences **667**(1): 1-12.

Murphy, G., M. I. Cockett, et al. (1991). "Matrix metalloproteinase degradation of elastin, type IV collagen and proteoglycan. A quantitative comparison of the activities of 95 kDa and 72 kDa gelatinases, stromelysins-1 and -2 and punctuated metalloproteinase (PUMP)." Biochem J. **277**: 277-9.

Mylonas, I., U. Jeschke, et al. (2007). "Steroid receptors ERalpha, ERbeta, PR-A and PR-B are differentially expressed in normal and atrophic human endometrium." Histol Histopathol. **22**(2): 169-76.

Niimi, T. and S. Fujita (2001). "Letter to the Editor: NMR structure of human fibronectin EDA." Journal of Biomolecular NMR **21**(3): 281-4.

Nikas, G. (1999). "Pinopodes as markers of endometrial receptivity in clinical practice." Hum Reprod **14**(Suppl 2): 99-106.

Noyes, R. W., A. T. Hertig, et al. (1975). "Dating the endometrial biopsy." Am J Obstet Gynaecol. **122**(2): 262-3.

O'Shea, K. S., L. H. Liu, et al. (1990). "Role of the extracellular matrix protein thrombospondin in the early development of the mouse embryo." J. Cell Biol. **111**(6): 2713-2723.

Obara, M., M. S. Kang, et al. (1988). "Site-directed mutagenesis of the cell-binding domain of human fibronectin: Separable, synergistic sites mediate adhesive function." Cell **53**(4): 649-657.

Okamura, Y., M. Watari, et al. (2001). "The Extra Domain A of Fibronectin Activates Toll-like Receptor 4." J. Biol. Chem. **276**(13): 10229-10233.

Olden, K., R. M. Pratt, et al. (1979). "Role of carbohydrate in biological function of the adhesive glycoprotein fibronectin." PNAS.

Olsen, B. R. and Y. Ninomiya (1999). Collagens. Guidebook to the Extracellular Matrix, Anchor, and Adhesion Proteins. T. Kreis and R. Vale. New York, Oxford University Press Inc.

Orend, G. and R. Chiquet-Ehrismann (2000). "Adhesion Modulation by Antiadhesive Molecules of the Extracellular Matrix." Experimental Cell Research **261**(1): 104-110.

Osterlund, C. and G. Fried (2000). "TGF{beta} receptor types I and II and the substrate proteins Smad 2 and 3 are present in human oocytes." Mol. Hum. Reprod. **6**(6): 498-503.

Palmer, E., C. Ruegg, et al. (1993). "Sequence and tissue distribution of the integrin alpha 9 subunit, a novel partner of beta 1 that is widely distributed in epithelia and muscle." J. Cell Biol. **123**(5): 1289-1297.

Pankov, R., E. Cukierman, et al. (2000). "Integrin Dynamics and Matrix Assembly: Tensin-dependent Translocation of α5β1 Integrins Promotes Early Fibronectin Fibrillogenesis." J. Cell Biol. **148**(5): 1075-1090.

Paolella, G., C. Henchcliffe, et al. (1988). "Sequence analysis and in vivo expression show that alternative splicing of ED-B and ED-A regions of the human fibronectin gene are independent events." Nucl. Acids Res. **16**(8): 3545-3557.

Parsons, J. T. (2003). "Focal adhesion kinase: the first ten years." J Cell Sci **116**(8): 1409-1416.

Paul, J. I. and R. O. Hynes (1984). "Multiple fibronectin subunits and their post-translational modifications." J. Biol. Chem. **259**(21): 13477-13487.

Peters, J. and R. Hynes (1996). "Fibronectin isoform distribution in the mouse. I. The alternatively spliced EIIIB, EIIIA, and V segments show widespread codistribution in the developing mouse embryo." Cell Adhesion and Communication **4**: 103-125.

Pierschbacher, M. D. and E. Ruoslahti (1984). "Cell attachment activity of fibronectin can be duplicated by small synthetic fragments of the molecule." Nature **309**(5963): 30-33.

Piestrzeniewicz-Ulanska, D., M. Brys, et al. (2002). "Expression of TGF-[beta] type I and II receptors in normal and cancerous human endometrium." Cancer Letters **186**(2): 231-239.

Popovici, R. M., L.-C. Kao, et al. (2000). "Discovery of New Inducible Genes in in vitroDecidualized Human Endometrial Stromal Cells Using Microarray Technology." Endocrinology **141**(9): 3510-3515.

Potts, J. R. and I. D. Campbell (1994). "Fibronectin structure and assembly." Current Opinion in Cell Biology **6**(5): 648-655.

Preissner, K. T. and D. Seiffert (1998). "Role of Vitronectin and Its Receptors in Haemostasis and Vascular Remodeling." Thrombosis Research **89**(1): 1-21.

Psychoyos, A. (1973). "Hormonal control of ovoimplantation." Vitamins and Hormones **31**: 201-56.

Rawdanowicz, T. J., A. L. Hampton, et al. (1994). "Matrix metalloproteinase production by cultured human endometrial stromal cells: identification of interstitial collagenase, gelatinase- A, gelatinase-B, and stromelysin-1 and their differential regulation by interleukin-1 alpha and tumor necrosis factor-alpha." J Clin Endocrinol Metab **79**(2): 530-536.

Reddy, K. V. R. and S. S. Mangale (2003). "Integrin receptors: the dynamic modulators of endometrial function." Tissue and Cell **35**(4): 260-273.

Reis, F. M., C. Lhullier, et al. (2005). "In Vivo Assessment of the Regulation of Transforming Growth Factor Alpha, Epidermal Growth Factor (EGF), and EGF Receptor in the Human Endometrium by Medroxyprogesterone Acetate." Journal of Assisted Reproduction and Genetics **22**(1): 19-24.

Ricard-Blum, S. and F. Ruggiero (2005). "The collagen superfamily: from the extracellular matrix to the cell membrane." Pathologie Biologie **53**(7): 430-442.

Rider, V., D. L. Carlone, et al. (1992). "Uterine fibronectin mRNA content and localization are modulated during implantation." Developmental Dynamics **195**(1): 1-14.

Riesewijk, A., J. Martin, et al. (2003). "Gene expression profiling of human endometrial receptivity on days LH+2 versus LH+7 by microarray technology." Mol Hum Reprod **9**: 253 - 264.

Rizzino, A. (1988). "Transforming growth factor-[beta]: Multiple effects on cell differentiation and extracellular matrices." Developmental Biology **130**(2): 411-422.

Robb, L., R. Li, et al. (1998). "Infertility in female mice lacking the receptor for interleukin 11 is due to a defective uterine response to implantation." Nature Medicine **4**(3): 303-8.

Roman, J., R. M. LaChance, et al. (1989). "The fibronectin receptor is organized by extracellular matrix fibronectin: implications for oncogenic transformation and for cell recognition of fibronectin matrices." J. Cell Biol. **108**(6): 2529-2543.

Rout, U. K., J. Wang, et al. (2004). "alpha5beta1, alphaVbeta3 and the platelet associated integrin alphaIIbbeta3 coordinately regulate adhesion and migration of differentiating mouse trophoblast cells." Dev Biol **268**: 135 - 151.

Rundhaug, J. E. (2005). "Matrix metalloproteinases and angiogenesis." Journal of Cellular and Molecular Medicine **9**(2): 267-285.

Ruoslahti, E. (1988). "Fibronectin and its Receptors." Annual Review of Biochemistry **57**(1): 375-413.

Ruoslahti, E. (1996). "RGD and other recognition sequencess for integrins." Annual Review of Cell and Developmental Biology **12**(1): 697-715.

Ruoslahti, E. and Y. Yamaguchi (1991). "Proteoglycans as modulators of growth factor activities." Cell **64**(5): 867-869.

Sahakian, V., J. Anners, et al. (1993). "Selective localization of interleukin-1 receptor antagonist in eutopic endometrium and endometriotic implants." Fertility And Sterility **60**(2): 276-279.

Saito, S., N. Yamaji, et al. (1999). "The Fibronectin Extra Domain A Activates Matrix Metalloproteinase Gene Expression by an Interleukin-1-dependent Mechanism." J. Biol. Chem. **274**(43): 30756-30763.

Salamonsen, L. and G. Nie (2002). "Proteases at the Endometrial–Trophoblast Interface: Their Role in Implantation." Reviews in Endocrine & Metabolic Disorders **3**(2): 133-43.

Salamonsen, L. A., G. Nie, et al. (2002). "Newly identified endometrial genes of importance for implantation." Journal of Reproductive Immunology **53**(1-2): 215-225.

Sambrook, J. and T. Maniatis (1989). Molecular Cloning: A Laboratory Manual, Cold Spring Harbor Laboratory Press

Sangha, R. K., X. F. Li, et al. (1997). "Fibroblast growth factor receptor-1 is a critical component for endometrial remodeling: localization and expression of basic fibroblast growth factor and FGF-R1 in human endometrium during the menstrual cycle and decreased FGF-R1 expression in menorrhagia." Lab Invest. **77**(4): 389-402.

Sarani, S. A., M. Ghaffari-Novin, et al. (1999). "Morphological evidence for the 'implantation window' in human luminal endometrium." Hum Reprod **14**: 3101 - 3106.

Satokata, I., G. Benson, et al. (2002). "Sexually dimorphic sterility phenotypes in HoxalO-deficient mice." Nature **374**(6521): 460-463.

Sayle, R. A. and E. J. Milner-White (1995). "RASMOL: biomolecular graphics for all." Trends in Biochemical Sciences **20**(9): 374-376.

Scarpino, S., A. Stoppacciaro, et al. (1999). "Expression of EDA/EDB isoforms of fibronectin in papillary carcinoma of the thyroid." Journal of Pathology **188**(2): 163-167.

Schultz, J. F., L. Mayernik, et al. (1997). "Integrin trafficking regulates adhesion to fibronectin during differentiation of mouse peri-implantation blastocysts." Dev Genet **21**: 31 - 43.

Schvartz, I., D. Seger, et al. (1999). "Vitronectin." The International Journal of Biochemistry & Cell Biology **31**(5): 539-544.

Schwartz, M. A. (2001). "Integrin signaling revisited." Trends in Cell Biology **11**(12): 466-470.

Schwarzbauer, J. E. and J. L. Sechler (1999). "Fibronectin fibrillogenesis: a paradigm for extracellular matrix assembly." Current Opinion in Cell Biology **11**(5): 622-627.

Schwarzbauer, J. E., J. W. Tarnkun, et al. (1983). "Three different fibronectin mRNAs arise by alternative splicing within the coding region." Cell **35**: 421-431.

Sechler, J. L., S. A. Corbett, et al. (1997). "Modulatory Roles for Integrin Activation and the Synergy Site of Fibronectin during Matrix Assembly." Mol. Biol. Cell **8**(12): 2563-2573.

Sechler, J. L., A. M. Cumiskey, et al. (2000). "A novel RGD-independent fibronectin assembly pathway initiated by alpha4beta1 integrin binding to the alternatively spliced V region." J Cell Sci **113**(8): 1491-1498.

Sechler, J. L., H. Rao, et al. (2001). "A novel fibronectin binding site required for fibronectin fibril growth during matrix assembly." J. Cell Biol. **154**(5): 1081-1088.

Sedele, M., S. Karaveli, et al. (2002). "Tenascin expression in normal, hyperplastic, and neoplastic endometrium." Int J Gynecol Pathol. **21**(2): 161-6.

Serini, G., M.-L. Bochaton-Piallat, et al. (1998). "The Fibronectin Domain ED-A Is Crucial for Myofibroblastic Phenotype Induction by Transforming Growth Factor-beta 1." J. Cell Biol. **142**(3): 873-881.

Seufferlein, T. and E. Rozengurt (1995). "Sphingosylphosphorylcholine Rapidly Induces Tyrosine Phosphorylation of p125FAK and Paxillin, Rearrangement of the Actin Cytoskeleton and Focal Contact Assembly." J. Biol. Chem. **270**(41): 24343-24351.

Sharma, A., Z. Rao, et al. (1997). "Specific Interactions between Human Integrin [alpha]v[beta]3and Chimeric Hepatitis B Virus Core Particles Bearing the Receptor-Binding Epitope of Foot-and-Mouth Disease Virus." Virology **239**(1): 150-157.

Shi, Y. and J. Massague (2003). "Mechanisms of TGF-[beta] Signaling from Cell Membrane to the Nucleus." Cell **113**(6): 685-700.

Shimao, Y., K. Nabeshima, et al. (1999). "Role of fibroblasts in HGF/SF-induced cohort migration of human colorectal carcinoma cells: Fibroblasts stimulate migration associated with increased fibronectin production via upregulated TGF-beta1." International Journal of Cancer **82**(3): 449-458.

Sieg, D. J., C. R. Hauck, et al. (2000). "FAK integrates growth-factor and integrin signals to promote cell migration." Nat Cell Biol **2**(5): 249-256.

Sieg, D. J., C. R. Hauck, et al. (1999). "Required role of focal adhesion kinase (FAK) for integrin-stimulated cell migration." J Cell Sci **112**(16): 2677-2691.

Simon, C., A. Frances, et al. (1994). "Interleukin-1 system in the materno-trophoblast unit in human implantation: immunohistochemical evidence for autocrine/paracrine function." J Clin Endocrinol Metab **78**(4): 847-854.

Simon, C., M. J. Gimeno, et al. (1997). "Embryonic Regulation of Integrins β3, α4, and α1 in Human Endometrial Epithelial Cells in Vitro." J Clin Endocrinol Metab **82**(8): 2607-2616.

Simon, C., J. C. Martin, et al. (2000). "Paracrine regulators of implantation." Best Practice & Research Clinical Obstetrics & Gynaecology **14**(5): 815-826.

Simón, C., C. Moreno, et al. (1998). "Cytokines and embryo implantation." Journal of Reproductive Immunology **39**(1-2): 117-131.

Simon, C., G. Piquette, et al. (1993). "Localization of interleukin-1 type I receptor and interleukin-1 beta in human endometrium throughout the menstrual cycle." J Clin Endocrinol Metab **77**(2): 549-555.

Singer, C. F., E. Marbaix, et al. (1999). "Local cytokines induce differential expression of matrix metalloproteinases but not their tissue inhibitors in human endometrial fibroblasts." European Journal of Biochemistry **259**(1-2): 40-45.

Smith, S. K. (1995). "Angiogenic growth factor expression in the uterus." Hum Reprod Update **1**(2): 162-172.

Somkuti, S. G., L. Yuan, et al. (1997). "Epidermal Growth Factor and Sex Steroids Dynamically Regulate a Marker of Endometrial Receptivity in Ishikawa Cells." J Clin Endocrinol Metab **82**(7): 2192-2197.

Spitzfaden, C., R. P. Grant, et al. (1997). "Module-module interactions in the cell binding region of fibronectin: stability, flexibility and specificity." Journal of Molecular Biology **265**(5): 565-579.

Stamm, S., S. Ben-Ari, et al. (2005). "Function of alternative splicing." Gene **344**: 1-20.

Staun-Ram, E. and E. Shalev (2005). "Human trophoblast function during the implantation process." Reproductive Biology and Endocrinology **3**(1): 56.

Stewart, C. L. and E. B. Cullinan (1997). "Preimplantation development of the mammalian embryo and its regulation by growth factors." Developmental Genetics **21**(1): 91-101.

Stewart, C. L., P. Kaspar, et al. (1992). "Blastocyst implantation depends on maternal expression of leukaemia inhibitory factor." Nature **359**: 76 - 79.

Sticht, H., A. R. Pickford, et al. (1998). "Solution structure of the glycosylated second type 2 module of fibronectin." Journal of Molecular Biology **276**(1): 177-187.

Sugino, N. (2007). "The Role of Oxygen Radical-mediated Signaling Pathways in Endometrial Function." Placenta **28**(Supplement 1): S133-S136.

Sutherland, A., P. Calarco, et al. (1988). "Expression and function of cell surface extracellular matrix receptors in mouse blastocyst attachment and outgrowth." J. Cell Biol. **106**(4): 1331-1348.

Sutherland, A. E., P. G. Calarco, et al. (1993). "Developmental regulation of integrin expression at the time of implantation in the mouse embryo." Development **119**(4): 1175-1186.

Suzuki, N., J. Zara, et al. (1998). "A cytoplasmic protein bystin, interacts with trophinin, tastin and cytokeratin." Proc Natl Acad Sci USA **95**: 5027 - 5032.

Swindle, C. S., K. T. Tran, et al. (2001). "Epidermal growth factor (EGF)-like repeats of human tenascin-C as ligands for EGF receptor." J. Cell Biol. **154**(2): 459-468.

Tabibzadeh, S., P. G. Satyaswaroop, et al. (1999). "Regulation of TNF-{alpha} mRNA expression in endometrial cells by TNF-{alpha} and by oestrogen withdrawal." Mol. Hum. Reprod. **5**(12): 1141-1149.

Tabibzadeh, S. and X. Z. Sun (1992). "Cytokine expression in human endometrium throughout the menstrual cycle." Hum. Reprod. **7**(9): 1214-1221.

Tabibzadeh, S., E. Zupi, et al. (1995). "Physiology: Site and menstrual cycle-dependent expression of proteins of the tumour necrosis factor (TNF) receptor family, and BCL-2 oncoprotein and phase-specific production of TNF{alpha} in human endometrium." Hum. Reprod. **10**(2): 277-286.

Taga, T. (1996). "gp130, a Shared Signal Transducing Receptor Component for Hematopoietic and Neuropoietic Cytokines." Journal of Neurochemistry **67**(1): 1-10.

Taguchi, M., T. Kubota, et al. (1999). "Immunohistochemical localization of tenascin and ki-67 nuclear antigen in human endometrium throughout the normal menstrual cycle." J. Med Dent Sci. **46**(1): 7-12.

Taipale, J. and J. Keski-Oja (1997). "Growth factors in the extracellular matrix." FASEB J. **11**(1): 51-59.

Tan, O., T. Ornek, et al. "Tenascin is highly expressed in endometriosis and its expression is upregulated by estrogen." Fertility and Sterility **In Press, Corrected Proof**.

Tanaka, T., T. Sakamoto, et al. (2001). "Interleukin-11 enhances cell survival of decidualized normal human endometrial stromal cells." Gynecological Endocrinology **15**(4): 272 - 278.

Tang, B., S. Guller, et al. (1993). "Mechanisms involved in the decidualization of human endometrial stromal cells." Acta Eur Fertil **24**(221-223).

Taylor, H. S., A. Arici, et al. (1998). "HOXA10 is Expressed in Response to Sex Steroids at the Time of Implantation in the Human Endometrium." J. Clin. Invest. **101**(7): 1379-1384.

Telgmann, R. and B. Gellersen (1998). "Marker genes of decidualization: activation of the decidual prolactin gene." Hum Reprod Update **4**(5): 472-479.

Thie, M. and H. Denker (2002). "In vitro Studies on Endometrial Adhesiveness for Trophoblast: Cellular Dynamics in Uterine Epithelial Cells." Cells Tissues Organs **172**(3): 237-252.

Timpl, R. (1996). "Macromolecular organization of basement membranes." Current Opinion in Cell Biology **8**(5): 618-624.

Troche, V., D. M. O'Connon, et al. (1991). "Measurement of human epidermal growth factor receptor in the endometrium during the menstrual cycle." American Journal of Obstetrics and Gynecology **165**: 1499-503.

Tsai, M. and B. W. O'Malley (1994). "Molecular Mechanisms of Action of Steroid/Thyroid Receptor Superfamily Members." Annual Review of Biochemistry **63**(1): 451-486.

Turner, C. E. (2000). "Paxillin and focal adhesion signalling." Nat Cell Biol **2**(12): E231-E236.

Turpeenniemi, T., R. F. Feinberg, et al. (1995). "Extracellular matrix interactions in early human embryos: implications for normal implantation events." Fertil. Steril. **64**(1): 132-8.

Usadi, R. S., M. J. Murray, et al. (2003). "Temporal and morphologic characteristics of pinopod expression across the secretory phase of the endometrial cycle in normally cycling women with proven fertility." Fertil Steril **79**: 970 - 974.

van der Walle, C. F., H. Altroff, et al. (2002). "Novel mutant human fibronectin FIII9-10 domain pair with increased conformational stability and biological activity." Protein Eng. **15**(12): 1021-1024.

Vassalli, J. D., A. P. Sappino, et al. (1991). "The plasminogen activator/plasmin system." J Clin Invest. **88**(4): 1067-1072.

Vogiagis, D., M. M. Marsh, et al. (1996). "Leukaemia inhibitory factor in human endometrium throughout the menstrual cycle." J Endocrinol **148**(1): 95-102.

Vollmer, G., M. I. Tan, et al. (1997). "Expression of tenascin-C by human endometrial adenocarcinoma and stromal cells: heterogeneity of splice variants and induction by TGF-beta." Biochem Cell Biol. **75**(6): 759-69.

Wang, J., L. Mayernik, et al. (2002). "Integrin Signaling Regulates Blastocyst Adhesion to Fibronectin at Implantation: Intracellular Calcium Transients and Vesicle Trafficking in Primary Trophoblast Cells." Developmental Biology **245**(2): 270-279.

Wegener, K. L., A. W. Partridge, et al. (2007). "Structural Basis of Integrin Activation by Talin." Cell **128**(1): 171-182.

Wijelath, E. S., S. Rahman, et al. (2006). "Heparin-II Domain of Fibronectin Is a Vascular Endothelial Growth Factor-Binding Domain: Enhancement of VEGF Biological Activity by a Singular Growth Factor/Matrix Protein Synergism." Circ Res **99**(8): 853-860.

Williams, M. J., I. Phan, et al. (1994). "Solution Structure of a Pair of Fibronectin Type 1 Modules with Fibrin Binding Activity." Journal of Molecular Biology **235**(4): 1302-1311.

Woessner, J. F., Jr. (1991). "Matrix metalloproteinases and their inhibitors in connective tissue remodeling." FASEB J. **5**(8): 2145-2154.

Wu, C., P. E. Hughes, et al. (1996). "Identification of a new biological function for the integrin alpha v beta 3: initiation of fibronectin matrix assembly." Cell Adhesion and Communication **4**(3): 149-58.

Wynn, R. M. (1969). "Noncellular components of the placenta." Am J Obstet Gynaecol. **103**(5): 723-39.

Wynn, R. M. (1974). "Ultrastructural development of the human decidua." Am J Obstet Gynaecol. **118**(5): 652-70.

Xiao, T., J. Takagi, et al. (2004). "Structural basis for allostery in integrins and binding to fibrinogen-mimetic therapeutics." Nature **432**(7013): 59-67.

Xu, P., Y.-l. Wang, et al. (2001). "Effects of Matrix Proteins on the Expression of Matrix Metalloproteinase-2, -9, and -14 and Tissue Inhibitors of Metalloproteinases in Human Cytotrophoblast Cells During the First Trimester." Biol Reprod **65**(1): 240-246.

Yamada, K. M. (1989). "Fibronectins: structure, functions and receptors." Current Opinion in Cell Biology **1**(5): 956-963.

Yamada, K. M., D. H. Schlesinger, et al. (1977). "Characterization of a major fibroblast cell surface glycoprotein." Biochemistry **16**(25): 5552-5559.

Yelian, F. D., Y. Yang, et al. (1995). "Molecular interactions between fibronectin and integrins during mouse blastocyst outgrowth." Molecular Reproduction and Development **41**(4): 435-448.

Yokosaki, Y., N. Matsuura, et al. (1998). "Identification of the Ligand Binding Site for the Integrin alpha 9beta 1 in the Third Fibronectin Type III Repeat of Tenascin-C." J. Biol. Chem. **273**(19): 11423-11428.

Yoo, H., D. Barlow, et al. (1997). "Temporal and spatial regulation of expression of heparin-binding epidermal growth factor-like growth factor in the human endometrium: A possible role in blastocyst implantation." Developmental Genetics **21**(1): 102-108.

Yoshino, O., Y. Osuga, et al. (2003). "Endometrial Stromal Cells Undergoing Decidualization Down-Regulate Their Properties to Produce Proinflammatory Cytokines in Response to Interleukin-1β via Reduced p38 Mitogen-Activated Protein Kinase Phosphorylation." J Clin Endocrinol Metab **88**(5): 2236-2241.

Young, B. A., Y. Taooka, et al. (2001). "The Cytoplasmic Domain of the Integrin alpha 9 Subunit Requires the Adaptor Protein Paxillin to Inhibit Cell Spreading but Promotes Cell Migration in a Paxillin-independent Manner." Mol. Biol. Cell **12**(10): 3214-3225.

Zachary, I. and E. Rozengurt (1992). "Focal adhesion kinase (p125FAK): A point of convergence in the action of neuropeptides, integrins, and oncogenes." Cell **71**(6): 891-894.

Zardi, L., B. Carnemolla, et al. (1987). "Transformed human cells produce a new fibronectin isoform by preferential alternative splicing of a previously unobserved exon." EMBO J. **6**(8): 2337-2342.

Zhu, J., B. Boylan, et al. (2007). "Tests of the Extension and Deadbolt Models of Integrin Activation." J. Biol. Chem. **282**(16): 11914-11920.

Zygmunt, M., F. Herr, et al. (2003). "Angiogenesis and vasculogenesis in pregnancy." Eur Journal of Obs & Gynecology and Reproductive Biology **110**: S10-S18

Appendix

Appendix I (a, b) Immunofluorescence staining for CNI produced by ESCs at day 0, day 6 and day 6 with cAMP, from different fields of view of one ESC cell number (890S) in the same experiment. Control sections treated with MoIgG instead of primary antibody are also shown. CNI is in green and nuclei in blue, scale bars are 50 μm.

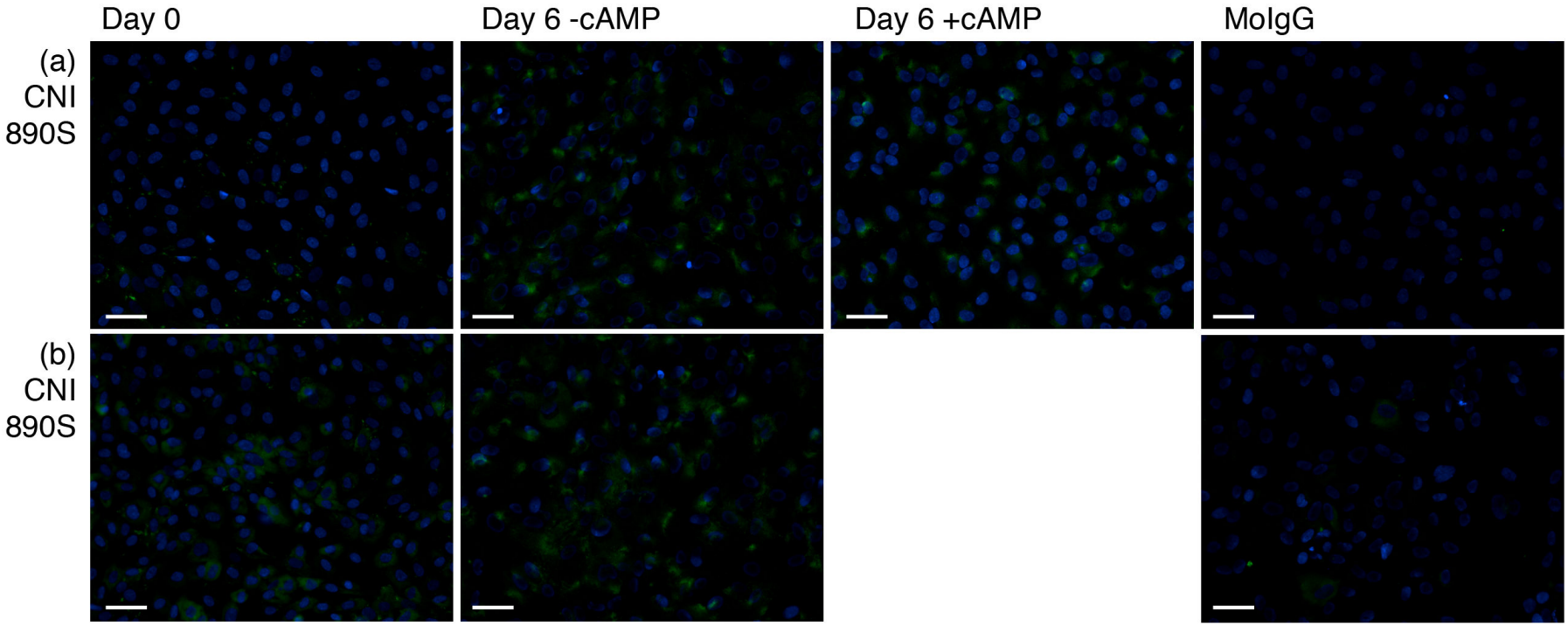

Appendix I (c, d) Immunofluorescence staining for CNI produced by ESCs at day 0, day 6 and day 6 with cAMP, from different fields of view of one ESC cell number (890S) in the same experiment. Control sections treated with MoIgG instead of primary antibody are also shown. CNI is in green and nuclei in blue, scale bars are 25 μm.

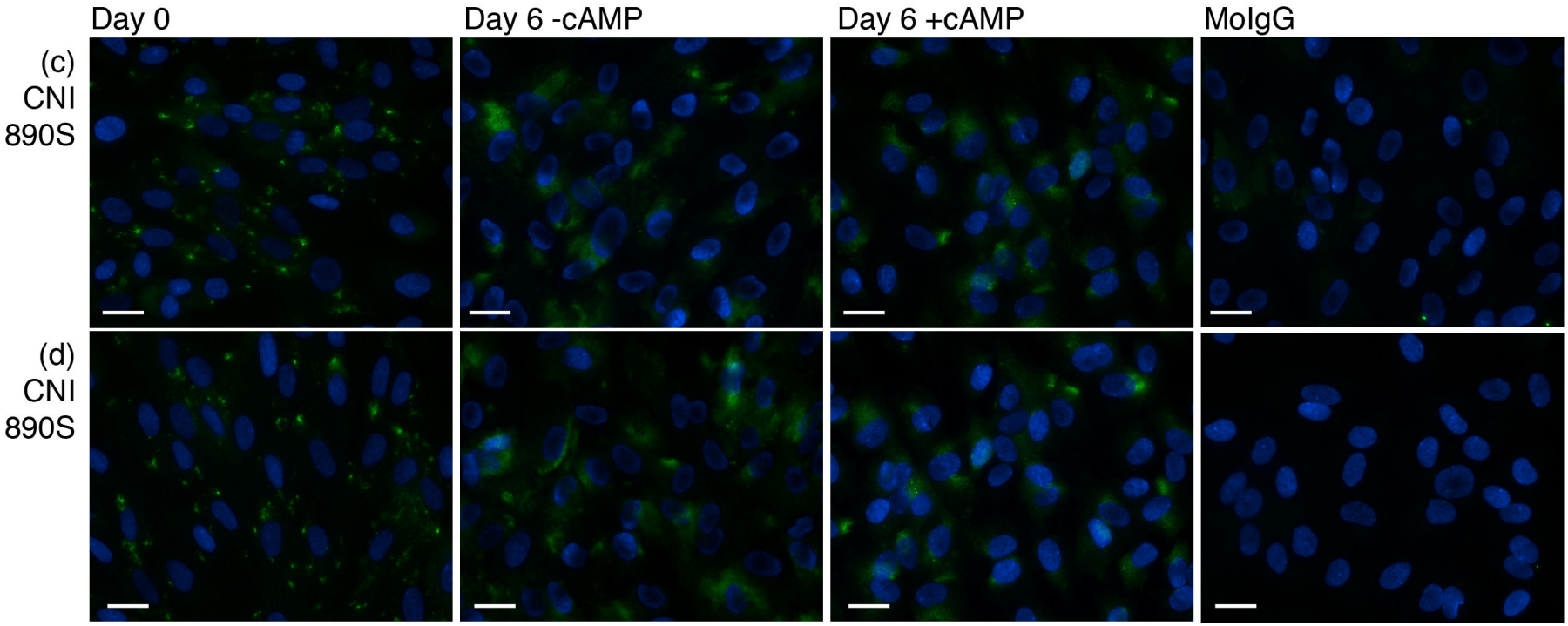

Appendix I (e, f) Immunofluorescence staining for CNI produced by ESCs at day 0, day 6 and day 6 with cAMP, from different fields of view of one ESC cell number (700S) in the same experiment. Control sections treated with MoIgG instead of primary antibody are also shown. CNI is in green and nuclei in blue, scale bars are 50 μm.

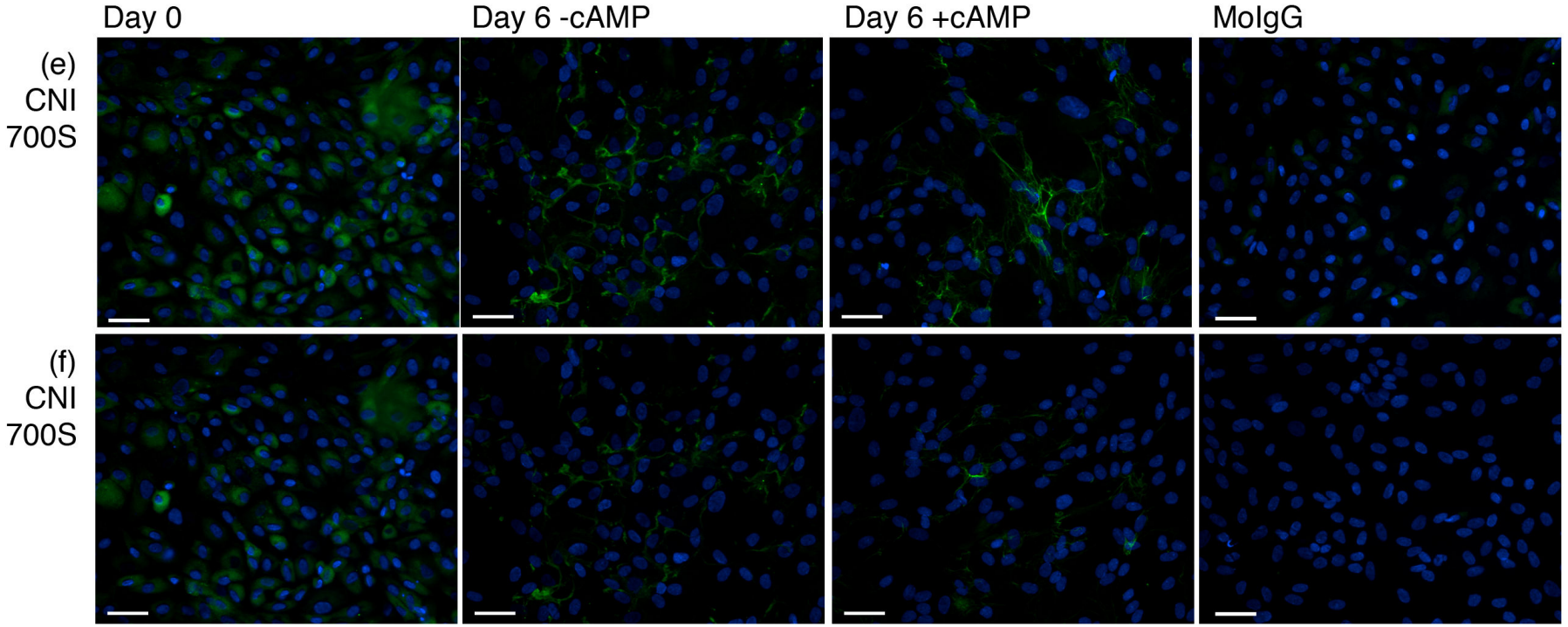

Appendix I (g, h) Immunofluorescence staining for CNI produced by ESCs at day 6 and day 6 with cAMP, from different fields of view of one ESC cell number (700S) in the same experiment. Control sections treated with MoIgG instead of primary antibody are also shown. CNI is in green and nuclei in blue, scale bars are 25 μm.

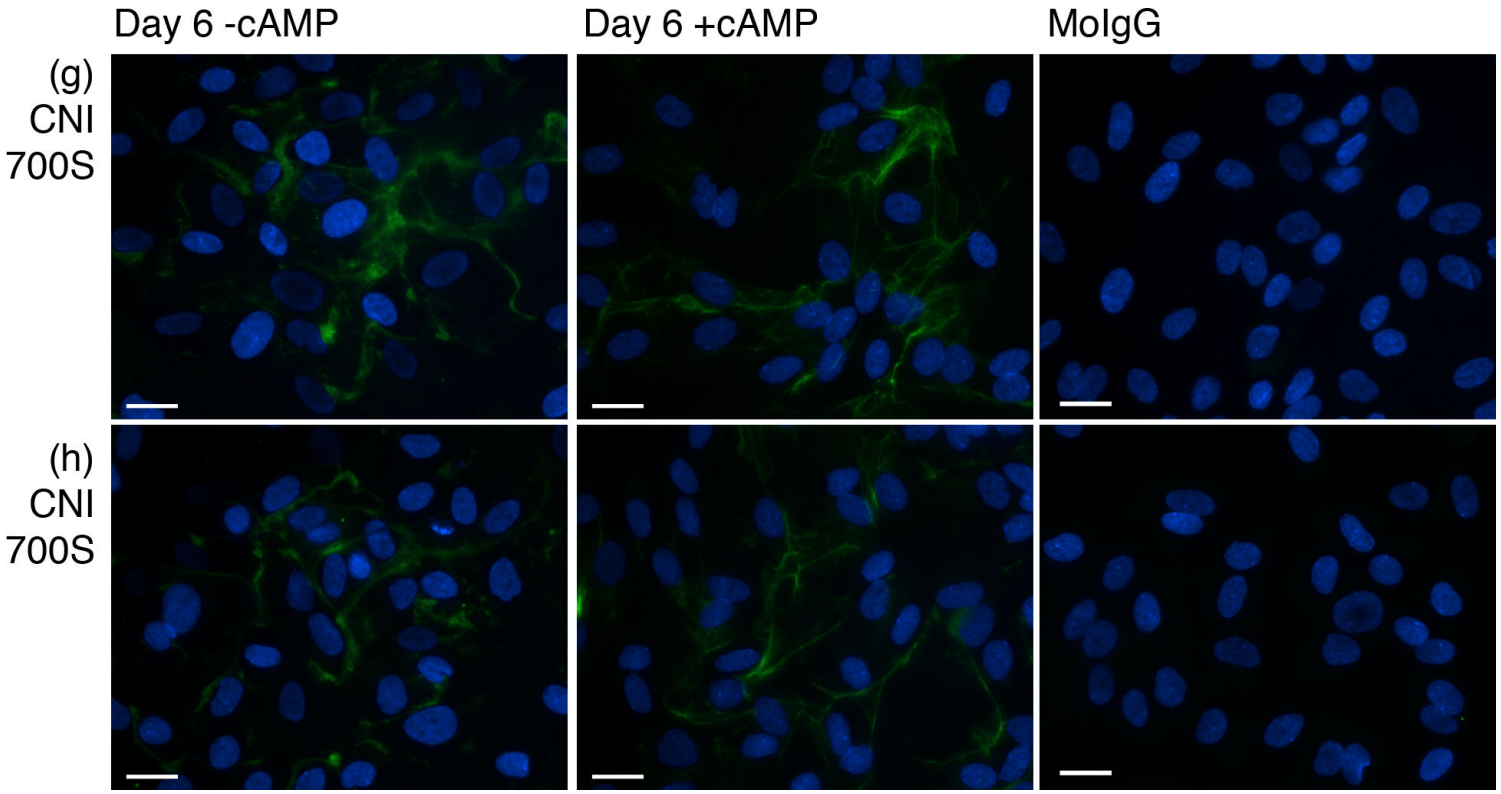

Appendix I (i, j) Immunofluorescence staining for CNI produced by ESCs at day 0, day 6 and day 6 with cAMP, from different fields of view of one ESC cell number (862S) in the same experiment. Control sections treated with MoIgG instead of primary antibody are also shown. CNI is in green and nuclei in blue, scale bars are (i) 50 μm and (j) 25 μm.

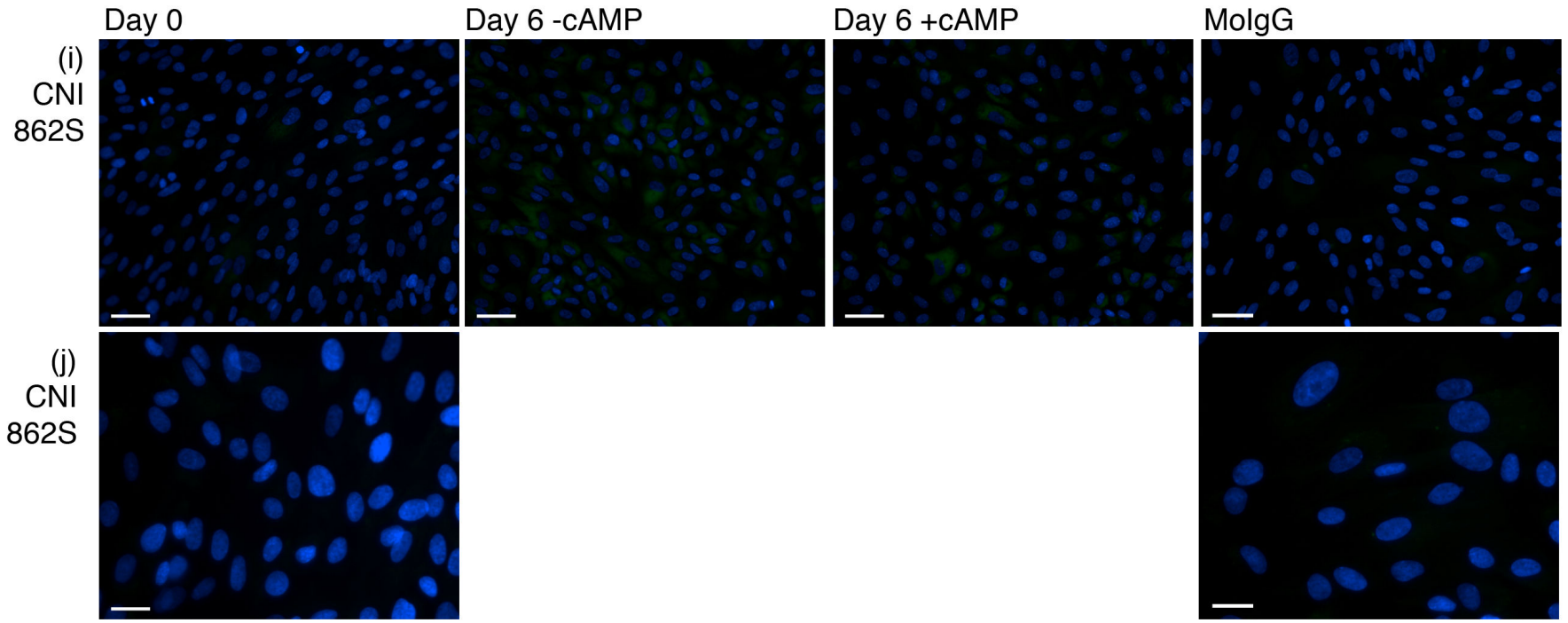

Appendix II (a,b) Immunofluorescence staining for CNIV produced by ESCs at day 0, day 6 and day 6 with cAMP, from different fields of view of one ESC cell number (862S) in the same experiment. Control sections treated with MoIgG instead of primary antibody are also shown. CNIV is in green and nuclei in blue, scale bars are 50 μm.

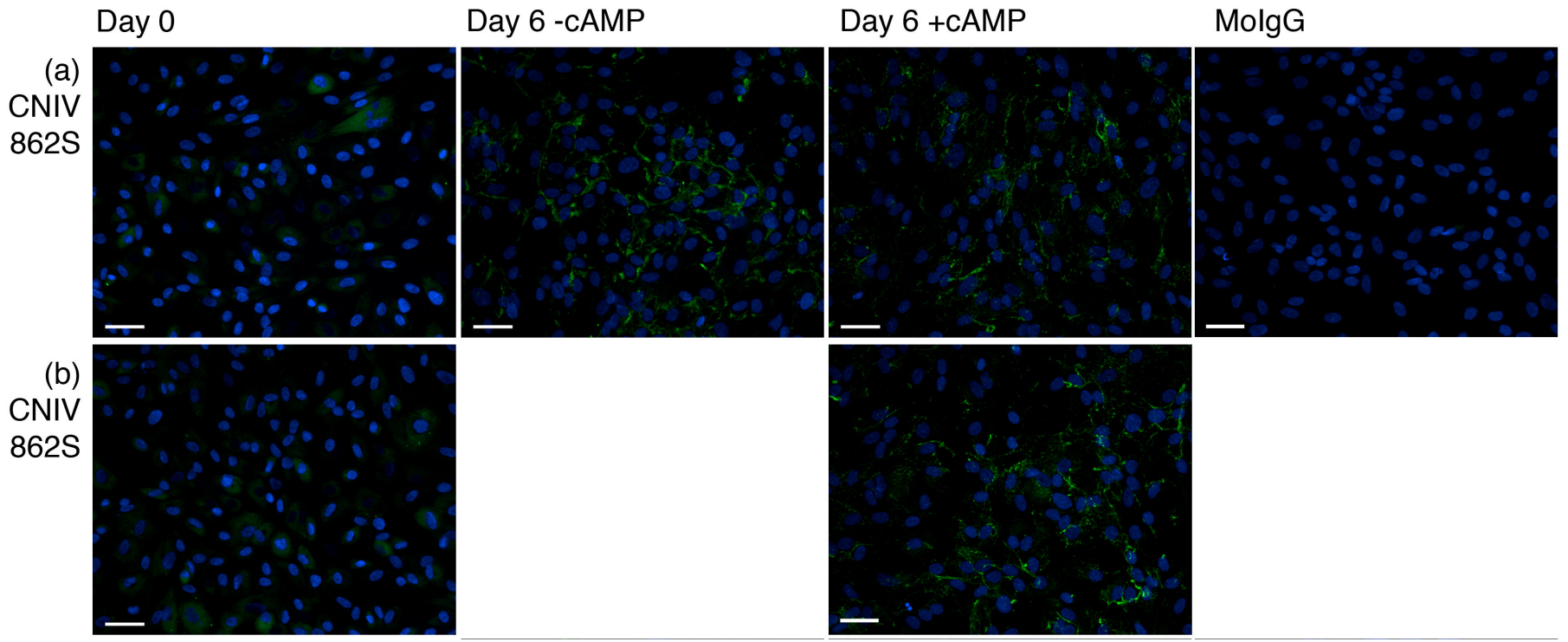

Appendix II (c, d) Immunofluorescence staining for CNIV produced by ESCs at day 6 and day 6 with cAMP, from different fields of view of one ESC cell number (862S) in the same experiment. Control sections treated with MoIgG instead of primary antibody are also shown. CNIV is in green and nuclei in blue, scale bars are 25 μm.

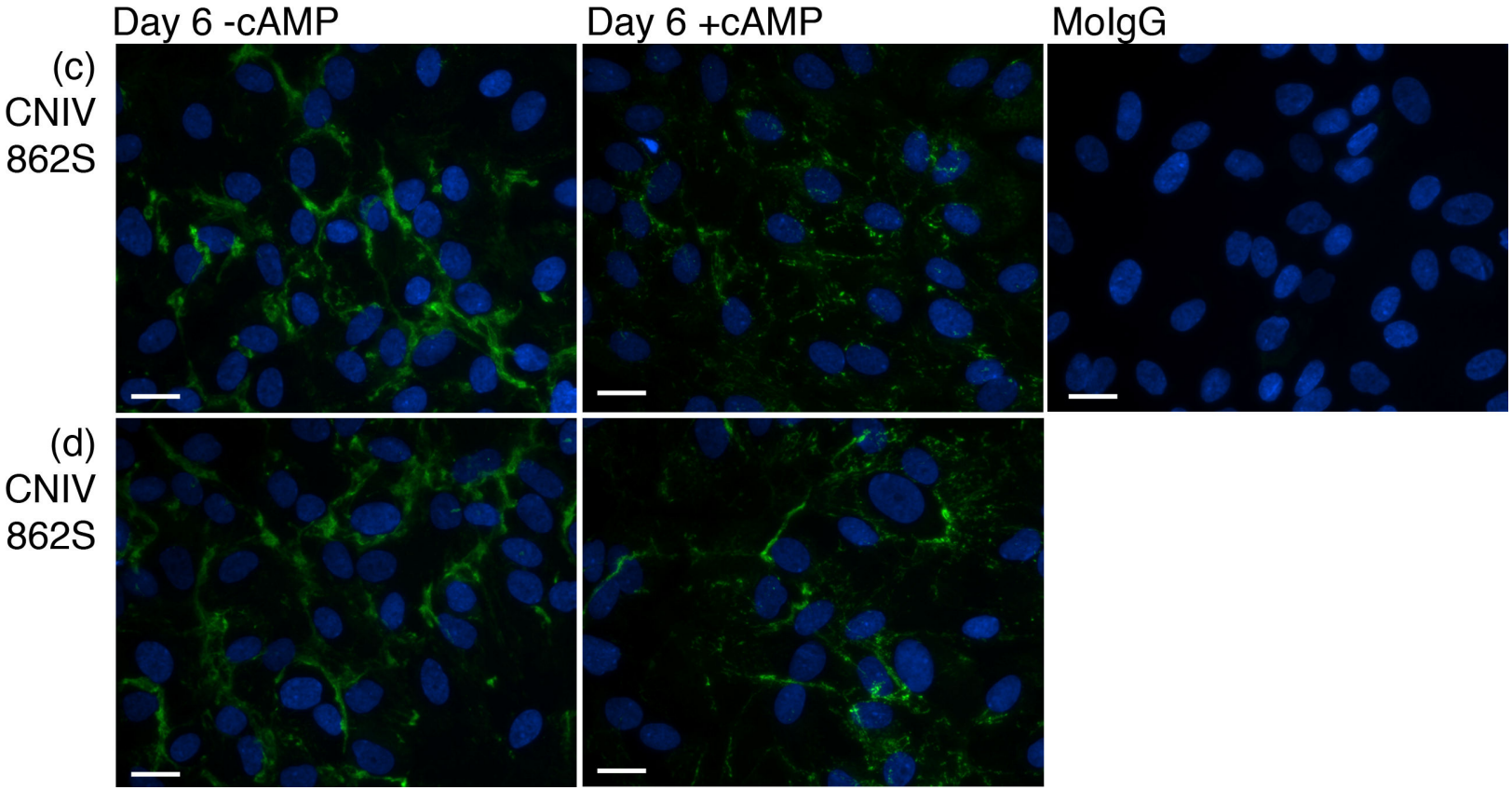

Appendix II (e, f) Immunofluorescence staining for CNIV produced by ESCs at day 0, day 6 and day 6 with cAMP, from different fields of view of one ESC cell number (890S) in the same experiment. Control sections treated with MoIgG instead of primary antibody are also shown. CNIV is in green and nuclei in blue, scale bars are 50 μm.

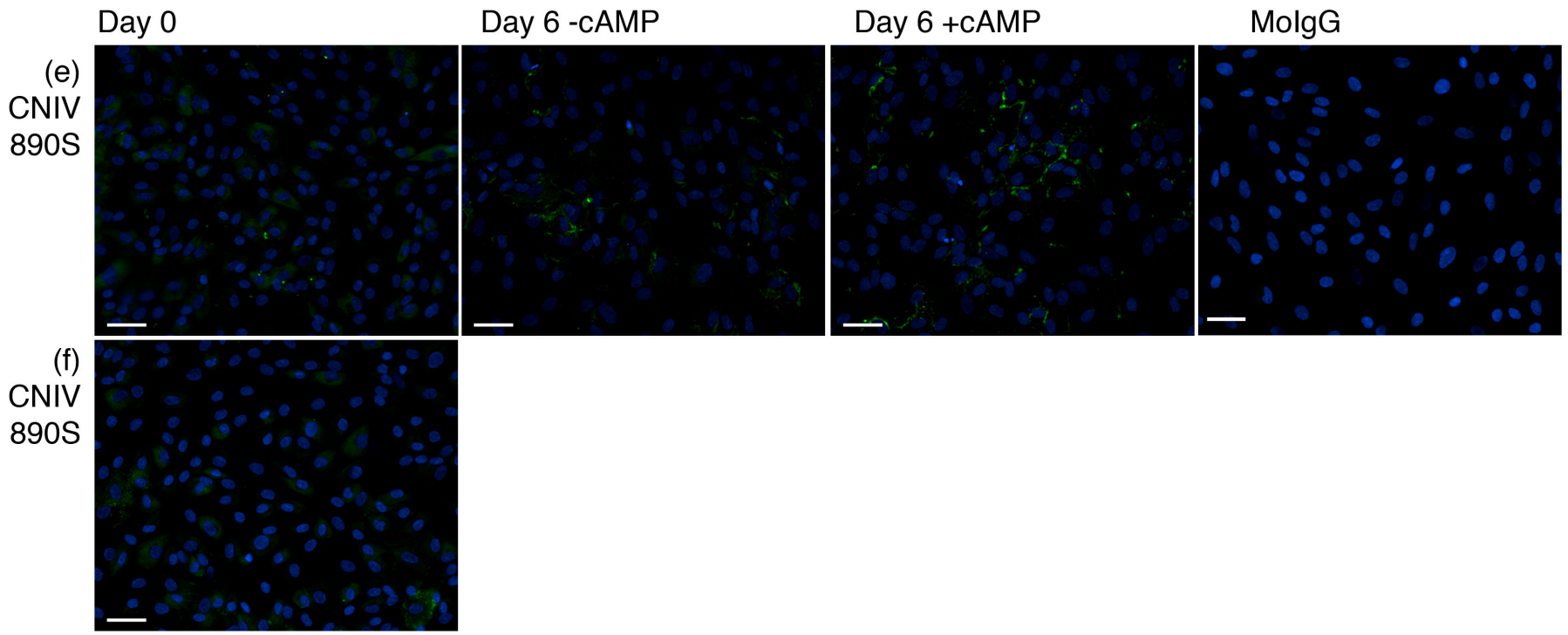

Appendix II (g, h) Immunofluorescence staining for CNIV produced by ESCs at day 0, day 6 and day 6 with cAMP, from different fields of view of one ESC cell number (890S) in the same experiment. Control sections treated with MoIgG instead of primary antibody are also shown. CNIV is in green and nuclei in blue, scale bars are 25 μm.

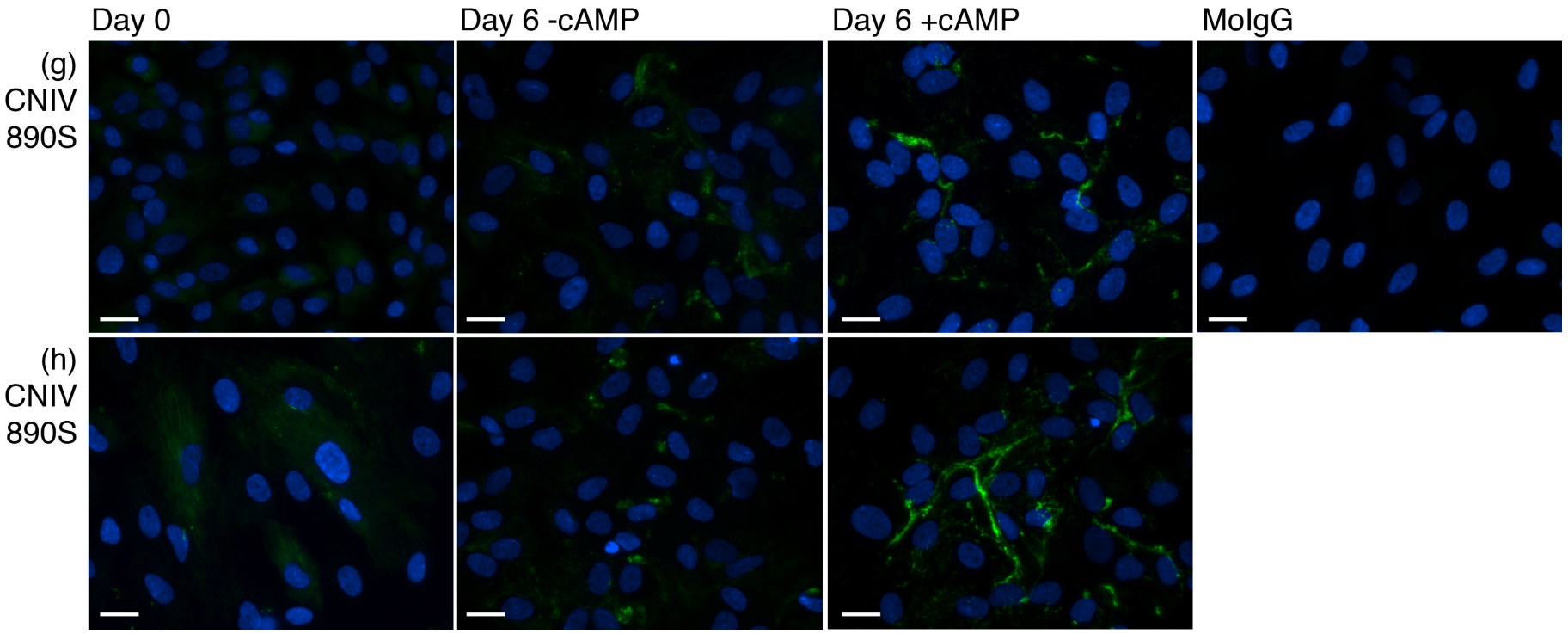

Appendix II (i-k) Immunofluorescence staining for CNIV produced by ESCs at day 0, day 6 and day 6 with cAMP, from different fields of view of one ESC cell number (700S) in the same experiment. Control sections treated with MoIgG instead of primary antibody are also shown. CNIV is in green and nuclei in blue, scale bars are (i, j) 50 μm and (k) 25 μm.

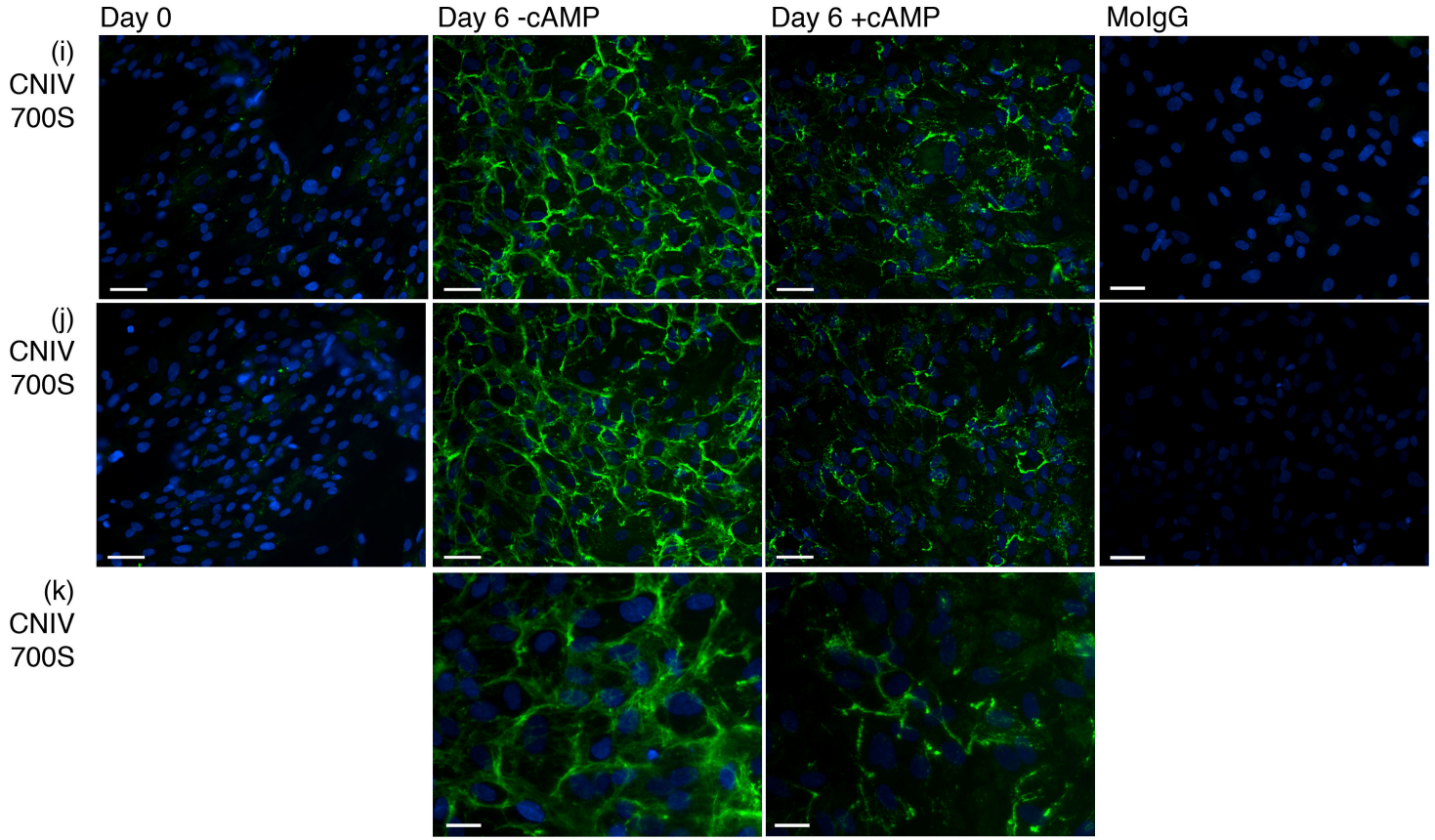

Appendix III (a, b) Immunofluorescence staining for LN produced by ESCs at day 0, day 6 and day 6 with cAMP, from different fields of view of one ESC cell number (890S) in the same experiment. Control sections treated with MoIgG instead of primary antibody are also shown. LN is in green and nuclei in blue, scale bars are 50 μm.

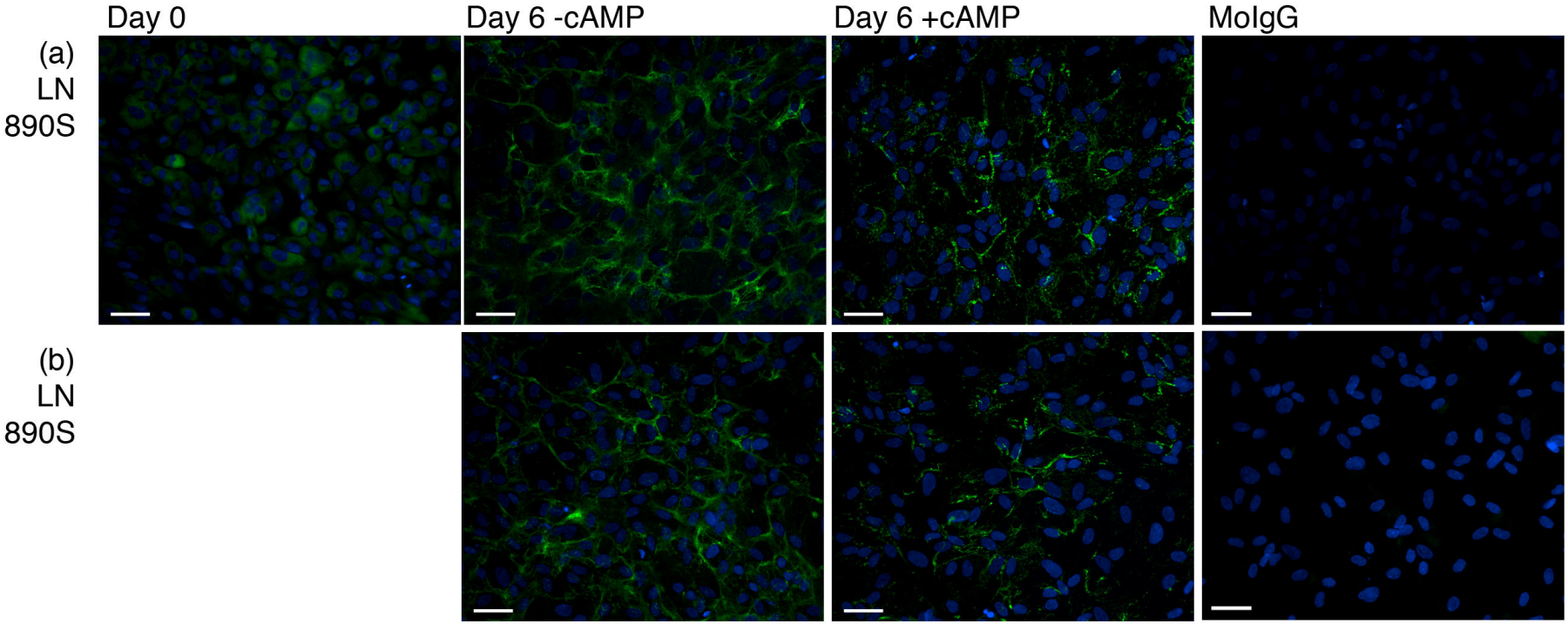

Appendix III (c, d) Immunofluorescence staining for LN produced by ESCs at day 6 and day 6 with cAMP, from different fields of view of one ESC cell number (890S) in the same experiment. Control sections treated with MoIgG instead of primary antibody are also shown. LN is in green and nuclei in blue, scale bars are (c) 50 μm and (d) 25 μm.

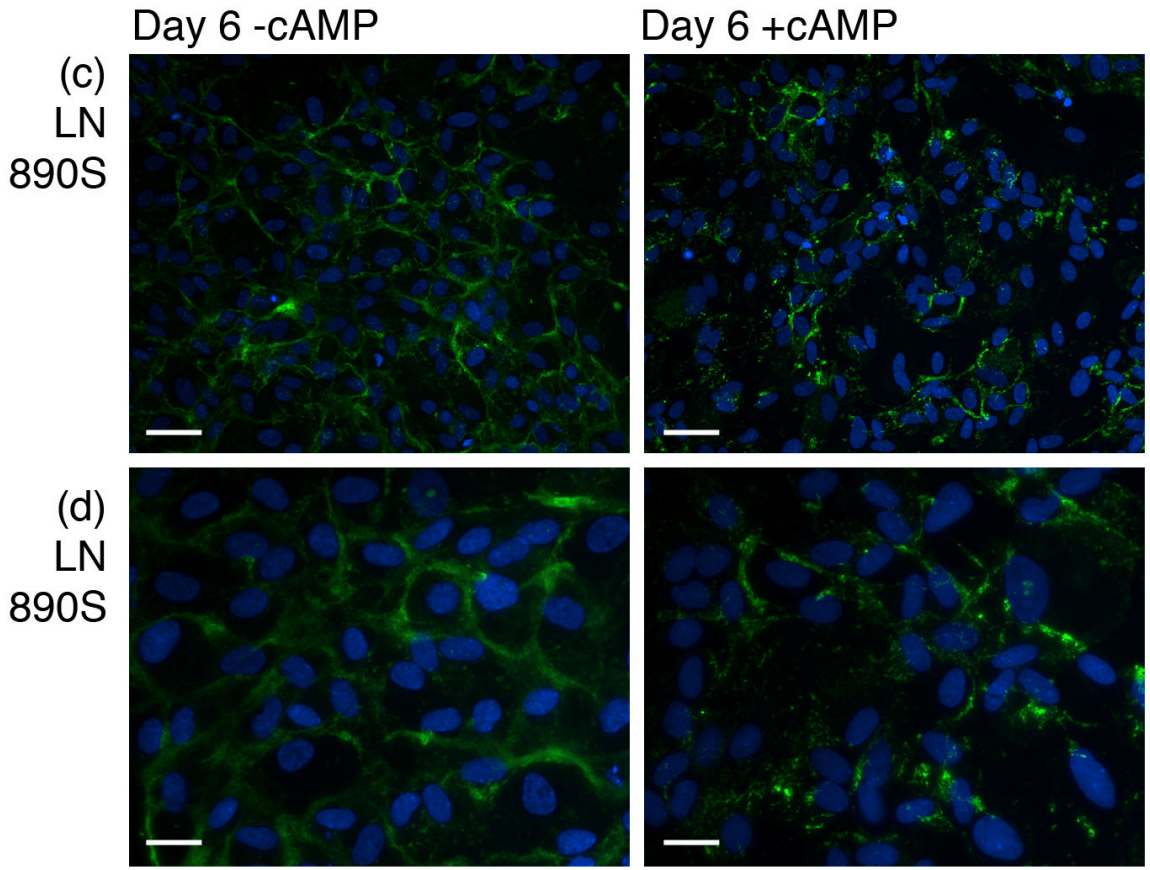

Appendix III (e, f) Immunofluorescence staining for LN produced by ESCs at day 0, day 6 and day 6 with cAMP, from different fields of view of one ESC cell number (629S) in the same experiment. Control sections treated with MoIgG instead of primary antibody are also shown. LN is in green and nuclei in blue, scale bars are 50 μm.

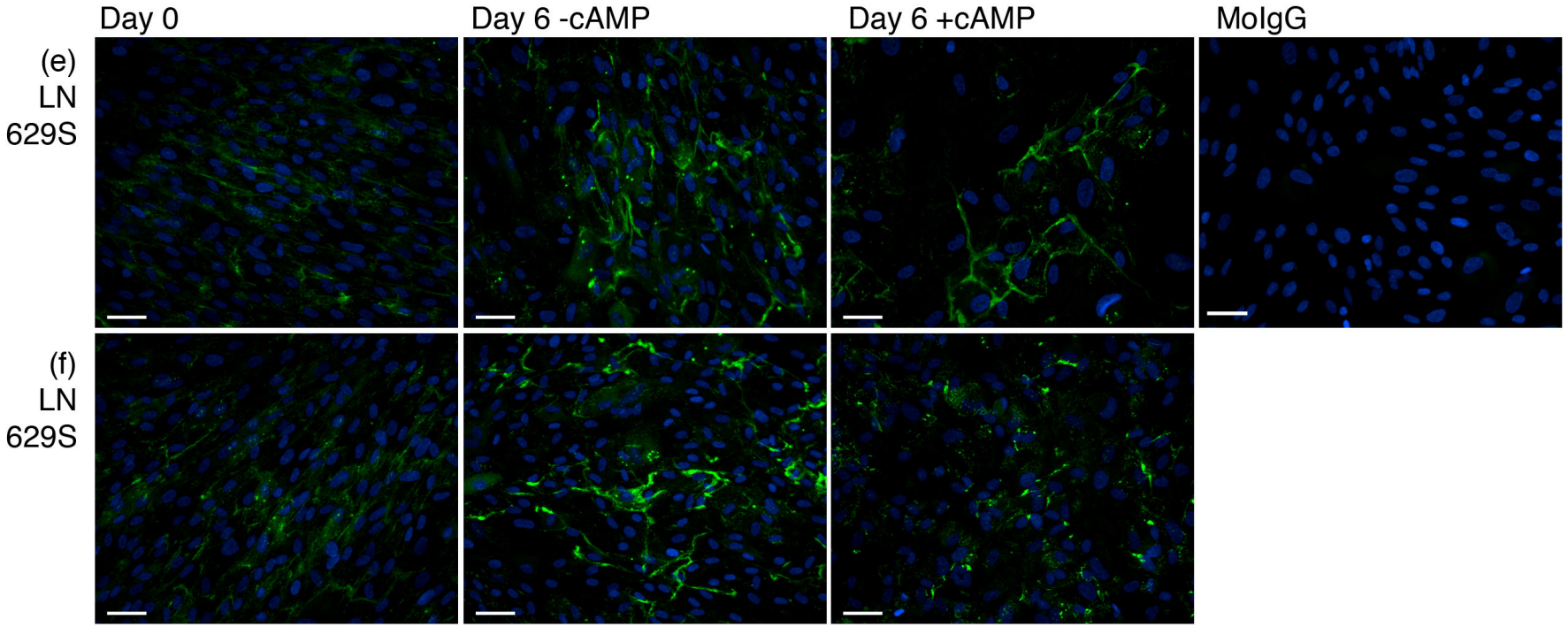

Appendix III (g, h) Immunofluorescence staining for LN produced by ESCs at day 6 and day 6 with cAMP, from different fields of view of one ESC cell number (629) in the same experiment. Control sections treated with MoIgG instead of primary antibody are also shown. LN is in green and nuclei in blue, scale bars are 25 μm.

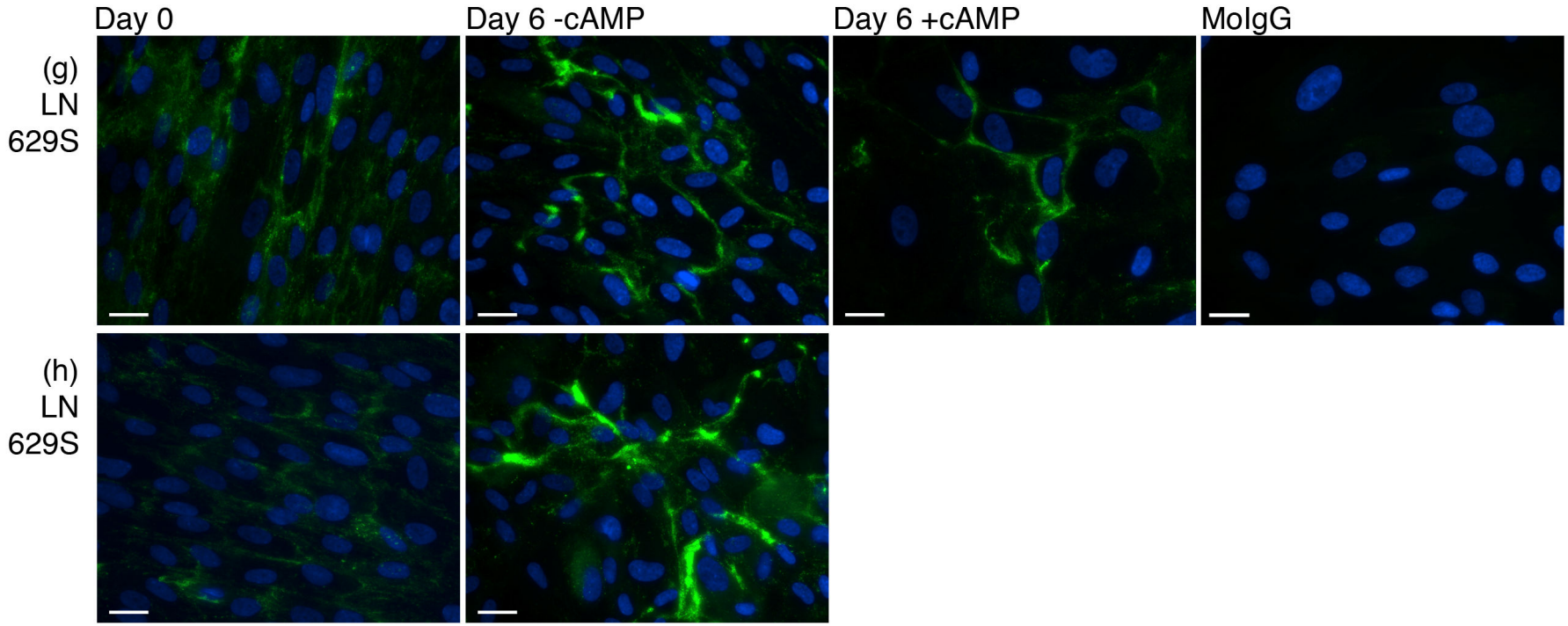

Appendix III (i, j) Immunofluorescence staining for LN produced by ESCs at day 6 and day 6 with cAMP, from different fields of view of one ESC cell number (826S) in the same experiment. Control sections treated with MoIgG instead of primary antibody are also shown. LN is in green and nuclei in blue, scale bars are 50 μm.

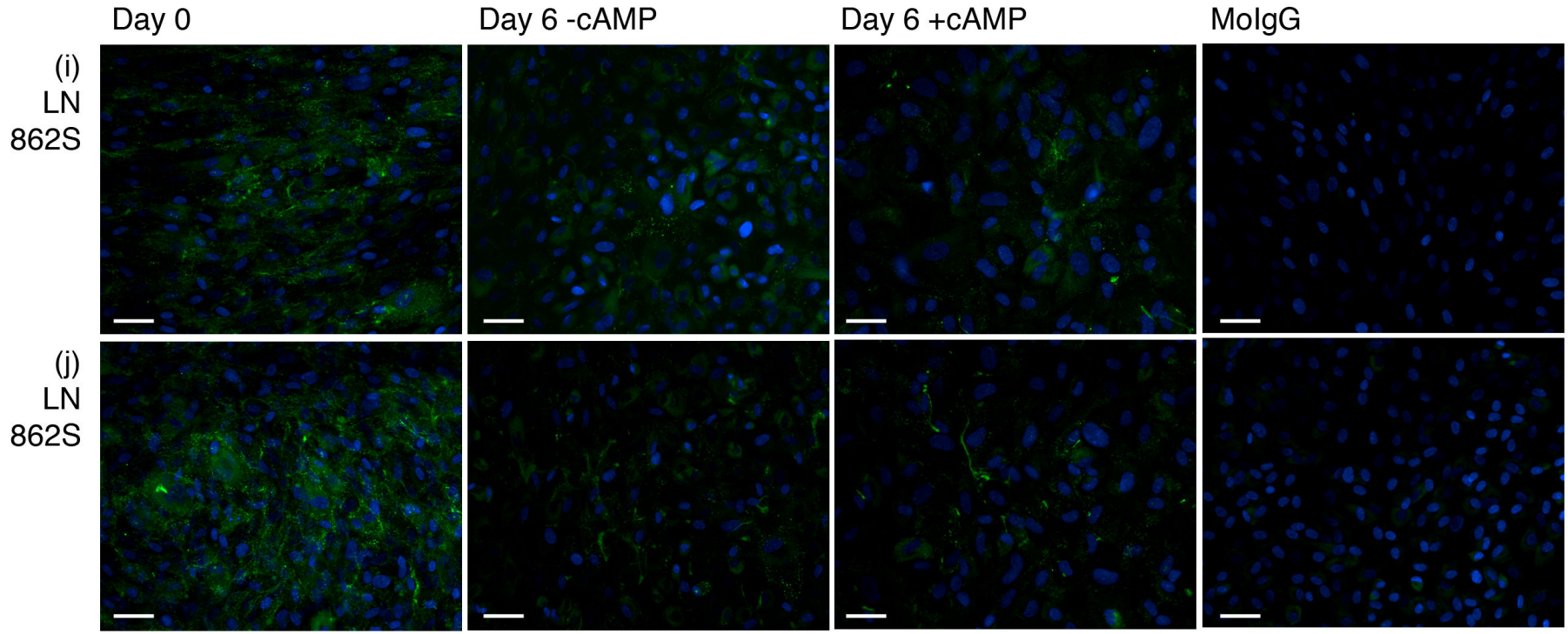

Appendix IV (a, b) Immunofluorescence staining for VN produced by ESCs (700S) at day 0, day 6 and day 6 with cAMP, using the anti-VN clone BV2, control sections were treated with MoIgG instead of primary antibody. VN is in green and nuclei in blue, scale bars are 50 μm.

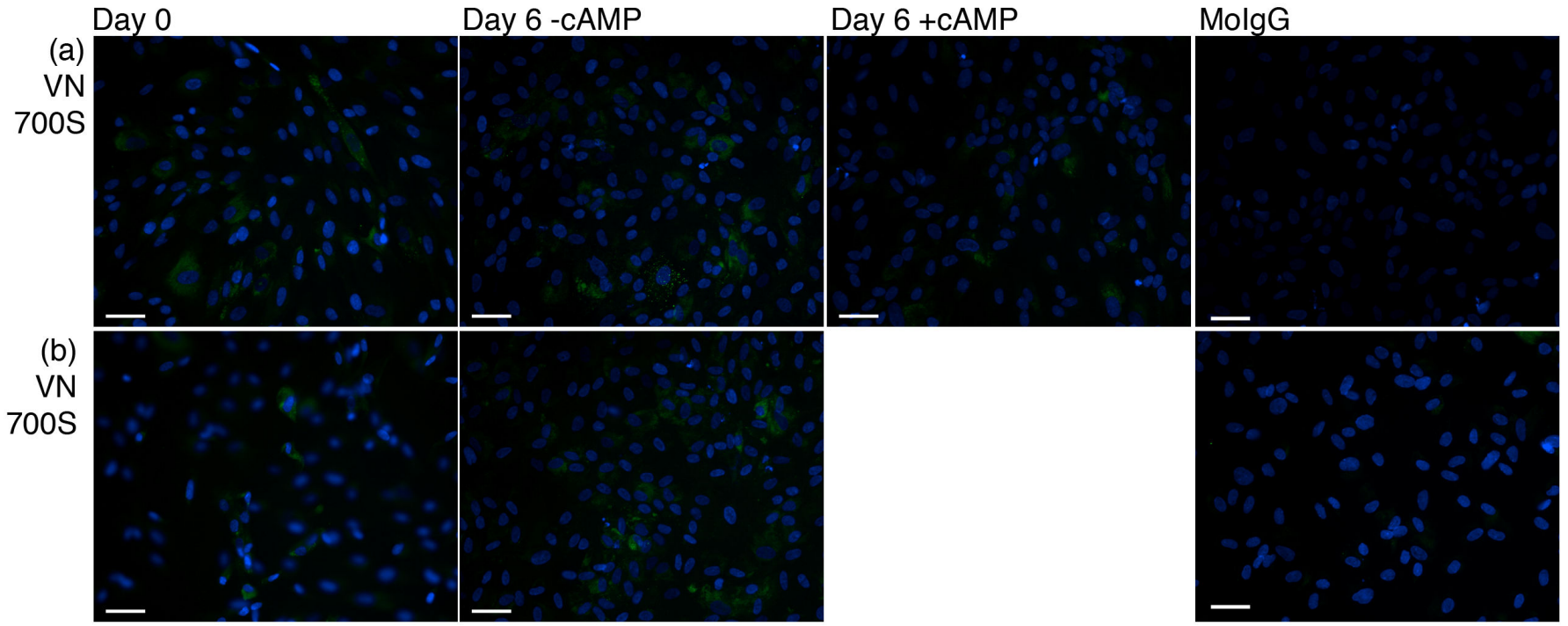

Appendix IV (c, d) Immunofluorescence staining for VN produced by ESCs (890S) at day 0, day 6 and day 6 with cAMP, using the anti-VN clone BV2, control sections were treated with MoIgG instead of primary antibody. VN is in green and nuclei in blue, scale bars are 50 μm.

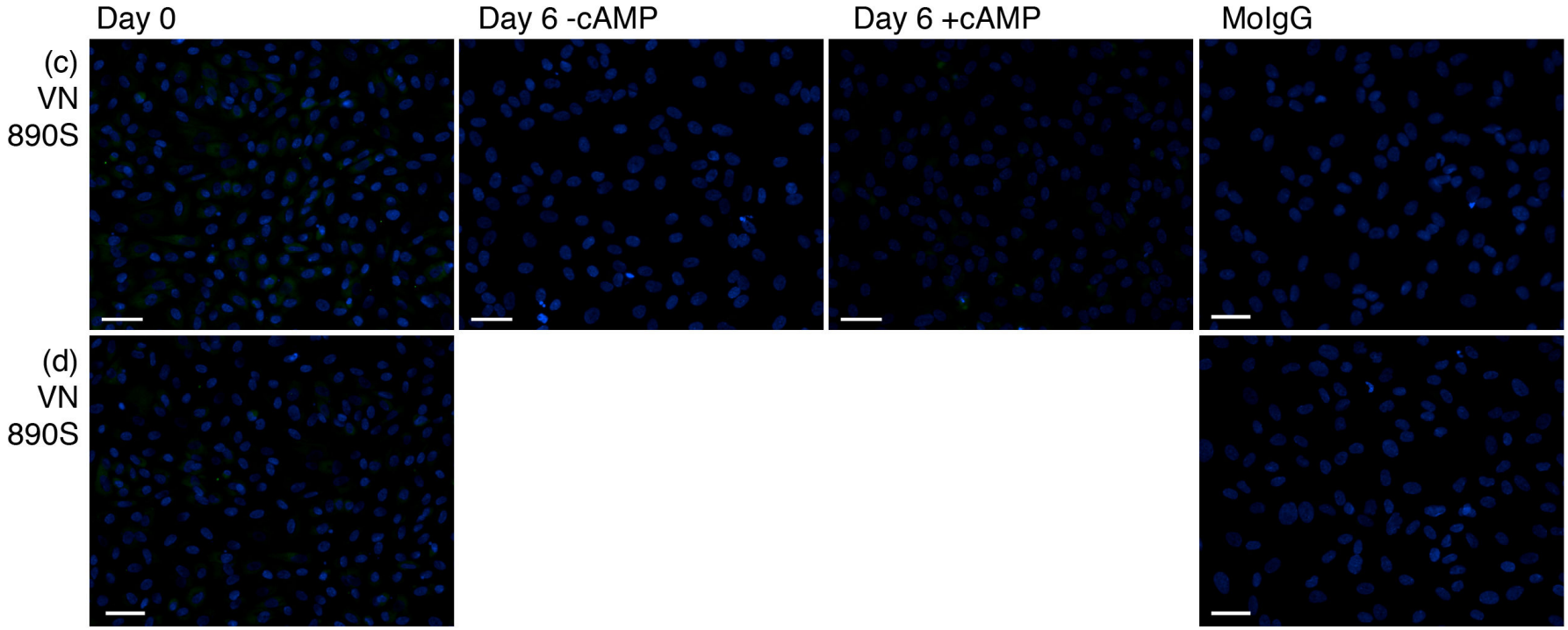

Appendix IV (e, f) Immunofluorescence staining for VN produced by ESCs (890S) at day 0, day 6 and day 6 with cAMP, using the anti-VN clone BV2, control sections were treated with MoIgG instead of primary antibody. VN is in green and nuclei in blue, scale bars are 25 μm.

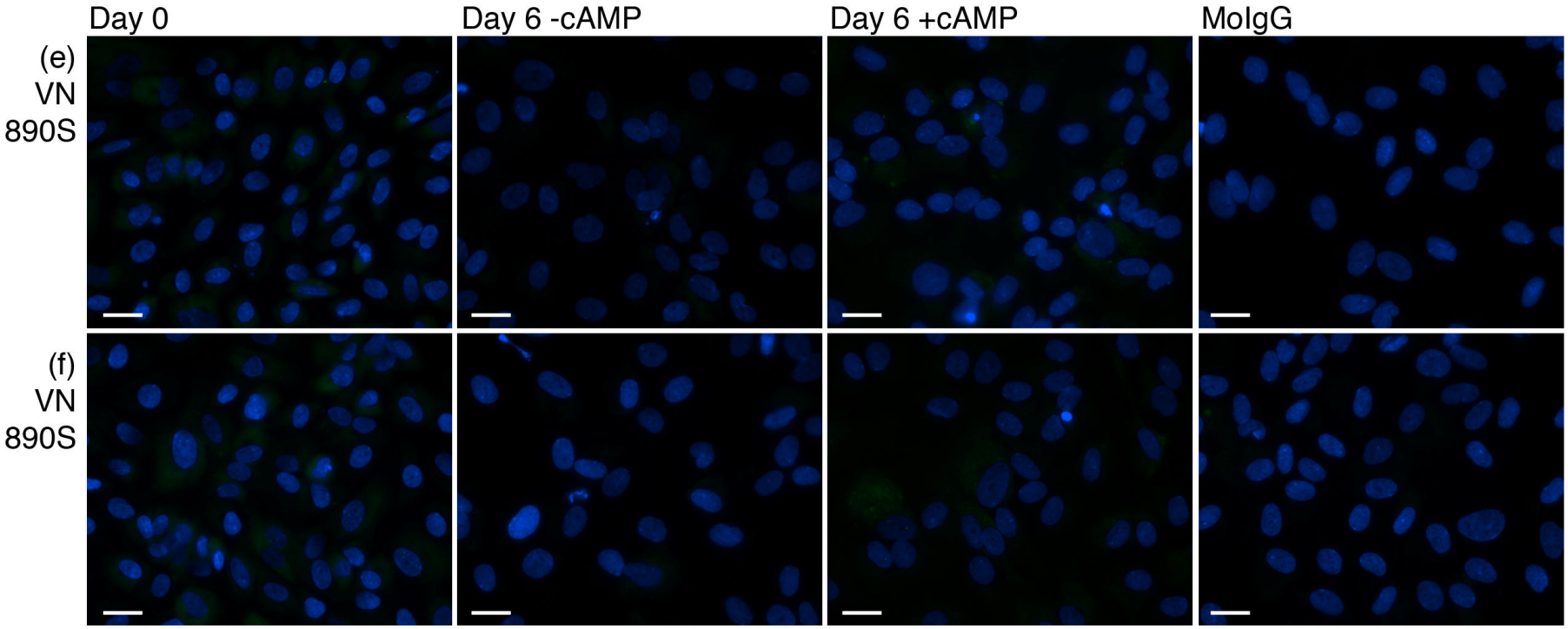

Appendix IV (g, h, i) Immunofluorescence staining for VN produced by ESCs (890S) at day 0, day 6 and day 6 with cAMP, using the anti-VN clone 342603, control sections were treated with MoIgG instead of primary antibody. VN is in green and nuclei in blue, scale bars are 50 μm.

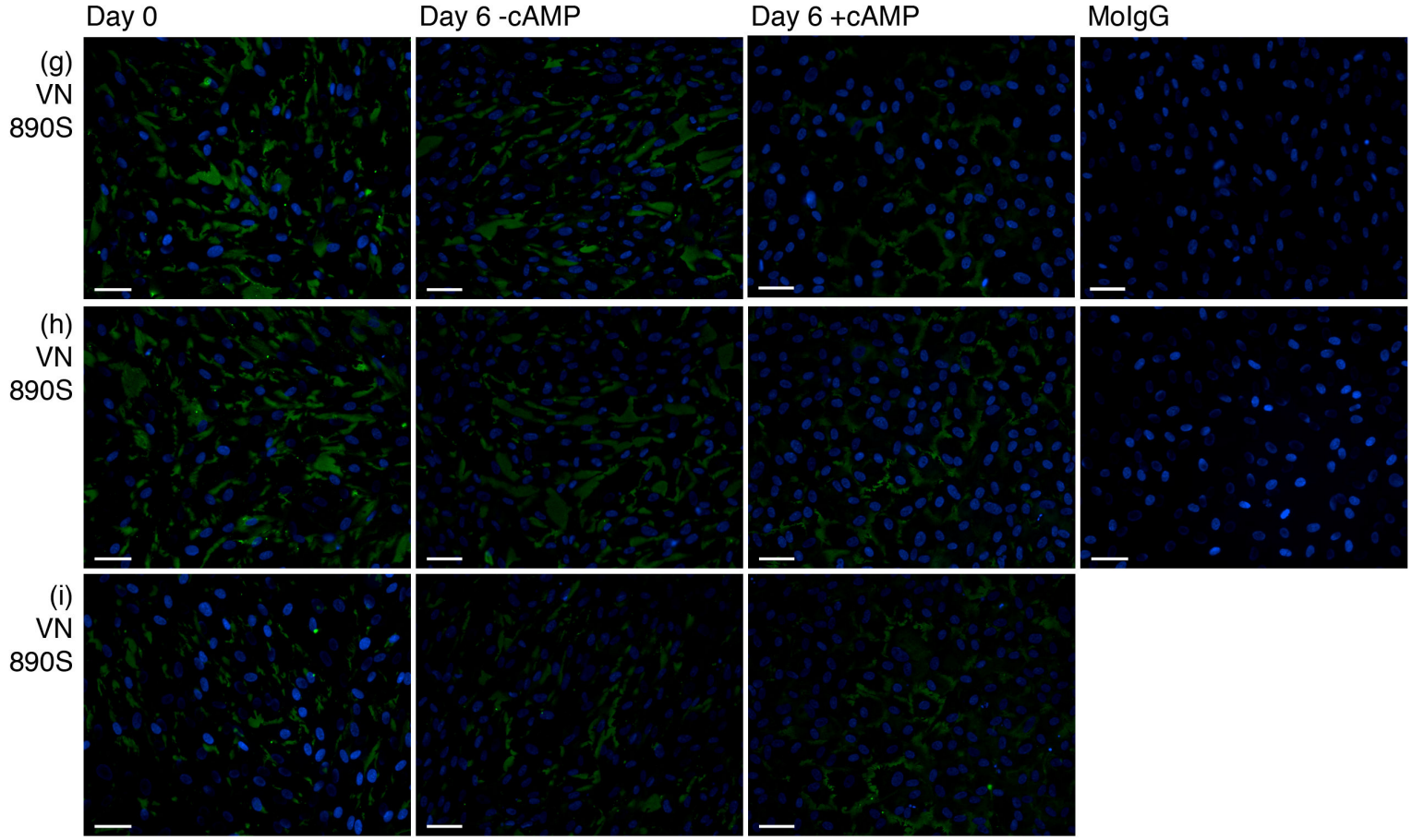

Appendix IV (j, k) Immunofluorescence staining for VN produced by ESCs (890S) at day 0, day 6 and day 6 with cAMP, using the anti-VN clone 342603, control sections were treated with MoIgG instead of primary antibody. VN is in green and nuclei in blue, scale bars are 50 μm.

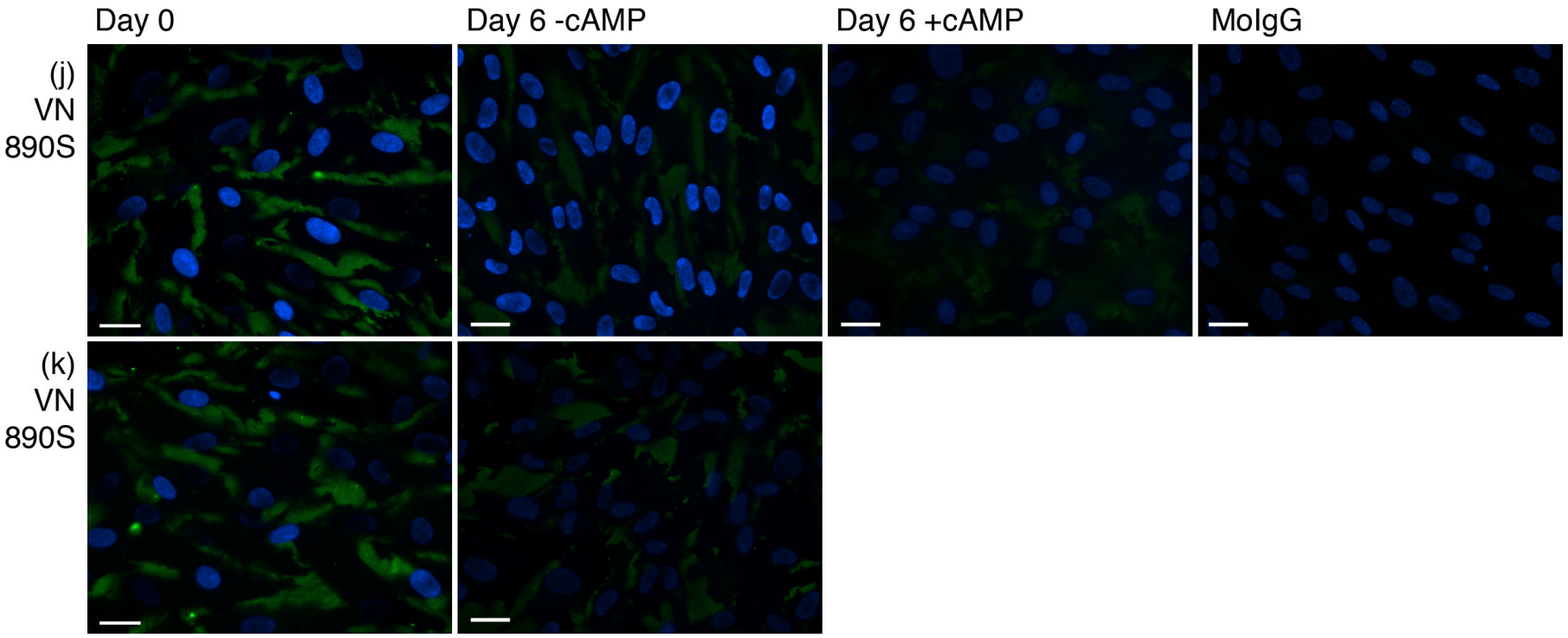

Appendix V (a, b) Immunofluorescence staining for TN produced by ESCs at day 0, day 6 and day 6 with cAMP, from different fields of view of one ESC cell number (890S) in the same experiment. Control sections treated with MoIgG instead of primary antibody are also shown. TN is in green and nuclei in blue, scale bars are 50 μm.

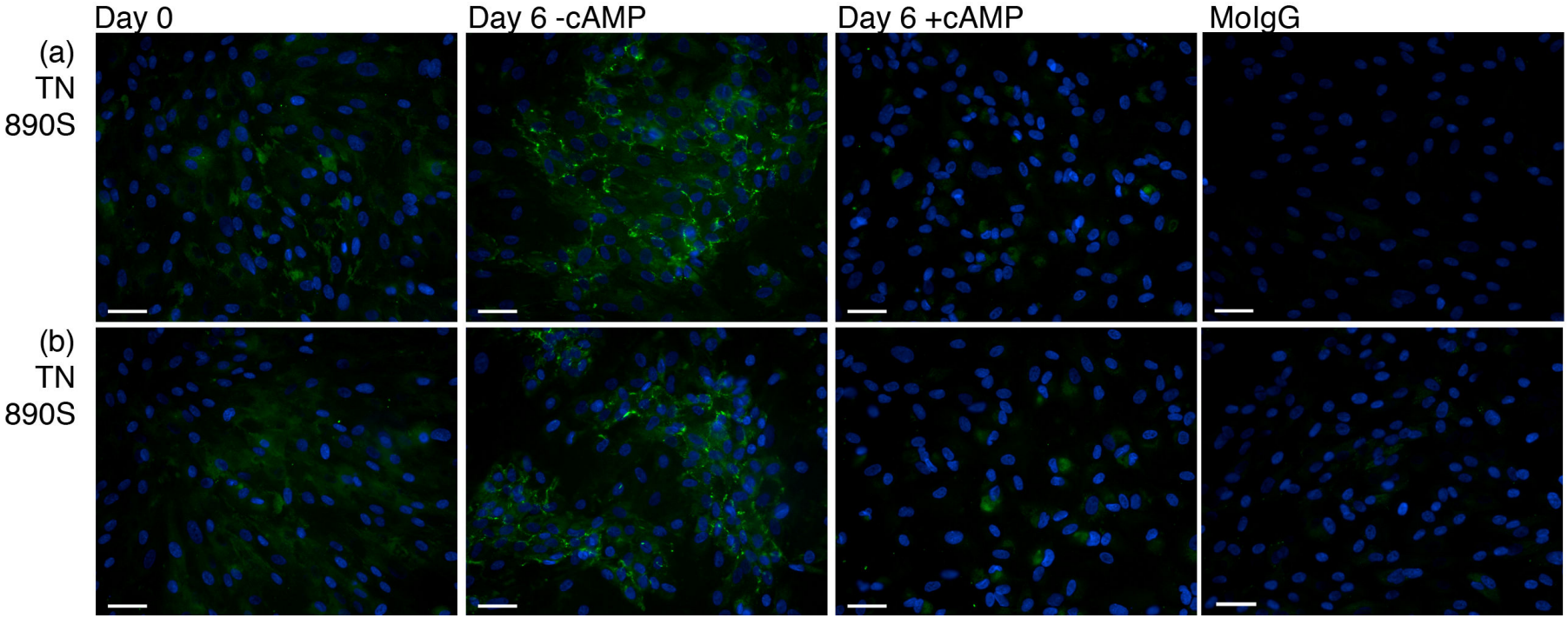

Appendix V (c, d) Immunofluorescence staining for TN produced by ESCs at day 6 and day 6 with cAMP, from different fields of view of one ESC cell number (890S) in the same experiment. Control sections treated with MoIgG instead of primary antibody are also shown. TN is in green and nuclei in blue, scale bars are 25 μm.

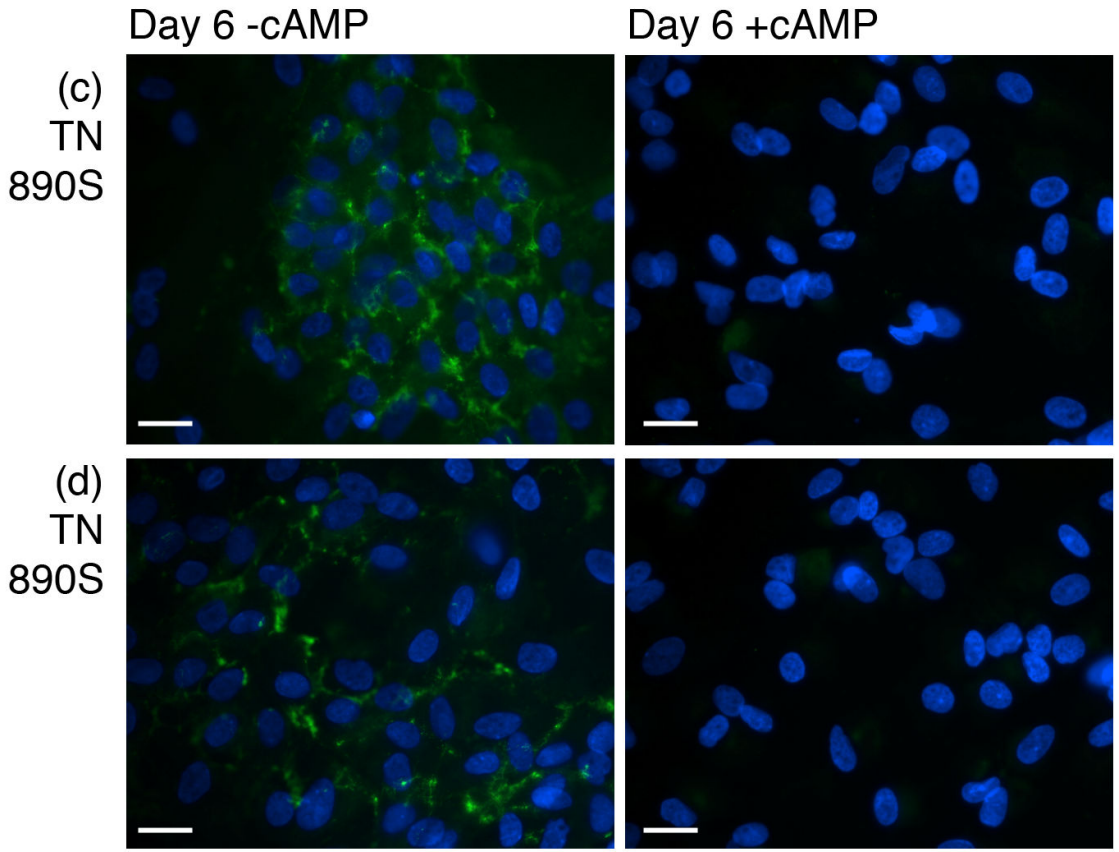

Appendix V (e, f) Immunofluorescence staining for TN produced by ESCs at day 0, day 6 and day 6 with cAMP, from different fields of view of one ESC cell number (700S) in the same experiment. Control sections treated with MoIgG instead of primary antibody are also shown. TN is in green and nuclei in blue, scale bars are (e) 50 μm and (f) 25 μm.

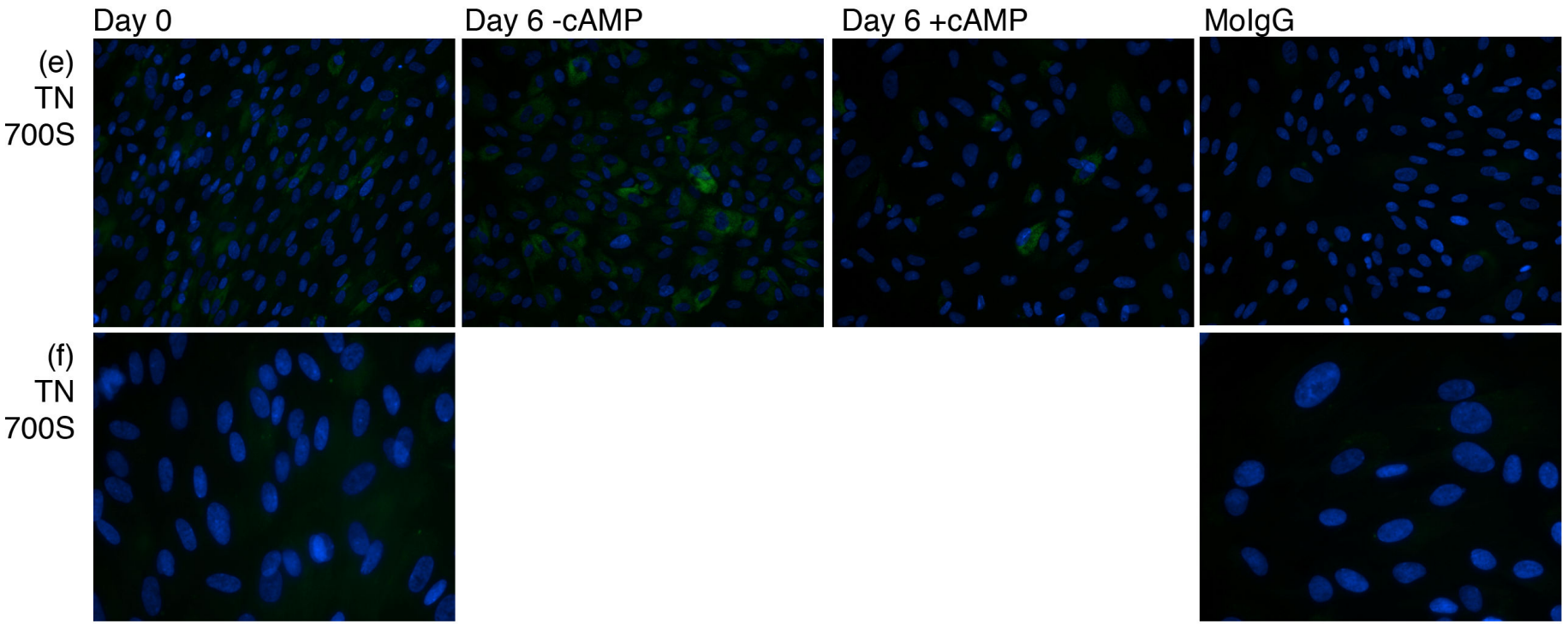

Appendix V (g, h) Immunofluorescence staining for TN produced by ESCs at day 0, day 6 and day 6 with cAMP, from different fields of view of one ESC cell number (629S) in the same experiment. Control sections treated with MoIgG instead of primary antibody are also shown. TN is in green and nuclei in blue, scale bars are 50 μm.

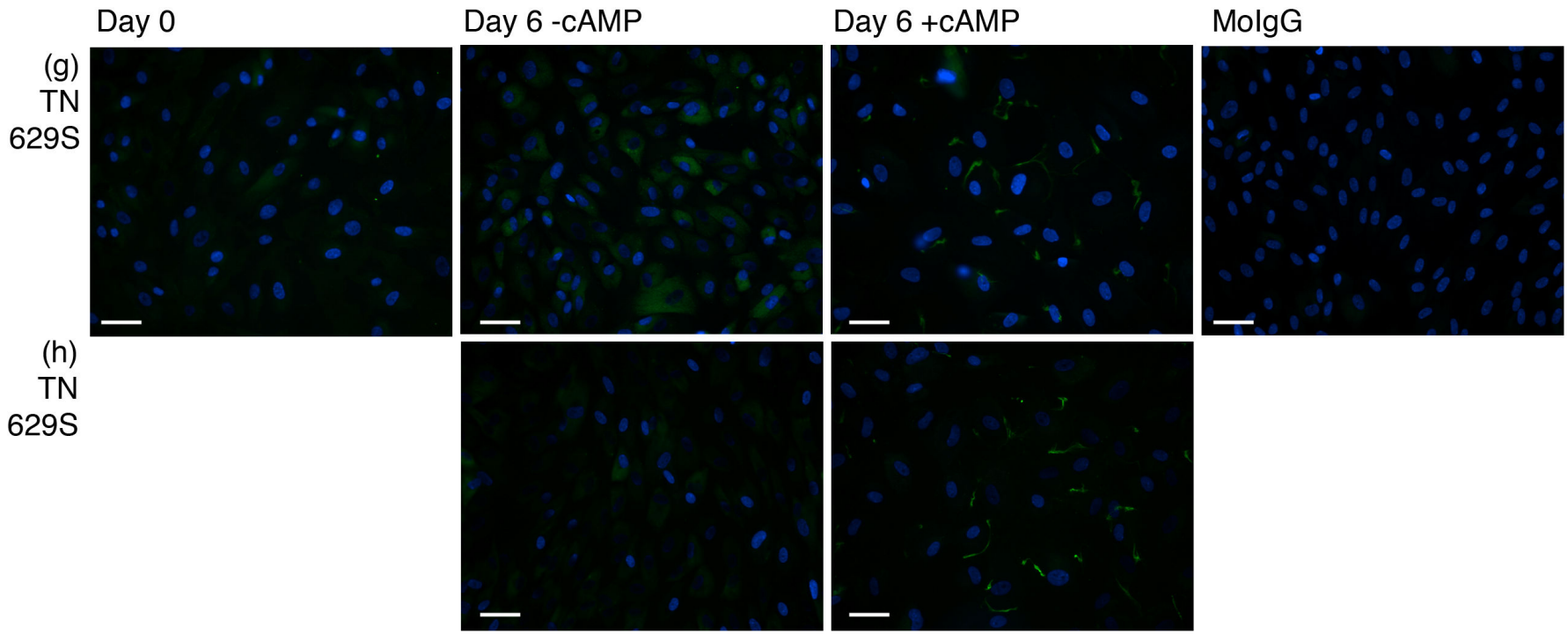

Appendix VI (a-c) Immunofluorescence staining for FN produced by ESCs (700S) at day 0, day 6 and day 6 with cAMP, control sections were treated with MoIgG instead of primary antibody. FN is in green and nuclei in blue, scale bars are 50μm.

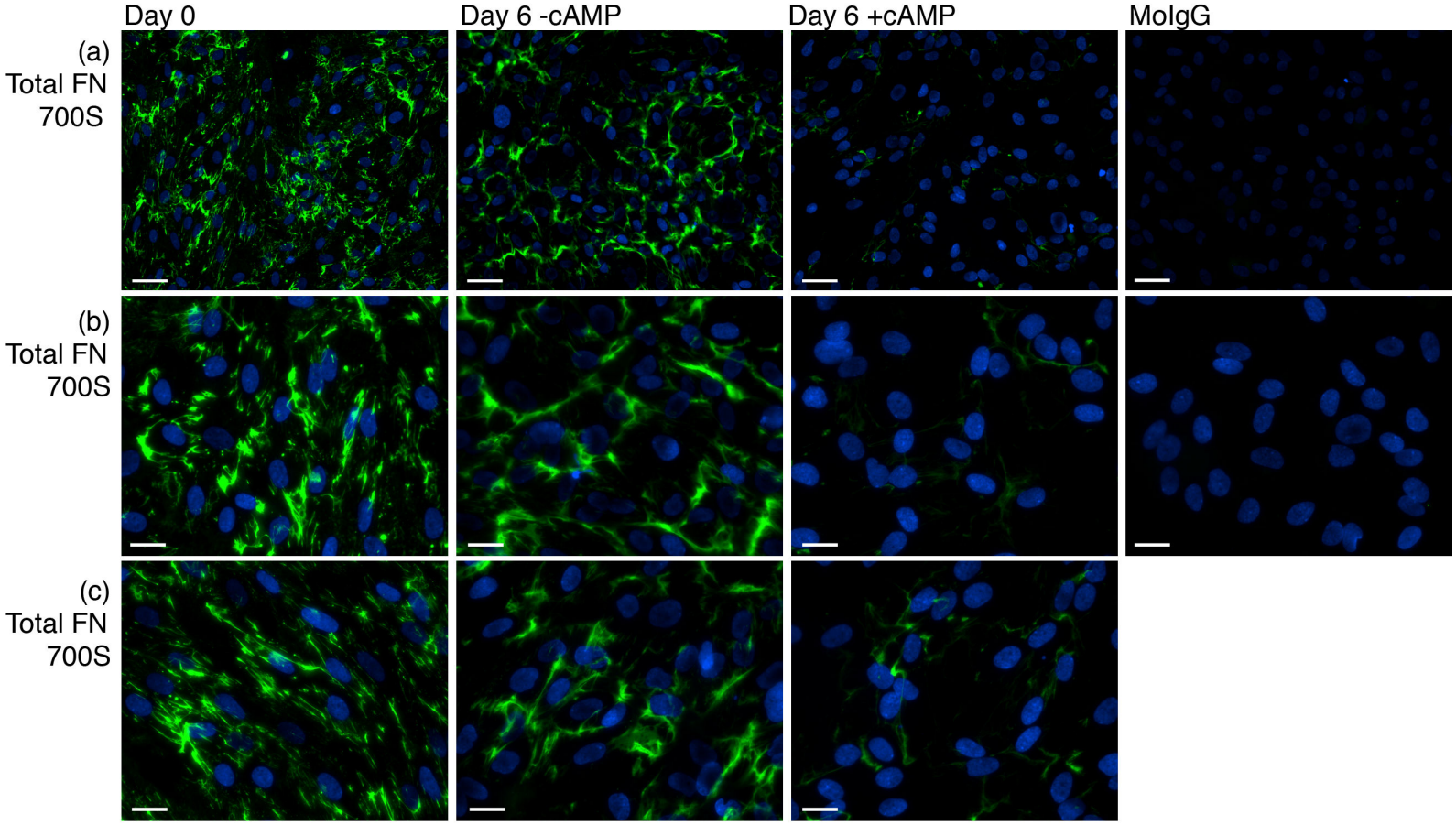

Appendix VI (d-f) Immunofluorescence staining for FN produced by ESCs (862S) at day 0, day 6 and day 6 with cAMP, control sections were treated with MoIgG instead of primary antibody. FN is in green and nuclei in blue, scale bars are 50μm.

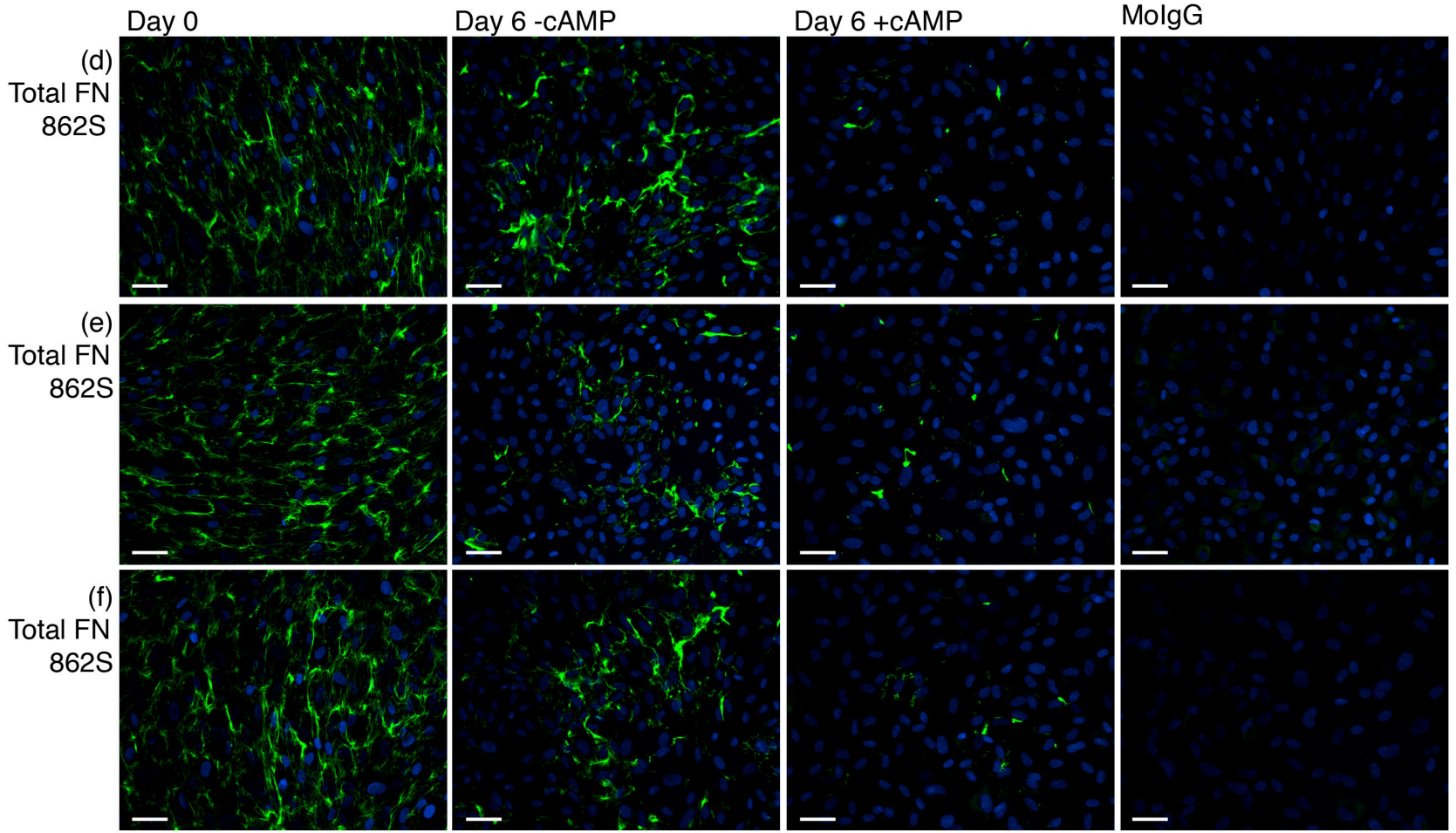

Appendix VI (g-i) Immunofluorescence staining for FN produced by ESCs (862S) at day 0, day 6 and day 6 with cAMP, control sections were treated with MoIgG instead of primary antibody. FN is in green and nuclei in blue, scale bars are 25μm.

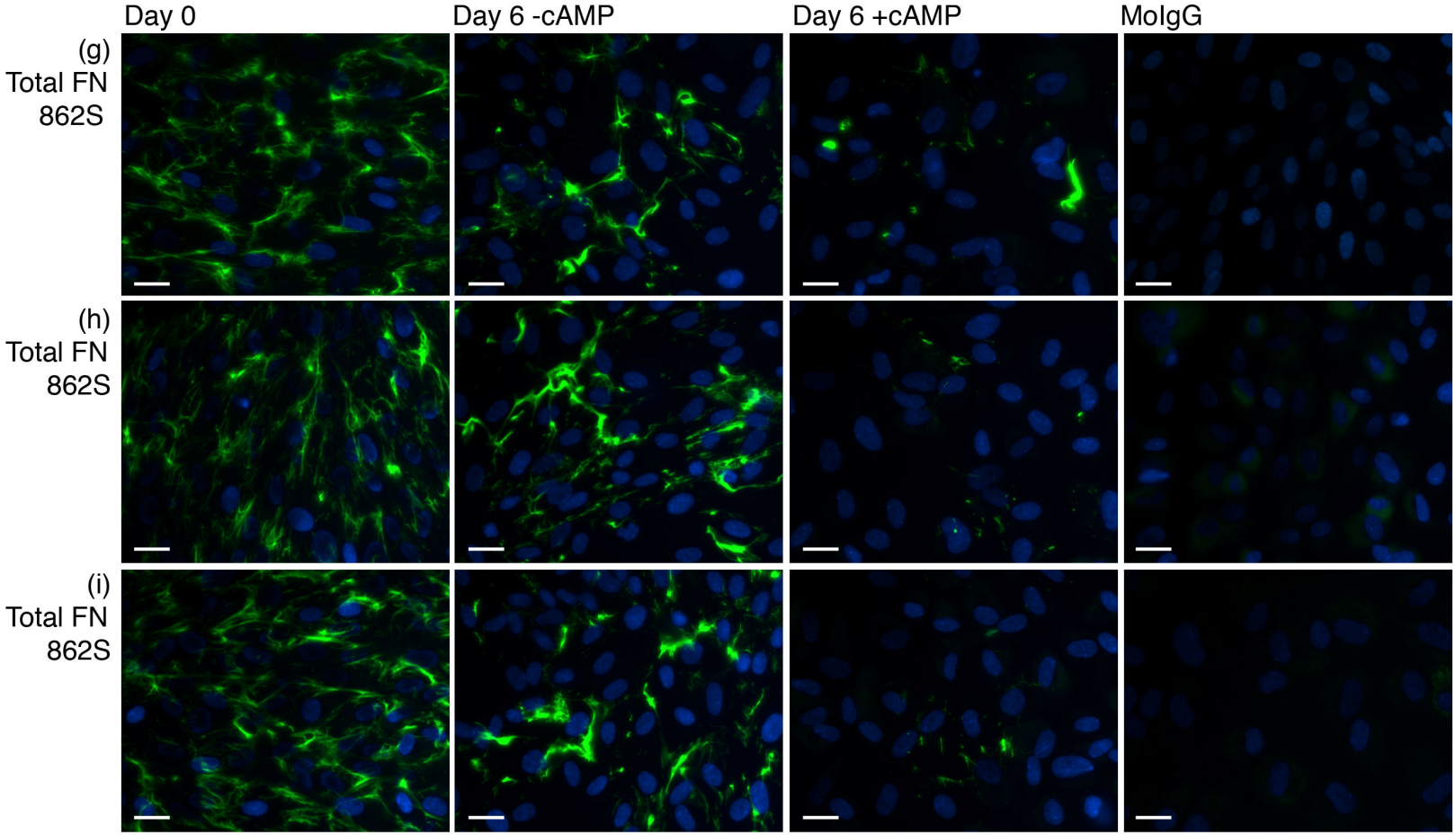

Appendix VI (j-l) Immunofluorescence staining for FN produced by ESCs (890S) at day 0, day 6 and day 6 with cAMP, control sections were treated with MoIgG instead of primary antibody. FN is in green and nuclei in blue, scale bars are (j, k) 50µm and (l) 25 µm.

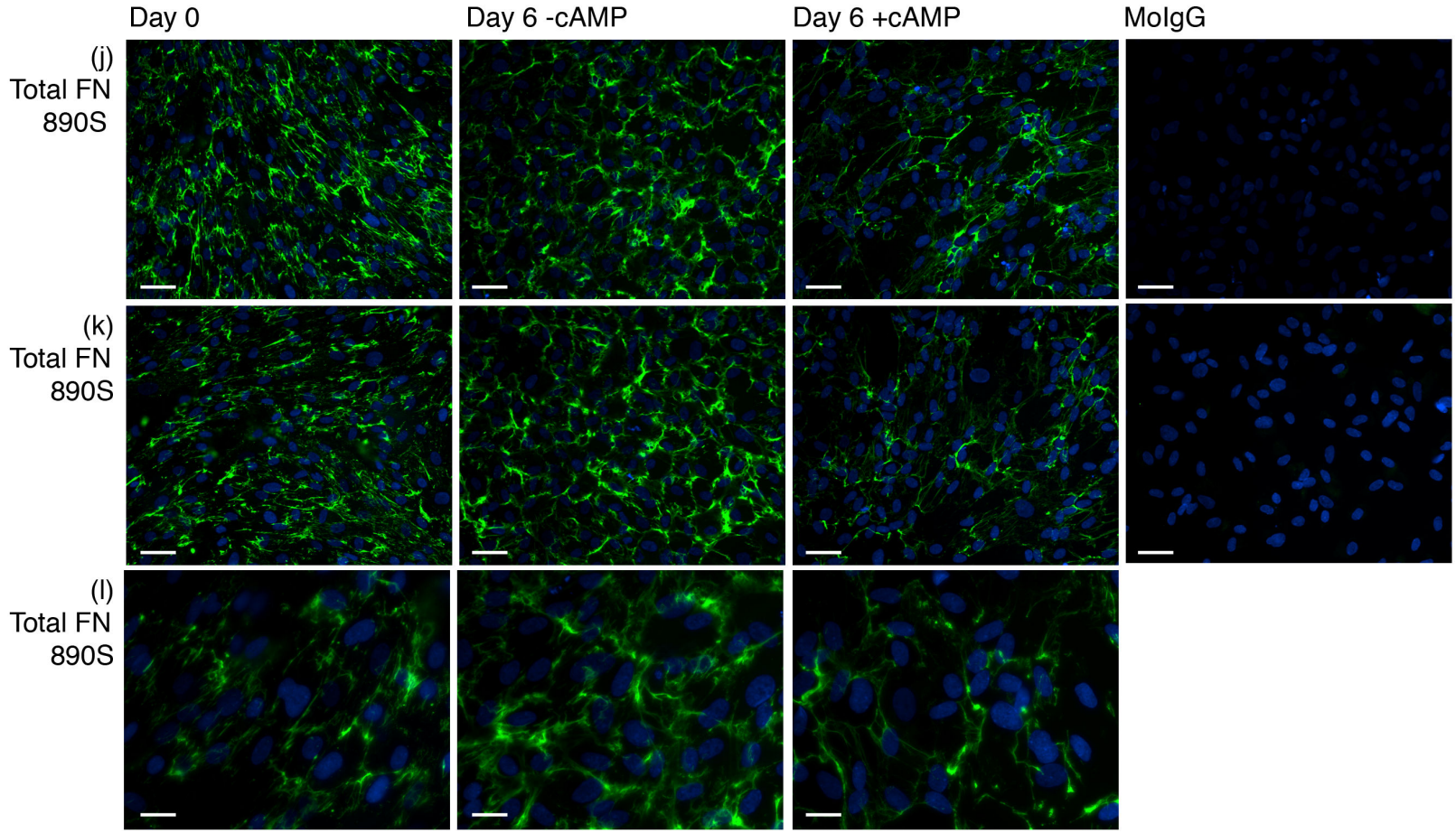

Appendix VII (a, b) Immunofluorescence staining for EDIIIA+FN produced by ESCs at day 0, day 6 and day 6 with cAMP, from different fields of view of one ESC cell number (700S) in the same experiment. Control sections treated with MoIgG instead of primary antibody are also shown. EDIIIA+FN is in green and nuclei in blue, scale bars are 50 μm.

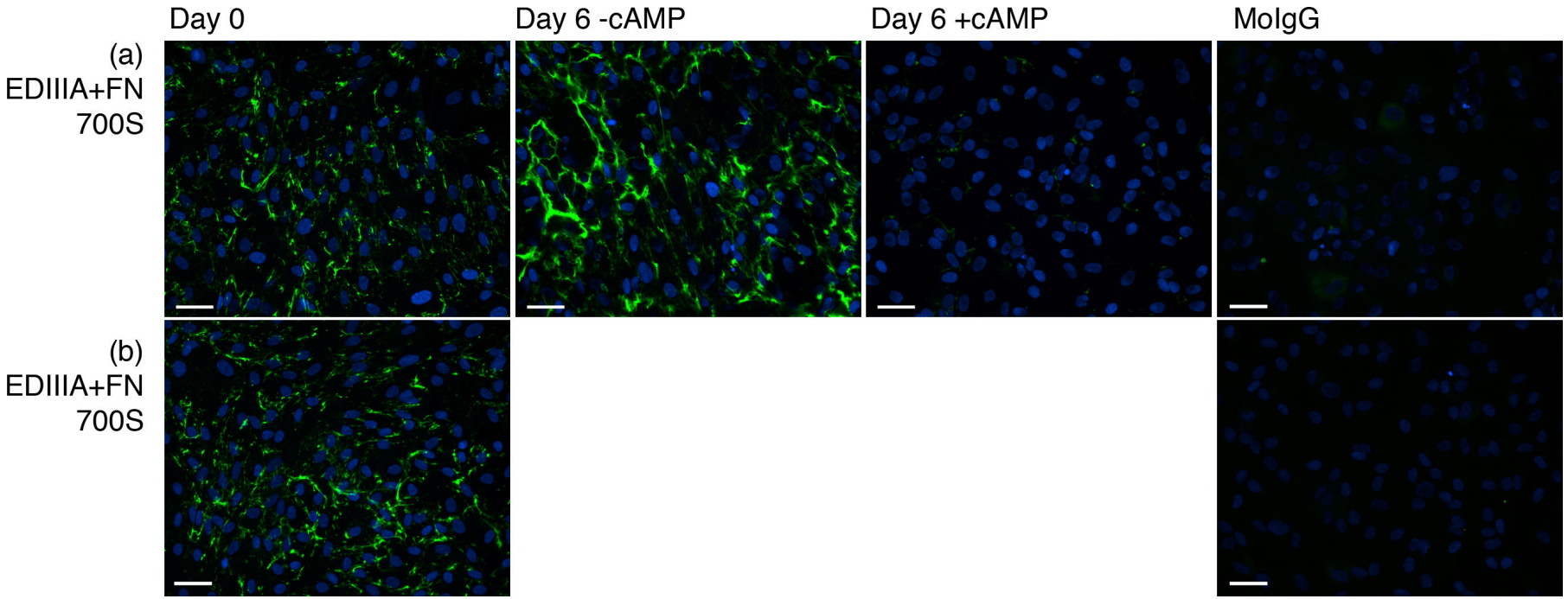

Appendix VII (c, d) Immunofluorescence staining for EDIIIA+FN produced by ESCs at day 0, day 6 and day 6 with cAMP, from different fields of view of one ESC cell number (700S), in the same experiment. Control sections treated with MoIgG instead of primary antibody are also shown. EDIIIA+FN is in green and nuclei in blue, scale bars are 25 μm.

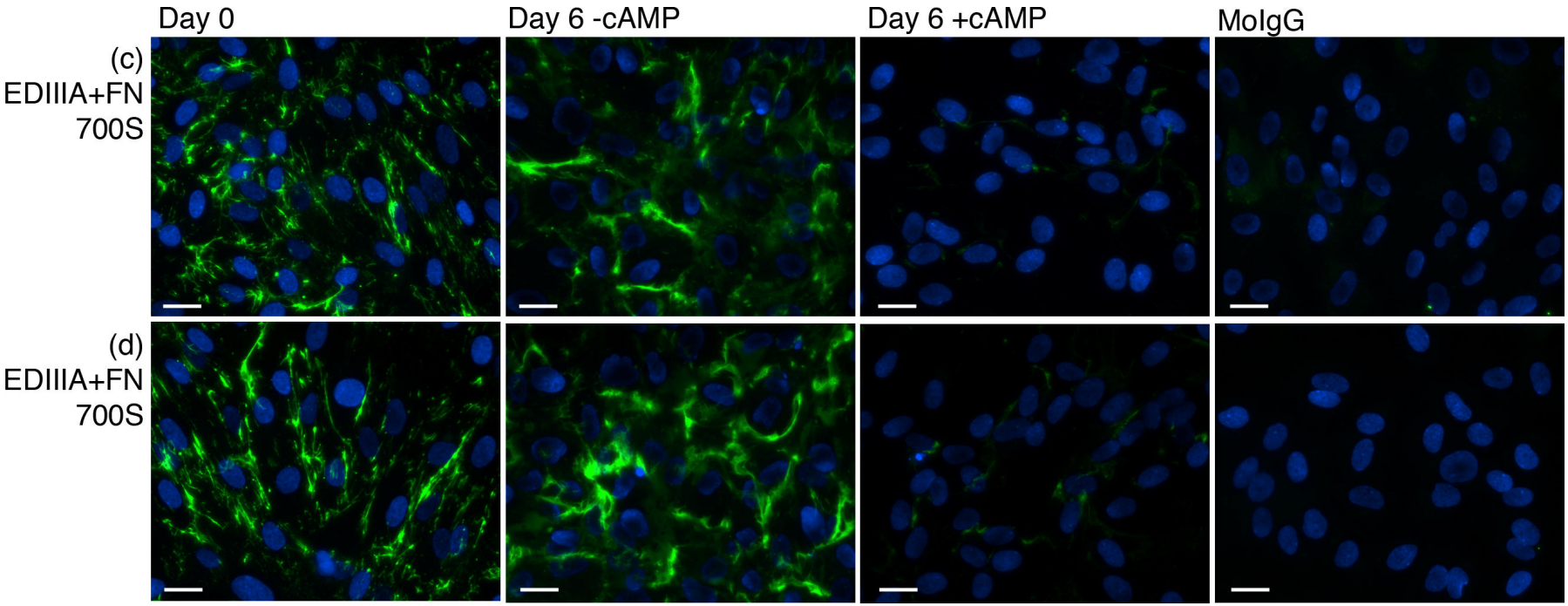

Appendix VII (e, f) Immunofluorescence staining for EDIIIA+FN produced by ESCs at day 0, day 6 and day 6 with cAMP, from different fields of view of one ESC cell number (862S) in the same experiment. Control sections treated with MoIgG instead of primary antibody are also shown. EDIIIA+FN is in green and nuclei in blue, scale bars are 50 μm.

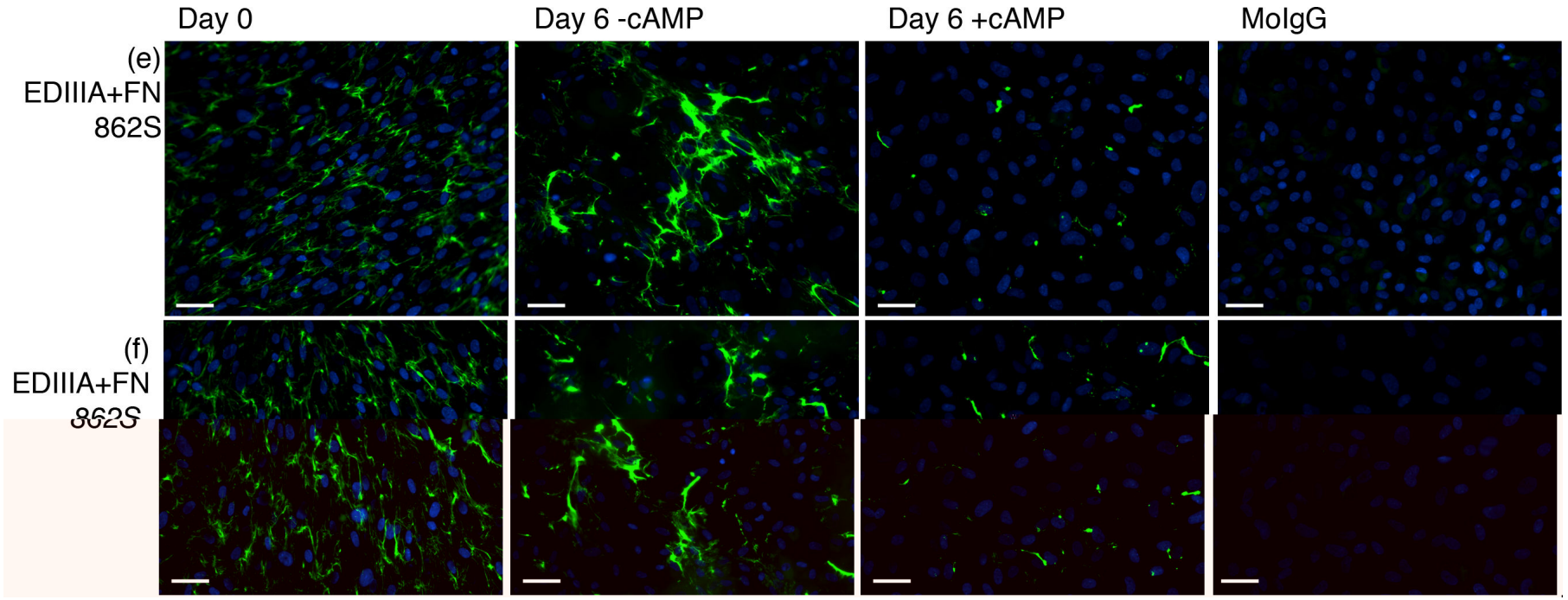

Appendix VII (g, h) Immunofluorescence staining for EDIIIA+FN produced by ESCs at day 0, day 6 and day 6 with cAMP, from different fields of view of one ESC cell number (862S) in the same experiment. Control sections treated with MoIgG instead of primary antibody are also shown. EDIIIA+FN is in green and nuclei in blue, scale bars are 25 μm.

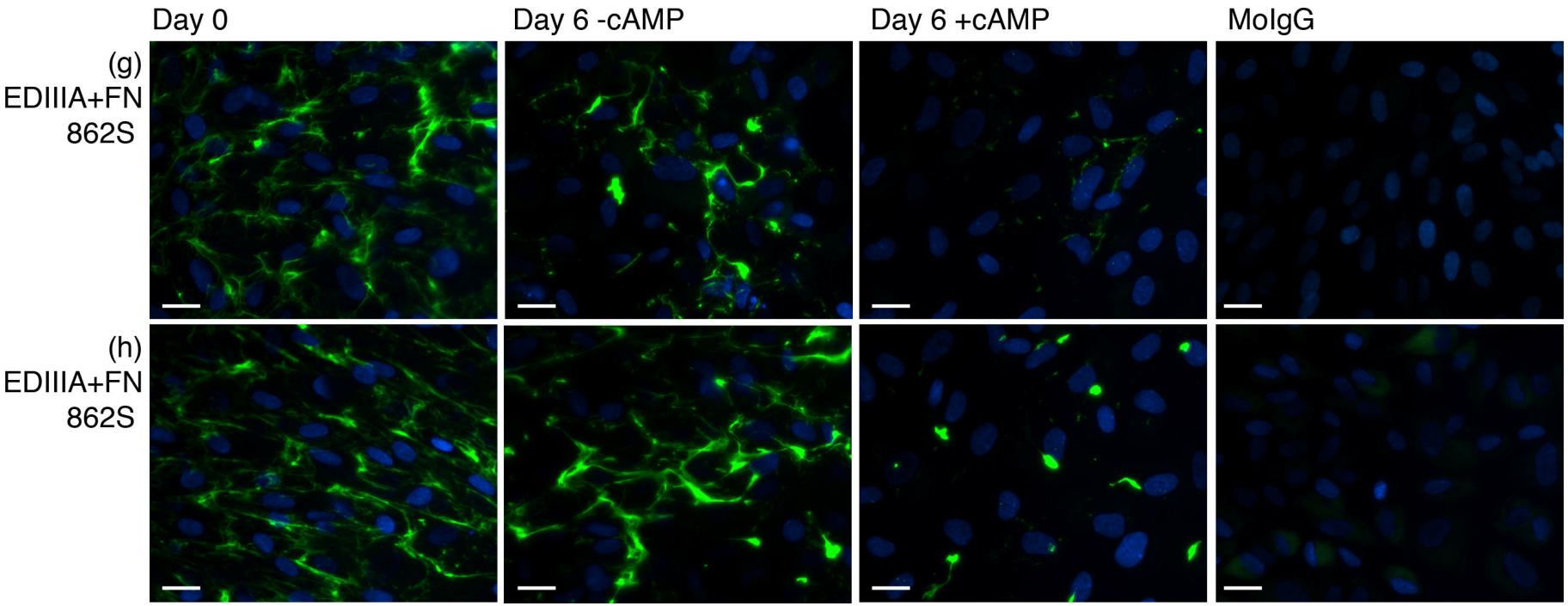

Appendix VII (i, j) Immunofluorescence staining for EDIIIA+FN produced by ESCs at day 0, day 6 and day 6 with cAMP, from different fields of view of one ESC cell number (629S) in the same experiment. Control sections treated with MoIgG instead of primary antibody are also shown. EDIIIA+FN is in green, actin in red and nuclei in blue, scale bars are 50 μm.

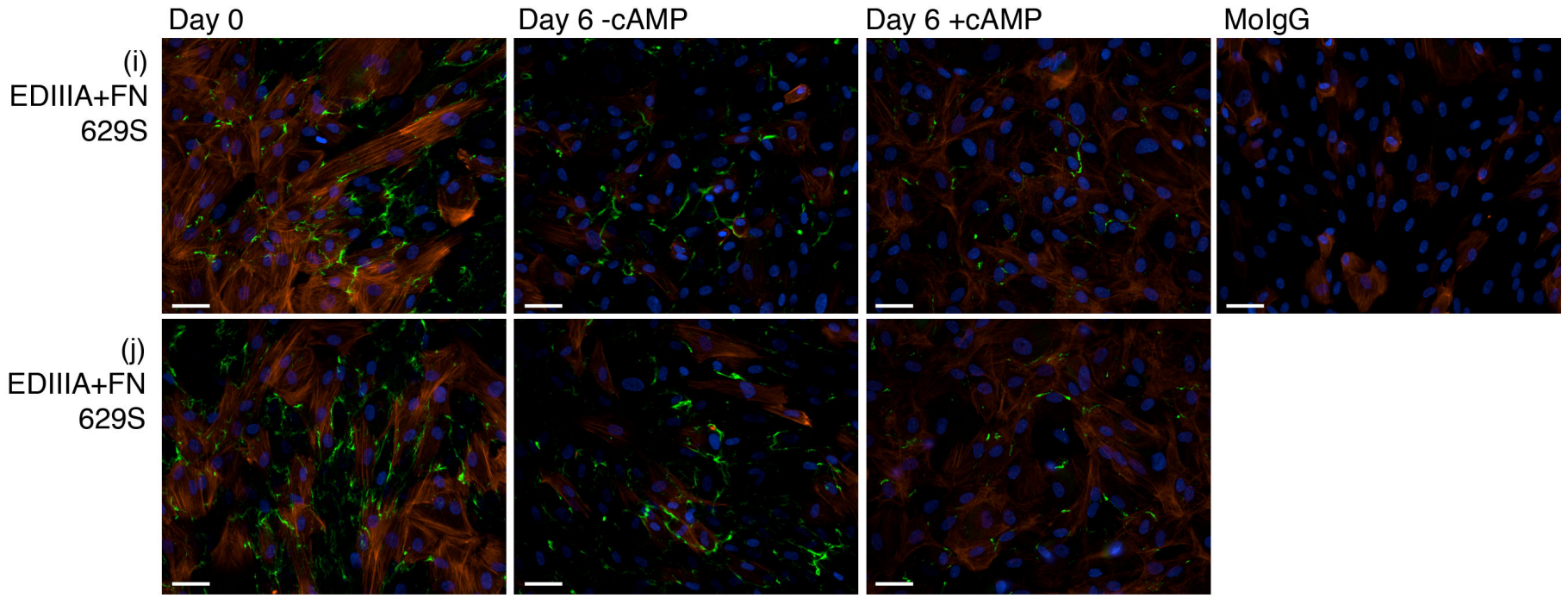

Appendix VIII (a, b) Immunofluorescence staining for EDIIIB+FN produced by ESCs at day 0, day 6 and day 6 with cAMP, from different fields of view of one ESC cell number (700S) in the same experiment. Control sections treated with MoIgG instead of primary antibody are also shown. EDIIIB+FN is in green and nuclei in blue, scale bars are 50 μm.

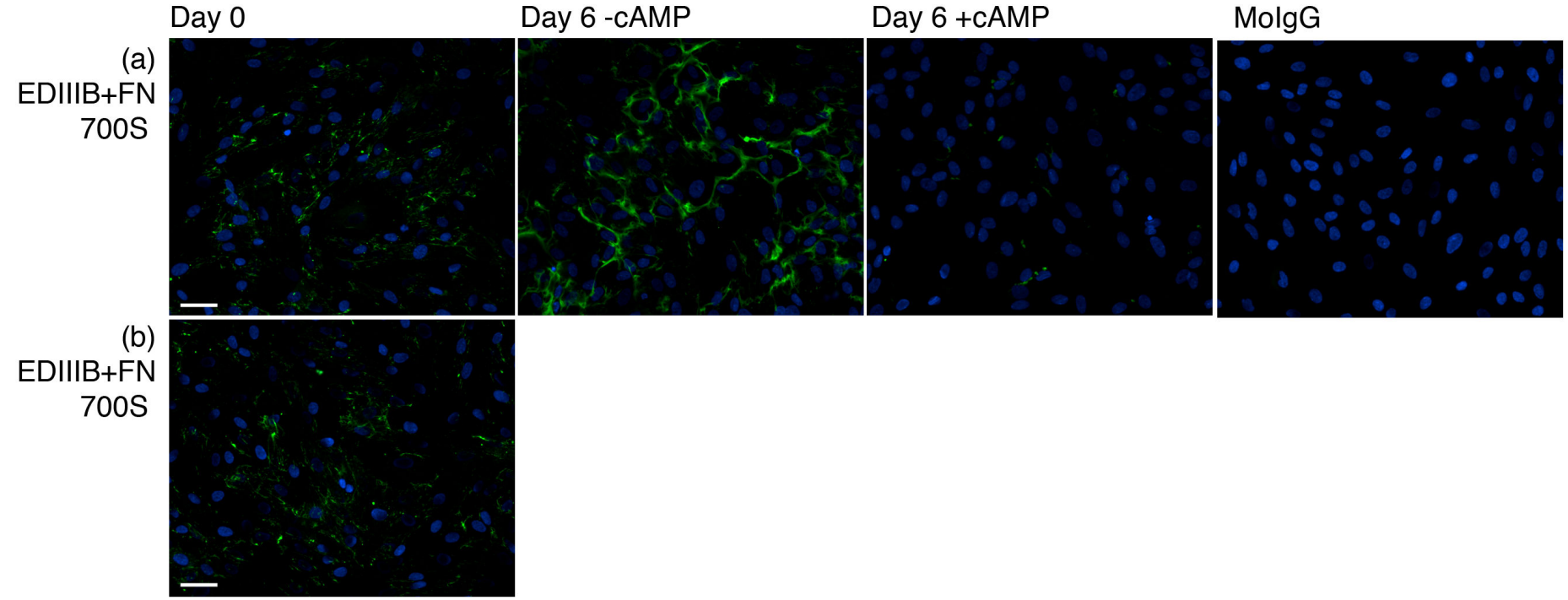

Appendix VIII (c, d) Immunofluorescence staining for EDIIIB+FN produced by ESCs at day 0, day 6 and day 6 with cAMP, from different fields of view of one ESC cell number (700S) in the same experiment. Control sections treated with MoIgG instead of primary antibody are also shown. EDIIIB+FN is in green and nuclei in blue, scale bars are 25 μm.

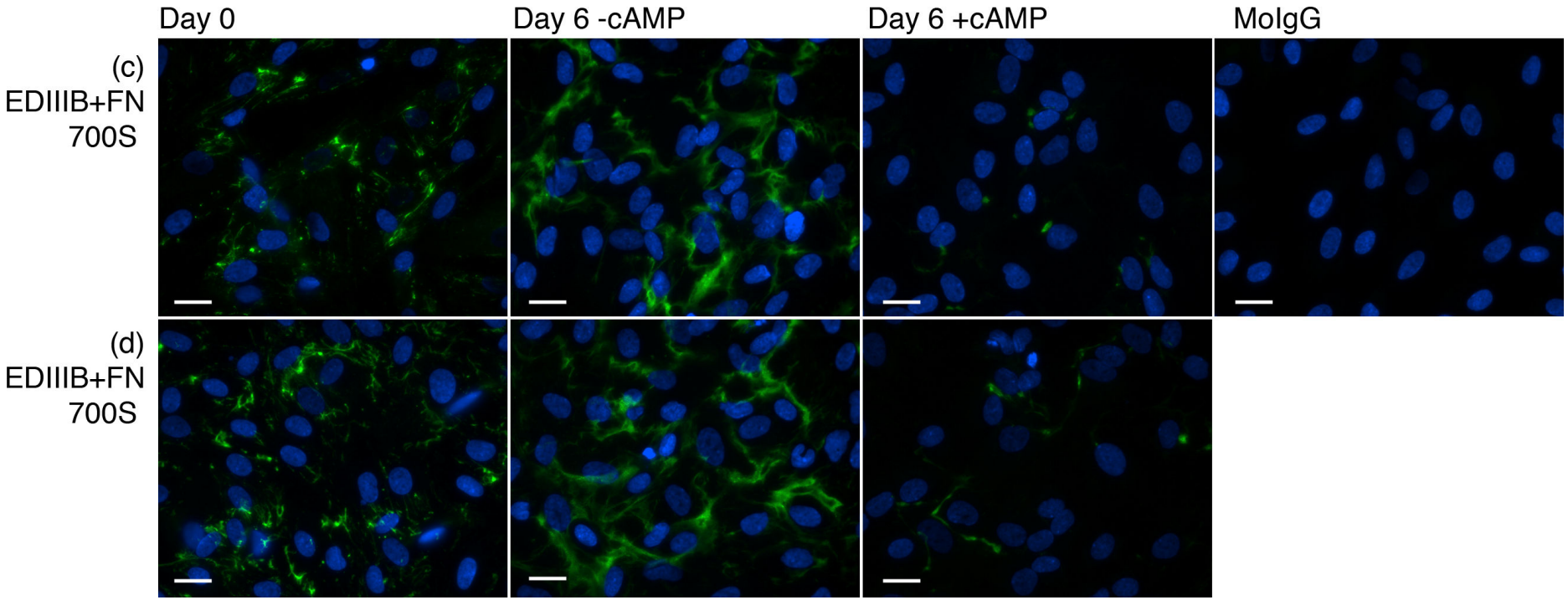

Appendix VIII (e, f) Immunofluorescence staining for EDIIIB+FN produced by ESCs at day 0, day 6 and day 6 with cAMP, from different fields of view of one ESC cell number (862S) in the same experiment. Control sections treated with MoIgG instead of primary antibody are also shown. EDIIIB+FN is in green and nuclei in blue, scale bars are 50 μm.

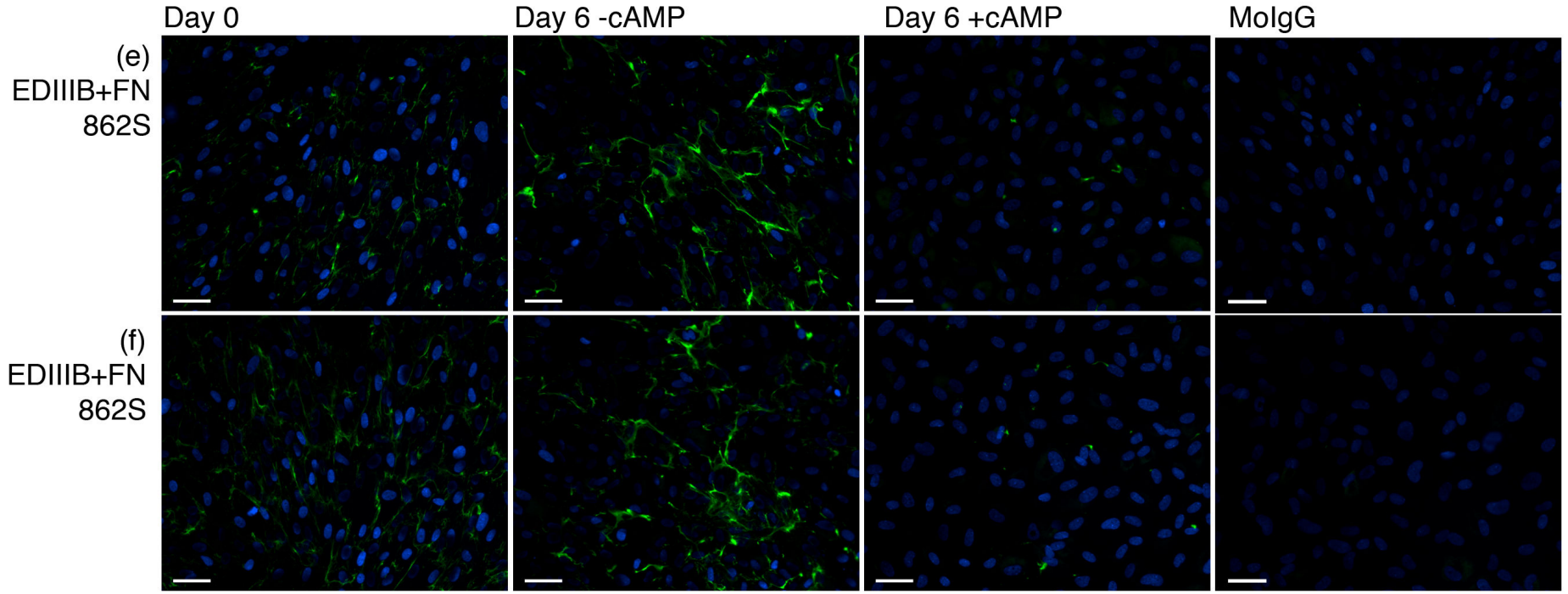

Appendix VIII (g, h) Immunofluorescence staining for EDIIIB+FN produced by ESCs at day 0, day 6 and day 6 with cAMP, from different fields of view of one ESC cell number (862S) in the same experiment. Control sections treated with MoIgG instead of primary antibody are also shown. EDIIIB+FN is in green and nuclei in blue, scale bars are 25 μm.

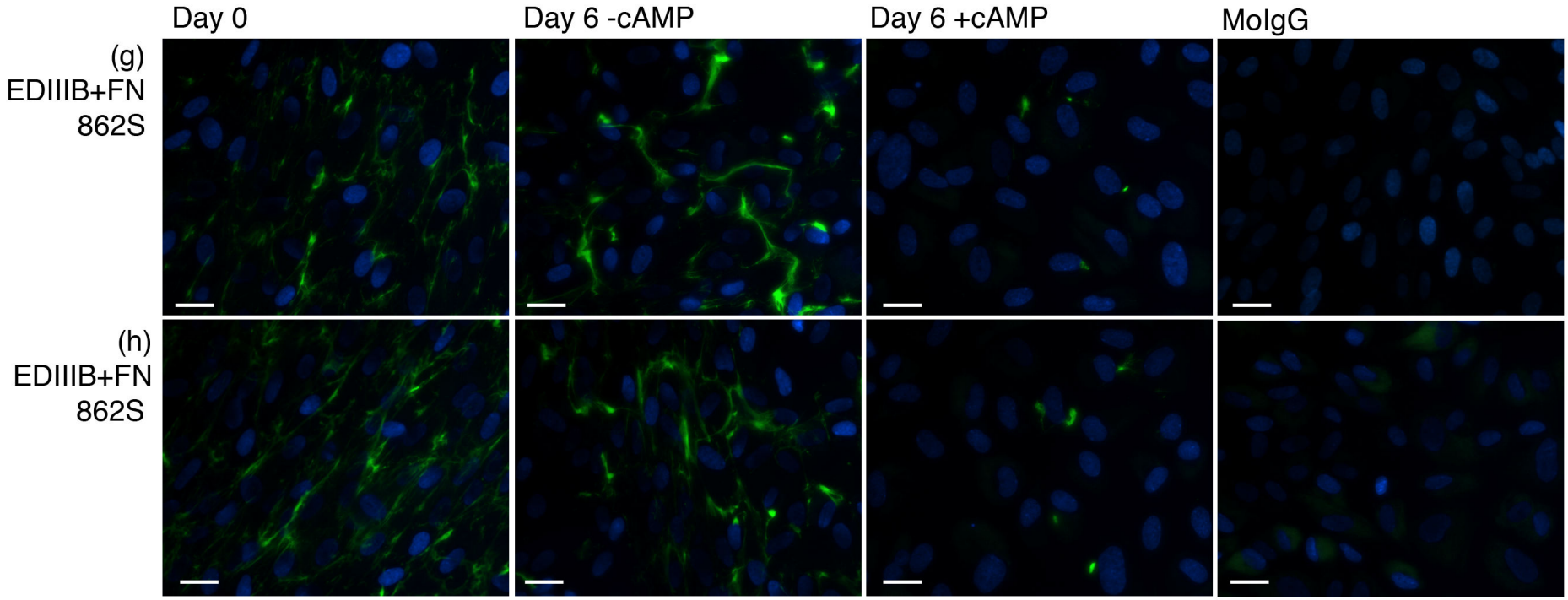

Appendix VIII (i-k) Immunofluorescence staining for EDIIIB+FN produced by ESCs (890S) at day 0, day 6 and day 6 with cAMP, control sections were treated with MoIgG instead of primary antibody. EDIIIB+FN is in green and nuclei in blue, scale bars are (i,j) 50 and (k) 25 μm.

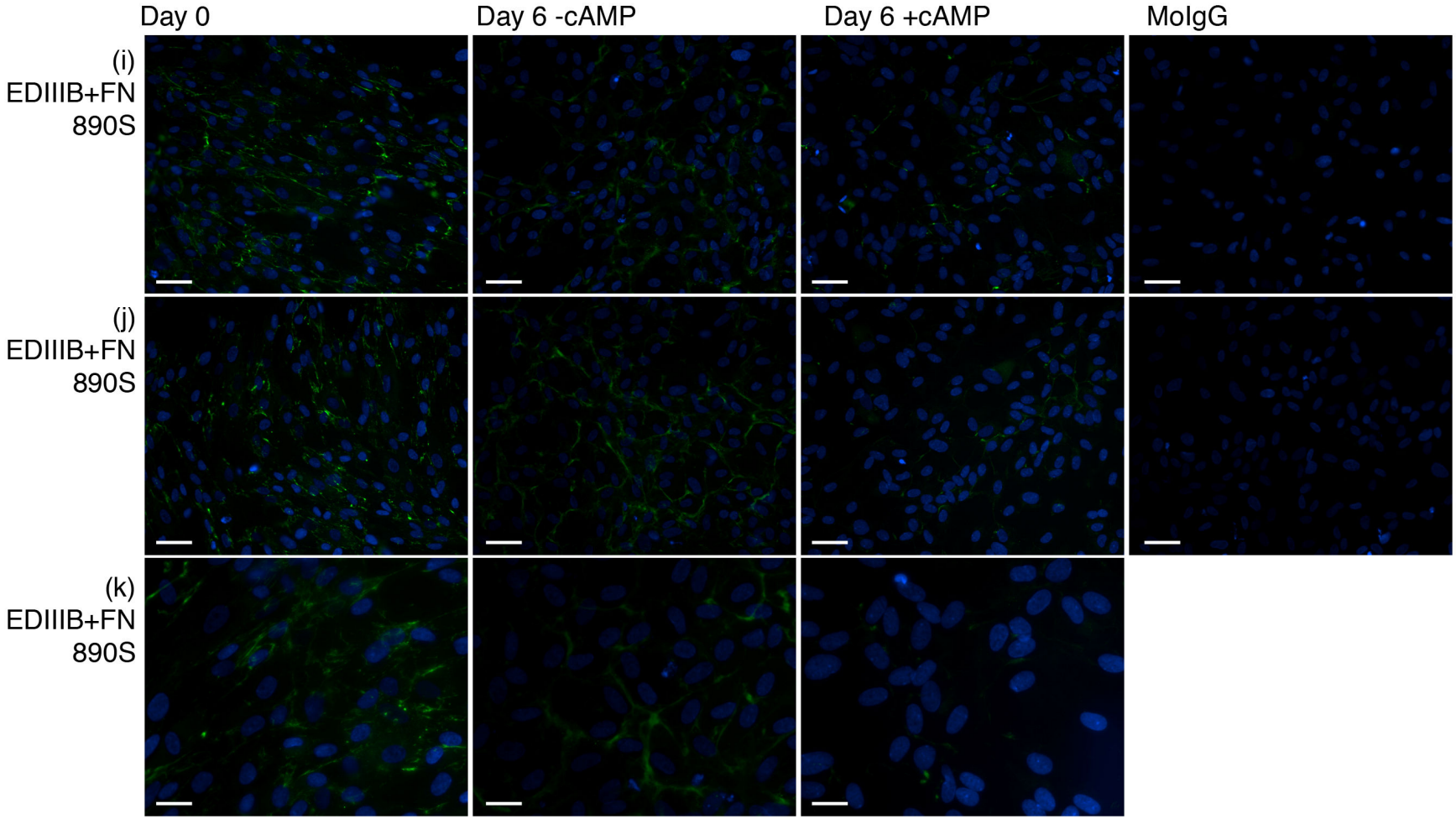

Appendix IX (a, b) Immunofluorescence staining for vinculin produced by ESCs at day 0, day 6 and day 6 with cAMP, from different fields of view of one ESC cell number (862S) in the same experiment. Control sections treated with MoIgG instead of primary antibody are also shown. Vinculin is in green, actin in red and nuclei in blue, scale bars are 50µm.

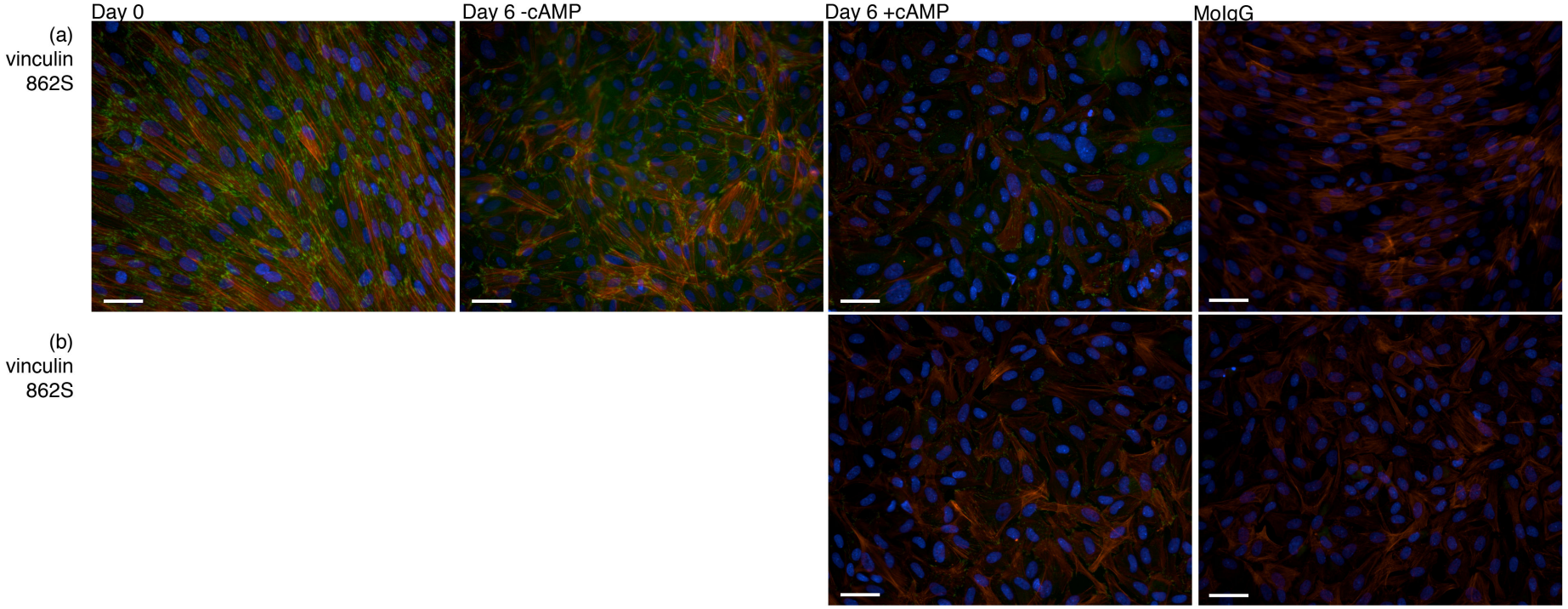

Appendix IX (c, d) Immunofluorescence staining for vinculin produced by ESCs at day 0, day 6 and day 6 with cAMP, from different fields of view of one ESC cell number (862S) in the same experiment. Vinculin is in green, actin in red and nuclei in blue, scale bars are 25μm.

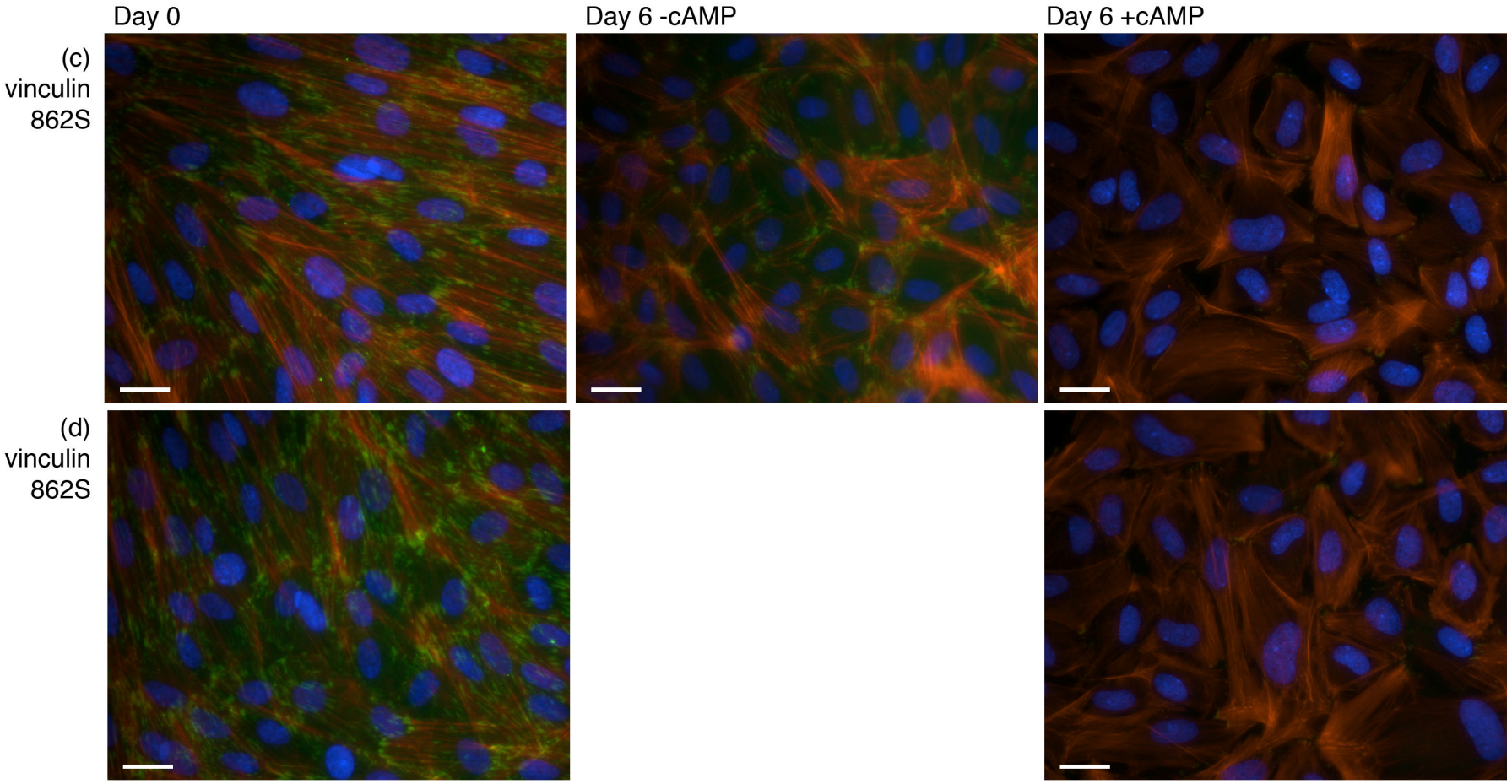

Appendix IX (e, f) Immunofluorescence staining for vinculin produced by ESCs at day 0, day 6 and day 6 with cAMP, from different fields of view of one ESC cell number (629S) in the same experiment. Control sections treated with MoIgG instead of primary antibody are also shown. Vinculin is in green, actin in red and nuclei in blue, scale bars are 50μm.

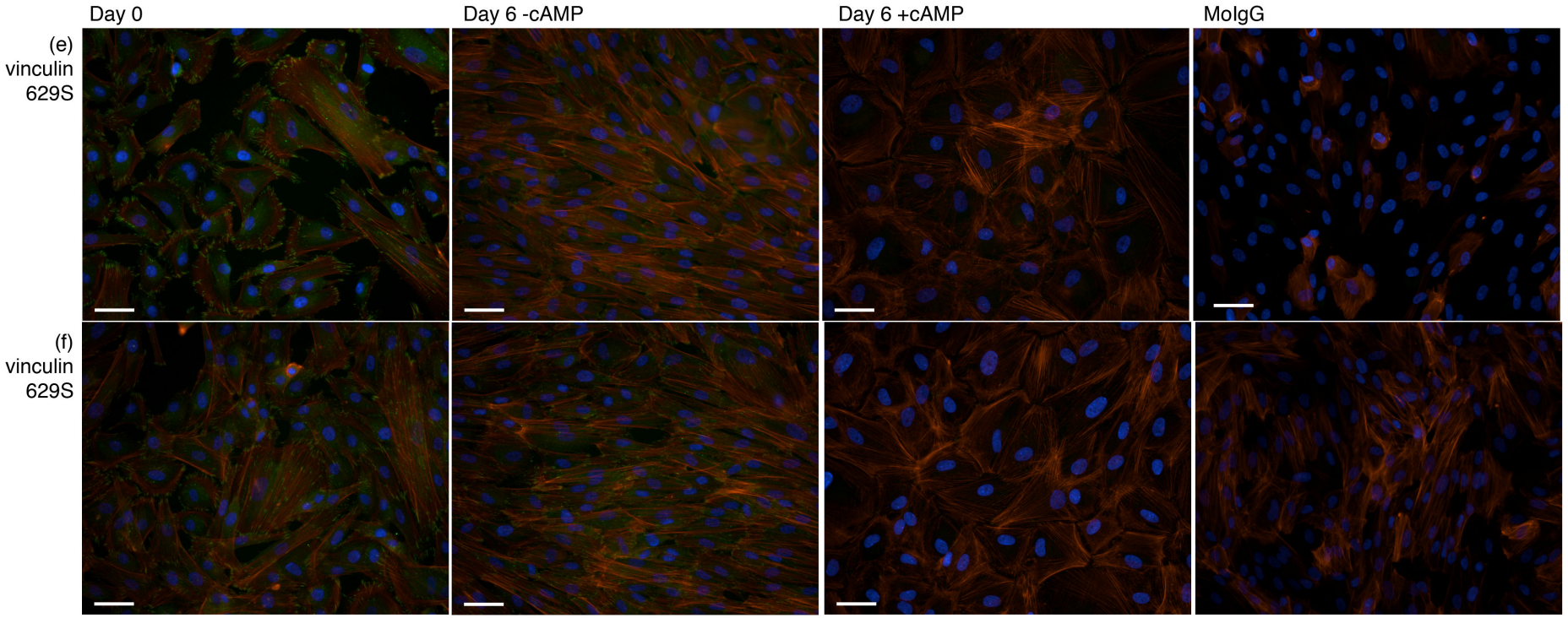

Appendix IX (g, h) Immunofluorescence staining for vinculin produced by ESCs at day 0, day 6 and day 6 with cAMP, from different fields of view of one ESC cell number (890S) in the same experiment. Control sections treated with MoIgG instead of primary antibody are also shown. Vinculin is in green, actin in red and nuclei in blue, scale bars are 50µm.

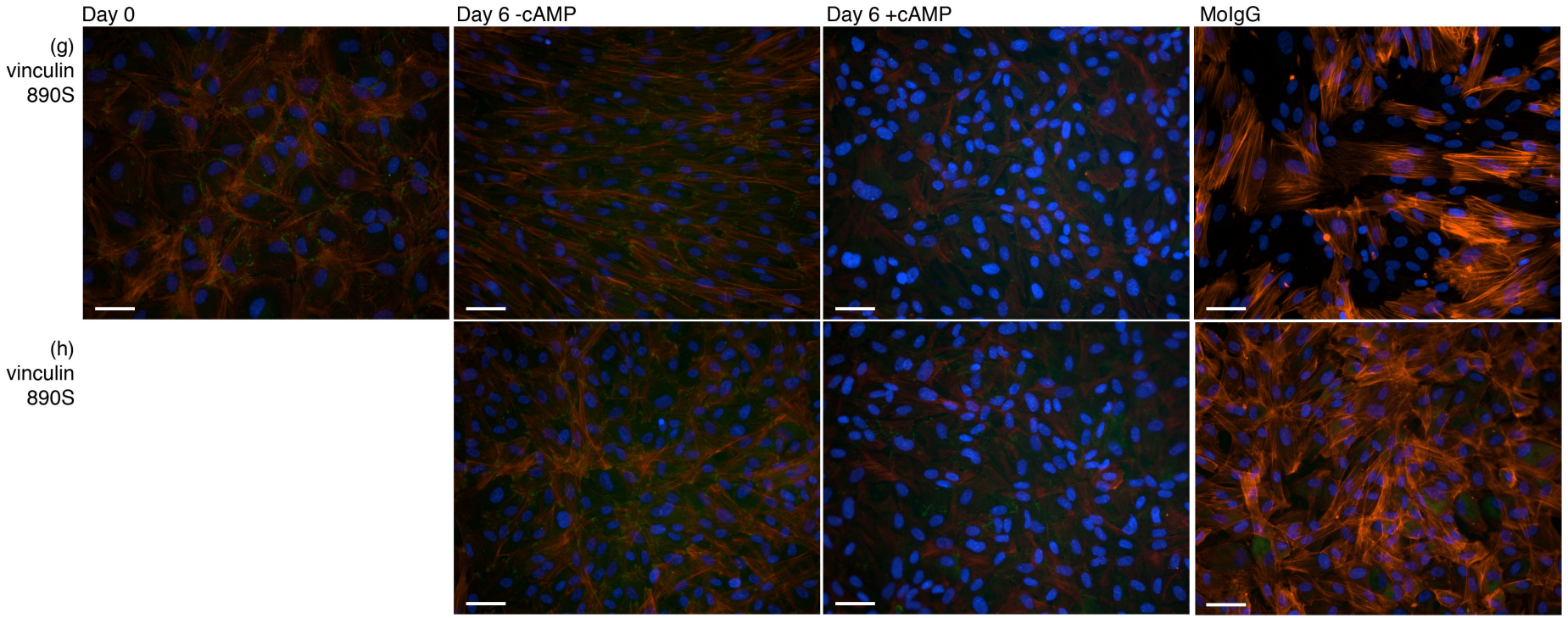

Appendix IX (i, j) Immunofluorescence staining for vinculin produced by ESCs at day 0, day 6 and day 6 with cAMP, from different fields of view of one ESC cell number (890S) in the same experiment. Control sections treated with MoIgG instead of primary antibody are also shown. Vinculin is in green, actin in red and nuclei in blue, scale bars are 25µm.

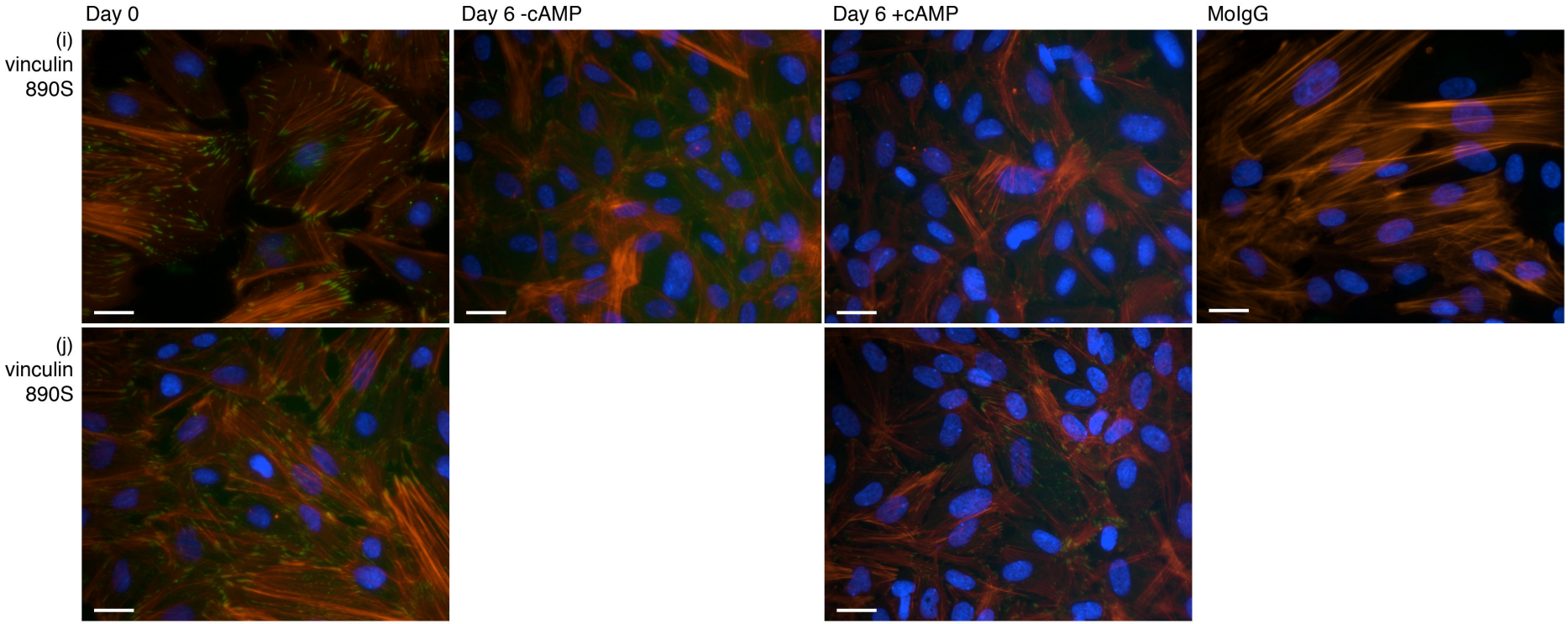

Appendix X (a, b) Immunofluorescence staining for paxillin produced by ESCs at day 0, day 6 and day 6 with cAMP, from different fields of view of one ESC cell number (862S) in the same experiment. Control sections treated with MoIgG instead of primary antibody are also shown. Paxillin is in green, actin in red and nuclei in blue, scale bars are 50 μm.

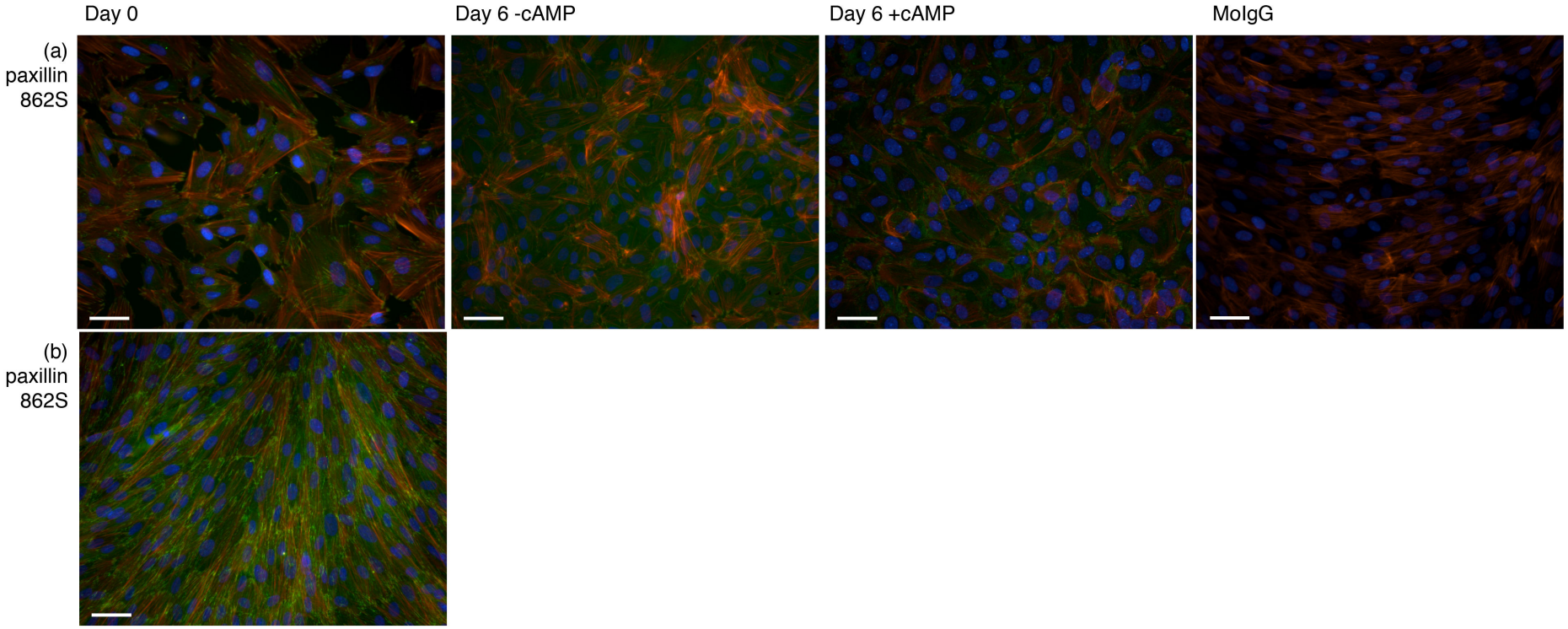

Appendix X (c, d) Immunofluorescence staining for paxillin produced by ESCs at day 0, day 6 and day 6 with cAMP, from different fields of view of one ESC cell number (862S) in the same experiment. Paxillin is in green, actin in red and nuclei in blue, scale bars are 25μm.

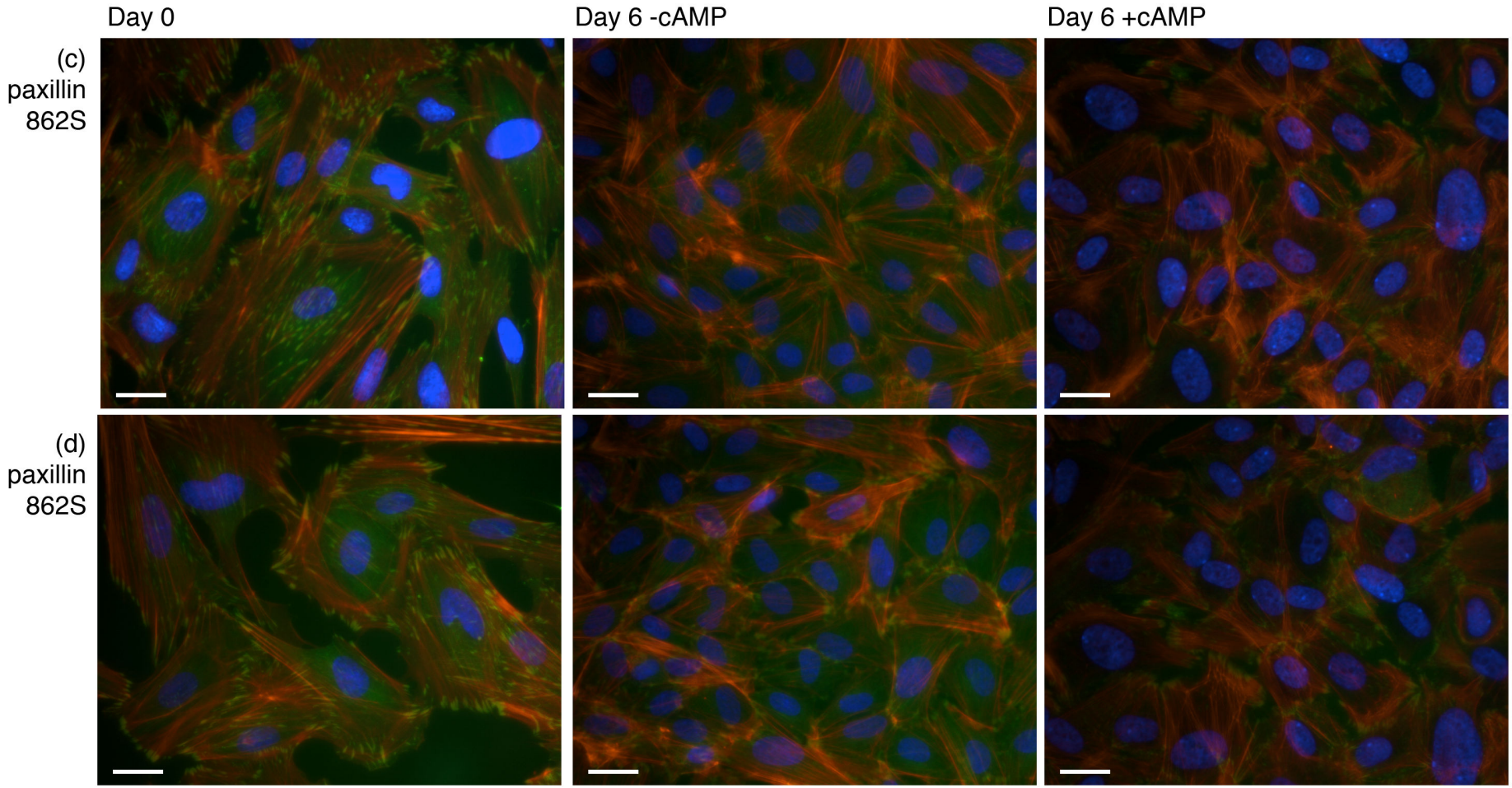

Appendix X (e, f) Immunofluorescence staining for paxillin produced by ESCs at day 0, day 6 and day 6 with cAMP, from different fields of view of one ESC cell number (890S) in the same experiment. Control sections treated with MoIgG instead of primary antibody are also shown. Paxillin is in green, actin in red and nuclei in blue, scale bars are 50 μm.

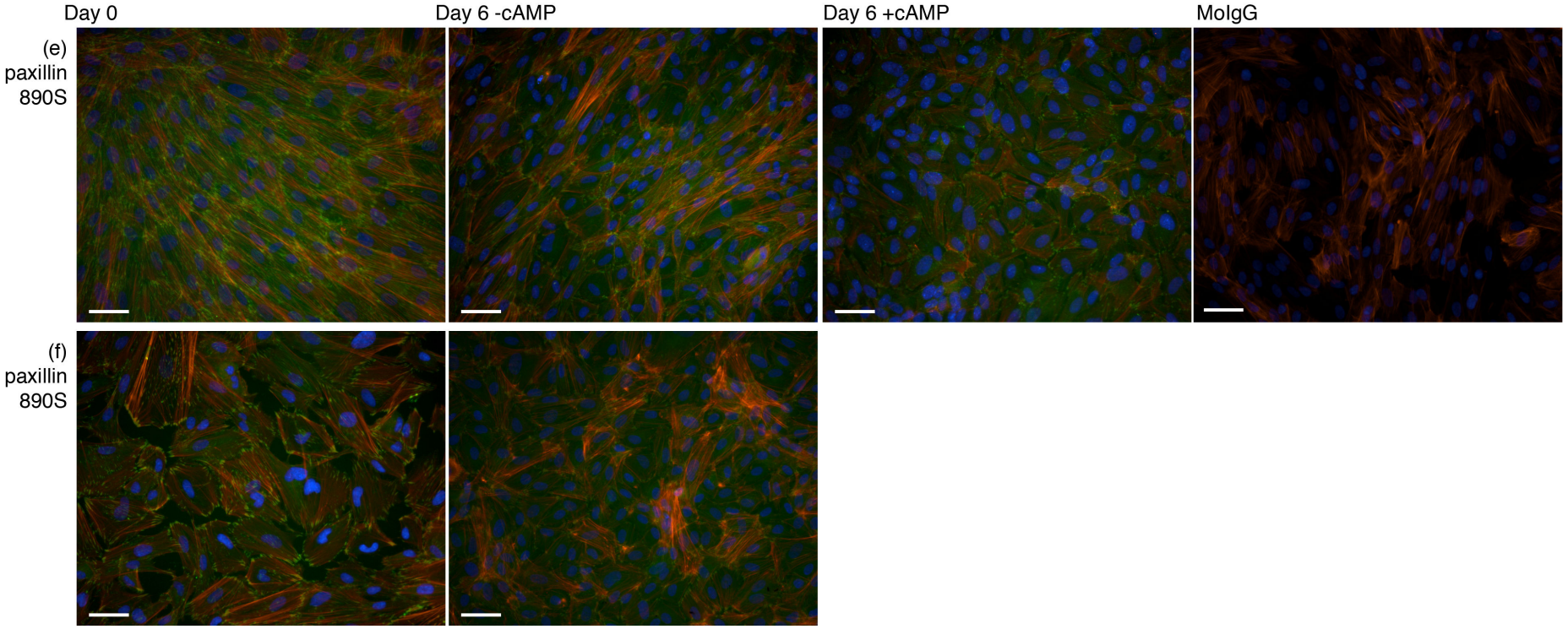

Appendix X (g, h) Immunofluorescence staining for paxillin produced by ESCs at day 0, day 6 and day 6 with cAMP, from different fields of view of one ESC cell number (890S) in the same experiment. Paxillin is in green, actin in red and nuclei in blue, scale bars are 25μm.

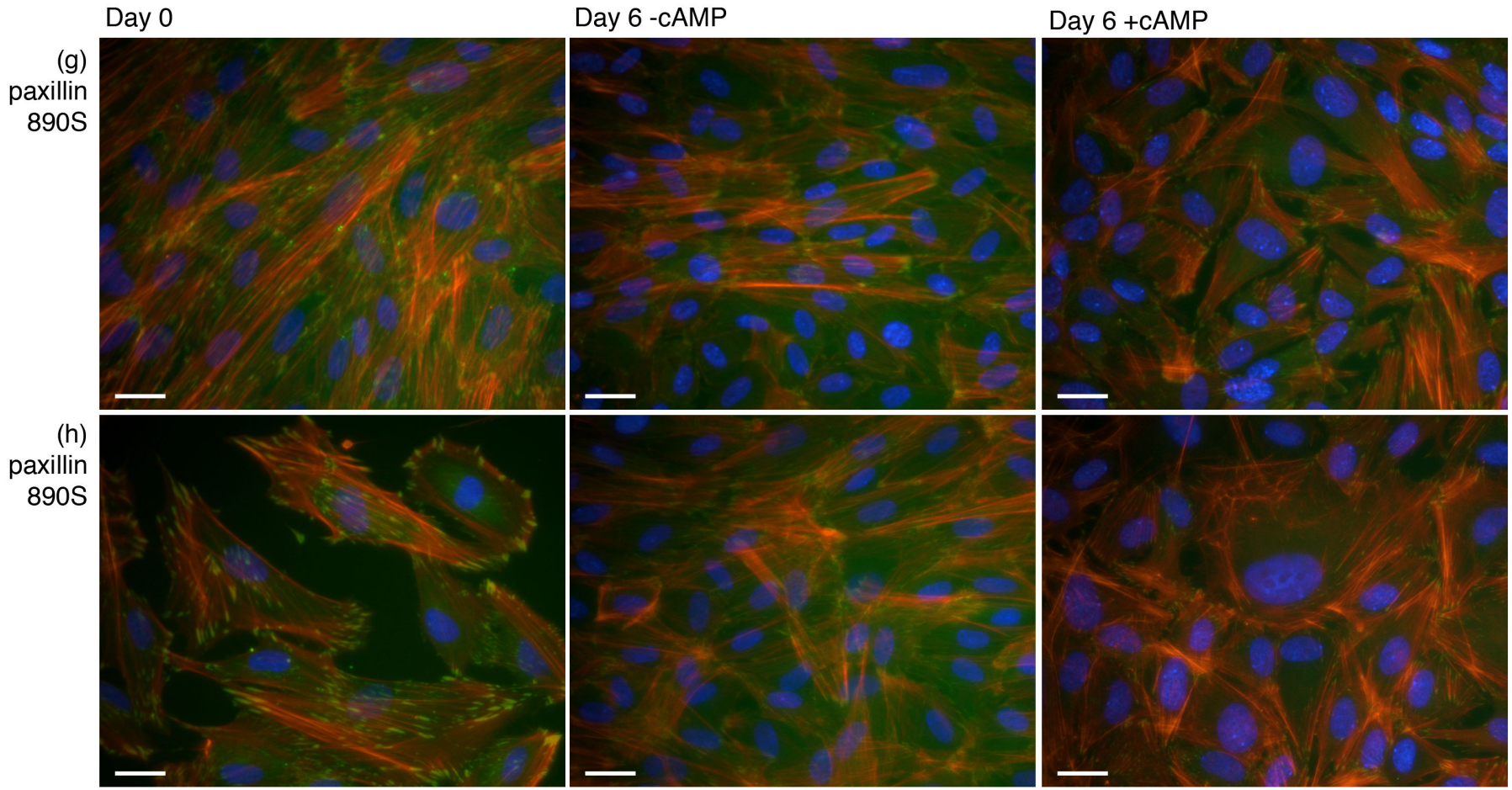

Appendix X (i-k) Immunofluorescence staining for paxillin produced by ESCs (629S) at day 0, day 6 and day 6 with cAMP. Control sections treated with MoIgG instead of primary antibody are also shown. Paxillin is in green, actin in red and nuclei in blue, scale bars are 50 μm.